



# Measurements of air quality at a hydraulic fracturing site in the Surat Basin, Queensland- Final Report

Task 3 Report for Project W.12

Air, water and soil impacts of hydraulic fracturing: Phase 2

June 2019

Erin Dunne<sup>1</sup>, Melita Keywood<sup>1</sup>, Paul Selleck<sup>1</sup>, Jennifer Powell<sup>1</sup>, Maximilien Desservettaz<sup>1</sup>, Alistair Williams<sup>2</sup>, Anthony Morrison<sup>3</sup>, Min Cheng<sup>1</sup>, James Harnwell<sup>1</sup>, Scott Henson<sup>1</sup>, Suzie Molloy<sup>1</sup>, Ot Sisoutham<sup>2</sup>, Jason Ward<sup>1</sup>, Sylvester Werczynski<sup>2</sup>, Grant Edwards<sup>3</sup>

<sup>1</sup> CSIRO Oceans & Atmosphere

<sup>2</sup> Australian Nuclear Science and Technology Organisation (ANSTO)

<sup>3</sup>Macquarie University- Dept. Environmental Sciences- MQ Centre for Energy & Environmental Contaminants





# GISERA

Gas Industry Social and  
Environmental Research Alliance



**QGC**



**Santos**



Australian Government  
Department of Industry, Science,  
Energy and Resources



Supported by  
**Government of  
South Australia**



**NORTHERN  
TERRITORY  
GOVERNMENT**



**PANGAEA**  
RESOURCE PTY LTD

GISERA, GPO Box 2583, Brisbane QLD 4001, Australia



# GISERA

Gas Industry Social and  
Environmental Research Alliance

## Document control

<b>Version</b>	<b>Date</b>	<b>Description</b>	<b>Author</b>	<b>Approved</b>
1	6/02/19	Draft Report for peer review	ED	MK
2	12/05/19	Draft Report- peer review comments addressed	ED	MK
3	11/06/2019	Final Report- CSIRO internal review comments incorporated. Version submitted to CSIRO EPublish	ED	MK
4	20/6/2019	Final Report- Approved in EPublish EP193832	MK	PK

## Report Title

**ISBN (print):** 978-1-4863-1312-9

**ISBN (online):** 978-1-4863-1313-6

The Gas Industry Social and Environmental Research Alliance (GISERA) undertakes publicly-reported research that addresses the socio-economic and environmental impacts of Australia's natural gas industries.

GISERA was co-founded by CSIRO and Australia Pacific LNG in July 2011. For further information visit [gisera.csiro.au](http://gisera.csiro.au).

## Citation

Dunne, E., Keywood, M., Selleck, P., Powell, J., Desservettaz, M., Williams, A M., Edwards, G., Morrison, A., Cheng, M., Harnwell, J., Henson, S., Molloy, S., Sisoutham, O., Ward, J., Werczynski, S. (2019) Measurements of air quality at a hydraulic fracturing site in the Surat Basin, Queensland- Draft Report. Task 3 Report for Project W.12 to the Gas Industry Social and Environmental Research Alliance (GISERA). March 2019. CSIRO, Canberra.

## Copyright

© 2019 CSIRO To the extent permitted by law, all rights are reserved and no part of this publication covered by copyright may be reproduced or copied in any form or by any means except with the written permission of CSIRO.

## Important Disclaimer

The partners in GISERA advise that the information contained in this publication comprises general statements based on scientific research. The reader is advised and needs to be aware that such information may be incomplete or unable to be used in any specific situation. No reliance or actions must therefore be made on that information without seeking prior expert professional, scientific and technical advice. To the extent permitted by law, GISERA (including its partners, employees and consultants) excludes all liability to any person for any consequences, including but not limited to all losses, damages, costs, expenses and any other compensation, arising directly or indirectly from using this publication (in part or in whole) and any information or material contained in it.

## Cover Photo

Photo of hydraulic fracturing activity in the Surat Basin. Photo credit to Erin Dunne

# Contents

<b>Glossary .....</b>	<b>xv</b>
<b>Acknowledgements.....</b>	<b>xviii</b>
<b>Executive summary .....</b>	<b>19</b>
<b>1 Introduction.....</b>	<b>22</b>
1.1 Out of Scope.....	24
<b>2 Measurement methods .....</b>	<b>25</b>
2.1 Target air pollutants and relevant air quality objectives .....	25
2.1.1 Air Quality Index .....	29
2.2 Measurement sites .....	30
2.3 HF activity and Sampling Timelines .....	32
2.4 Measurement systems.....	35
2.4.1 North and South-AQMS .....	35
2.4.2 Solar-AQMS.....	37
<b>3 Meteorology .....</b>	<b>38</b>
3.1.1 Data capture for air masses impacted by HF.....	42
<b>4 Ambient Air Quality .....</b>	<b>46</b>
4.1 Nitrogen dioxide, carbon monoxide, ozone, sulphur dioxide.....	49
4.1.1 Nitrogen dioxide .....	49
4.1.2 Carbon monoxide.....	54
4.1.3 Ozone.....	57
4.1.4 Sulfur dioxide .....	61
4.2 Particulate Matter (PM <sub>2.5</sub> , PM <sub>10</sub> , TSP) mass concentrations.....	64
4.2.1 PM <sub>10</sub> concentrations at the North and South-AQMS .....	67
4.2.2 PM <sub>10</sub> concentrations at the Solar-AQMS sites.....	71
4.2.3 PM <sub>2.5</sub> concentrations at the North and South-AQMS and Solar-AQMS sites .....	73
4.2.4 Total suspended particles (TSP) .....	77
4.2.5 Summary of PM Exceedances .....	81
4.3 Chemical Composition Analysis of Particulate Matter .....	82
4.3.1 Queensland EPP air pollutants present in PM <sub>10</sub> .....	84
4.3.2 PM <sub>10</sub> Source Apportionment.....	84

4.3.2.1	PMF factors and source tracers.....	85
4.3.2.2	Source indicator species.....	87
4.3.2.3	Factor 1 Soil .....	91
4.3.2.4	Factor 2 Secondary Ammonium Sulfate.....	97
4.3.2.5	Factor 3 Secondary Nitrate-Aged Sea Salt.....	98
4.3.2.6	Factor 4 Aged Biomass Smoke .....	99
4.3.2.7	Factor 5 Fresh Sea Salt .....	101
4.3.2.8	Factor 6 Wood Smoke.....	102
4.3.2.9	Factor 7 Glucose .....	103
4.3.2.10	Factor 8 Primary Biological Aerosol.....	104
4.3.3	Summary of the sources of PM at the HF study site .....	105
<b>5</b>	<b>NEPM Air Toxics, other VOCs and hydrogen sulphide .....</b>	<b>106</b>
5.1	Formaldehyde .....	109
5.2	Benzene, Toluene, Xylenes.....	117
5.2.1	Benzene .....	118
5.2.2	Toluene .....	120
5.2.3	Xylenes.....	123
5.2.4	HF and non-HF related sources of BTX.....	126
5.2.5	BTX Summary.....	130
5.3	Polycyclic Aromatic Hydrocarbons .....	130
5.4	Other Queensland EPP air pollutants .....	137
5.5	Other VOCs .....	139
<b>6</b>	<b>Mercury and Radon .....</b>	<b>143</b>
6.1	Mercury.....	143
6.2	Radon.....	146
<b>7</b>	<b>Methane .....</b>	<b>151</b>
<b>8</b>	<b>Discussion and Summary .....</b>	<b>155</b>
	<b>References .....</b>	<b>162</b>
<b>9</b>	<b>Appendix: Comparison of particulate matter (PM) measurement methods .....</b>	<b>168</b>
<b>10</b>	<b>Appendix - Analysis of PM<sub>10</sub> chemical composition data .....</b>	<b>170</b>
10.1	Data Quality .....	170
10.1.1	Blank filters .....	170

10.1.2 Ion balance.....	170
10.1.3 Comparison of species from IC and IBA analysis.....	171
10.1.4 Species correlations and tracer time series.....	172
10.1.5 Reconstructed chemical mass.....	176
10.2 Data analysis by PMF (positive matrix factorisation).....	177
10.2.1 Selection of species.....	178
10.2.2 Species correlations and tracer time series.....	180
10.2.3 PMF configuration.....	180
10.2.4 PMF mass closure .....	182
<b>11 Appendix –VOC Measurements .....</b>	<b>183</b>
11.1 PTR-MS.....	183
11.2 Active sampling of formaldehyde and BTX on adsorbent cartridges.....	185
11.3 Analysis of DNPH tubes for formaldehyde.....	186
11.4 Analysis of VOC adsorbent tubes .....	187
11.5 Precision of active sampling on VOC adsorbent tubes and DNPH cartridges .....	189
11.5.1 VOC adsorbent tubes.....	189
11.5.2 DNPH cartridges.....	189
11.6 Passive Radiello sampling.....	190
11.7 Comparison of VOC measurements made by PTR-MS, VOC adsorbent tubes, DNPH and Passive Radiello sampling.....	192
<b>12 Appendix-Sampling and Analysis of polycyclic aromatic hydrocarbons .....</b>	<b>194</b>
12.1 Sampling efficiency, analytical recovery and blank levels .....	196
<b>13 Appendix-Mercury sampling and analysis .....</b>	<b>200</b>
<b>14 Appendix – Fire Hotspot data.....</b>	<b>201</b>

## List of Tables

Table 1 Target air pollutants, their potential HF-related sources and associated air quality objectives. See Glossary for definition of acronyms.....	27
Table 2 Air Quality Index categories and their respective Index value ranges. ....	29
Table 3 Timeline of sampling and well site activities for the measurement period July – December 2017. HF is Hydraulic Fracturing, WC is well completions.....	34
Table 4 Summary of meteorology data from the BoM site at Roma and meteorology data from the North-AQMS at the study site.....	40

Table 5 The distance and heading from the North and South-AQMS to each well and the proportion of time the AQMS was downwind of the well during HF + WC activity.....	44
Table 6 Distance of each Solar-AQMS from the closest well, the heading from the closet well and the proportion of time the Solar QMS was downwind of the nearest well during HF + WC activities. ....	45
Table 7 Number of occasions and the proportion (%) of total observations air pollutant concentrations fell into each of the 5 air quality index categories.....	47
Table 8 Monthly maximum and average 1-hour concentrations of NO <sub>2</sub> (ppm) for North and South-AQMS for the HF study period (Jul – Dec 2018). Data availability (%), overall average NO <sub>2</sub> concentrations, and concentrations during HF + WC are also presented. The NEPM 1-hour air quality objective for NO <sub>2</sub> is 0.12 ppm. ....	51
Table 9 Proportion of total NO <sub>2</sub> observations (1-hour averages) in each air quality index category from the North and South-AQMS at the HF study site, and from Hopeland, Miles Airport and Burncluith sites operated as part of the Surat Basin Ambient Air Monitoring Network. ....	52
Table 10 Monthly maximum and average rolling 8-hour concentrations of CO (ppm) for North and South-AQMS during the HF study period (Jul – Dec 2017). Data availability (%), overall average and maximum CO concentrations and concentrations during the HF + WC period are also presented. The NEPM rolling 8-hour air quality objective for CO is 9 ppm. ....	54
Table 11 Proportion of total CO observations (rolling 8-hour averages) in each air quality index category from the North and South-AQMS' at the HF study site, and from Hopeland, Miles Airport and Burncluith sites operated as part of the Surat Basin Ambient Air Monitoring Network.....	55
Table 12 Monthly maximum and average 1-hour and rolling 4-hour concentrations of O <sub>3</sub> (ppm) for the North and South-AQMS during the HF study period (Jul – Dec 2018). Data availability (%), overall average O <sub>3</sub> concentrations, and average concentrations during the HF + WC period are also presented. The NEPM 1-hour air quality objective for O <sub>3</sub> is 0.100 ppm and the NEPM 4-hour air quality objective for O <sub>3</sub> is 0.08 ppm. ....	58
Table 13 Proportion of total 1-hour averages and rolling 4-hour average observations of O <sub>3</sub> in each air quality index category from the North and South-AQMS at the HF study site, and from Hopeland, Miles Airport and Burncluith sites operated as part of the Surat Basin Ambient Air Monitoring Network. ....	60
Table 14 Ambient concentrations of SO <sub>2</sub> for the North-AQMS including monthly average and maximum 1-hour and 24-hour concentrations (ppm) during the HF study period July – December 2017. Data capture rates, overall average and maximum SO <sub>2</sub> concentrations, and concentrations during HF + WC are also included; The NEPM 1-hour air quality objective for SO <sub>2</sub> is 0.2 ppm. ....	63
Table 15 Proportion of 1-hour and rolling 24-hour observations of SO <sub>2</sub> in each air quality index category from the North and South-AQMS at the HF study site, and from Flinders View, a suburban air quality monitoring site located in the Ipswich area of SE Queensland. SO <sub>2</sub> measurements were not made at Hopeland, Miles Airport or Burncluith.....	63
Table 16 Monthly maximum and average 24-hour concentrations of PM <sub>10</sub> (µg m <sup>-3</sup> ) for North and South-AQMS for the HF study period (Jul – Dec 2017). Data capture (%), overall average PM <sub>10</sub> , and	

concentrations during HF +WC are also presented. The NEPM 24-hour air quality objective for PM <sub>10</sub> is 50 µg m <sup>-3</sup> .....	69
Table 17 Proportion of total 24-hour observations of PM <sub>10</sub> in each air quality index category from the FIDAS measurements at the North and South-AQMS at the HF study site, and from Hopeland and Miles Airport sites operated as part of the Surat Basin Ambient Air Monitoring Network. PM was not measured at Burncluith. ....	70
Table 18 Average concentrations of all PM <sub>10</sub> filter samples collected via the Microvol low volume samplers at the five Solar-AQMS. The annual Ambient Air NEPM (2016) guideline of 25 µg m <sup>-3</sup> ...	73
Table 19 Ambient concentrations of PM <sub>2.5</sub> including average and monthly maximum and average 24-hour concentrations (µg.m <sup>-3</sup> ), monthly data capture (%), overall average PM <sub>2.5</sub> , percentage of data collected downwind of activities including HF, and average and maximum PM <sub>2.5</sub> downwind of HF +WC activities for North and South-AQMS for 2017.....	74
Table 20 Proportion of total 24-hour observations of PM <sub>2.5</sub> in each air quality index category from the North and South-AQMS' and five Solar-AQMS at the HF study site, and from Hopeland and Miles Airport sites operated as part of the Surat Basin Ambient Air Monitoring Network. PM was not measured at Burncluith. ....	75
Table 21 Ambient concentrations of TSP including average and monthly maximum and average 24-hour concentrations (µg.m <sup>-3</sup> ) for the North and South-AQMS (Jul – Dec 2017). Data capture (%), overall average and maximum TSP, and TSP concentrations during HF + WC are also included.....	78
Table 22 Proportion of total 24-hour observations of TSP in each air quality index category from the North and South-AQMS' at the HF study site, and from Hopeland and Miles Airport sites operated as part of the Surat Basin Ambient Air Monitoring Network. PM including TSP was not measured at Burncluith.....	79
Table 23 Detection frequency and average concentrations of arsenic, manganese, nickel and sulfate from the North-AQMS, and the QLD EPP air quality objectives for these elements/compounds .....	84
Table 24 Summary of factors identified by the PMF, the chemical species that contribute to the factors, the percentage of total mass that the factor comprises and the potential sources that contribute to the factor. ....	87
Table 25 Key species used to identify sources contributing to the multi-day samples collected with the Microvol samplers at the Solar-AQMS sites .....	88
Table 26 Ratios of chloride and magnesium to sodium in seawater (Millero et al., 2008), produced waters and influent and brine from the water treatment facility and the Fresh Sea Salt Factor identified by PMF in the PM <sub>10</sub> samples. ....	102
Table 27 Monthly maximum and average 24-hour concentrations of formaldehyde (ppm) for North-AQMS (PTR-MS & DNPH methods) and for Solar-AQMS #1-#5 (DNPH method) for the HF study period (Jul – Dec 2017). Data capture (%), overall average formaldehyde, and concentrations during HF +WC are also presented. The NEPM 24-hour MIL for formaldehyde is 0.040 ppm.....	111
Table 28 The detection frequency (% samples > Detection limit, DL) and the range of ~ 14-day integrated average concentrations of formaldehyde measured by Radiello at the HF study site,	

another HF site in the Miles-Condamine region in 2016/17 (Dunne et al., 2018), and from two regional sites (Burncluith & Tara region) and two gas field sites (Wilgas & Hopeland) operated as part of the Surat Basin Ambient Air Monitoring Network (Lawson et al. 2018).....	113
Table 29 Monthly maximum and average 24-hour concentrations of benzene (ppb) for North-AQMS by PTR-MS and AT-VOC methods for the HF study period (Jul – Dec 2017). Data capture (%), overall average benzene, and concentrations during HF +WC are also presented. The annual NEPM MIL for benzene is 180 ppb. Note: Benzene data from Solar-AQMS #1 –# 5 excluded due to poor precision (Appendix 11). .....	118
Table 30 Comparison of the detection frequency (% samples > DL) and concentration ranges of benzene measured by Radiello at the HF study site, with data from another HF site in the Miles-Condamine region collected in 2016/17 (Dunne et al., 2018), and with data from two regional sites (Burncluith & Tara region) and two gas field sites (Wilgas & Hopeland) operated as part of the Surat Basin Ambient Air Monitoring Network (Lawson et al., 2018).....	120
Table 31 Monthly maximum and average 24-hour concentrations of toluene (ppm) for North-AQMS by the PTR-MS and active sampling on adsorbent tube methods (AT-VOC) and for Solar-AQMS #1-#5 for the HF study period (Jul – Dec 2017). Data capture (%), overall average toluene, and concentrations during HF +WC are also presented. The NEPM 24-hour MIL for toluene is 0.1 ppm.....	121
Table 32 Comparison of the detection frequency (% samples > DL) and concentration ranges of toluene measured by Radiello at the HF study site, with data from another HF site in the Miles-Condamine region collected in 2016/17 (Dunne et al 2018), and with data from two regional sites (Burncluith & Tara region) and two gas field sites (Wilgas & Hopeland) operated as part of the Surat Basin Ambient Air Monitoring Network (Lawson et al 2018).....	123
Table 33 Monthly maximum and average 24-hour concentrations of xylenes (ppm) for North-AQMS and for Solar-AQMS 1-5 for the HF study period (Jul – Dec 2017). Data capture (%), overall average xylenes, and concentrations during HF +WC are also presented. The NEPM 24-hour MIL for formaldehyde is 0.04 ppm.....	124
Table 34 Comparison of the detection frequency (% samples > DL) and concentration ranges of xylenes measured by Radiello at the HF study site, with data from another HF site in the Miles-Condamine region collected in 2016/17 (Dunne et al., 2018), and with data from two regional sites (Burncluith & Tara region) and two gas field sites (Wilgas & Hopeland) operated as part of the Surat Basin Ambient Air Monitoring Network (Lawson et al., 2018).....	125
Table 35 Summary statistics for Benzo[a]Pyrene concentrations .....	131
Table 36 Concentrations of ten PAH species measured at other Queensland sites. BaP, the marker used to assess levels of PAHs against the annual NEPM, is highlighted in bold. ....	133
Table 37 Diagnostic ratios of different PAH sources from the literature and measured in this study. ....	136
Table 38 Mean and max concentrations, detection frequency, detection limit method employed, averaging time and air quality objective for 1,2 dichloromethane, styrene, Tetrachloroethylene and Hydrogen Sulphide.....	138

Table 39 The concentration range and detection frequency (DF) for each VOC detected in Radiello samples at the HF study site and their relevant annual/ long term ambient air quality objective values. Also presented are data from another HF study site in the Miles-Condamine region collected in 2016/17 (Dunne et al 2018), and data from the regional sites (Tara and Burncluith) and gas field sites (Miles Airport and Hopeland) collected over the same period as the present study. ....	141
Table 40 Summary statistics for mercury concentrations, in ng/m <sup>3</sup> sampled from 15 <sup>th</sup> August 2017 to 6 <sup>th</sup> December 2017 .....	144
Table 41 Concentrations of mercury measured in other locations in Australia. ....	145
Table 42 Summary radon concentration statistics, including monthly average and maximum concentrations from the South-AQMS and the Tara region reference measurements. The ARPANSA Recommendations for Limiting Exposure to Ionizing Radiation (ARPANSA 2002) (Guidance note [NOHSC:3022(1995)]) are: 200 Becquerel per cubic metre Bq m <sup>-3</sup> for households and 1000 Bq m <sup>-3</sup> for workplaces. ....	147
Table 43 Species excluded from the PMF analysis .....	178
Table 44 Species included in PMF analysis of PM <sub>2.5</sub> data listing PMF category, and the median concentration and signal-to-noise ratio calculated by EPA PMF at each site. ....	179
Table 45 MDL and calibration response for the NEPM air toxics compounds.....	185
Table 46 MDL, mean rang of replicates and %RSD for replicate analyses on DNPH and VOC absorbent tubes.....	189
Table 47 Ambient concentrations of air toxics formaldehyde, benzene, toluene and xylenes measured with the different methods outlined in Section 5. ....	193
Table 48 Target compounds, internal standards and transitions monitored .....	196
Table 49 Recovery of spike deuterated PAHs added (a) before sampling; and (b) before extraction of exposed sample .....	197
Table 50 Masses of laboratory blanks, field blanks, sample MDL and number of detects .....	199

## List of Figures

Figure 1 Surat Basin study region. The site of the study presented here was ~ 35 km North of Yuleba. The Surat Basin Ambient Air Quality Study Monitoring area in the Miles Condamine region is also shown. (Source Lawson et al 2017). ....	20
Figure 2 Conceptual model for the potential pathway of pollutants from the source to the atmosphere (from Keywood et al., 2017). ....	23
Figure 3 The study site within the Roma–Yuleba region of the Surat Basin. The orange dots represent CSG wells. Source: Queensland Globe (2019).....	30
Figure 4 Map showing locations of wells that underwent HF (labelled by Well ID" Combabula ###), and the location of the North-AQMS and South-AQMS (yellow pins) and the well sites where the	

five solar powered air monitoring stations were also located (within 100 meters of the well pads). Source: Qld Globe (date).....	31
Figure 5 North-AQMS with HF spread present at adjacent well (COM 313) in the foreground. The distance from the COM 313 to the North-AQMS was approximately 100 m. ....	31
Figure 6 South-AQMS (right) with water storage tank, fuel storage tank and truck/equipment laydown area in the background. The distance from the laydown area to the South-AQMS was approximately 100 m. ....	32
Figure 7 Two enclosures at North-AQMS located adjacent to a well pad undergoing drilling. ....	36
Figure 8 Solar-AQMS #4 located adjacent to a well pad (COM 314) undergoing well perforation..	37
Figure 9 24-hour average temperature and relative humidity measured at 2m at the North and South-AQMS and the five Solar-AQMS sites and daily rainfall. Shaded areas represent periods of well development activity on the HF study site, including drilling, HF and well completion (WC)..	41
Figure 10 Wind roses summarising the frequency (length) of 5-minute average wind speed (colour) and direction (angle) measured at 2m height at the five Solar-AQMS sites and wind roses of the 1-hour average wind speed and direction measured at 10 m height at the North and South-AQMS for the entire study period (Jul- Nov 2017). ....	41
Figure 11 Wind roses summarising the frequency (length) of average 1-hour wind speed (colour) and direction (angle) for the months of July to November 2017 measured at 10 m height at the North-AQMS, and separated between night time (20:00 – 08:00) and day time (08:00 – 20:00)...	42
Figure 12 1-hour average NO <sub>2</sub> concentration (ppm) at both North and South-AQMS. Shaded areas represent periods of well development activity on the HF study site, including drilling (grey) and HF + WC (purple).....	51
Figure 13: Box and whisker plots of the 5-minute average NO <sub>2</sub> data from the North and South-AQMS measured when downwind of drilling (A) and HF + WC (C). For comparison NO <sub>2</sub> data from other WDRs during drilling (B) and from other WDRs during HF + WC (D), as well as during non-activity periods (E) are presented. Note the box represents the inter-quartile range (IQR) (range of 25 <sup>th</sup> to 75 <sup>th</sup> percentiles), the blue line is the median (50 <sup>th</sup> percentile), the whiskers represent the 5 <sup>th</sup> and 95 <sup>th</sup> percentiles and the points above/below the whiskers represent the top/bottom 5% of values. NO <sub>2</sub> was not measured at the North-AQMS during drilling (see Table 8). ....	53
Figure 14 Daily maximum 8-hour averages for CO at both North and South-AQMS. Shaded areas represent periods of well development activity on the HF study site, including drilling (grey) and HF + WC (purple).....	55
Figure 15: Box and whisker plots of the 5-minute average CO data (ppm) from the North and South-AQMS measured when downwind of drilling and HF + WC. For comparison CO data from other WDRs during drilling and HF +WC, as well as during non-activity periods are presented. Note the box represents the range between the 25 <sup>th</sup> and 75 <sup>th</sup> percentiles, the blue line is the median (50 <sup>th</sup> percentile), the whiskers represent the 5 <sup>th</sup> and 95 <sup>th</sup> percentiles and the points above/below the whiskers represent the top/bottom 5% of values. Note: CO wasn't measured during drilling at the North-AQMS (see Table 10). ....	57

Figure 16 1-hour averages for O<sub>3</sub> at both North and South-AQMS. Shaded areas represent periods of well development activity on the HF study site, including drilling (grey) and HF + WC (purple). 59

Figure 17 Daily maximum 4-hour averages for O<sub>3</sub> at both North and South-AQMS. Shaded areas represent periods of well development activity on the HF study site, including drilling (grey) and HF + WC (purple). ..... 59

Figure 18: Box and whisker plots of the 5-minute average O<sub>3</sub> data (ppb) from the North and South-AQMS measured when downwind of HF + WC (C). For comparison O<sub>3</sub> data from other WDRs during and HF +WC (D), as well as during non-activity periods (E) are presented. Note the box represents the range between the 25<sup>th</sup> and 75<sup>th</sup> percentiles, the blue line is the median (50<sup>th</sup> percentile), the whiskers represent the 5<sup>th</sup> and 95<sup>th</sup> percentiles and the points above/below the whiskers represent the top/bottom 5% of values. Note: ozone wasn't measured during drilling at the North or South-AQMS (see Table 12)..... 61

Figure 19 1-hour averages for SO<sub>2</sub> at the North-AQMS. Shaded areas represent periods of well development activity on the HF study site, including drilling (grey) and HF + WC (purple). ..... 62

Figure 20 24-hour averages for SO<sub>2</sub> at the North-AQMS. Shaded areas represent periods of well development activity on the HF study site, including drilling (grey) and HF + WC (purple). ..... 62

Figure 21 Box and whisker plots of the 5-minute average SO<sub>2</sub> data (ppm) from the North and South-AQMS measured when downwind of drilling and HF + WC. For comparison SO<sub>2</sub> data from other WDRs during drilling and HF +WC, as well as during non-activity periods are presented. Note the box represents the range between the 25<sup>th</sup> and 75<sup>th</sup> percentiles, the blue line is the median (50<sup>th</sup> percentile), the whiskers represent the 5<sup>th</sup> and 95<sup>th</sup> percentiles and the points above/below the whiskers represent the top/bottom 5% of values. Note: SO<sub>2</sub> was not measured at the South-AQMS during this study or at the North-AQMS during drilling due to equipment faults. .... 64

Figure 22 Comparison of PM<sub>10</sub> and PM<sub>2.5</sub> measurement methods employed during the HF study. Lines represent 1:1 agreement. (Left panel) (blue) 24-hour average PM<sub>10</sub> by low-volume Derenda sampler with gravimetric mass determination versus 24-hour average of continuous PM<sub>10</sub> measurement by FIDAS light scattering method ( $R^2 = 0.94$ ). (red) Multi-day integrated average PM<sub>10</sub> by low-volume Microvol sampler with gravimetric mass determination versus FIDAS PM<sub>10</sub> integrated average over the same sample duration as Microvol ( $R^2 = 0.97$ ). (Right Panel) 24-hour average of continuous PM<sub>10</sub> measurements by E-sampler light scattering technique with gravimetric mass correction versus 24-hour average of continuous PM<sub>10</sub> measurement by FIDAS light scattering method ( $R^2 = 0.84$ ). ..... 67

Figure 23 24-hour average PM<sub>10</sub> at both North and South-AQMS. Shaded areas represent periods of well development activity on the HF study site, including drilling (grey) and HF + WC (purple). 68

Figure 24 Box and whisker plots of the 5-minute average PM<sub>10</sub> data from the North and South-AQMS measured when downwind of drilling and HF + WC. For comparison PM<sub>10</sub> data from other WDRs during drilling and HF +WC, as well as during non-activity periods are presented. Note the box represents the range between the 25<sup>th</sup> and 75<sup>th</sup> percentiles, the blue line is the median (50<sup>th</sup> percentile), the whiskers represent the 5<sup>th</sup> and 95<sup>th</sup> percentiles and the points above/below the whiskers represent the top/bottom 5% of values..... 71

Figure 25 Multi-day integrated averages for PM <sub>10</sub> at the five Solar-AQMS. Bars represent average PM <sub>10</sub> concentrations at each site. The length of the bar represents the sample duration. Shaded areas represent periods of well development activity on the HF study site, including drilling (grey) and HF + WC (purple).....	72
Figure 26 24-hour average PM <sub>2.5</sub> measured at the North and South-AQMS by Palas FIDAS and at the five Solar-AQMS sites measured by MetOne E-Sampler. Site 5 was co-located with the South-AQMS. Shaded areas represent periods of well development activity on the HF study site, including drilling (grey) and HF + WC (purple).....	75
Figure 27 Box and whisker plots of the 5-minute average PM <sub>2.5</sub> data from the North and South-AQMS measured when downwind of drilling and HF + WC. For comparison PM <sub>10</sub> data from other WDRs during drilling and HF +WC, as well as during non-activity periods are presented. Note the box represents the range between the 25 <sup>th</sup> and 75 <sup>th</sup> percentiles, the blue line is the median (50 <sup>th</sup> percentile), the whiskers represent the 5 <sup>th</sup> and 95 <sup>th</sup> percentiles and the points above/below the whiskers represent the top/bottom 5% of values.....	77
Figure 28 24-hour averages for total suspended particles at both North and South-AQMS. Shaded areas represent periods of well development activity on the HF study site, including drilling (grey) and HF + WC (purple).....	79
Figure 29 Box and whisker plots of the 5-minute average PM <sub>2.5</sub> data from the North and South-AQMS measured when downwind of drilling and HF + WC. For comparison PM <sub>10</sub> data from other WDRs during drilling and HF +WC, as well as during non-activity periods are presented. Note the box represents the range between the 25 <sup>th</sup> and 75 <sup>th</sup> percentiles, the blue line is the median (50 <sup>th</sup> percentile), the whiskers represent the 5 <sup>th</sup> and 95 <sup>th</sup> percentiles and the points above/below the whiskers represent the top/bottom 5% of values.....	81
Figure 30 Chemical fingerprints for each Factor. Left axis and blue bars represents the concentration of each species contributing to the fingerprint. Right axis and red square represent the fraction of the total mass of the species accounted for by the factor .....	86
Figure 31 The average concentration of the indicator species and other key species from each factor from the 12-hour samples of PM <sub>10</sub> collected by the Comde-Derenda low volume sampler (top) and the multi-day samples of PM <sub>10</sub> collected by Microvols (middle) and PM <sub>2.5</sub> collected by E-Samplers (bottom) at the Solar-AQMS sites (#1 - #5). Error bars represent ± one standard deviation.....	89
Figure 32 Time series of the contribution of each PMF Factor to PM <sub>10</sub> at the North-AQMS (µg m <sup>-3</sup> ). Shaded areas represent drilling (grey) and HF + WC (purple) periods .....	90
Figure 33 Soil Factor- polar frequency plot of the weighted mean statistic (left) and polar frequency of the maximum statistic (right).....	92
Figure 34 Map of HF study site with North and South-AQMS (red dots), roads, wells (COM###) and laydown area near South-AQMS shown. Source: Origin Energy. ....	93
Figure 35 Composition of multi-day sample collected at Solar-AQMS #4 with Microvol 6-13 Sept 2017. The species are plotted in order of decreasing concentration. In this sample the soil indicator species Si and Al displayed the highest concentrations indicating a soil dust contribution to this sample.....	94

Figure 36 Composition of multi-day sample collected at South-AQMS with Microvol 22-29 Sept 2017. The species are plotted in order of decreasing concentration. In this sample the soil indicator species Si, BC and Al displayed the highest concentrations indicating a soil dust contribution to this sample.....	95
Figure 37 PM <sub>10</sub> (top) and TSP (bottom) mass measured at the South-AQMS by Palas FIDAS - polar frequency plot of the weighted mean statistic (left) and polar frequency of the maximum statistic (right). .....	96
Figure 38 Ammonium Sulfate Factor- polar frequency plot of the weighted mean statistic (left) and polar frequency of the maximum statistic (right).....	98
Figure 39 Secondary Nitrate-Aged Sea Salt Factor- polar frequency plot of the weighted mean statistic (left) and polar frequency of the maximum statistic (right). .....	99
Figure 40 NASA Worldview map of fire hotspots (Appendix 15) on the 27th September 2017 when the highest 24-hour average concentrations of the Aged Biomass Smoke Factor (Factor 4) were recorded. Note the mixing of Wood Smoke (Factor 6) from forest fires ~ 200 km to the NW and Aged Biomass Smoke (Factor 4) from fires further afield (~ 400 km) to the NNE over the study site. ....	100
Figure 41 Aged Biomass Smoke Factor- polar frequency plot of the weighted mean statistic (left) and polar frequency of maximum statistic (right). .....	101
Figure 42 Sea salt Factor- polar frequency plot of the weighted mean statistic (left) and polar frequency of maximum statistic (right). .....	102
Figure 43 Wood Smoke Factor- polar frequency plot of the weighted mean statistic (left) and polar frequency of maximum statistic (right). .....	103
Figure 44 Glucose Factor- polar frequency plot of the weighted mean statistic (left) and polar frequency of maximum statistic (right). .....	104
Figure 45 Primary Biological Aerosol Factor- polar frequency plot of the weighted mean statistic (left) and polar frequency of maximum statistic (right). .....	105
Figure 46 24-hour averages of formaldehyde measured at the North-AQMS and Solar-AQMS sites by active sampling on the DNPH tubes and the NEPM 24-hour objective. Shaded areas represent periods of well development activity on the HF study site, including drilling (grey) and HF + WC (purple). .....	112
Figure 47 Time series of the 24-hour averages of formaldehyde and the biomass burning tracer acetonitrile measured by PTR-MS at the North-AQMS. ....	114
Figure 48 Box and whisker plots of the 10 min average formaldehyde data from the North-AQMS measured by PTR-MS when downwind of drilling and HF + WC. For comparison formaldehyde data from other WDRs during drilling and HF +WC, as well as during non-activity periods are presented. Note the box represents the range between the 25 <sup>th</sup> and 75 <sup>th</sup> percentiles, the blue line is the median (50 <sup>th</sup> percentile), the whiskers represent the 5 <sup>th</sup> and 95 <sup>th</sup> percentiles and the points above/below the whiskers represent the top/bottom 5% of values.....	115
Figure 49 24-hour averages of benzene measured at the North-AQMS by PTR-MS and NEPM Air Toxics annual objective for benzene. Shaded areas represent periods of well development activity	

on the HF study site, including drilling (grey) and HF + WC (purple). Note that North AQMS tubes represents the samples collected using the AT-VOC method at the North-AQMS.....	119
Figure 50 24-hour averages of toluene measured at the North-AQMS by PTR-MS and by absorbent tubes (AT-VOC) at the Solar-AQMS sites with the NEPM Air Toxics annual objective for toluene. Shaded areas represent periods of well development activity on the HF study site, including drilling (grey) and HF + WC (purple).....	122
Figure 51 24-hour averages of xylenes measured at the North-AQMS by PTR-MS and by absorbent tubes at the Solar-AQMS sites with the NEPM Air Toxics annual objective for xylene. Shaded areas represent periods of well development activity on the HF study site, including drilling (grey) and HF + WC (purple).....	125
Figure 52 Time series of 24-hour concentrations of BTX species benzene, toluene and xylene (top panel) and acetonitrile (bottom panel) measured by PTR-MS measured at the North-AQMS. Shaded areas represent periods of well development activity on the HF study site, including drilling (grey) and HF + WC (purple).....	127
Figure 53 Box and whisker plots of the 10 min average benzene, toluene, xylene data from the North-AQMS measured by PTR-MS when downwind of drilling (A) and HF + WC (C). For comparison BTX data from other WDRs during drilling (B) and HF +WC (D), as well as during non-activity periods (E) are presented. Note the box represents the range between the 25 <sup>th</sup> and 75 <sup>th</sup> percentiles, the blue line is the median (50 <sup>th</sup> percentile), the whiskers represent the 5 <sup>th</sup> and 95 <sup>th</sup> percentiles and the points above/below the whiskers represent the top/bottom 5% of values. .	129
Figure 54 Time series of 48-hour average benzo[a]pyrene concentrations in ng m <sup>-3</sup> during the study compared to the annual NEPM objective of 0.3 ng m <sup>-3</sup> . Shaded areas represent periods of well development activity on the HF study site, including drilling (grey) and HF + WC (purple). ...	132
Figure 55 Time series of 48-hour PAH concentrations measured at the South-AQMS site. ....	133
Figure 56 Time series of BaP, the sum of 8 aerosol phase PAH (BaA, BaP, Cr, Bbf+BkF, Bep, i123cdP, DahA and BghiP) and 2 gas phase PAH (Flu and Pyr). Shaded areas represent periods of well development activity on the HF study site, including drilling (grey) and HF + WC (purple). The green shaded area represents activity at COM 359R and COM 444. ....	135
Figure 57 24-hour averages of styrene measured at the North-AQMS by PTR-MS and by absorbent tubes at the Solar-AQMS sites with the NEPM Air Toxics annual objective for styrene. Shaded areas represent periods of well development activity on the HF study site, including drilling (grey) and HF + WC (purple).....	138
Figure 58 Time series of mercury concentrations. Shaded areas represent periods of well development activity on the HF study site, including drilling (grey) and HF + WC (purple). ....	144
Figure 59 Box and whisker plots of the 5-minute average mercury data from the South-AQMS measured when downwind of drilling and HF + WC. For comparison mercury data from other WDRs during drilling and HF +WC, as well as during non-activity periods are presented. Note the box represents the range between the 25 <sup>th</sup> and 75 <sup>th</sup> percentiles, the blue line is the median (50 <sup>th</sup> percentile), the whiskers represent the 5 <sup>th</sup> and 95 <sup>th</sup> percentiles and the points above/below the whiskers represent the top/bottom 5% of values.....	146

Figure 60 Time series of 24-hour average radon concentrations from the South-AQMS. Shaded areas represent periods of well development activity on the HF study site, including drilling (grey) and HF + WC (purple). The ARPANSA Recommendations for Limiting Exposure to Ionizing Radiation (ARPANSA 2002) (Guidance note [NOHSC:3022(1995)]) are: 200 Becquerel per cubic metre Bq m <sup>-3</sup> for households and 1000 Bq m <sup>-3</sup> for workplaces.....	148
Figure 61 Box and whisker plots of the 10 min average radon data from the South-AQMS measured when downwind of drilling and HF + WC. For comparison radon data from other WDRs during drilling and HF +WC, as well as during non-activity periods are presented. Note the box represents the range between the 25 <sup>th</sup> and 75 <sup>th</sup> percentiles, the blue line is the median (50 <sup>th</sup> percentile), the whiskers represent the 5 <sup>th</sup> and 95 <sup>th</sup> percentiles and the points above/below the whiskers represent the top/bottom 5% of values.....	149
Figure 62 Time series of radon concentration and wind speed (WS) measured at the South-AQMS .....	149
Figure 63 Time series of methane measured at the North and South-AQMS. Shaded areas represent periods of well development activity on the HF study site, including drilling (grey) and HF + WC (purple).....	152
Figure 64 Box and whisker plots of the 5-minute average methane data from the North and South-AQMS measured when downwind of drilling and HF + WC. For comparison methane data from other WDRs during drilling and HF + WC, as well as during non-activity periods are presented. Note the box represents the range between the 25 <sup>th</sup> and 75 <sup>th</sup> percentiles, the blue line is the median (50 <sup>th</sup> percentile), the whiskers represent the 5 <sup>th</sup> and 95 <sup>th</sup> percentiles and the points above/below the whiskers represent the top/bottom 5% of values.....	154
Figure 65 Comparison of PM <sub>10</sub> and PM <sub>2.5</sub> measurement methods employed during the HF study. Lines represent 1:1 agreement. (Left panel) (blue) 24-hour average PM <sub>10</sub> by low-volume Derenda sampler with gravimetric mass determination versus 24-hour average of continuous PM <sub>10</sub> measurement by FIDAS light scattering method (R2 = 0.94). (red) Multi-day integrated average PM <sub>10</sub> by low-volume Microvol sampler with gravimetric mass determination versus FIDAS PM <sub>10</sub> integrated average over the same sample duration as Microvol (R2 = 0.97). (Right Panel) 24-hour average of continuous PM <sub>10</sub> measurements by E-Sampler light scattering technique with gravimetric mass correction versus 24-hour average of continuous PM <sub>10</sub> measurement by FIDAS light scattering method (R2 = 0.84).....	169
Figure 66 Ion balance for the ion chromatography measurements with the anions and cations .	171
Figure 67 Comparison of chloride ion (Cl <sup>-</sup> ) concentrations determined by ion chromatography and elemental chlorine (Cl) concentrations determined by ion beam analysis.....	172
Figure 68 Scatter plot of titanium versus aluminium .....	173
Figure 69 Scatter plot of silicon versus aluminium.....	173
Figure 70 Scatter plot showing the strong linear relationship between magnesium and sodium concentrations .....	174
Figure 71 Scatter plot showing that for a given sodium concentration, the observed chloride concentrations are always lower than for fresh sea salt (Cl <sup>-</sup> /Na <sup>+</sup> = 1.80).....	174

Figure 72 Scatter plot showing the strong linear relationship between nss sulfate and ammonium concentrations .....	175
Figure 73 Scatter plot of mannosan versus levoglucosan in the PM <sub>10</sub> measured during the study	175
Figure 74 Time series plot of levoglucosan in the PM <sub>10</sub> measured during the study .....	176
Figure 75 Time series plot of arabitol and mannitol in the PM <sub>10</sub> measured during the study.....	176
Figure 76 Scatter plot of gravimetric mass versus reconstructed chemical mass in the PM <sub>10</sub> measured during the study .....	177
Figure 77 EPA PMF diagnostic tables.....	182
Figure 78 Scatter plot of 24-hour PM <sub>10</sub> concentrations from the gravimetric mass determination and the reconstructed mass from the PMF solution.....	182

# Glossary

## Units of measurement

ha	hectare, unit of area equal to 10 000 m <sup>2</sup> , or approximately 2.47 acres. There are 100 hectares in one square kilometre.
µg m <sup>-3</sup>	micrograms per cubic metre (1 microgram = one millionth of a gram)
ng m <sup>-3</sup>	nanograms per cubic metre (1 nanogram = 1 billionth of a gram)
ppm	parts per million by volume
ppb	parts per billion by volume
l min <sup>-1</sup>	litres per minute
ml min <sup>-1</sup>	millilitres per minute
Bqm <sup>-3</sup>	Becquerel per cubic metre, a unit of radioactivity
µm	micrometre (1 micrometre = 1 millionth of a metre)

## Nomenclature

Aldehyde	A class of oxygenated volatile organic compounds
Ambient air	Outdoor air
Bioaerosols	Biological aerosols which can include living and non-living components of biological organisms (animals, plants, fungi, lichen, microorganisms), including spores and pollens.
Biomass burning	The combustion or burning of any biomass e.g. trees, grasses, agricultural waste etc
BTX	Benzene, toluene, xylenes (a subset of VOCs)
Coal Seam Gas (CSG)	A type of natural gas, composed primarily of methane, extracted from coal seams
Detection limit	The lowest reliably measurable concentration of a pollutant for a particular analytical technique
Flowback	Following hydraulic fracturing, the target coal seams which have become pressurised, may be allowed to depressurise by opening a discharge valve on the wellhead, which allows the well to flowback fluid to surface.

Flowback fluids	Flowback fluids are fluids that are returned to the surface via the well directly after hydraulic fracturing during flowback. These fluids may contain HF fluids, groundwater from the coal seam, and coal seam gas.
Gas processing facility (GPF)	A facility which compresses and dries gas
Ground water	Refers to water present beneath the earth's surface in rock formations and soil pore spaces.
Hydraulic Fracturing (HF)	a well stimulation process that is used to increase the flow of gas and water from a gas well. HF involves the high pressure injection of a large volume of fluids into a well in order to fracture targeted coal seams and open pathways for gas and fluids to flow into the well.
Hydraulic Fracturing Fluids	HF fluids are predominantly water and proppant (~ 97 - 98%) with a small amount of chemical additives
Isowipes	Alcohol (isopropanol) wipes
Kimwipes	Lint free tissues
pH	A scale used to assess the acidity or alkalinity of a solution
Proppants	Solids, usually sand, treated sand or manufactured ceramic material, added to hydraulic fracturing fluids in order to prop open the fractures in the target coal / shale seam induced by the hydraulic fracturing treatment.
Geogenic	Of geological origin
Surface water	Surface water refers to water that collects on the surface of the planet and includes rivers, lakes, wetlands, oceans.
Tracer	A gas or particle measurement used as a proxy for other atmospheric constituents not directly measured or used to indicate the likely impact of a specific pollution source.

## Abbreviations

ANSTO	Australian Nuclear Science and Technology Organisation
AQMS	Air Quality Monitoring Station
AQI	Air Quality Index
ARPANSA	Australian Radiation Protection and Nuclear Safety Agency
BTX	A subset of VOCs including benzene, toluene and xylenes
CO	Carbon monoxide
CO <sub>2</sub>	carbon dioxide

CSG	Coal seam gas
CSIRO	Commonwealth Scientific and Industrial Research Organisation
DNPH	Dinitrophenylhydrazine
EPP	Environment Protection Policy- Queensland
CH <sub>4</sub>	Methane
GISERA	Gas Industry Social and Environmental Research Alliance
HF	Hydraulic Fracturing
lpm	Litres per minute
NEPM	National Environment Protection Measure
NO <sub>x</sub>	Oxides of nitrogen
NO <sub>2</sub>	Nitrogen dioxide
NPI	National Pollutant Inventory
O <sub>3</sub>	Ozone
PAH	Polycyclic aromatic hydrocarbons
PM <sub>2.5</sub>	Particulate mass with an aerodynamic diameter of < 2.5 µm
PM <sub>10</sub>	Particulate mass with an aerodynamic diameter of < 10 µm
QAEHS	Queensland Alliance of Environmental Health Sciences
Texas ACMV	Texas Commission on Environmental Quality Air Monitoring Comparison Values
TSP	Total suspended particles
VOC	Volatile organic compound

# Acknowledgements

This report was supported by the Gas Industry Social and Environmental Research Alliance (GISERA). GISERA is a collaboration between CSIRO, Commonwealth and state governments and industry established to undertake publicly-reported independent research. The purpose of GISERA is to provide quality assured scientific research and information to communities living in gas development regions focusing on social and environmental topics including: groundwater and surface water, greenhouse gases and air quality, biodiversity, land management, the marine environment, and socio-economic impacts. The governance structure for GISERA is designed to provide for and protect research independence and transparency of research. Visit [gisera.csiro.au](https://gisera.csiro.au) for more information about GISERA's governance structure, projects and research findings.

We gratefully acknowledge Xianyu (Fisher) Wang and team from the Queensland Alliance for Environmental Health Sciences (QAEHS) and Armand Atanacio and team from the Australian Nuclear Science and technology Organisation (ANSTO) for their assistance in sample media preparation and analysis.

The field work component of this project would not have been possible without the cooperation of the landholders who hosted this study. We also gratefully acknowledge assistance from Origin Energy and the field operations team at Origin Energy's Reedy Creek gas processing facility for facilitating access to the study site.

## Executive summary

Hydraulic fracturing (HF) is a well stimulation process that is used to increase the flow of gas and water from a gas well. HF involves the high-pressure injection of a large volume of fluids and solids, with minor chemical additives, into a well in order to fracture targeted coal seams and open pathways for gas and fluids to flow into the well. The potential impact on air, surface water, groundwater and soil of HF operations in coal seam gas (CSG) production are of concern to communities living in gas development regions, particularly given the lack of high quality publicly available data on air, water and soil impacts.

The GISERA Air, Water and Soil Impacts of Hydraulic Fracturing: Phase 2 (W.12) project aims to address the concern around the lack of available data on air, water and soil impacts by carrying out a comprehensive investigation of air, water and soil quality during HF at a site in the Surat Basin in Queensland (Figure 1). It continues on from the Phase 1 project (W.11) during which comprehensive peer-reviewed study designs were developed for air quality (Dunne et al., 2017) and water and soil quality (Apte et al., 2017) studies.

This report presents the air quality data measured during well pad development operations (including HF) at a 600 ha field containing 10 CSG wells that underwent HF in August-October 2017.

The ambient air quality measurement program was designed to achieve three main objectives

- **Objective 1-** Provide comparisons of the air quality observed at a HF site with Australian federal and state air quality objectives, as well as data from other air quality studies undertaken in areas not directly impacted by HF operations both within the Surat Basin and in other locations in Australia.
- **Objective 2-** Quantify changes in air pollutant levels above background that occur during HF operations.
- **Objective 3-** Provide information on the contribution of HF and non-HF related sources of air pollutants to local air quality at the selected study site.

Ambient air quality is determined by pollutants emitted into the atmosphere as well atmospheric transport, mixing, transformation, and removal processes which are heavily influenced by meteorological variables. An assessment of meteorological data collected at the nearest Bureau of Meteorology (BoM) weather observation site (at Roma) and measured by instruments at several locations within the HF field showed that meteorological variables were broadly consistent between the BoM site and the locations measured at the HF field. Meteorological conditions observed at the study site were also typical of the wider region over the study period and the meteorology at the study site in 2017 was consistent with the longer-term climate based on the Roma BoM data. Sampling occurred under a variety of different meteorological conditions typical of the changing seasons between July and November.

While the primary aim of the sampling program was to provide measurements to assess the impact of HF on air quality, other well site activities in addition to HF occurred during the measurement period including drilling and well completion.

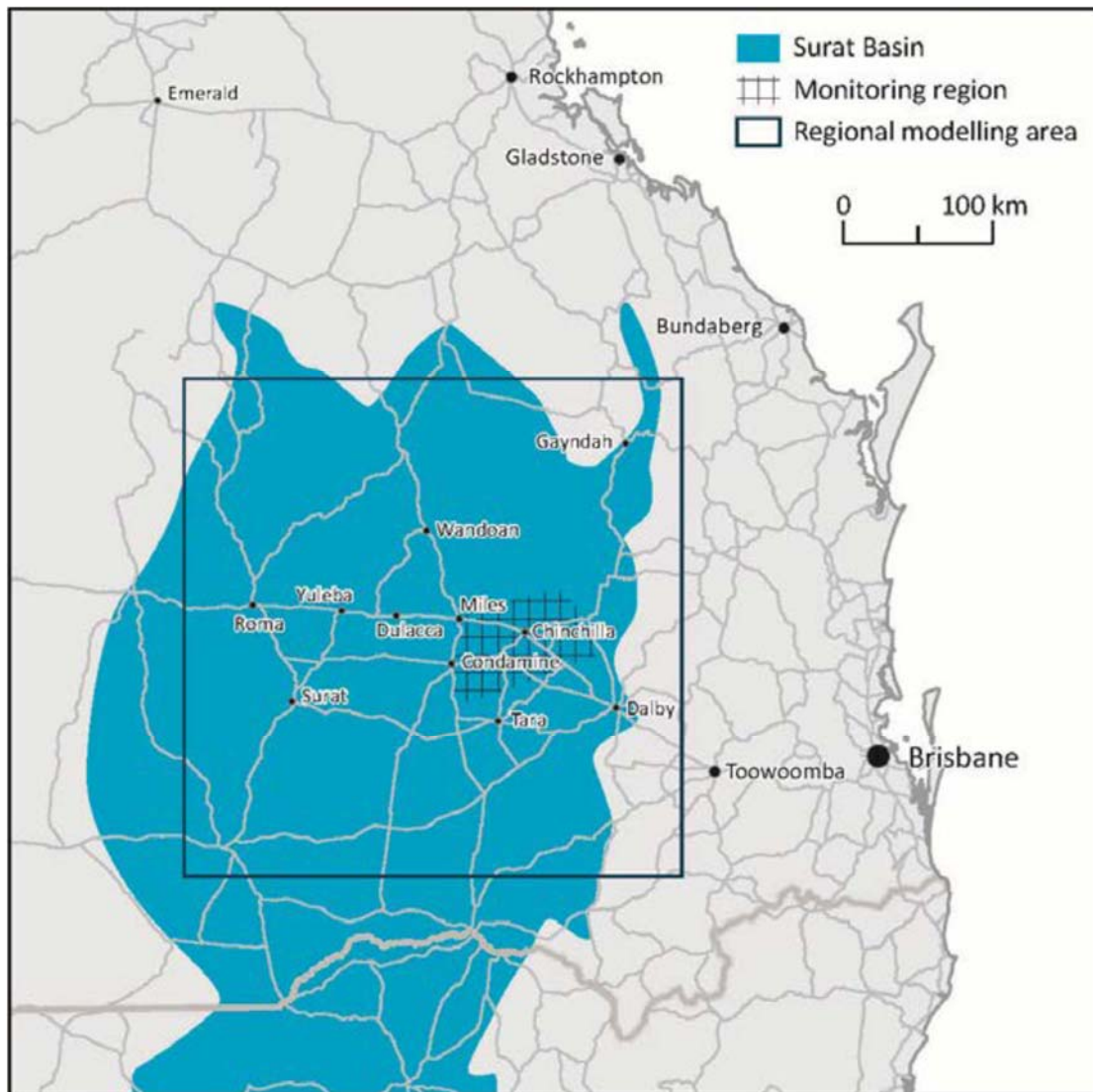


Figure 1 Surat Basin study region. The site of the study presented here was ~ 35 km North of Yuleba. The Surat Basin Ambient Air Quality Study Monitoring area in the Miles Condamine region is also shown. (Source Lawson et al 2017).

In relation to the study objectives, the data presented in this report showed that:

**Objective 1** - with the exception of a few, infrequent high airborne particle concentrations, the levels of atmospheric pollutants were well below relevant air quality objectives for the entire duration of the study period. The range of concentrations observed at the HF study site, including occasional exceedances of PM<sub>10</sub> and TSP, were not different to those observed at other sites in the Surat Basin or other locations in Australia that were not directly impacted by HF activity.

**Objective 2** - short term increases in the concentrations of NO<sub>2</sub>, CO, PM<sub>10</sub>, PM<sub>2.5</sub>, TSP, BTX and formaldehyde above background were associated with well development activities in this study. These impacts occurred at levels below air quality objectives, with the exception of infrequent dust events.

Well development activity was not associated with measurable enhancements in O<sub>3</sub>, SO<sub>2</sub>, mercury, radon and methane.

**Objective 3-** the dominant sources of air pollutants in the background atmosphere at the HF study site were:

- Biomass burning (NO<sub>2</sub>, CO, formaldehyde, BTX, PM<sub>2.5</sub>);
- Regional transport of pollutants from industry and agriculture (NO<sub>2</sub>, CO, ammonium sulfate aerosol, nitrate aged sea salt aerosol);
- Secondary production in the atmosphere (O<sub>3</sub>, formaldehyde, nitrate aged sea salt aerosol)
- Natural sources (sea salt, biological aerosol).

The data presented showed that in addition to occasional high airborne dust events associated with the movement of vehicles and equipment on unsealed roads, emissions from diesel powered vehicles and equipment on site during well development also contributed to small increases above background in NO<sub>2</sub>, CO, PM<sub>2.5</sub>, formaldehyde, BTX, and PAHs which were still well within relevant ambient air quality objectives. Impacts on air quality associated with well development were short term (hours to days) and were transient within gas development regions as drilling, HF and well development operations moved from well site to well site.

Analysis of limited data of the composition of HF fluids, drilling fluids, CSG and flowback/produced waters showed these HF-specific sources did not contain high levels of contaminants which may potentially impact air quality, or they were only present in trace amounts, suggesting that direct emissions of pollutants to the air from these HF-specific sources was unlikely to have contributed significantly to airborne concentrations. It is important to note that accidental or uncontrolled releases (spills, leaks) of HF fluids and CSG were not observed during this study and the impact on air quality of these events was not assessed.

In summary, this is the first comprehensive study of the impact of HF on air quality in an Australian onshore gas field and provides important information about the concentrations and potential sources of air pollutants associated with well development activities. The data generated in this study will be made publicly available on the CSIRO data access portal in late 2019. This report and the data provided will assist the assessment of human health risks from exposures via ambient air (NICNAS 2017c) including the GISERA health study, Keywood et al., (2018), and other studies on the environmental and health impacts of CSG development in Australia. The data also provides a useful resource for policy makers, landholders, and other stakeholders to inform decision making around future well development in the region and to inform improvements in industry practice.

# 1 Introduction

Hydraulic fracturing (HF) is a well stimulation process that is used to increase the flow of gas and water from a gas well. HF involves the high pressure injection of a large volume of fluids into a well in order to fracture targeted coal seams or oil shales so that pathways open for gas and fluids to flow into the well. The fractures created are kept open by solids called proppants, usually sand, which are added to the injected fluids.

In the case of coal seam gas (CSG) extraction by HF, the injected fluids are predominantly water and proppant (~ 97 – 98 %) with a small amount of chemical additives used to optimise the HF fluid performance and enhance well production. HF can involve the injection of several hundred thousand to over a million litres of fluids per well (CSIRO , 2015), and while chemical additives make up a small fraction (~2 – 3 %), there may be 5000 to greater than (>) 10 000 litres of chemical additives stored, mixed and injected at each well pad. The general classes of chemicals used and their application are:

- **Water** – major component of HF fluids used to fracture the coal seam when injected under high pressure. Bore water, surface water or groundwater previously extracted from coal seams is often used;
- **Proppant** – Props open fractures in coal seam once the high pressure fluid is removed. Typically sand of varying mesh sizes are used;
- **Water conditioning** – includes controls for microbial growth using biocides (e.g. 2-methyl-2h-isothiazol-3-one, 5-chloro-2-methyl-2h-isothiazolol-3-one); pH control (e.g. – hydrochloric acid).
- **Clay management** – to prevent swelling and or migration of clays into fluid stream. Potassium chloride commonly used;
- **Corrosion inhibitor** – to prevent corrosion of well casings and equipment e.g. gelatines;
- **Fluid viscosity management** – to control viscosity of fluids. For example, guar gum is used to form linear gels that hold the proppant in suspension enabling its spread through fractures. More viscous, crosslinked gels are formed by addition of formulations often containing borate salts, ethylene glycol, and potassium hydroxide. Once the desired proppant has been placed, gel breakers such as ammonium peroxydisulfates and nitroethanol are added to reduce viscosity in order to maximise recovery of HF fluids during flowback.

Once the required volumes of fluid have been pumped into the well and fracturing has taken place, the coal seam is depressurised and the fluids are allowed to flowback to the surface via the well. Initially flowback fluid will contain a mixture of HF fluids, proppant and groundwater from the coal seam. The flowback fluids may also contain a number of contaminants mobilised from the coal seam during HF activities. These geogenic contaminants include trace elements (e.g. arsenic, manganese, barium, boron and zinc), radionuclides (e.g. isotopes of radium, thorium, and uranium) and organic compounds such as hydrocarbons, and phenols (Apte et al., 2017, Schinteie et al., 2015). When geogenic contaminants are mobilized in fluids there is a potential for an emission to the atmosphere (Field et al., 2014).

At the surface flowback fluids are stored on site either in large (~30 000 – 80 000 L) storage tanks, in on-site ponds, or captured directly at the wellhead and removed by a gathering network and

transferred to a water treatment facility. Flowback occurs over several hours to days and ends once the majority of solids have cleared from the fluids. Overall, the handling and storage of HF fluids, flowback fluids and CSG at the surface will determine the impact of HF activities on air quality.

A literature review (Keywood et al., 2017) conducted as part of the air quality component of the project identified potential sources of air pollutants associated with HF and a conceptual model of the potential pathways of pollutants from the source to the atmosphere was developed (Figure 2) to inform the development of the study design.

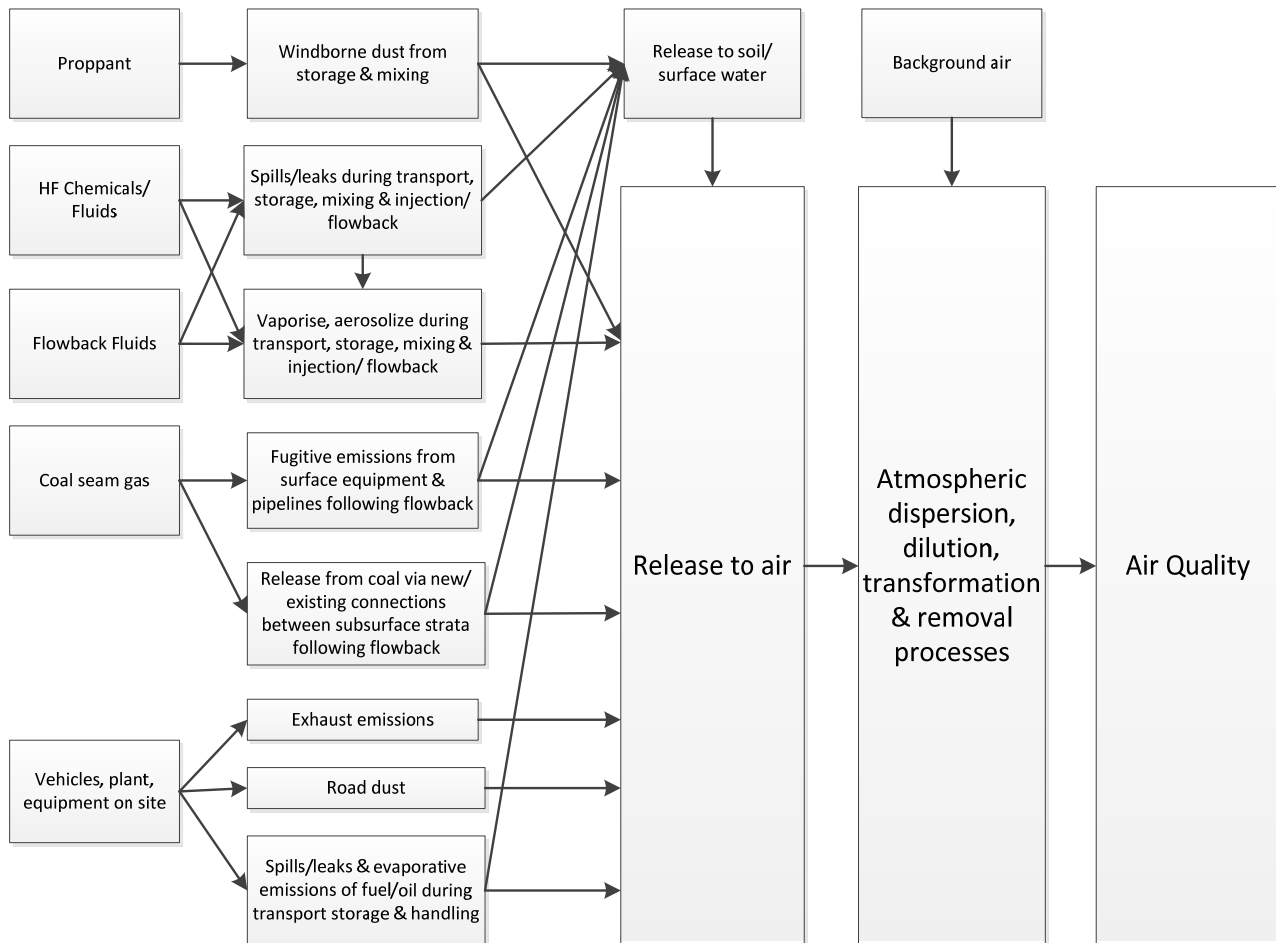


**Figure 2 Conceptual model for the potential pathway of pollutants from the source to the atmosphere (from Keywood et al., 2017).**

In addition to air pollutants emitted from HF and flowback fluids, emissions will also occur from equipment and vehicles on site including diesel exhaust emissions, evaporative fuel emissions, and road dust.

The potential impacts on air, surface water, groundwater and soil of HF operations in coal seam gas production are of concern to communities living in gas development regions. Community concerns centre on disclosure of the nature and type of chemicals used in the HF operations; potential enhanced

mobilization of geogenic contaminants (e.g. organic compounds, radon, mercury) from the coal seam; the environmental fate of HF chemicals and geogenic contaminants; and the potential for impacts on human health and the environment (Cham and Stone 2013).

An Australian Government assessment of chemicals used in coal seam gas extraction in Australia identified 113 chemicals used in drilling and HF during the period 2010 – 2012 (NICNAS 2017a), 44 of which were determined to be of low concern for human health and the remaining 69 chemicals were identified as requiring further assessment (NICNAS 2017b). Hazard and exposure assessments for these 44 chemicals found that:

- *No Australian information is available on the concentrations of drilling and hydraulic fracturing chemicals in the atmosphere and dust / soil in close proximity to coal seam gas extraction activities;*
- *More monitoring data on ambient air emissions from CSG developments would assist the assessment of human health risks from exposures via ambient air (NICNAS 2017c).*

The GISERA Air, Water and Soil Impacts of Hydraulic Fracturing: Phase 2 (W.12) project addresses some of these concerns and gaps by carrying out a comprehensive investigation of air, water and soil quality during HF at a site in the Surat Basin in Queensland. It continues on from the Phase 1 project (W.11) during which comprehensive peer-reviewed study designs were developed for air quality (Dunne et al., 2017) and water and soil quality (Apte et al., 2017) studies.

The ambient air quality measurement program was designed to achieve three main objectives

- **Objective 1-** Provide comparisons of the air quality observed at a HF site with Australian federal and state air quality objectives, as well as data from other air quality studies undertaken in areas not directly impacted by HF operations both within the Surat Basin and in other locations in Australia.
- **Objective 2-** Quantify changes in air pollutant levels above background that occur during HF operations.
- **Objective 3-** Provide information on the contribution of HF and non-HF related sources of air pollutants to local air quality at the selected study site.

This report presents the air quality data measured during well pad development operations (including HF) at a 600 ha field containing 10 CSG wells that underwent HF in August-October 2017. The summary of the measurement program was provided in a previous report (Dunne et al., 2017). In this report the air quality data are discussed in relation to Australian federal and state air quality objectives and compared to data collected in other Australian locations not directly impacted by HF during the study period thus providing information on the influence of HF at the measurement sites.

## 1.1 Out of Scope

The scope of the study described here does not provide the following:

**A formal risk assessment:** Prior to commencing HF activities as part of their Environmental Authority Permit, companies must update the stimulation risk assessment in their Environmental Management Plan related to HF “to ensure that stimulation activities are managed to prevent environmental harm

and meet the additional requirements within this environmental authority”. The study described here does not provide an assessment of risk.

**An assessment of impacts on human health:** This study did not determine the impacts of HF on human health. Instead the data collected in this study were compared with federal, state and other air quality objectives determined to protect human health and the environment. The data from the study will be made publicly available for potential use in studies specifically targeting the impact of CSG activities on human health (GISERA 2018).

**An assessment of representativeness and scalability:** The study presented here is specific to HF activity being carried out at the sites identified. The representativeness of this study, and the scalability of data to other well sites in the Surat Basin or other locations will depend on a number of factors including the representativeness of the HF processes employed, underlying geology, structure of the coal seams, well depths as well as meteorology etc.

## 2 Measurement methods

### 2.1 Target air pollutants and relevant air quality objectives

The study design developed for assessment of the impact of HF on air quality (Dunne et al., 2017) identified a list of key pollutants to be targeted as part of the sampling program and their potential HF related sources. The target air pollutants, their potential HF-related sources and associated air quality objectives are listed in Table 1.

Air quality is assessed by comparing the measured pollutant concentrations against federal and state air quality objectives which are designed to protect human health, wellbeing and the environment.

Air quality criteria relevant to this report include:

- National Environment Protection (Ambient Air Quality) Measure – 2016. The pollutants to which this NEPM measure applies are nitrogen dioxide (NO<sub>2</sub>), carbon monoxide (CO), ozone (O<sub>3</sub>), sulphur dioxide (SO<sub>2</sub>), particulate mass < 2.5 µm diameter (PM<sub>2.5</sub>), and < 10 µm diameter (PM<sub>10</sub>);
- National Environment Protection (Air Toxics) Measure – 2011. The pollutants to which this NEPM measure applies are benzene, toluene, xylenes, formaldehyde and benzo[a]pyrene as a marker for polycyclic aromatic hydrocarbons (PAHs);
- Queensland Environmental Protection (Air) Policy– 2008. The Queensland EPP (2008) includes all air pollutants and air toxics prescribed in the NEPM along with total suspended particulates (TSP) and 18 other organic and inorganic pollutants, including mercury, 4 organic gaseous pollutants and 4 compounds which may be present in particulate matter (PM). No recognised Australian 24-hour ambient air objective exists for total TSP and the 24-hour air quality objective used here is based on the New Zealand Ministry for the Environment’s nuisance trigger level of 60 µg m<sup>-3</sup> for high sensitivity areas (MFE 2016) , as recommended by Queensland’s Department of Environment and Science (DES);

- Australian Radiation Protection and Nuclear Safety Agency (ARPANSA) Radiation Recommendations for Limiting Exposure to Ionizing Radiation (ARPANSA 2002) (Guidance note [NOHSC:3022(1995)]). Provides recommended action levels for radon-222 concentration in air for households and workplaces.

Australian federal or state ambient air quality objectives are not available for many of the volatile organic compounds (VOCs) expected to be measured in this study. In the absence of Australian objectives, international objectives that covered the range of VOCs measured in this study have been consulted, in particular:

- Texas Commission on Environmental Quality Air Monitoring Comparison Values (ACMV) and Effects Screening Levels (ESLs). The ACMV and ESL values are “chemical specific air concentrations set to protect human health and welfare”. Where ACMV values were not available for a specific compound the appropriate ESL was used. For details on the difference between ACMVs and ESLs the reader is referred to TCEQ (2016a) and TCEQ (2016b).

**Table 1 Target air pollutants, their potential HF-related sources and associated air quality objectives. See Glossary for definition of acronyms**

Pollutant	Ambient Air Quality Standard			Potential HF Activity Sources
	Averaging Period	Max Concentration	Relevant Standard	
Nitrogen dioxide	1-hour 1 year	0.12 ppm 0.03 ppm	NEPM (2016) EPP (2008)	Exhaust from diesel powered equipment and vehicles
Sulphur dioxide	1-hour 1 day 1 year	0.20 ppm 0.08 ppm 0.02 ppm	NEPM (2016) EPP (2008)	
Carbon Monoxide	8-hour	9 ppm	NEPM (2016) EPP (2008)	
Ozone	1-hour 4 h	0.10 ppm 0.08 ppm	NEPM (2016) EPP (2008)	Secondary pollutant- No direct emissions. Product of reactive processes in air between VOCs and oxides of nitrogen (NO <sub>x</sub> )
Total Suspended Particles (TSP)	24-hour	nuisance trigger level 60 µg m <sup>-3</sup> for high sensitivity areas	MFE (2016)	Windborne soil, sand, road dust. Mechanical generation of PM during mixing and storage of HF fluids and flowback.
Particles <10 µm PM <sub>10</sub>	1 day 1 year	50 µg m <sup>-3</sup> 25 µg m <sup>-3</sup>	NEPM (2016) EPP (2008)	Windborne soil, sand, road dust. Mechanical generation of PM during mixing and storage of HF fluids and flowback.
Particles <2.5 µm PM <sub>2.5</sub>	1 day 1 year	25 µg m <sup>-3</sup> 8 µg m <sup>-3</sup>	NEPM (2016)	Vehicle exhaust and other combustion emissions. Secondary pollutant- No direct emissions. Product of reactive processes in air between gases or between gases and other particles.
Arsenic	Annual	6 ng m <sup>-3</sup>	EPP (2008)	Potential components of PM
Manganese	Annual	0.16 µg m <sup>-3</sup>	EPP (2008)	
Nickel	Annual	20 ng m <sup>-3</sup>	EPP (2008)	

Pollutant	Ambient Air Quality Standard			Potential HF Activity Sources
Sulfate	24-hour	27 $\mu\text{g m}^{-3}$	EPP (2008)	
Formaldehyde	24-hour	0.04 ppm	NEPM (2011) EPP (2008)	Exhaust from diesel powered equipment & vehicles  Secondary pollutant -Product of reactive processes in atmosphere between VOCs and NOx  Minor component or secondary product of CSG and Flowback Fluids
Benzene	1 year	0.003 ppm	NEPM (2011) EPP (2008)	Exhaust and Evaporative emissions from vehicles and equipment  Minor components of CSG and Flowback Fluids (Day et al., 2016)
Toluene	24-hour 1 year	1 ppm 0.1 ppm	NEPM (2011) EPP (2008)	
Xylenes	24-hour 1 year	0.25 ppm 0.20 ppm	NEPM (2011) EPP (2008)	
Styrene	1 week	0.06 ppm	EPP(2008)	
benzo(a)pyrene as a marker of Poly aromatic hydrocarbons (PAHs)	1 year	0.3 $\text{ng m}^{-3}$	NEPM (2011) EPP (2008)	Exhaust from diesel powered equipment & vehicles  Minor components of CSG and Flowback Fluids
1,2-Dichloroethane	24-hour	0.17 ppm	EPP (2008)	unknown
Tetrachloroethylene	Annual	0.036 ppm	EPP (2008)	unknown
Mercury	1 year	1.1 $\mu\text{g m}^{-3}$	EPP (2008)	Minor components of CSG and Flowback Fluids
Radon		Households: 200 $\text{Bq m}^{-3}$ Workplaces: 1000 $\text{Bq m}^{-3}$	ARPANSA (2002)	Minor component of CSG
Hydrogen sulphide	24-hour 90 days	0.110 ppm 0.014ppm	EPP (2008) WA DOH (2009)	Minor component of CSG
Methane	na	na	na	Major component of CSG

### 2.1.1 Air Quality Index

The data for pollutants included in the ambient air NEPM (2016) (CO, NO<sub>2</sub>, O<sub>3</sub>, SO<sub>2</sub>, PM<sub>2.5</sub>, PM<sub>10</sub>) and TSP included in the Qld EPP for Air (2008) were converted into air quality index (AQI) values, which express the observed concentration of an air pollutant as a percentage of the relevant air quality objective value. The index value was calculated from the ratio of the pollutant concentration to the relevant air quality objective expressed as a percentage;

$$\text{Air quality index value (\%)} = \frac{\text{Pollutant concentration}}{\text{Air quality objective value}} \times 100$$

The AQI values were then graded into one of five qualitative air quality categories ('very good' 0–33, 'good' 34–66, 'fair' 67–99, 'poor' 100–149, and 'very poor' 150+) as shown in Table 2. The AQI approach is commonly used by state government agencies including the Queensland Government to report air quality so that it is easier for the general community to understand what the measured concentrations mean to air quality (Keywood et al., 2017). The proportion of time air pollutant levels fell into each of the five air quality index categories reported in Sections 4 – 5 and the circumstances that resulted in poor air quality conditions are discussed.

It is important to note that this report provides an assessment of air quality in the near vicinity of HF activities. When air pollutants are emitted during HF activities, they will undergo dilution by mixing with background air as they are transported away from the source. As such the levels of pollutants emitted, meteorological factors, and the capacity of the air in the region to add to, or dilute/remove the pollutants will determine the air quality experienced by nearby residents and communities.

**Table 2 Air Quality Index categories and their respective Index value ranges.**

AQI Categories	AQI value range (% of air quality objective value)	AQI Category Description (Source: Keywood et al 2016)
Very good	0 - 33	Air quality is considered very good, and air pollution poses little or no risk
Good	34 - 66	Air quality is considered good, and air pollution poses little or no risk
Fair	67 - 99	Air quality is acceptable. However, there may be health concerns for very sensitive people
Poor	100 - 149	Air quality is unhealthy for sensitive groups. The general population is not likely to be affected in this range
Very Poor	> 150	Air quality is unhealthy, and everyone may begin to experience health effects. People from sensitive groups may experience more serious health effects

## 2.2 Measurement sites

The study location was a farmland property of approximately 600 ha. Roma, the largest nearby population centre is located approximately 80 km to the SW. The property is predominantly flat, semi-arid open grassland with stands of native tree vegetation. Linked by Horse Creek Road, the township of Yuleba (population <200) lies approximately 35 km to the SSW of the study site (Figure 3).

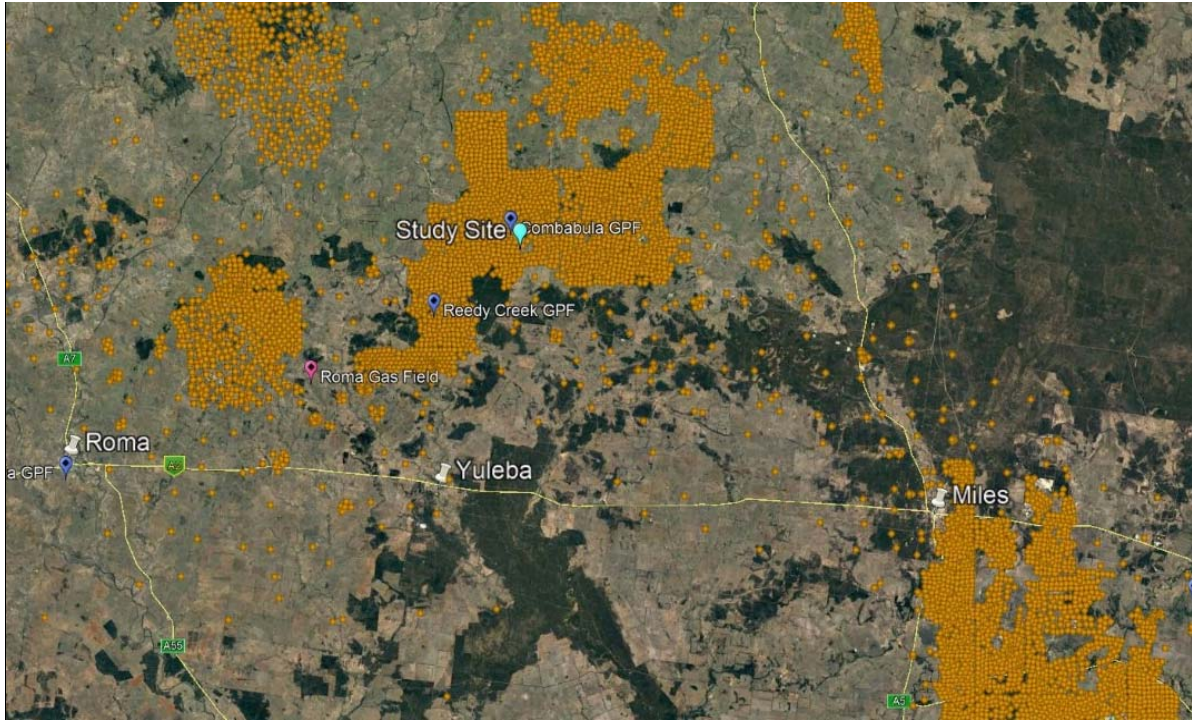


**Figure 3** The study site within the Roma–Yuleba region of the Surat Basin. The orange dots represent CSG wells. Source: Queensland Globe (2019)

The property contains 10 coal seam gas wells, grid spaced at ~600 – 800 m intervals. The wells are operated by Origin Energy Resources Pty Ltd and were drilled and constructed in 2017 targeting the Walloon Coal Measures. All 10 wells underwent HF between September and October 2017. The location of the wells and the sampling locations are shown in Figure 4.

Two different types of air quality measurement systems were deployed in this study: two fixed air quality monitoring stations (AQMS) located at the northern and southern ends of the HF field, and five solar-powered air quality monitoring stations (Solar-AQMS), four of which were located adjacent to wells and one co-located with the South-AQMS. The North- and South-AQMS were located alongside two electricity sub-stations which provided the only available access to mains power necessary for the air conditioning and monitoring equipment within each of these enclosures. The North-AQMS was located adjacent to well COM 313 (Figure 5). The South-AQMS was located adjacent to a laydown yard which was a cleared area that contained a large above ground water tank used to store groundwater for HF sourced from a nearby bore. This area also served as a storage area for diesel refuelling tanks, trailers holding HF chemicals and proppant, trucks and equipment and the area experienced frequent truck traffic (Figure 6).

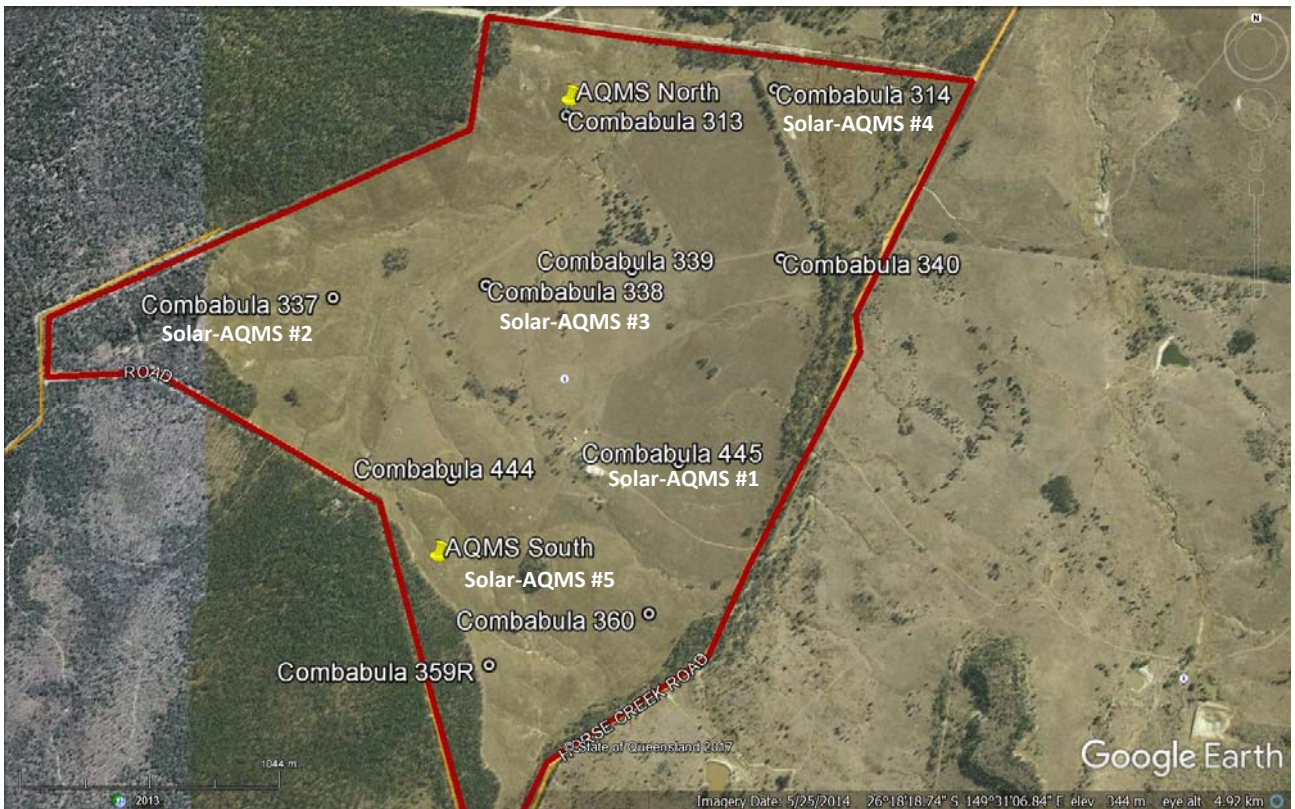


Figure 4 Map showing locations of wells that underwent HF (labelled by Well ID" Combabula ###), and the location of the North-AQMS and South-AQMS (yellow pins) and the well sites where the five solar powered air monitoring stations were also located (within 100 meters of the well pads). Source: Qld Globe (date)



Figure 5 North-AQMS with HF spread present at adjacent well (COM 313) in the foreground. The distance from the COM 313 to the North-AQMS was approximately 100 m.



**Figure 6 South-AQMS (right) with water storage tank, fuel storage tank and truck/equipment laydown area in the background. The distance from the laydown area to the South-AQMS was approximately 100 m.**

The locations of the measurement sites, as shown in Figure 4, were determined with consideration given to:

- Locating sites on the northern, southern, eastern and western sides of the property to provide measurements upwind and downwind of HF under variable wind conditions (wind direction data presented in Section 3);
- Locating one Solar-AQMS site adjacent to the South-AQMS site to provide validation of the Solar-AQMS instrumentation against higher-quality AQMS instrumentation;
- Locating sites in proximity to wells (within ~ 100 m of well pad boundary) in order to enhance the probability of capturing changes in air pollutant levels during HF operations;
- Compliance with AS/NZ S 3580.1.1:2016- Method for sampling and analysis of ambient air Part 1.1 Guide to siting air monitoring equipment.

### 2.3 HF activity and Sampling Timelines

The primary aim of the sampling program was to provide measurements to assess the impact of HF on air quality, however other well site activities in addition to HF occurred during the measurement period. The range of activities that occurred at the study site during sampling, included:

- **Drilling and well construction** – nine out of ten of the wells were drilled and constructed in 2017 with depths of 826 – 876 m, targeting the Walloon Coal Measures. Drilling took approximately 1- 3 days;
- **Well integrity testing** – down-hole survey of the well. This took approximately 24-hours;
- **Well casing perforation** – the well was perforated at target intervals using specialised explosive charges to create connection of the coal seam to the well. This took approximately 24-hours;
- **Well head changeover** – installation of a specialised HF well head. This took approximately 24-hours;

- **Site set-up** – HF operations required a number of pieces of equipment including above-ground water storage ponds, mixing units, high pressure pumps, coiled tubing unit to convey HF fluids down the well, crane, chemical and proppant storage trailers, flowback tanks, control vans. This took approximately 2 – 3 days;
- **Hydraulic Fracturing** – the injection of HF fluids (water, sand, chemicals) into targeted intervals at high pressure via the coiled tubing unit. This took approximately 1 – 3 days;
- **Well Completion** – the well was flowed back, production equipment installed in the well and connected to surface production equipment (pumps, separators, and pipelines). This took approximately 1-2 days.

Each of these activities required specialised rigs/equipment and during the measurement period it was common to observe several different activities occurring at different well pads at the same time. Consequently, the ambient air quality across the study site was likely to be impacted by multiple well-site activities and not exclusively HF.

For the purposes of this report, two distinct periods of well development are highlighted in the time series of the air pollutant data presented:

- Drilling - 26/7/2017 – 28/8/2017;
- Hydraulic Fracturing and Well Completion- 21/9/2017 – 2/11/2017.

A timeline of sampling and the timing of some key well site activities for the study period (Drilling, HF, and Well Completion) is shown in Table 3.

**Table 3 Timeline of sampling and well site activities for the measurement period July – December 2017. HF is Hydraulic Fracturing, WC is well completions**

	July 2017	August 2017	September 2017	October 2017	November 2017	December 2017
Well ID (Sampling Site)		Drilling 26/7 – 28/8/2017		Hydraulic Fracturing (HF) & Well Completion (WC) 21/9 – 2/11/2017		
COM 360		26/7 – 31/7		HF 21/9 – 22/9 WC 22/9 – 24/9		
COM 445 (Solar-AQMS #1)		31/7 – 3/8		HF 23/9 – 24/9 WC 27/9 – 29/9		
COM 340		3/8 – 6/8		HF 27/9 WC 29/9 – 30/9		
COM 313 (North-AQMS)		10/8 – 14/8		HF 6/10 – 7/10 WC 9/10 – 11/10		
COM 337 (Solar-AQMS #2)		14/8 – 18/8		HF 9/10 – 10/10 WC 11/10 – 13/10		
COM 338 (Solar-AQMS #3)		18/8 – 22/8		HF 11/10 WC 13/10 – 15/10		
COM 444		25/8 – 28/8		HF 12/10 – 13/10 WC 15/10 – 16/10		
COM 359R		<i>drilled 17/3 – 21/3 2016</i>		HF 14/10 WC 16/10 – 20/10		
COM 339		22/8 – 25/8		HF 16/10 – 19/10 WC 20/10 – 23/10		
COM 314 (Solar-AQMS #4)		6/8 – 10/8		HF 26/10 WC 1/11 – 2/11		
<i>Note: South-AQMS and Solar-AQMS Site 5 were co-deployed at a location adjacent to laydown yard and HF water storage tank, not directly adjacent to any wells</i>						
Sampling Activity						
Continuous sampling	19/7 – 24/11					subset of measurements ongoing at AQMS
Intensive sampling		7/8 – 19/8		15/9 – 29/10	subset of measurements until 21/11	

The sampling program consisted of two overlapping phases:

- **Continuous monitoring** at the North and South-AQMS sites which began in July 2017 and concluded in November 2017 with a subset of measurements ongoing until December 2017;
- **Intensive monitoring** phase which occurred for periods before, during and after HF activities commenced at co-located wells, involving both the North and South-AQMS and the five Solar-AQMS. The intensive monitoring phase comprised 56 days in which CSIRO scientists and technicians visited all six sampling locations daily to deploy and retrieve samples of gases and particulate matter (PM) collected on specialised sample media (filters, adsorbent tubes, cartridges), to undertake daily checks of continuous monitoring equipment. During this intensive monitoring phase CSIRO team members maintained written logs of the HF operations and other activities relevant to air quality that were occurring in the field during sampling.

## 2.4 Measurement systems

The sampling and analysis methods employed in this study provided measurements of six air pollutants listed in the NEPM for Ambient Air Quality (NEPM 2016) and all five of the NEPM Air Toxics (NEPM 2011), as well as mercury listed in the Queensland Government EPP (Air) Policy (Queensland EPP 2008), and radon listed in the ARPANSA recommendations (ARPANSA, 2002). Instruments were operated continuously, and integrated samples were collected for defined periods, on sample media that was subsequently analysed for their chemical composition in an analytical laboratory.

In this section we describe the instrumentation deployed at the North- and South-AQMS as well as the five Solar-AQMS sites. The large suite of instrumentation deployed in this study were operated by CSIRO along with partner research organisations including the Australian Nuclear Science and Technology Organisation (ANSTO), Macquarie University, University of Queensland and external contractors Ecotech (Brisbane, Queensland, Australia) and SGS-Leeder (Chinchilla, Qld). Details of the measurement program that was undertaken and data capture are provided in a previous report for this project (Dunne et al., 2018).

### 2.4.1 North and South-AQMS

The North-AQMS and South-AQMS were air-conditioned mobile laboratories provided by Ecotech Pty Ltd. These enclosures were purpose-built for housing high-quality, sensitive measurement systems and were complete with masts and inlets and required mains 240 V power supply.

The North-AQMS was comprised of two separate but co-located enclosures (Figure 7). One enclosure housed a suite of Ecotech operated instrumentation to measure CO, oxides of nitrogen

(as NO<sub>2</sub>, NO and NO<sub>x</sub>), O<sub>3</sub>, SO<sub>2</sub>, methane (CH<sub>4</sub>), carbon dioxide (CO<sub>2</sub>), particulate matter (TSP, PM<sub>10</sub>, PM<sub>2.5</sub>), and meteorology including wind speed and wind direction at 10 meters height and temperature, humidity, solar radiation, rainfall and barometric pressure at 10 meters and 2 meters. Details of the Ecotech operated instruments, their calibration and maintenance as well as QA/QC processes were provided in previous reports for this project (Dunne et al 2017, 2018a).

For measurements of gas phase species at the North-AQMS and South-AQMS, ambient air was drawn through a glass inlet ~3.5 m in length, into a common manifold via an inlet fan that provided ~20 litres per minute (lpm) of constant flow at low pressure, from which instruments drew their sampling flows via Teflon tubing by way of individual vacuum pumps. For measurement of particles, there was a separate inlet which contained a drying system designed to reduce the influence of moisture on particle size while preserving semi-volatile particles. The dryer used real-time ambient temperature and humidity measurements to dynamically adjust heating of the inlet tube to keep the relative humidity of the sampled air to less than 60%.

A second enclosure located at the North-AQMS housed CSIRO instrumentation including a proton transfer reaction mass spectrometer (PTR-MS) for continuous measurements of VOCs, and a sampling system that collected two 12-hour samples per day of VOCs on specialised sample media for analysis offline at CSIRO's laboratories in Aspendale, Victoria.

Also located outside at the North-AQMS were two particulate samplers, one collected PM<sub>10</sub> samples (particles with diameter ≤ 10 μm) from midnight to midday and the second collected samples from midday to midnight. These filter samples were analysed for gravimetric mass and elemental composition at ANSTO's laboratories at Lucas Heights, NSW and subsequently analysed for ionic composition and carbohydrates at CSIRO's laboratories in Aspendale, Victoria.



**Figure 7** Two enclosures at North-AQMS located adjacent to a well pad undergoing drilling.

The South-AQMS was comprised of a single AQMS enclosure housing a matching suite of Ecotech operated instrumentation to measure CO, oxides of nitrogen (as NO<sub>2</sub>, NO and NO<sub>x</sub>), O<sub>3</sub>, CH<sub>4</sub>, CO<sub>2</sub> and particulates (TSP, PM<sub>10</sub>, PM<sub>4</sub>, PM<sub>2.5</sub> and PM<sub>1</sub>) and meteorology including 10-metre wind speed and direction, 10-metre and 2-metre temperature, humidity, solar radiation, rainfall and barometric pressure. Instrumentation for the measurement of gaseous elemental mercury (operated by Macquarie University) was also located in the South-AQMS enclosure. Located outside at this site was a radon monitor operated by the Australian Nuclear Science and Technology Organisation (ANSTO) and a CSIRO sampler for the collection of polycyclic aromatic hydrocarbons (PAHs).

### 2.4.2 Solar-AQMS

Five solar-powered air quality monitoring stations (Solar-AQMS) custom built by CSIRO were deployed in this project (Figure 8). All instruments in the Solar-AQMS were operated by CSIRO. Each Solar-AQMS included an Ecotech Microvol PM<sub>10</sub> sampler for ~weekly integrated mass and chemical composition analysis, and a Met-One E-sampler for continuous PM<sub>2.5</sub> concentration measurement and ~weekly integrated mass and chemical composition analysis. The Solar-AQMS sites also contained sampling equipment for integrated 12-hour sampling of VOCs onto adsorbent tubes and 24-hour sampling of aldehydes onto DNPH (Dinitrophenylhydrazine) cartridges and a Lufft WS 500UMB Weather Sensor for the measurement of 2-metre wind speed and direction, air temperature, relative humidity and barometric air pressure.



Figure 8 Solar-AQMS #4 located adjacent to a well pad (COM 314) undergoing well perforation.

## 3 Meteorology

Ambient air quality is determined by the pollutants emitted into the atmosphere as well as by atmospheric transport, mixing, transformation, and removal processes which are heavily influenced by meteorological variables. For example, strong winds can result in higher levels of windborne dust that can be transported long distances whereas periods of rain will remove gas and particulate matter from the air via wet deposition to the surface.

The following section describes the meteorological data measured at the study site and places the observed meteorology into the context of long term measurements from the study region. This provides an assessment of how representative the weather and climatic conditions were during the study period. The meteorological conditions that affected levels of air pollutants as well as the fraction of observations that were downwind of HF operations will be discussed.

### **Regional Meteorology**

The nearest Bureau of Meteorology (BoM) weather observation station in the project area was located at Roma Airport (BOM Station No. 043091) where meteorological data has been collected since 1992. Temperature, rainfall and wind speed data from Roma Airport for the period 1992 – 2017 is presented in Table 4 to describe the overall climate of the region. This long term meteorology record shows the climate of the project area is characterised as sub-tropical with cool, dry, winter seasons (Apr-Sept) and hot, wet summers (Nov- Feb). Data from Roma Airport for the year 2017, coinciding with the study period (Jul – Dec), is also presented in Table 4 showing the temperature, rainfall and wind speeds were fairly typical in comparison to the long term averages.

Meteorological data from the North-AQMS located at the study site (Jul – Dec 2017) is also presented in Table 4. Based on the data from the two stations (Roma and North-AQMS) for each month of 2017, temperature and wind speed were consistent between the two sites suggesting that the meteorology at the Roma and the North-AQMS was similar during the study period. In addition, the temperature and wind speeds measured at the North-AQMS during the study for each month of 2017 were consistent with the longer term (1992-2017) temperatures and windspeeds measured at Roma suggesting that the meteorology at the North-AQMS during the study period was similar to longer term averages. Rainfall variability between Roma and the HF study site appears large, despite similar totals over the six months of data.

### **Local meteorology during the study period**

Meteorological parameters were measured at seven locations across the HF study site: one at the North-AQMS, one at the South-AQMS and one at each of the five Solar-AQMS sites. Daily average temperature, relative humidity, wind speed and direction are shown in Figure 9 for the seven sites. Daily rainfall was only measured at the North-AQMS and the South-AQMS and is also shown

in Figure 9. Coinciding with the transition from winter (Jun – Aug) to spring and summer (Sept-Dec) the 24-hour averaged temperature increased from  $\sim 10^{\circ}$  to  $\sim 30^{\circ}\text{C}$  with increasing rainfall and relative humidity towards the end of the campaign. A period of increased temperatures was observed during the second half of September 2017, with 24-hour averaged temperature also reaching close to  $30^{\circ}\text{C}$ . This was followed by an abrupt fall in average temperature on October 1<sup>st</sup> coinciding with a shift in the local weather, the arrival of thunderstorms and a steep increase in relative humidity.

Figure 10 shows wind roses summarising the frequency of wind speed (colour) and directions (angle) measured at the North and South-AQMS and the five Solar-AQMS. The plots show wind directions dominated by SW and NE winds at each site. Solar-AQMS #5 and the South-AQMS which were co-located, also both measured wind directions directly from the north and south. Measured wind speeds appear to be consistent across the sites with maximum speeds measured at the North-AQMS.

In Figure 11 the wind rose for each month measured at the North-AQMS are shown. Dividing the data between night time (20:00-08:00) and day time (08:00 – 20:00) periods highlights the prevalence of lower wind speeds at night compared to during the day. In addition, from July to November there was a clear shift from SW winds at the beginning of the campaign, during the winter months, to NE winds at the end of the campaign, as summer approached. As a consequence of this shift in the dominant wind direction, it is likely regional air pollutant sources to the SW would have had a greater impact on air quality at the study site during the winter months, and sources to the NE of the site would have had a greater influence during the summer months.

**Table 4 Summary of meteorology data from the BoM site at Roma and meteorology data from the North-AQMS at the study site.**

		Jan	Feb	Mar	Apr	May	Jun	Jul	Aug	Sep	Oct	Nov	Dec
<b>Temperature (°C)</b>													
Roma Airport 1992-2017	Daily min average	21	20	18	13	8	5	4	5	10	14	18	20
	Daily max average	34	33	31	28	24	20	20	22	26	29	31	33
Roma Airport 2017	Daily min average							5	3	9	16	15	20
	Daily max average							23	24	30	29	31	35
HF study site 2017	Daily min average	-	-	-	-	-	-	1	4	9	16	15	19
	Daily max average	-	-	-	-	-	-	23	24	29	27	29	33
<b>Rainfall (mm)</b>													
Roma Airport 1992-2017	Average total	65	86	60	27	24	29	18	23	29	44	59	84
Roma Airport 2017	Total	-	-	-	-	-	-	28	6	1	92	70	83
HF study site 2017	Total	-	-	-	-	-	-	0	6	0	85	112	49
<b>Wind speed (m/s)</b>													
Roma Airport 1992-2017	Average 9am	5.4	4.9	4.7	4.0	3.2	3.1	3.3	4.3	5.2	5.6	5.5	5.2
	Average 3pm	5.0	5.0	4.5	4.4	4.2	4.3	4.6	4.9	5.1	5.3	5.1	5.0
Roma Airport 2017	Average 9am							2.8	3.3	4.4	4.7	5.0	5.0
	Average 3pm							3.6	4.7	4.4	4.7	3.9	4.2
HF study site 2017	Average 9am	-	-	-	-	-	-	1.8	3.4	4.0	4.1	4.2	4.3
	Average 3pm	-	-	-	-	-	-	2.8	3.9	3.5	3.8	3.5	3.0

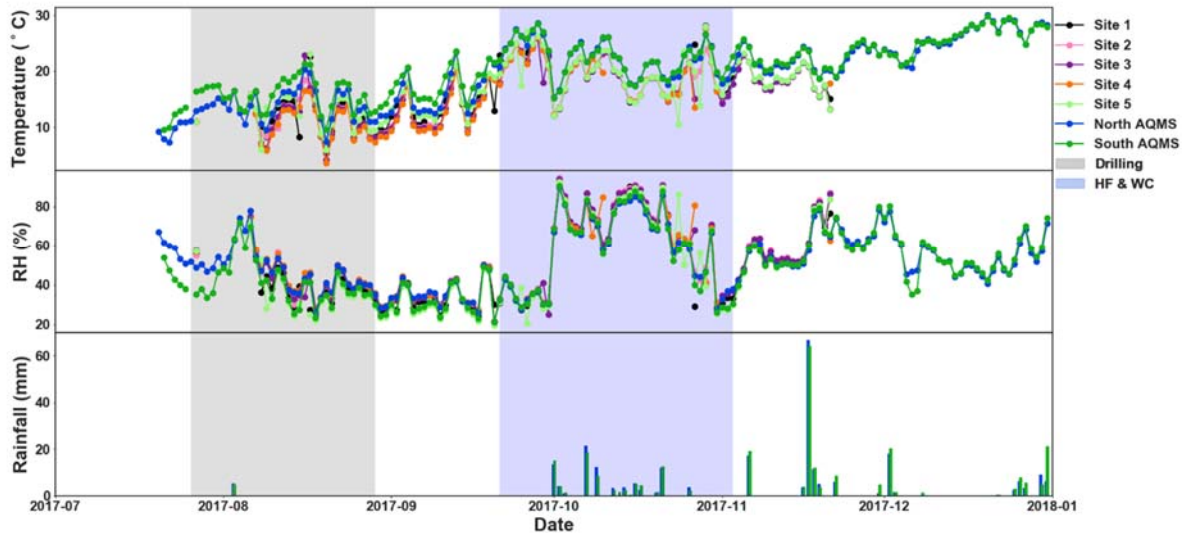


Figure 9 24-hour average temperature and relative humidity measured at 2m at the North and South-AQMS and the five Solar-AQMS sites and daily rainfall. Shaded areas represent periods of well development activity on the HF study site, including drilling, HF and well completion (WC).

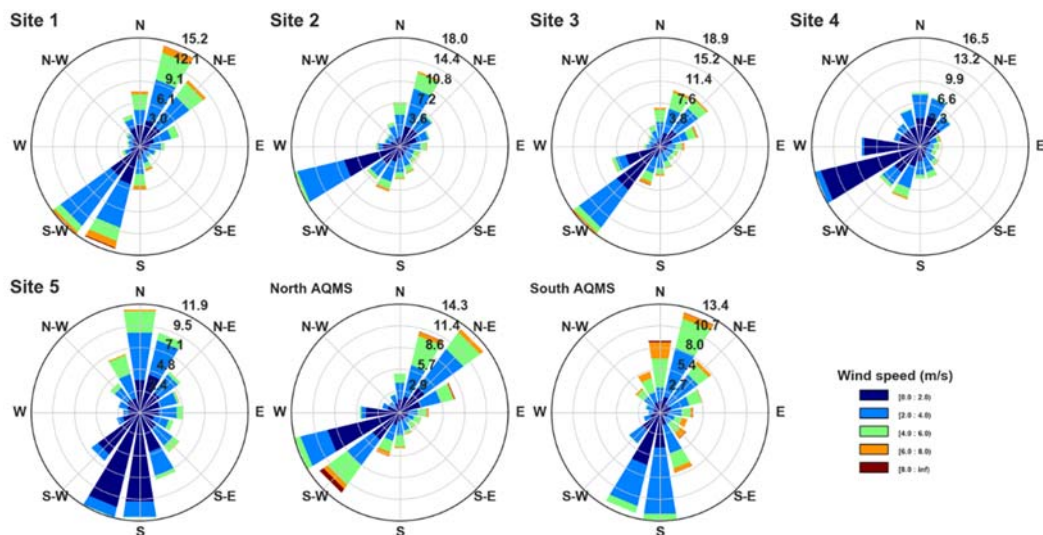
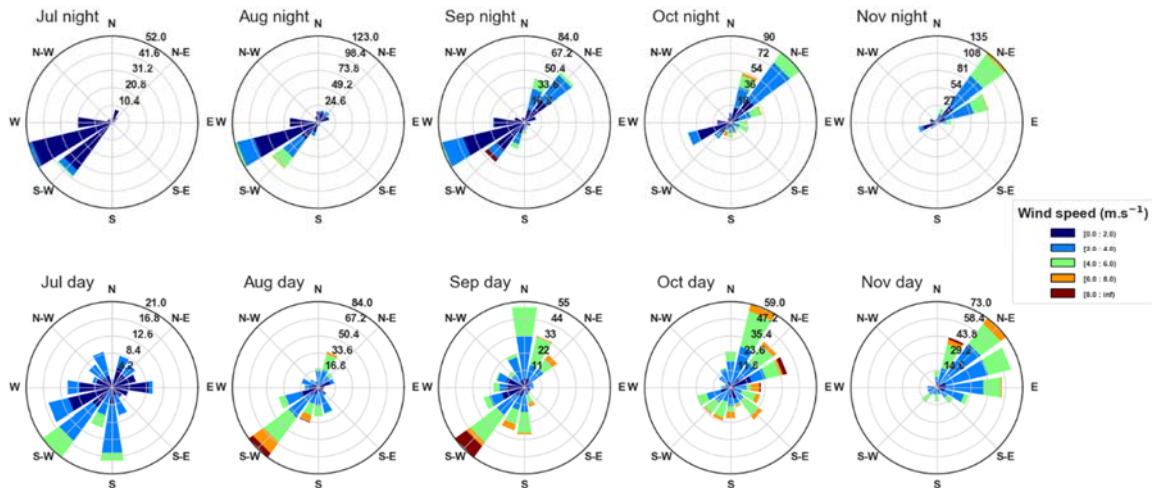


Figure 10 Wind roses summarising the frequency (length) of 5-minute average wind speed (colour) and direction (angle) measured at 2m height at the five Solar-AQMS sites and wind roses of the 1-hour average wind speed and direction measured at 10 m height at the North and South-AQMS for the entire study period (Jul- Nov 2017).



**Figure 11** Wind roses summarising the frequency (length) of average 1-hour wind speed (colour) and direction (angle) for the months of July to November 2017 measured at 10 m height at the North-AQMS, and separated between night time (20:00 – 08:00) and day time (08:00 – 20:00).

### 3.1.1 Data capture for air masses impacted by HF

Two important factors were identified that would influence the amount of time an air mass, impacted by HF and well completion activity, was sampled at the North, South and Solar-AQMS sites. These were:

- Wind direction - the air mass must be transported from the well to the sampling site i.e. the sampling site must be downwind of the well pad when the activity is occurring;
- Wind speed and distance from well pad to sampling site– wind speed affects the amount of time the air mass is impacted by emissions from HF and well completion, and the amount of time the air mass spends over the sampling site. Wind speed and distance from well to sampling site affects the extent of dilution of emissions by mixing with cleaner background air as they are transported away from the source.

As discussed in Section 2.2, the locations of the North-AQMS and South-AQMS were limited to two sites adjacent to electricity sub-stations which provided the only available access to mains power necessary for the air conditioning and monitoring equipment contained within each of these enclosures. As such, there was little flexibility in the choice of location for the North and South-AQMS and the co-located Solar-AQMS.

For the remaining four Solar-AQMS units, the locations were selected based on consideration of the prevailing meteorological conditions, safety and accessibility. The study design included

assessment of meteorological observations from previous studies (Dunne et al., 2017) that determined winds from the south and ENE sectors were expected to dominate when HF operations were underway. The solar-AQMS units were positioned to maximise exposure to these sectors while allowing for safety and accessibility factors.

To estimate the proportion of time each AQMS was exposed to an air mass influenced by HF or WC activities the following definitions were used:

- Downwind – an AQMS was considered downwind of a well when the wind direction was directly towards the AQMS  $\pm 20^\circ$ ;
- Calm – wind speeds were  $< 1 \text{ m sec}^{-1}$ .

Five-minute averages of wind direction and wind speed were calculated for each AQMS. The proportion of time an AQMS was exposed to an air mass influenced by HF or WC activity was estimated as the number of 5-minute averages that were either downwind or calm as a percentage of the total number of 5-minute averages for that AQMS.

The proportion of time each AQMS was downwind of a well during HF +WC activity are presented in Table 5 and Table 6.

The South-AQMS was located adjacent to a laydown yard ( $< 100 \text{ m}$ , heading  $0 - 90^\circ$ ). The laydown yard was a cleared area that served as a store for ground water used in well development operations, diesel refuelling tanks, trailers holding HF chemicals and proppant, trucks and equipment. Consequently, the area experienced frequent truck traffic. It is likely emissions from the laydown had an impact on local air quality especially in the vicinity of the South-AQMS.

Table 5 shows that the South-AQMS was downwind of the laydown area or under calm conditions, for 42% of the entire South-AQMS sampling period (Jul – Nov). The North-AQMS was downwind of HF + WC occurring at different wells between 9 and 30% of the time and the South-AQMS was downwind of HF + WC occurring at the different wells between 8 and 37% of the time. Table 6 shows that the Solar-AQMS sites were downwind of HF + WC occurring at the closest well between 13 and 37 % of the time.

**Table 5 The distance and heading from the North and South-AQMS to each well and the proportion of time the AQMS was downwind of the well during HF + WC activity.**

Well ID	HF + WC period	Distance from North-AQMS	Heading from North-AQMS to well <sup>1</sup>	Proportion of time North-AQMS was downwind of well during HF + WC <sup>2</sup>	Distance from South-AQMS	Heading from South-AQMS to well <sup>1</sup>	Proportion of time South-AQMS was downwind of well during HF + WC <sup>2</sup>
		(km)			(km)		
COM 360	21/9 – 24/9/2017	2.23	168 °	15 %	0.82	113 °	3 %
COM 445	23/9 – 29/9/2017	1.58	157 °	20 %	0.97	66 °	8 %
COM 340	27/9 – 30/9/2017	1.22	126 °	12 %	1.69	48 °	14 %
COM 313	6/10 – 11/10/2017	0.11	118 °	13 %	1.83	12 °	37 %
COM 337	9/10 – 13/10/2017	1.15	226 °	30 %	1.18	332 °	15 %
COM 338	11/10 - 15/10/2017	0.77	197 °	15 %	1.12	3 °	23 %
COM 444	12/10 –16/10/2017	1.58	195 °	15 %	0.35	339 °	10 %
COM 359R	14/10 –20/10/2017	2.29	185 °	9 %	0.43	171 °	8 %
COM 339	16/10 –23/10/2017	0.86	159 °	18 %	1.20	29 °	12 %
COM 314	26/10 – 2/11/2017	1.00	92 °	15 %	2.22	35 °	11 %
Laydown	NA <sup>3</sup>				< 0.1	0 - °90	42%
<b>Overall proportion of time North-AQMS was downwind of HF + WC<sup>4</sup></b>						16%	
<b>Overall proportion of time South-AQMS was downwind of HF + WC<sup>4</sup></b>						16%	

<sup>1</sup> The heading from the AQMS to the well  $\pm 20^\circ$  was the wind direction range used to define when the AQMS was downwind of the well.

<sup>2</sup> The proportion of time the AQMS was downwind of the well was calculated from the proportion of 5-minute average wind direction observations that were within the wind direction range (defined as the heading from the AQMS to the well  $\pm 20^\circ$ ) plus the proportion of observations (5-minute) when calm conditions prevailed (wind speed  $< 1 \text{ m sec}^{-1}$ ).

<sup>3</sup> Site activity (truck traffic, refuelling, fuel and chemical storage) occurred at the laydown area for the entire period of the study (Jul – Nov), not just during HF + WC periods.

<sup>4</sup> Overall proportion of time North-AQMS was downwind of HF + WC for period 21/9 – 2/11/2017, the period when HF and / or WC was occurring at one or more wells on site.

**Table 6 Distance of each Solar-AQMS from the closest well, the heading from the closet well and the proportion of time the Solar QMS was downwind of the nearest well during HF + WC activities.**

Solar-AQMS Site	Adjacent Well ID	HF + WC period	Distance from AQMS to well (km)	Heading from site to well <sup>1</sup>	Proportion of time site was downwind of well during HF + WC <sup>2</sup>
1	COM 445	23/9 – 29/9/20-17	0.12	45	37%
2	COM 337	9/10 – 13/10/2017	0.11	235	36%
3	COM 338	11/10 – 15/10/2017	0.11	220	22%
4	COM 314	26/10 – 2/11/2017	0.13	165	13%

<sup>1</sup> The heading from the Solar-AQMS site to the well  $\pm 20^\circ$  was the wind direction range used to define when the solar AQMS was downwind of the well.

<sup>2</sup> The proportion of time the Solar-AQMS site was downwind of the well was calculated from the proportion of 5-minute average wind direction observations that were within the wind direction range (defined as the heading from the Solar-AQMS to the well  $\pm 20^\circ$ ) plus the proportion of observations (5-minute) when calm conditions prevailed (wind speed  $< 1 \text{ m sec}^{-1}$ ).

## 4 Ambient Air Quality

The major objectives of this study were to provide comparisons of the air quality observed at a site with HF activities with Australian federal and state air quality objectives, and with data from other air quality studies undertaken in areas not directly impacted by HF operations both within the Surat Basin and in other locations in Australia. This section reports data for pollutants included in the National Environment Protection Measure for Ambient Air Quality (2015) namely NO<sub>2</sub>, CO, O<sub>3</sub>, SO<sub>2</sub>, PM<sub>2.5</sub> and PM<sub>10</sub> and TSP included in the Queensland EPP (2008). Also included are data on components of PM<sub>10</sub> (arsenic, manganese, nickel and sulfate) and TSP included in the Queensland EPP for Air (2008).

Air quality in relation to NO<sub>2</sub>, CO, O<sub>3</sub>, SO<sub>2</sub>, PM<sub>2.5</sub> and PM<sub>10</sub> and TSP is assessed by comparing pollutant concentrations against the air quality objectives set within the air quality standards outlined in Section 2.1. As discussed, state government agencies including the Queensland Government commonly report air quality index values (AQI) (see Section 2.1). Air quality indexes are reported in five categories – ‘very good’, ‘good’, and ‘fair’ representing concentrations at or below air quality objective values; and ‘poor’ to ‘very poor’ representing concentrations in exceedance of air quality objective values.

During the HF study the number of occasions and the proportion of air pollutant levels measured at the North-AQMS and the South-AQMS that fell into each of the five air quality index categories is reported in Table 7. Air quality at the study site in relation to each of the seven pollutants was classified as ‘good’ to ‘very good’ in 93% to 100% of the measurements during the period Aug – Dec 2017. Concentrations of NO<sub>2</sub>, CO, and SO<sub>2</sub> never exceeded relevant air quality objectives and concentrations were always less than two-thirds of the NEPM /EPP objectives. Air quality in relation to O<sub>3</sub> and PM<sub>2.5</sub> was classified as ‘good’ to ‘very good’ more than 98% of the time and ‘fair’ for the remaining <2%. Concentrations of PM<sub>10</sub> and TSP exceeded the relevant air quality objectives and air quality was classified as ‘poor’ to ‘very poor’ for ≤2% of the time. The remainder of the time air quality in relation to PM<sub>10</sub> and TSP was classified as ‘good’ to ‘very good’ with 93% to 99% of the measurements being less than two-thirds of the relevant air quality objectives.

Table 7 Number of occasions and the proportion (%) of total observations air pollutant concentrations fell into each of the 5 air quality index categories.

AQ Index categories		Occurrences					Proportion of total observations in each AQ index category					
		Very Good	Good	Fair	Poor	Very Poor	Very Good	Good	Fair	Poor	Very Poor	
Pollutant	AQ objective											
North-AQMS	NO <sub>2</sub>	NEPM 1-h	2777	0	0	0	0	100%	0%	0%	0%	0%
	CO	NEPM 8-h	2842	0	0	0	0	100%	0%	0%	0%	0%
	O <sub>3</sub>	NEPM 1-h	1882	896	0	0	0	68%	32%	0%	0%	0%
		NEPM 4-h	1307	1591	19	0	0	45%	55%	1%	0%	0%
	SO <sub>2</sub>	NEPM 1-h	2771	0	0	0	0	100%	0%	0%	0%	0%
		NEPM 24-h	121	0	0	0	0	100%	0%	0%	0%	0%
	PM <sub>2.5</sub>	NEPM 24-h	138	21	3	0	0	85%	13%	2%	0%	0%
	PM <sub>10</sub>	NEPM 24-h	142	19	1	0	0	88%	12%	1%	0%	0%
	TSP	DES 24-h	131	27	2	2	0	81%	17%	1%	1%	0%
South-AQMS	NO <sub>2</sub>	NEPM 1-h	3424	0	0	0	0	100%	0%	0%	0%	0%
	CO	NEPM 8-h	1955	0	0	0	0	100%	0%	0%	0%	0%
	O <sub>3</sub>	NEPM 1-h	1703	1065	0	0	0	62%	38%	0%	0%	0%
		NEPM 4-h	1005	1903	31	0	0	34%	65%	1%	0%	0%
	PM <sub>2.5</sub>	NEPM 24-h	130	19	2	0	0	86%	13%	1%	0%	0%
	PM <sub>10</sub>	NEPM 24-h	126	20	4	1	0	83%	13%	3%	1%	0%
	TSP	DES 24-h	105	34	6	3	3	70%	23%	4%	2%	2%

The following Sections provide a more detailed summary of measurements for each pollutant from both the North and South-AQMS as well as PM<sub>10</sub> and PM<sub>2.5</sub> data from the five Solar-AQMS sites. Air quality in relation to the concentrations of each air pollutant observed at the study site are compared to Australian federal and state air quality objectives and comparisons provided with data from other air quality studies undertaken in areas not directly impacted by HF operations.

Data from the present study are compared to measurements from three air quality monitoring stations - Hopeland, Miles Airport and Burncluith - that operated as part of GISERA's Surat Basin Ambient Air Quality Study (Lawson et al., 2018) over the same period as the present study. A fourth station at the Tara Region site suffered significant data loss during this period due to issues with power supply and will not be referred to here. The Hopeland and Miles Airport monitoring stations were located within operational CSG fields, 1 - 5 km from gas processing facilities, and were within 100 – 450 m of CSG wells with 15 to 25 wells within a 2 km radius of each site. A regional background site at Burncluith was > 10 km away from any major CSG infrastructure (Lawson et al., 2018). HF activities were not known to have occurred near these Surat Basin air monitoring sites during the period of the present study hence data from these sites provides a useful comparison of regional air quality from locations not directly impacted by HF activities.

Time series of key air pollutants are presented and periods when well development activities were occurring at the study site (drilling, HF + WC) are identified to provide a 'first look' at ambient air quality across the site during activity and non-activity periods.

Using higher time resolution data (5-minute average), the concentrations of pollutants measured at the North and South-AQMS when downwind of drilling, HF + WC activities are presented. For comparison, data for periods when the AQMS were upwind of drilling, HF + WC, and during periods where none of these activities were occurring are also presented. For the purposes of this discussion, the following definitions were used:

- Downwind of drilling: Includes data for the periods when drilling was occurring (see Section 2.3, Table 3), and the wind direction (WDR) was within a defined range for each well (defined as the heading from the AQMS to the well  $\pm 20^\circ$ )(see Section 3, Table 5 and Table 6) plus periods when calm conditions prevailed (wind speed < 1 m sec<sup>-1</sup>);
- Downwind of HF+ WC: Includes data for the periods when HF + WC activity was occurring (see Section 2.3, Table 3), and the WDR was within a defined range for each well (defined as the heading from the AQMS to the well  $\pm 20^\circ$ )(see Section 3, Table 5 and Table 6) plus periods when calm conditions prevailed (wind speed < 1 m sec<sup>-1</sup>);
- Other WDR excluding downwind of drilling or other WDR excluding downwind of HF + WC: Includes data for the periods when drilling or when HF + WC activity was occurring (see Section 2.3, Table 3), but the WDR was NOT within the defined ranges for each well (see above) and excludes periods when calm conditions prevailed;

- Non-activity periods: Includes data for the periods when no drilling, HF or WC activity was occurring on site. Data from all WDRs is included.

If pollutant emissions are associated with drilling or HF +WC it would be reasonable to expect that higher pollutant concentrations will be observed downwind of these activities than observed for other WDRs during the same periods, and higher than observed during non-activity periods.

## **4.1 Nitrogen dioxide, carbon monoxide, ozone, sulphur dioxide**

Australian standard measurement methods for pollutant monitoring as described in the ambient air NEPM were employed by Ecotech for the measurement of NO<sub>x</sub>, CO, O<sub>3</sub>, and SO<sub>2</sub>. Ecotech was responsible for instrument installation, calibration and maintenance as well as data validation and reporting. Ecotech performed daily data checks on all the instruments via remote connection to identify any issues with instrument performance. CSIRO also undertook an independent daily check of instrument performance remotely for all sites and communicated any identified issues to Ecotech for action as they arose.

Ecotech were responsible for QA/QC of data and ensuring compliance with relevant Australian Standards. Reports of monthly validated data were provided to CSIRO who performed additional checks and independent assessments of data quality. Data capture rates <100% in the final validated data sets reported here resulted from instrument performance, maintenance and calibration issues and power outages. Monthly data capture rates for each pollutant are reported in the following sections. Monthly averages were not calculated for months where data capture was < 60%. Further details of the measurement methods, maintenance, calibration, QA/QC and data capture rates were provided in a previous report for this project Dunne et al. (2018a).

### **4.1.1 Nitrogen dioxide**

Nitrogen dioxide (NO<sub>2</sub>) is primarily emitted from combustion sources including exhaust emissions from vehicles and equipment, biomass burning and flaring in gas production regions. Summary NO<sub>2</sub> concentration statistics including monthly average and maximum concentrations and data capture rates for the North and South-AQMS are listed in Table 8. The time series of hourly average NO<sub>2</sub> concentrations from the North-AQMS and the South-AQMS and the NEPM 1-hour air

quality objective for NO<sub>2</sub> are shown in Figure 12.

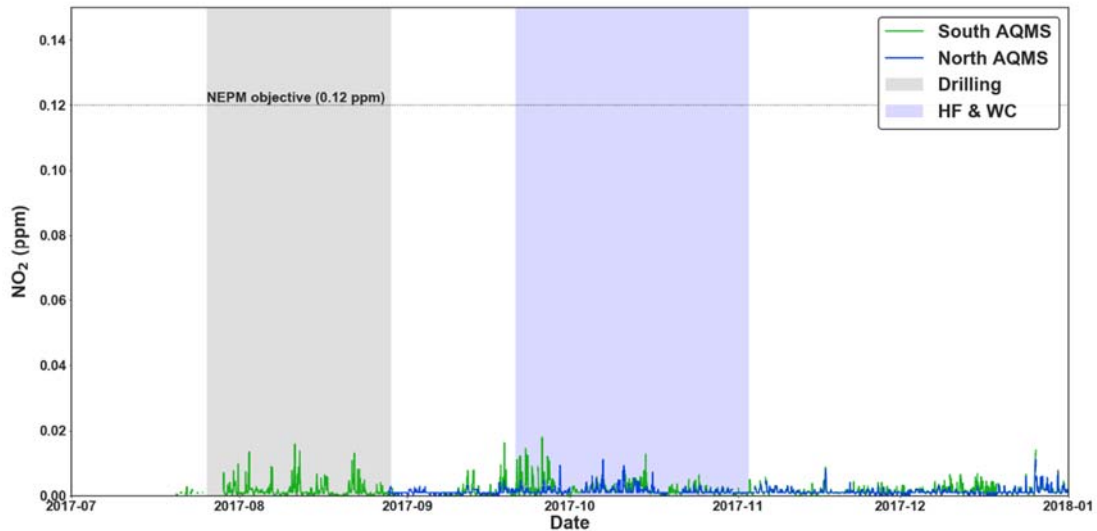


**Figure 12. 24-hour average NO<sub>2</sub> at both North and South-AQMS. Shaded areas represent periods of well development activity on the HF study site, including drilling (grey) and HF + WC (purple).**

The NEPM 1-hour air quality objective for NO<sub>2</sub> is 0.12 ppm. Shaded areas represent periods of well development activity on the HF study site, including drilling (grey) and HF + WC (purple).

While peaks in NO<sub>2</sub> concentrations were observed more frequently during the drilling period and HF + WC periods, air quality in relation to NO<sub>2</sub> was always classified as ‘very good’ and the observed levels never close to or exceeded the NEPM 1-hour air quality objective for NO<sub>2</sub> at the North and South-AQMS during the study period. Across the Surat Basin region similar AQI values were also reported for the same period at Hopeland, Miles Airport, and Burncluth (Table 9).

At the North and South-AQMS the overall averages of NO<sub>2</sub> for the whole measurement period were 0.001 ppm and 0.002 ppm respectively. If average NO<sub>2</sub> concentrations for these approximately four months of monitoring were representative of the concentrations across one whole year, then the inferred annual concentrations of NO<sub>2</sub> were well below the annual Ambient Air NEPM (2016) guideline of 0.03 ppm.

**Table 8 Monthly maximum and average 1-hour concentrations of NO<sub>2</sub> (ppm) for North and South-AQMS for the HF study period (Jul – Dec 2018). Data availability (%), overall average NO<sub>2</sub> concentrations, and concentrations during HF + WC are also presented. The NEPM 1-hour air quality objective for NO<sub>2</sub> is 0.12 ppm.**

NO <sub>2</sub> - 2017	Jul	Aug	Sep	Oct	Nov	Dec	Jul – Dec 2017	HF + WC period 21 <sup>st</sup> Sept – 2 <sup>nd</sup> Nov
<b>North-AQMS</b>								
Max1-hour	n.d.	0.003	0.009	0.011	0.008	0.011	0.011	0.011
Average 1-hour	n.d.	i.d.	0.001	0.002	0.001	0.001	0.001	0.002
% Data Avail	0 <sup>g</sup>	10 <sup>g</sup>	95	83 <sup>e</sup>	95	96	63 <sup>e,g</sup>	86 <sup>e</sup>
<b>South-AQMS</b>								
Max 1-hour	0.010	0.016	0.018	0.013	0.009	0.014	0.018	0.018
Average 1-hour	i.d.	0.002	0.002	0.002	0.001	0.002	0.002	0.002
% Data Avail	14 <sup>c</sup>	91	74 <sup>e</sup>	96	96	96	78 <sup>c,e</sup>	95

n.d. indicates no data are available; i.d. indicates insufficient data were available to calculate value (< 60% data available). Reasons for data availability < 90 %: a = power outage; b = instrument failure; c = instrument commissioned/de-commissioned part way through month; d = air-conditioning failure; e = calibration out of tolerance; f = communication / logger failure; g = sample manifold inlet fault.

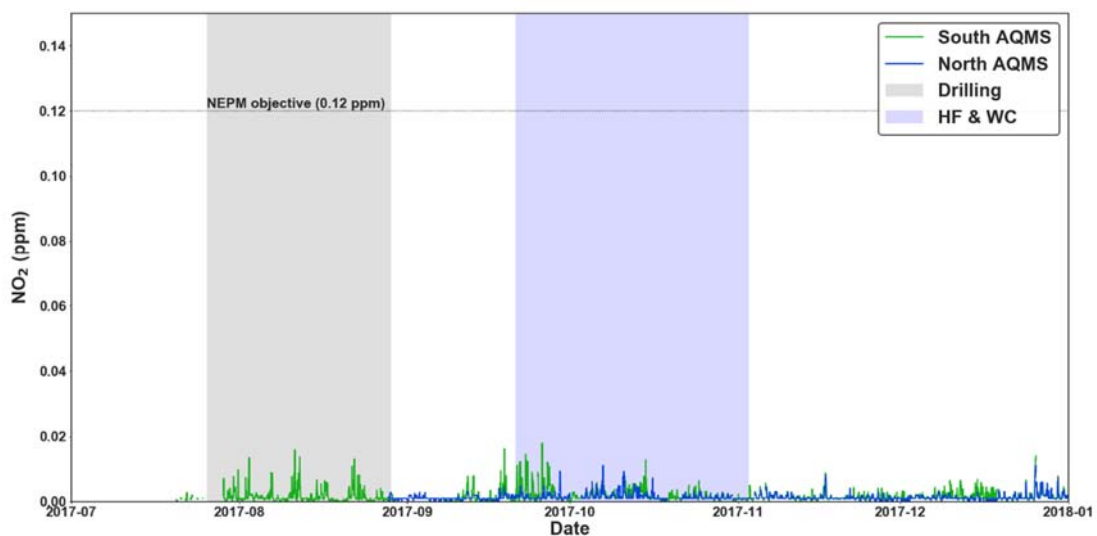


**Figure 12 1-hour average NO<sub>2</sub> concentration (ppm) at both North and South-AQMS. Shaded areas represent periods of well development activity on the HF study site, including drilling (grey) and HF + WC (purple).**

**Table 9 Proportion of total NO<sub>2</sub> observations (1-hour averages) in each air quality index category from the North and South-AQMS at the HF study site, and from Hopeland, Miles Airport and Burncluith sites operated as part of the Surat Basin Ambient Air Monitoring Network.**

AQ Index categories		Proportion of total observations in each AQ index category				
		Very Good	Good	Fair	Poor	Very Poor
NO <sub>2</sub> 1-hour average	North-AQMS (all)	100%	0%	0%	0%	0%
	North-AQMS (HF + WC)	100%	0%	0%	0%	0%
	South-AQMS (all)	100%	0%	0%	0%	0%
	South-AQMS (HF + WC)	100%	0%	0%	0%	0%
	Hopeland	100%	0%	0%	0%	0%
	Miles Airport	100%	0%	0%	0%	0%
	Burncluith	100%	0%	0%	0%	0%

### HF and non-HF related sources of NO<sub>2</sub>

Higher time resolution (5-minute) NO<sub>2</sub> and wind direction data were used to assess the likelihood that increases in NO<sub>2</sub> concentration were a result of well development activity.

Figure 13 shows the distributions of 5-minute averaged NO<sub>2</sub> data measured at the North and South-AQMS when downwind of drilling (A) and when downwind of HF or WC (C), alongside data from other WDRs during the same periods (B and D) and during periods where no drilling/HF/WC activities were occurring (E). The characteristics of the distributions for the NO<sub>2</sub> data from the North and South-AQMS were as follows:

#### North-AQMS:

- The median and inter quartile ranges (IQR, 25<sup>th</sup> – 75<sup>th</sup> percentiles) of NO<sub>2</sub> concentrations for all activity and non-activity periods, and all WDRs were similarly low (medians = 0.001 to 0.002ppm, IQRs = 0.001 to 0.003 ppm);
- **Drilling** - NO<sub>2</sub> was not measured at the North-AQMS during drilling due to instrument failure;

- **HF + WC** - the top 5 % of NO<sub>2</sub> values when measuring downwind of HF + WC (C in Figure 13) were slightly higher than the top 5% of values when measuring air masses from other WDRs during the same period (D) and when compared to non-activity periods (E).

#### South-AQMS:

- The median and inter quartile concentration ranges (IQR, 25<sup>th</sup> – 75<sup>th</sup> percentiles) of NO<sub>2</sub> for all activity and non-activity periods were low (medians = 0.000 to 0.001 ppm, IQRs = 0.001 to 0.004 ppm);
- **Drilling** - the top 5 % of NO<sub>2</sub> concentrations when measuring downwind of drilling (A) were higher than the top 5% of values when measuring air masses from other WDRs during the same period (B) and when compared to non-activity periods (E);
- **HF +WC** - the top 5 % of NO<sub>2</sub> values when measuring downwind of HF + WC (C) were higher than the top 5% of values when measuring air masses from other WDRs during the same period (D) and for all WDRs during non-activity periods (E).

NO<sub>2</sub> is not a component of drilling fluids, HF fluids, flowback fluids or CSG. Exhaust emissions from diesel powered equipment and vehicles on site may have contributed to the observed changes in NO<sub>2</sub> concentrations that coincided with drilling and HF + WC activities.

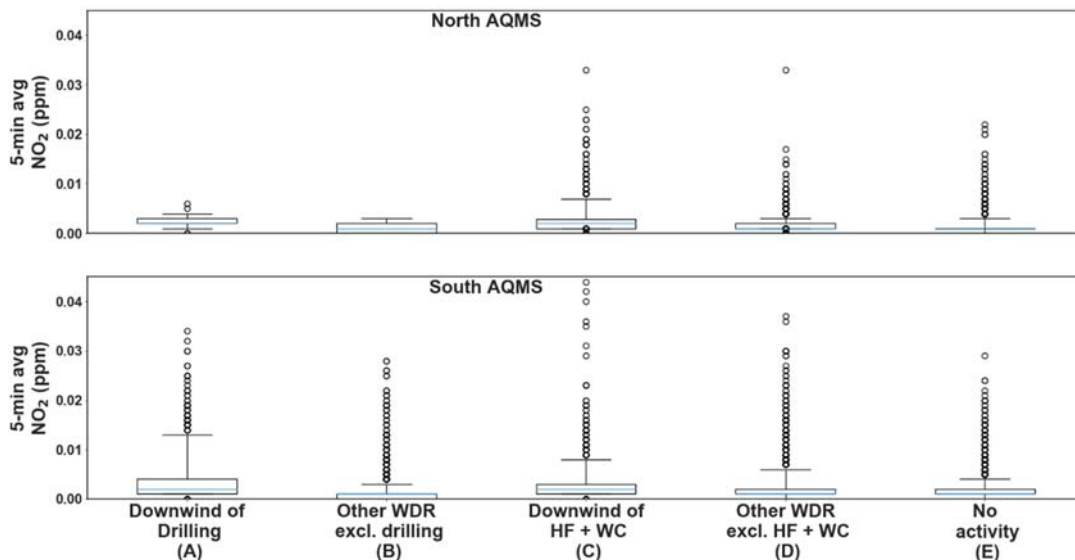


**Figure 13: Box and whisker plots of the 5-minute average NO<sub>2</sub> data from the North and South-AQMS measured when downwind of drilling (A) and HF + WC (C). For comparison NO<sub>2</sub> data from other WDRs during drilling (B) and from other WDRs during HF + WC (D), as well as during non-activity periods (E) are presented. Note the box represents the inter-quartile range (IQR) (range of 25<sup>th</sup> to 75<sup>th</sup> percentiles), the blue line is the median (50<sup>th</sup> percentile), the whiskers represent the 5<sup>th</sup> and 95<sup>th</sup> percentiles and the points above/below the whiskers represent the top/bottom 5% of values. NO<sub>2</sub> was not measured at the North-AQMS during drilling (see Table 8).**

#### 4.1.2 Carbon monoxide

Carbon monoxide (CO) is a gas produced from combustion processes such as motor vehicle exhaust, gas combustion and fires. Summary CO concentration statistics, including monthly average and maximum concentrations and data capture rates for the North and South-AQMS, are listed in Table 10. The time series of the daily maximum 8-hour average CO concentration at the North-AQMS and the South-AQMS and the NEPM 8-hour air quality objective for CO of 9 ppm are shown in Table 10. While frequent peaks in CO were observed during the drilling period, air quality in relation to CO was always classified as ‘very good’ and the observed levels did not exceed the NEPM 8-hour air quality objective for CO at the North-AQMS or South-AQMS. Across the Surat Basin region similar AQI values were also reported for the same period at Hopeland, Miles Airport, and Burncluth (Table 11).

**Table 10 Monthly maximum and average rolling 8-hour concentrations of CO (ppm) for North and South-AQMS during the HF study period (Jul – Dec 2017). Data availability (%), overall average and maximum CO concentrations and concentrations during the HF + WC period are also presented. The NEPM rolling 8-hour air quality objective for CO is 9 ppm.**

CO - 2017	Jul	Aug	Sep	Oct	Nov	Dec	Jul – Dec 2017	HF + WC period 21 <sup>st</sup> Sept – 2 <sup>nd</sup> Nov
<b>North-AQMS</b>								
Max 8-hour	n.d.	0.1	0.3	0.2	0.2	0.2	0.3	0.3
Average 8-hour	n.d.	0.0	0.1	0.1	0.1	0.1	0.1	0.1
% Data Avail	0 <sup>g</sup>	10 <sup>g</sup>	95	77 <sup>e</sup>	95	93	61 <sup>e,g</sup>	82 <sup>e</sup>
<b>South-AQMS</b>								
Max 8-hour	0.3	0.6	0.3	0.4	0.3		0.4	0.4
Average 8-hour	i.d.	0.1	0.1	0.1	0.1		0.1	0.1
% Data Avail	16 <sup>b,c</sup>	85 <sup>b</sup>	74 <sup>e</sup>	96	10 <sup>b</sup>	0 <sup>b</sup>	47 <sup>b</sup>	95

n.d. indicates no data are available; i.d. indicates insufficient data were available to calculate value (< 60% data available). Reasons for data availability < 90 %: a = power outage; b = instrument failure; c = instrument commissioned /de-commissioned part way through month; d = air-conditioning failure; e = calibration out of tolerance; f = communication / logger failure; g = sample manifold inlet fault.

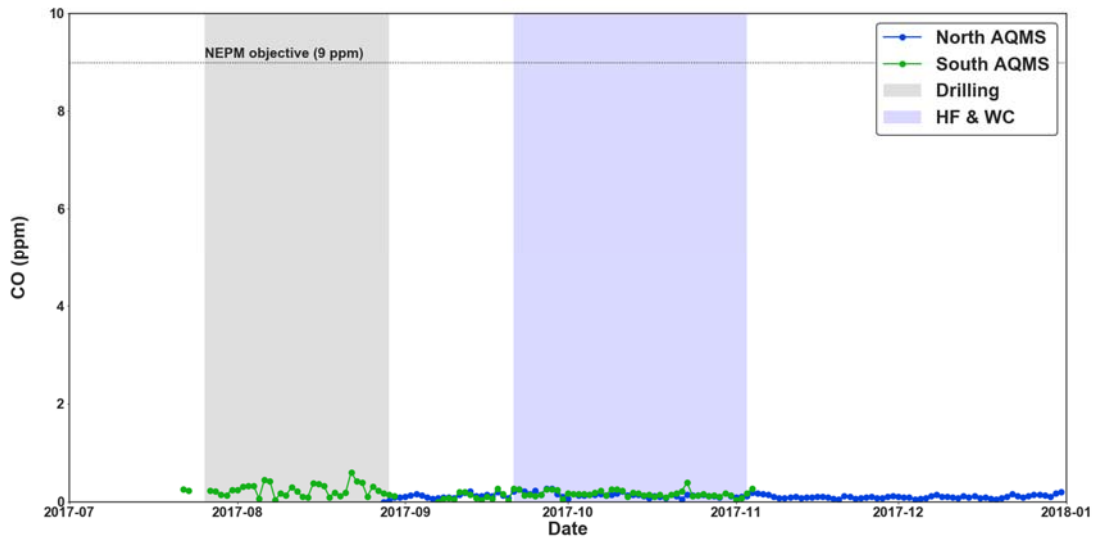


Figure 14 Daily maximum 8-hour averages for CO at both North and South-AQMS. Shaded areas represent periods of well development activity on the HF study site, including drilling (grey) and HF + WC (purple).

Table 11 Proportion of total CO observations (rolling 8-hour averages) in each air quality index category from the North and South-AQMS' at the HF study site, and from Hopeland, Miles Airport and Burncluith sites operated as part of the Surat Basin Ambient Air Monitoring Network.

AQ Index categories		Proportion of total observations in each AQ index category				
		Very Good	Good	Fair	Poor	Very Poor
CO 8-hour average	North-AQMS (all)	100%	0%	0%	0%	0%
	North-AQMS (downwind of HF)	100%	0%	0%	0%	0%
	South-AQMS (all)	100%	0%	0%	0%	0%
	South-AQMS (downwind of HF)	100%	0%	0%	0%	0%
	Hopeland	100%	0%	0%	0%	0%
	Miles Airport	100%	0%	0%	0%	0%
	Burncluith	100%	0%	0%	0%	0%

### HF and non-HF related sources of CO

Higher time resolution (5-minute) CO and wind direction data were used to assess the likelihood that increases in CO concentration were a result of well development activity.

Figure 15 shows the distributions of 5-minute average CO data measured at the North and South-AQMS when downwind of drilling (A) and when downwind of HF + WC (C) alongside data from

other WDRs during the same periods (B and D) and during periods where no drilling/HF/WC activities were occurring (E). The characteristics of the distributions for the CO data from the North and South-AQMS were as follows:

**North-AQMS:**

- The median and inter quartile ranges (IQR, 25<sup>th</sup> – 75<sup>th</sup> percentiles) of CO values for all activity and non-activity periods and all WDRs were low (medians = 0.0 to 0.1 ppm, IQRs = 0.0 to 0.1 ppm);
- **Drilling** - CO was not measured at the North-AQMS during drilling due to instrument faults;
- **HF + WC** - The highest values were associated with measurements of air masses from WDRs other than downwind of HF + WC (D) and during periods when there was no activity on site (E).

**South-AQMS:**

- The median and inter quartile ranges (IQR, 25<sup>th</sup> – 75<sup>th</sup> percentiles) of CO were higher downwind of drilling (A) than for measurements during other activity and non-activity periods and WDRs (B and E);
- **Drilling** - The top 5% of values when downwind of drilling (A) were higher than the top 5% of values when measuring air masses from other WDRs during the same period (B) and during non-activity periods (E);
- **HF + WC** - The top 5% of values when downwind of HF +WC (C) were lower than the top 5% of values when measuring air masses from other WDRs during the same period (D) and similar to those observed during non-activity periods (E).

Overall, drilling was associated with higher concentrations of CO at the South-AQMS, whereas HF + WC was not associated with the highest observed peaks in CO concentrations at either the North or South-AQMS. Other sources of CO, including biomass burning and gas combustion, may have contributed to CO concentrations when measuring air masses from other WDRs during the HF + WC period and during non-activity periods.

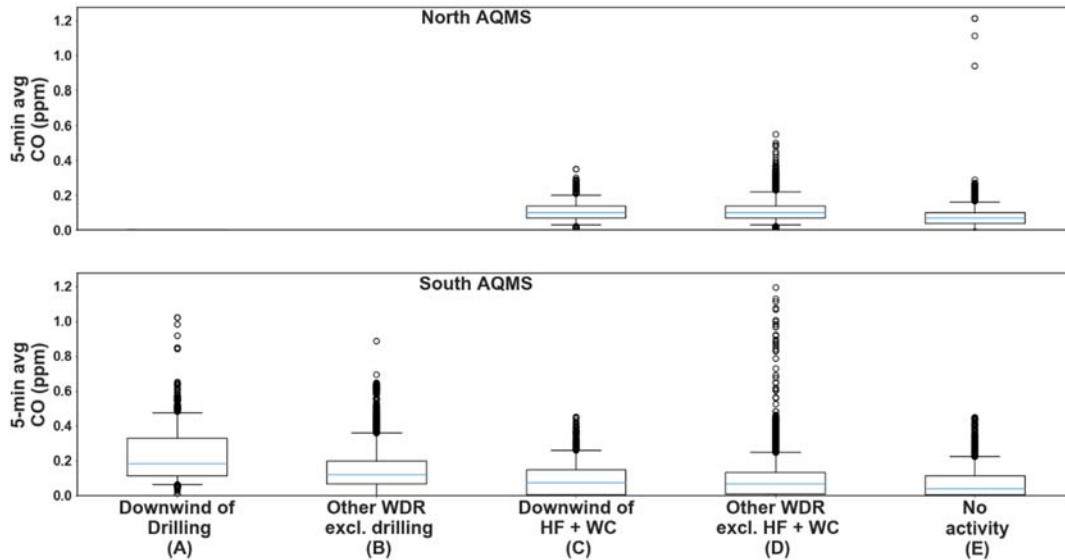


**Figure 15: Box and whisker plots of the 5-minute average CO data (ppm) from the North and South-AQMS measured when downwind of drilling and HF + WC. For comparison CO data from other WDRs during drilling and HF + WC, as well as during non-activity periods are presented. Note the box represents the range between the 25<sup>th</sup> and 75<sup>th</sup> percentiles, the blue line is the median (50<sup>th</sup> percentile), the whiskers represent the 5<sup>th</sup> and 95<sup>th</sup> percentiles and the points above/below the whiskers represent the top/bottom 5% of values. Note: CO wasn't measured during drilling at the North-AQMS (see Table 10).**

### 4.1.3 Ozone

Ozone (O<sub>3</sub>) in the troposphere (lower atmosphere) is not directly emitted into the atmosphere from ground-based sources. It is instead a secondary product of reactions between air pollutants NO<sub>x</sub> (oxides of nitrogen) and VOCs with additional contributions from transportation of O<sub>3</sub> from the stratosphere (upper atmosphere) where it is formed from reactions involving sunlight and oxygen.

Summary O<sub>3</sub> concentration statistics, including monthly average and maximum concentrations for both the 1-hour data and rolling 4-hour average data, as well as data capture rates for the North and South-AQMS are listed in Table 12. The time series of hourly and daily 4-hour maximum O<sub>3</sub> concentrations at the North-AQMS and the South-AQMS and the NEPM 1-hour and 4-hour, air quality objectives for O<sub>3</sub> are shown in Figure 16 and Figure 17. The NEPM 1-hour air quality objective for O<sub>3</sub> is 0.10 ppm. The 4-hour air quality objective for O<sub>3</sub> is 0.08 ppm.

Air quality in relation to the 4-hourly O<sub>3</sub> objective at the North-AQMS and the South-AQMS was classified as 'good' to 'very good' for 99% of the time and the remaining 1% was classed as 'fair'. There were no exceedances of the NEPM/EPP 1-hour nor 4-hour, O<sub>3</sub> air quality objectives. Across the Surat Basin region similar AQI values were also reported for the same period at Hopeland,

Miles Airport, and Burncluith (Table 13). Given the similarity in O<sub>3</sub> concentrations across the Surat Basin, the levels of O<sub>3</sub> observed at the study site were likely to be dominated by regional sources.

**Table 12 Monthly maximum and average 1-hour and rolling 4-hour concentrations of O<sub>3</sub> (ppm) for the North and South-AQMS during the HF study period (Jul – Dec 2018). Data availability (%), overall average O<sub>3</sub> concentrations, and average concentrations during the HF + WC period are also presented. The NEPM 1-hour air quality objective for O<sub>3</sub> is 0.100 ppm and the NEPM 4-hour air quality objective for O<sub>3</sub> is 0.08 ppm.**

O <sub>3</sub> - 2017	Jul	Aug	Sep	Oct	Nov	Dec	Aug – Dec 2017	HF + WC period 21 <sup>st</sup> Sept – 2 <sup>nd</sup> Nov
<b>North-AQMS</b>								
Max 1-hour	n.d.	0.043	0.062	0.053	0.053	0.061	0.062	0.062
Average 1-hour	n.d.	i.d.	0.033	0.029	0.025	0.028	0.029	0.031
Max 4-hour	n.d.	0.043	0.057	0.052	0.052	0.056	0.057	0.057
Average 4-hour	n.d.	i.d.	0.033	0.028	0.025	0.027	0.028	0.030
% Data Avail	0 <sup>g</sup>	10 <sup>g</sup>	83 <sup>g</sup>	95	96	96	63 <sup>g</sup>	94
<b>South-AQMS</b>								
Max 1-hour	n.d.	n.d.	0.060	0.059	0.054	0.062	0.062	0.060
Average 1-hour	n.d.	n.d.	0.035	0.031	0.028	0.029	0.031	0.033
Max 4-hour	n.d.	n.d.	0.059	0.058	0.053	0.057	0.057	0.059
Average 4-hour	n.d.	n.d.	0.035	0.030	0.028	0.029	0.031	0.032
% Data Avail	0 <sup>b,c</sup>	2 <sup>b</sup>	93	94	94	95	63 <sup>b,c</sup>	94

n.d. indicates no data are available; i.d. indicates insufficient data were available to calculate value (< 60% data available). Reasons for data availability < 90 %: a = power outage; b = instrument failure; c = instrument commissioned /de-commissioned part way through month; d = air-conditioning failure; e = calibration out of tolerance; f = communication / logger failure; g = sample manifold inlet fault.

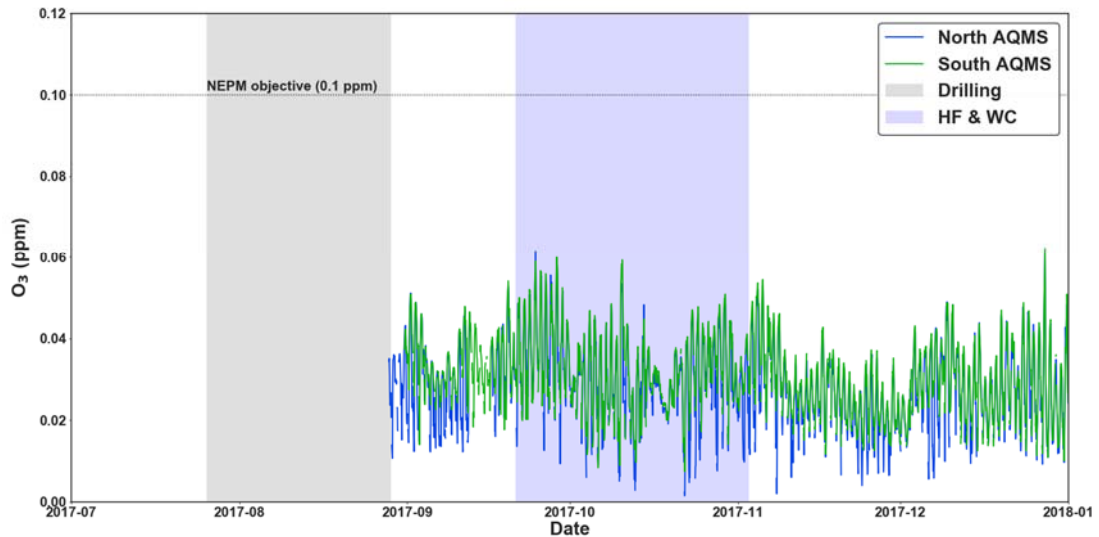


Figure 16 1-hour averages for O<sub>3</sub> at both North and South-AQMS. Shaded areas represent periods of well development activity on the HF study site, including drilling (grey) and HF + WC (purple).

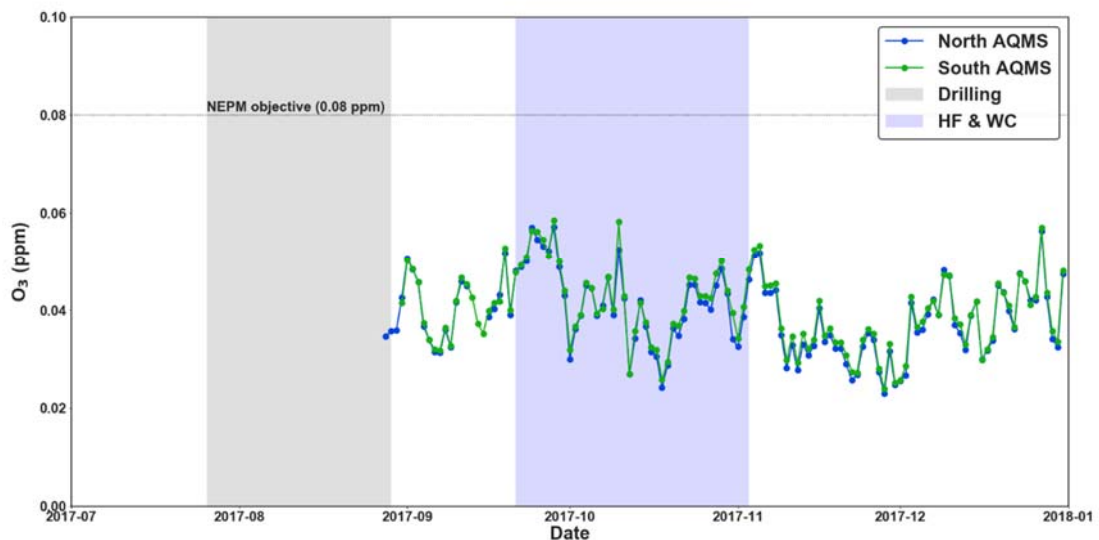


Figure 17 Daily maximum 4-hour averages for O<sub>3</sub> at both North and South-AQMS. Shaded areas represent periods of well development activity on the HF study site, including drilling (grey) and HF + WC (purple).

**Table 13 Proportion of total 1-hour averages and rolling 4-hour average observations of O<sub>3</sub> in each air quality index category from the North and South-AQMS at the HF study site, and from Hopeland, Miles Airport and Burncluith sites operated as part of the Surat Basin Ambient Air Monitoring Network.**

AQ Index categories		Proportion of total observations in each AQ index category				
		Very Good	Good	Fair	Poor	Very Poor
O <sub>3</sub> 1-hour average	North-AQMS (all)	68%	32%	0%	0%	0%
	North-AQMS (HF + WC)	61%	39%	0%	0%	0%
	South-AQMS (all)	62%	38%	0%	0%	0%
	South-AQMS (HF + WC)	56%	44%	0%	0%	0%
	Hopeland	63%	37%	0%	0%	0%
	Miles Airport	70%	30%	0%	0%	0%
	Burncluith	64%	36%	0%	0%	0%
O <sub>3</sub> 4-hour average	North-AQMS (all)	45%	55%	1%	0%	0%
	North-AQMS (HF + WC)	35%	64%	2%	0%	0%
	South-AQMS	34%	65%	1%	0%	0%
	South-AQMS (HF + WC)	28%	69%	3%	0%	0%
	Hopeland	42%	58%	1%	0%	0%
	Miles Airport	48%	51%	1%	0%	0%
	Burncluith	42%	58%	0%	0%	0%

### HF and non-HF related sources of O<sub>3</sub>

Higher time resolution (5-minute) O<sub>3</sub> and wind direction data were used to assess the likelihood that increases in O<sub>3</sub> concentration were a result of well development activity.

Figure 18 shows the distributions of 5-minute average O<sub>3</sub> data measured at the North and South-AQMS when downwind of HF + WC (C), alongside data from other WDRs during the same period (D) and during periods where no HF + WC activities were occurring (E). Ozone was not measured at the North and South-AQMS during drilling due to equipment faults.

The distribution in the concentration of ozone measured at both the North and South-AQMS for all periods and all WDRs were similar. The similarity across sites and for all WDRs is further evidence the ozone concentrations observed at the study site were dominated by regional sources (regional photochemical production and transport) and were not directly associated with emissions from HF + WC.

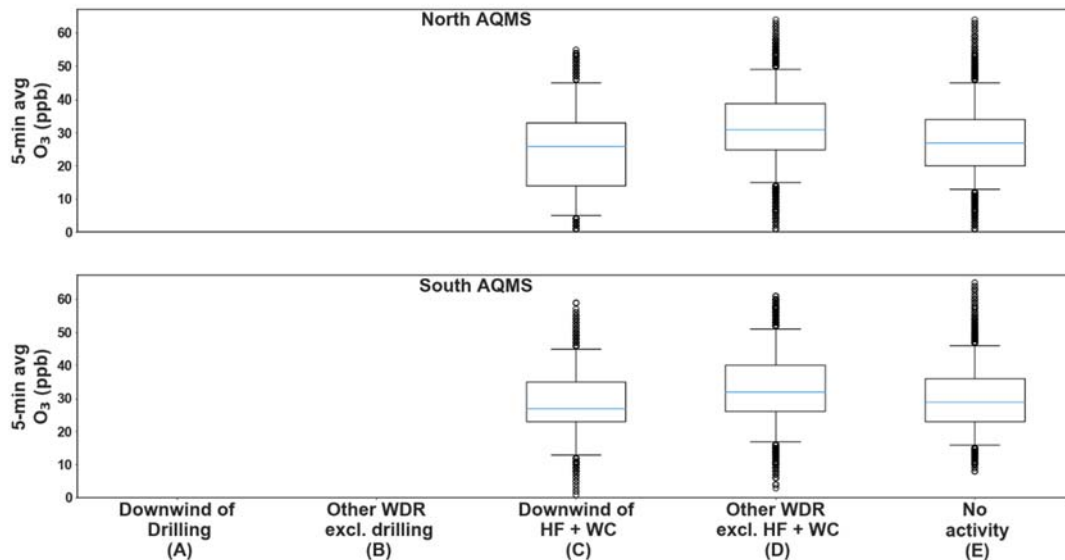


**Figure 18: Box and whisker plots of the 5-minute average O<sub>3</sub> data (ppb) from the North and South-AQMS measured when downwind of HF + WC (C). For comparison O<sub>3</sub> data from other WDRs during and HF +WC (D), as well as during non-activity periods (E) are presented. Note the box represents the range between the 25<sup>th</sup> and 75<sup>th</sup> percentiles, the blue line is the median (50<sup>th</sup> percentile), the whiskers represent the 5<sup>th</sup> and 95<sup>th</sup> percentiles and the points above/below the whiskers represent the top/bottom 5% of values. Note: ozone wasn't measured during drilling at the North or South-AQMS (see Table 12).**

#### 4.1.4 Sulfur dioxide

Sulfur dioxide (SO<sub>2</sub>) is a gas predominantly produced from the burning of fossil fuels. SO<sub>2</sub> was only measured at the North-AQMS. Summary SO<sub>2</sub> concentration statistics including monthly 1-hour and 24-hour average and maximum concentrations and data capture rates for the North-AQMS are listed in Table 14.

The time series showing hourly and 24-hour averaged SO<sub>2</sub> concentrations and the NEPM 1-hour and 24-hour air quality objectives for SO<sub>2</sub> are shown in Figure 19 and Figure 20. The NEPM 1-hour air quality objective for SO<sub>2</sub> is 0.2 ppm and the 24-hour air quality objective for SO<sub>2</sub> is 0.08 ppm. Air quality in relation to SO<sub>2</sub> was always classified as 'very good' and the observed levels did not exceed the NEPM 1-hour or 24-hour air quality objectives (Table 15). Note that SO<sub>2</sub> was not measured at Hopeland, Miles Airport or Burncluth. However similar AQI values were observed over the same period at a Queensland Department of Environment and Science air quality monitoring site at Flinders View, a suburban air quality monitoring site located in the Ipswich area of southeast Queensland (Table 15).

At the North-AQMS the overall average of SO<sub>2</sub> for the whole measurement period was 0.001 ppm. Assuming that the average SO<sub>2</sub> concentrations for these ~ 4 months of monitoring were similar to

the concentrations across one whole year, the inferred annual concentrations of SO<sub>2</sub> were well below the annual Ambient Air NEPM (2016) guideline of 0.02 ppm.

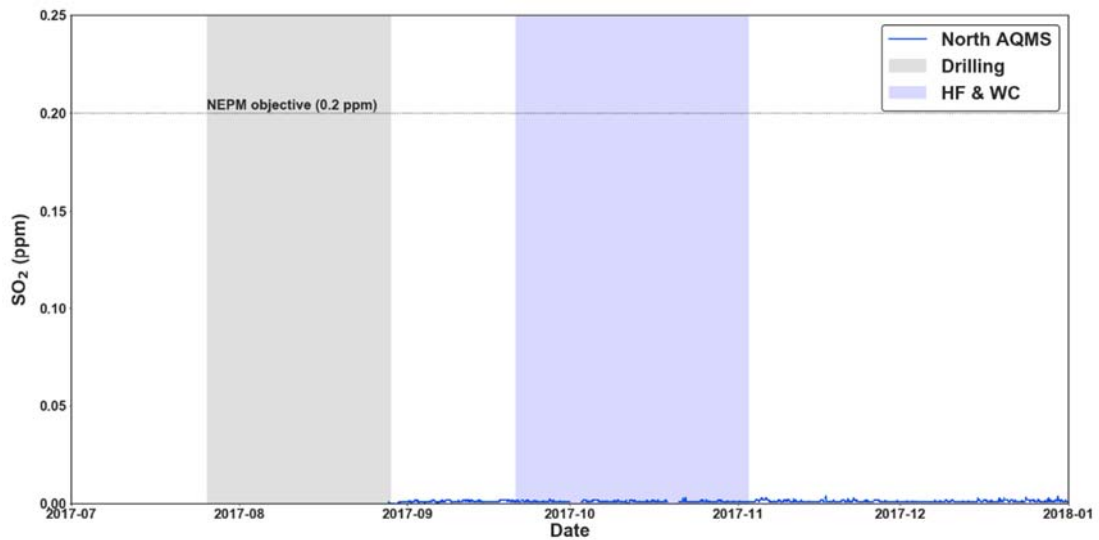


**Figure 19 1-hour averages for SO<sub>2</sub> at the North-AQMS. Shaded areas represent periods of well development activity on the HF study site, including drilling (grey) and HF + WC (purple).**

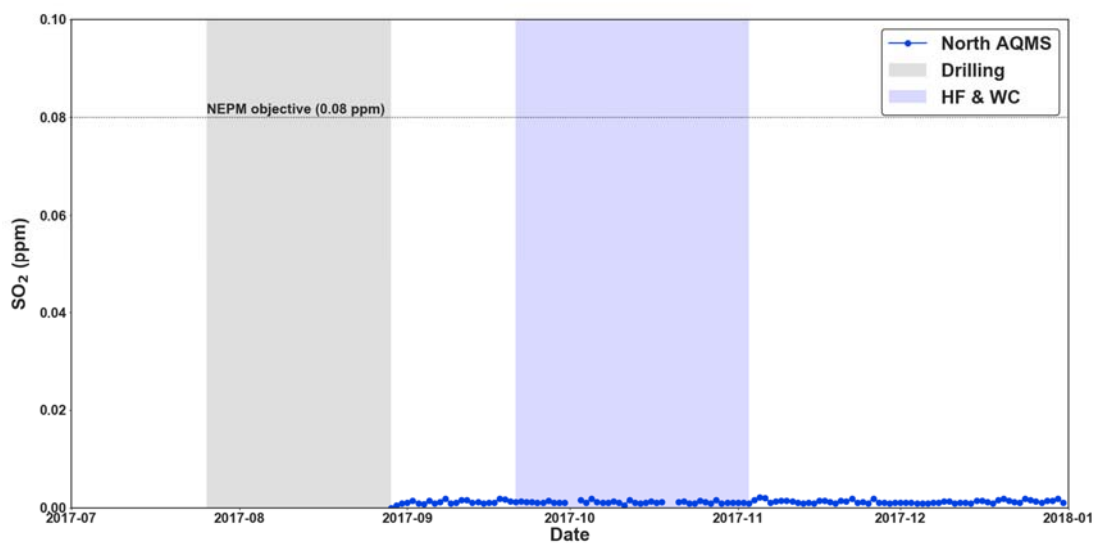


**Figure 20 24-hour averages for SO<sub>2</sub> at the North-AQMS. Shaded areas represent periods of well development activity on the HF study site, including drilling (grey) and HF + WC (purple).**

**Table 14 Ambient concentrations of SO<sub>2</sub> for the North-AQMS including monthly average and maximum 1-hour and 24-hour concentrations (ppm) during the HF study period July – December 2017. Data capture rates, overall average and maximum SO<sub>2</sub> concentrations, and concentrations during HF + WC are also included; The NEPM 1-hour air quality objective for SO<sub>2</sub> is 0.2 ppm.**

SO <sub>2</sub> - 2017	Jul	Aug	Sep	Oct	Nov	Dec	Aug – Dec 2017	HF + WC period 21 <sup>st</sup> Sept – 2 <sup>nd</sup> Nov
<b>North-AQMS</b>								
Max 1-hour	n.d.	0.001	0.002	0.003	0.004	0.004	0.004	0.003
Average 1-hour	n.d.	i.d.	0.001	0.001	0.001	0.001	0.001	0.001
Max 24-hour	n.d.	0.001	0.002	0.002	0.002	0.002	0.002	0.002
Average 24-hour	n.d.	i.d.	0.001	0.001	0.001	0.001	0.001	0.001
% Data Avail	0 <sup>b</sup>	10 <sup>b</sup>	95	83 <sup>e</sup>	95	96	63 <sup>e,g</sup>	86 <sup>e</sup>

n.d. indicates no data are available; i.d. indicates insufficient data were available to calculate value (< 60% data available). Reasons for data availability < 90 %: a = power outage; b = instrument failure; c = instrument commissioned /de-commissioned part way through month; d = air-conditioning failure; e = calibration out of tolerance; f = communication / logger failure; g = sample manifold inlet fault.

**Table 15 Proportion of 1-hour and rolling 24-hour observations of SO<sub>2</sub> in each air quality index category from the North and South-AQMS at the HF study site, and from Flinders View, a suburban air quality monitoring site located in the Ipswich area of SE Queensland. SO<sub>2</sub> measurements were not made at Hopeland, Miles Airport or Burncluth.**

AQ Index categories		Proportion of total observations in each AQ index category				
		Very Good	Good	Fair	Poor	Very Poor
SO <sub>2</sub> 1-hour average	North-AQMS (all)	100%	0%	0%	0%	0%
	North-AQMS (HF + WC)	100%	0%	0%	0%	0%
	South-AQMS (all)	100%	0%	0%	0%	0%
	South-AQMS (HF + WC)	100%	0%	0%	0%	0%
	Flinders View	100%	0%	0%	0%	0%
SO <sub>2</sub> 24-hour average	North-AQMS	100%	0%	0%	0%	0%
	North-AQMS (HF + WC)	100%	0%	0%	0%	0%
	South-AQMS	100%	0%	0%	0%	0%
	North-AQMS (HF + WC)	100%	0%	0%	0%	0%
	Flinders View	100%	0%	0%	0%	0%

## HF and non-HF related sources of SO<sub>2</sub>

Higher time resolution (5-minute) SO<sub>2</sub> and wind direction data were used to assess the likelihood that increases in SO<sub>2</sub> concentration were a result of well development activity.

Figure 21 shows the distribution of 5-minute average SO<sub>2</sub> data measured at the North and South-AQMS when downwind of HF +WC alongside data from other WDRs during the same period and during periods where no HF + WC activities were occurring. The range of SO<sub>2</sub> concentrations reported downwind of HF +WC were within the range of the observations from other WDRs during the same period and during non-activity periods. This indicates that emissions of SO<sub>2</sub> measured during this study were likely not associated with HF+WC activities.

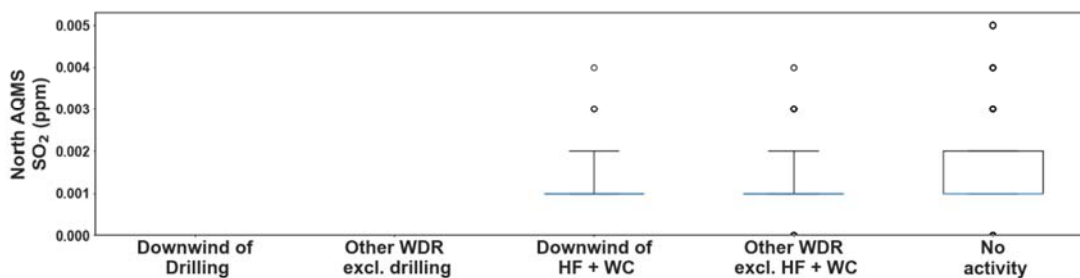


Figure 21 Box and whisker plots of the 5-minute average SO<sub>2</sub> data (ppm) from the North and South-AQMS measured when downwind of drilling and HF + WC. For comparison SO<sub>2</sub> data from other WDRs during drilling and HF +WC, as well as during non-activity periods are presented. Note the box represents the range between the 25<sup>th</sup> and 75<sup>th</sup> percentiles, the blue line is the median (50<sup>th</sup> percentile), the whiskers represent the 5<sup>th</sup> and 95<sup>th</sup> percentiles and the points above/below the whiskers represent the top/bottom 5% of values. Note: SO<sub>2</sub> was not measured at the South-AQMS during this study or at the North-AQMS during drilling due to equipment faults.

## 4.2 Particulate Matter (PM<sub>2.5</sub>, PM<sub>10</sub>, TSP) mass concentrations

Particulate matter (PM) is a mixture of airborne solid and liquid particles of varying size and composition. PM is emitted from a variety of natural and man-made sources and includes dust, smoke, sea salt, vehicle exhaust, industrial emissions and agricultural chemical sprays. Direct emissions of PM during HF operations may occur during storage handling and mixing of proppant (sand) and dry chemicals (e.g. potassium chloride, gelling agents, gel breakers and biocides). Like O<sub>3</sub>, PM can also be formed in the atmosphere as a secondary product of reactions between gaseous air pollutants.

## Relevant PM air quality objectives

The EPP (Air) and NEPM (Ambient Air) prescribe 24-hour air quality objectives for the mass concentrations ( $\mu\text{g m}^{-3}$ ) of two different size ranges of PM.

- $\text{PM}_{10}$  (particles with diameters  $< 10 \mu\text{m}$ )
  - NEPM/EPP 24-hour  $\text{PM}_{10}$  air quality objective is  $50 \mu\text{g m}^{-3}$
  - NEPM/EPP annual  $\text{PM}_{10}$  air quality objective is  $25 \mu\text{g m}^{-3}$
- $\text{PM}_{2.5}$  (particles with diameters  $< 2.5 \mu\text{m}$ )
  - NEPM/EPP 24-hour  $\text{PM}_{2.5}$  air quality objective is  $25 \mu\text{g m}^{-3}$
  - NEPM/EPP annual  $\text{PM}_{2.5}$  air quality objective is  $8 \mu\text{g m}^{-3}$

The NEPM for Ambient Air Quality does not prescribe an air quality guideline for TSP, however the Queensland EPP for Air prescribes an annual air quality objective value of  $90 \mu\text{g m}^{-3}$  for TSP. An Australian 24-hour ambient air objective does not exist for total TSP. Instead the 24-hour air quality objective used here is based on the New Zealand Ministry for the Environment's nuisance trigger level of  $60 \mu\text{g m}^{-3}$  for high sensitivity areas (MFE 2016), as recommended by Queensland's Department of Environment and Science (DES).

## PM Measurement Methods

There were four methods used in this study to measure air quality in relation to PM. Two methods were compliant with Australian Standards for  $\text{PM}_{10}$  sampling (AS/NZ 3580.9.9.2006.):

1. Sampling of  $\text{PM}_{10}$  by Low Volume Sampler-Gravimetric Method: Two x 12-hour samples of  $\text{PM}_{10}$  were collected per day on 47 mm Teflon Filters using Comde-Derenda low volume samplers at the North-AQMS. The flow rate of the Comde-Derenda sampler was  $\sim 38 \text{ lpm}$  (volumetric flow) which resulted in an average volume of air sampled per filter of  $\sim 27 \text{ m}^3$  (STP) over the 12-hour sample period. This was sufficient to collect enough particle mass for accurate gravimetric mass determination and chemical composition analysis. The average of the 2 x 12-hour samples per day were comparable with the NEPM (2016) 24-hour  $\text{PM}_{10}$  objective;
2.  $\text{PM}_{10}$  by Low Volume Sampler-Gravimetric Method: Multi-day ( $\sim 9$  days) samples of  $\text{PM}_{10}$  were collected on 47 mm Teflon Filters using Ecotech Microvol low volume samplers at the five Solar-AQMS sites. While sample periods of 24-hour allow a direct comparison with the 24-hour NEPM (2016)  $\text{PM}_{10}$  objective, the flow rate of the Microvol samplers was only  $\sim 3 \text{ lpm}$  (volumetric flow) so that a longer sampling time ( $\sim 7$  days) was required to sample a volume of air ( $\sim 30 \text{ m}^3$ ) sufficient to collect enough particle mass for accurate gravimetric mass determination and chemical composition analysis.

In addition, two non-standard methods were used:

1. Continuous measurements of  $\text{PM}_{2.5}$  by MetOne E-Sampler: E-samplers were operated at the five Solar-AQMS sites and provided continuous measurements of  $\text{PM}_{2.5}$  by near forward light

scattering technique plus gravimetric PM<sub>2.5</sub> mass by multi-day sampling on 47 mm Teflon filters. While the continuous PM<sub>2.5</sub> from light scattering is not an Australian Standard Method for determination of PM<sub>2.5</sub>, the filter measurements used for calibration did comply with Australian Standard Method AS/NZ 3580.9.10:2017;

2. Continuous measurements of PM<sub>10</sub> and PM<sub>2.5</sub> were performed simultaneously by Palas FIDAS 200s aerosol spectrometers located at both the North and South-AQMS: FIDAS instruments were also used for PM measurements at Miles Airport and Hopeland sites operated as part of the Surat Basin Ambient Air Quality Study (Lawson et al., 2018).

Ecotech were responsible for the operation and QA/QC of the PM<sub>10</sub>, PM<sub>2.5</sub> and TSP data from the Palas FIDAS instrument. Reports of monthly validated data were provided to CSIRO who performed additional checks and independent assessments of data quality. Data capture rates <100% in the final validated data sets reported here resulted from power outages. Further details of the measurement methods, maintenance, calibration, QA/QC and data capture rates were provided in a previous report for this project Dunne et al. (2018a).

CSIRO were responsible for the operation and QA/QC of the data from the PM<sub>10</sub> low volume samplers (Comde Derenda and Ecotech Microvols) and the measurements of PM<sub>2.5</sub> by MetOne e-Samplers. All three of these techniques involved the collection of PM onto filters. These filters were subsequently analysed for gravimetric mass. The mass concentrations reported by these methods are discussed below.

The PM filter samples also underwent chemical composition analysis. The composition of PM differs depending on the sources of PM present so that chemical composition data was used to identify the likely sources of PM at the HF study site and the factors that contributed to exceedances of PM air quality objectives. The results of the chemical composition analysis will be discussed later in the proceeding section 4.3.

### **PM Measurement Method Comparison**

A comparison of the mass concentration data reported by each of these PM measurement methods is provided in Figure 22. Good agreement Regression analysis produced slopes of 0.98 – 1.09, intercepts of -2 to 1  $\mu\text{g m}^{-3}$  and correlation coefficient ( $R^2$ ) values of 0.84 – 0.97 (Figure 22) between both co-located Australian Standard PM<sub>10</sub> Low Volume Sampler-Gravimetric Methods (Derenda and Microvol) and co-located continuous measurements of PM<sub>2.5</sub> by E-Sampler. An exact match would give a slope of 1, an intercept of 0 and  $R^2$  of 1. Thus, for the purposes of this study, the non-standard and Australian Standard PM measurement methods provided comparable results and were of sufficient quality for direct comparison with the NEPM (2016) and Qld EPP (2008) PM<sub>10</sub> and PM<sub>2.5</sub> air quality objectives.

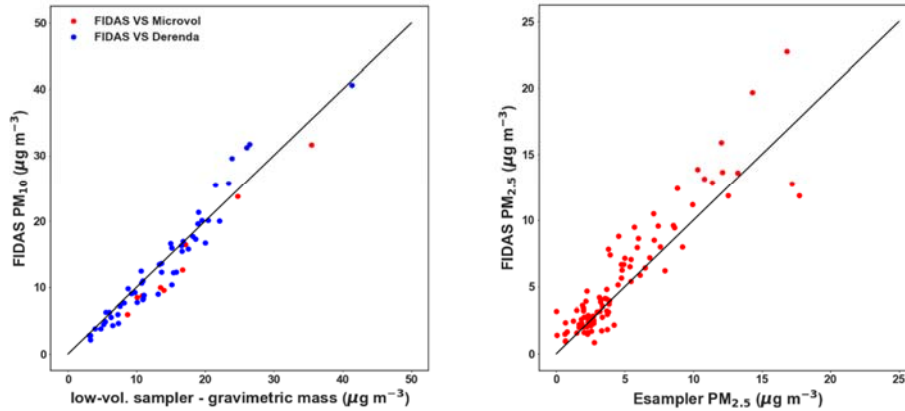


**Figure 22 Comparison of PM<sub>10</sub> and PM<sub>2.5</sub> measurement methods employed during the HF study. Lines represent 1:1 agreement. (Left panel) (blue) 24-hour average PM<sub>10</sub> by low-volume Derenda sampler with gravimetric mass determination versus 24-hour average of continuous PM<sub>10</sub> measurement by FIDAS light scattering method ( $R^2 = 0.94$ ). (red) Multi-day integrated average PM<sub>10</sub> by low-volume Microvol sampler with gravimetric mass determination versus FIDAS PM<sub>10</sub> integrated average over the same sample duration as Microvol ( $R^2 = 0.97$ ). (Right Panel) 24-hour average of continuous PM<sub>10</sub> measurements by E-sampler light scattering technique with gravimetric mass correction versus 24-hour average of continuous PM<sub>10</sub> measurement by FIDAS light scattering method ( $R^2 = 0.84$ ).**

#### 4.2.1 PM<sub>10</sub> concentrations at the North and South-AQMS

Summary statistics for PM<sub>10</sub> concentrations including monthly 24-hour average and maximum concentrations and data capture rates for the North-AQMS and South-AQMS are listed in Table 16. The time series of 24-hour average PM<sub>10</sub> concentrations from the North and South-AQMS and the NEPM 24-hour air quality objective for PM<sub>10</sub> are shown in Figure 23.

The NEPM 24-hour air quality objective for PM<sub>10</sub> is 50  $\mu\text{g m}^{-3}$ . Air quality in terms of 24-hour average PM<sub>10</sub> was classified as ‘good’ to ‘very good’ in 96 % of the measurements (Table 17) and ‘fair’ to ‘poor’ the remaining 4% of the time. There were no exceedances of the NEPM 24-hour air quality objective at the North-AQMS (Figure 23). At the South-AQMS there was one exceedance of the NEPM 24-hour air quality objective for PM<sub>10</sub> on September 27th, 2017 (Figure 23). The possible source/s of this PM<sub>10</sub> exceedance at the South-AQMS site on 27 September 2017 were investigated using chemical composition analysis and are discussed in Section 4.3.

At the North and South-AQMS the overall averages of PM<sub>10</sub> measured by the Palas FIDAS instruments for the whole measurement period (late July – December) were 10 and 14  $\mu\text{g m}^{-3}$  respectively. If the average PM<sub>10</sub> concentrations for these approximately four months of monitoring are representative of concentrations across one year then the inferred annual concentrations of PM<sub>10</sub> were below the annual Ambient Air NEPM (2016) guideline of 25  $\mu\text{g m}^{-3}$ .

PM<sub>10</sub> levels observed at the North and South-AQMS using the Palas FIDAS instruments were fairly typical of the Surat Basin region with similar PM<sub>10</sub> AQI values reported for Palas FIDAS data from the Hopeland and Miles Airport monitoring sites during the same period (Table 17).

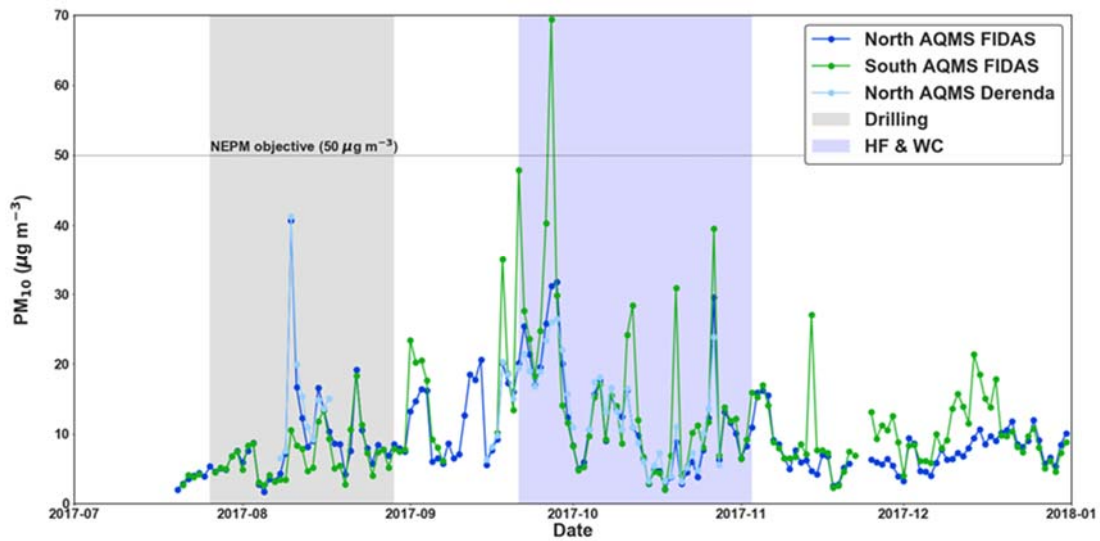


**Figure 23** 24-hour average PM<sub>10</sub> at both North and South-AQMS. Shaded areas represent periods of well development activity on the HF study site, including drilling (grey) and HF + WC (purple).

**Table 16 Monthly maximum and average 24-hour concentrations of PM<sub>10</sub> (µg m<sup>-3</sup>) for North and South-AQMS for the HF study period (Jul – Dec 2017). Data capture (%), overall average PM<sub>10</sub>, and concentrations during HF +WC are also presented. The NEPM 24-hour air quality objective for PM<sub>10</sub> is 50 µg m<sup>-3</sup>.**

PM <sub>10</sub> - 2017	Jul	Aug	Sep	Oct	Nov	Dec	Aug – Dec 2017	HF + WC period 21 <sup>st</sup> Sept – 2 <sup>nd</sup> Nov
<b>North-AQMS – low volume sampler</b>								
Max 24-hour	n.d.	41	27	24	n.d.	n.d.	41	27
Average 24-hour	n.d.	15	18	10	n.d.	n.d.	14	13
% Data Avail	0	55	53	94	0	0	31 <sup>h</sup>	77 <sup>i</sup>
<b>North-AQMS – FIDAS</b>								
Max 24-hour	8	41	32	30	16	12	41	32
Average 24-hour	i.d.	9	16	9	7	8	10	12
% Data Avail	39 <sup>c</sup>	100	100	100	93	100	88 <sup>c</sup>	100
<b>South-AQMS - FIDAS</b>								
Max 24-hour	7	18	69	40	27	21	69	69
Average 24-hour	i.d.	7	23	12	10	10	11	16
% Data Avail	32 <sup>c</sup>	98	70 <sup>a</sup>	98	96	98	82 <sup>a,c</sup>	98

n.d. indicates no data are available; i.d. indicates insufficient data were available to calculate value (< 60% data available). Reasons for data availability < 90 %: a = power outage; b = instrument failure; c = instrument commissioned/ de-commissioned part way through month; d = air-conditioning failure; e = calibration out of tolerance; f = communication / logger failure; g = sample manifold inlet fault; h = sampling only conducted when CSIRO personnel on site 8/8/2017 – 17/8/2017 and 15/9/2017 – 28/10/2017; i= samples not collected due to bad weather or sample media shortage

**Table 17 Proportion of total 24-hour observations of PM<sub>10</sub> in each air quality index category from the FIDAS measurements at the North and South-AQMS at the HF study site, and from Hopeland and Miles Airport sites operated as part of the Surat Basin Ambient Air Monitoring Network. PM was not measured at Burncluth.**

Proportion of total observations in each AQ index category						
AQ Index categories		Very Good	Good	Fair	Poor	Very Poor
PM <sub>10</sub> 24-hour average	North-AQMS (all)	88%	12%	1%	0%	0%
	North-AQMS (HF + WC)	75%	25%	0%	0%	0%
	South-AQMS (all)	83%	13%	3%	1%	0%
	South-AQMS (HF + WC)	70%	20%	7%	2%	0%
	Hopeland	93%	7%	0%	0%	0%
	Miles Airport	87%	11%	2%	0%	0%

#### HF and non-HF related sources of PM<sub>10</sub>

Higher time resolution (5-minute) PM<sub>10</sub> and wind direction data were used to assess the likelihood that increases in PM<sub>10</sub> concentration were a result of well development activity.

Table 19 shows the distributions of 5-minute average PM<sub>10</sub> data measured at the North and South-AQMS when downwind of drilling (A) and when downwind of HF + WC (C), alongside data from other WDRs during the same periods (B and D) and during periods where no drilling/HF/WC activities were occurring (E). The characteristics of the distributions for the PM<sub>10</sub> data from the North and South-AQMS were as follows:

#### North-AQMS:

- The median and inter quartile ranges (IQR, 25<sup>th</sup> – 75<sup>th</sup> percentiles) of PM<sub>10</sub> concentrations were similar for all activity periods and non-activity periods, and all WDRs (medians = 6 to 10 µg m<sup>-3</sup>, IQRs = 4 to 17 µg m<sup>-3</sup>);
- **Drilling** - the top 5 % of values when measuring downwind of drilling were higher than the top 5% of values when measuring air masses from other WDRs during the same period and higher than non-activity periods;
- **HF + WC** - The lowest range in concentrations was observed downwind of HF + WC.

#### South-AQMS:

- The median and inter quartile ranges (IQR, 25<sup>th</sup> – 75<sup>th</sup> percentiles) of PM<sub>10</sub> concentrations were also similar for all activity periods and WDRs (medians = 5 to 13 µg m<sup>-3</sup>, IQRs = 4 to 19 µg m<sup>-3</sup>);

- **Drilling** - The top 5 % of values when measuring downwind of drilling were lower than the top 5% of values when measuring air masses from other WDRs during the same period and lower than during non-activity periods;
- **HF + WC** - The top 5 % of values when measuring downwind of HF +WC were lower than the top 5% of values when measuring air masses from other WDRs during the same period and lower than during non-activity periods.

Overall, measurements downwind of drilling at the North-AQMS coincided with higher PM<sub>10</sub> concentrations, while measurements downwind of HF + WC activity did not coincide with the highest peaks in PM<sub>10</sub> at either the North or South-AQMS sites. Lower PM<sub>10</sub> concentrations downwind of HF + WC than for other WDRs during the same period indicates that activities on site, but not necessarily on the well pads, may be a source of PM<sub>10</sub> during peak events. This is consistent with vehicle traffic on unsealed roads being a source of PM<sub>10</sub> at the study site. The sources of PM<sub>10</sub> at the HF study site were further investigated using chemical composition analysis in Section 4.3.

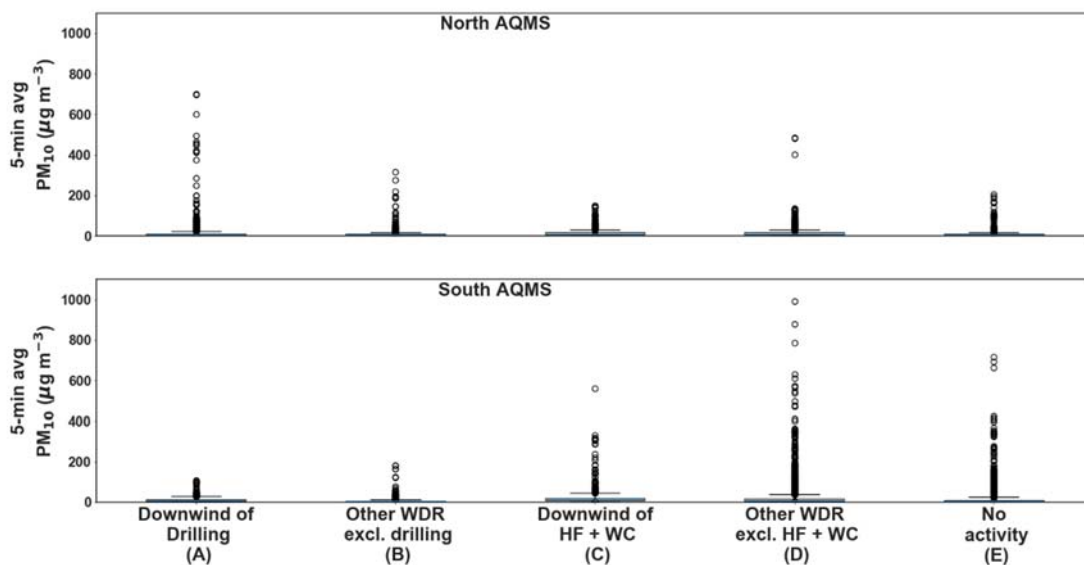


Figure 24 Box and whisker plots of the 5-minute average PM<sub>10</sub> data from the North and South-AQMS measured when downwind of drilling and HF + WC. For comparison PM<sub>10</sub> data from other WDRs during drilling and HF +WC, as well as during non-activity periods are presented. Note the box represents the range between the 25<sup>th</sup> and 75<sup>th</sup> percentiles, the blue line is the median (50<sup>th</sup> percentile), the whiskers represent the 5<sup>th</sup> and 95<sup>th</sup> percentiles and the points above/below the whiskers represent the top/bottom 5% of values.

#### 4.2.2 PM<sub>10</sub> concentrations at the Solar-AQMS sites

PM<sub>10</sub> was also collected on Teflon filters at the five Solar-AQMS sites by Ecotech Microvol low-volume samplers followed by gravimetric mass determination. Between August and November

2017 eight or nine filter samples were intermittently collected at each site. The average duration of these multi-day samples was 8.8 days with approximately 75 days of sampling occurring at each site (Table 18). The time series of the integrated average PM<sub>10</sub> concentrations from the multi-day samples for each of the five Solar-AQMS sites are shown in Figure 25.

The overall average values of PM<sub>10</sub> measured at each of the five Solar-AQMS sites across the sampling period (Aug – Nov) ranged from 16.7 – 22.2 µg m<sup>-3</sup> (Table 18). If the average PM<sub>10</sub> concentrations measured during these approximately four months of sampling were representative of concentrations across one full year, then the inferred annual concentrations of PM<sub>10</sub> were below the annual Ambient Air NEPM (2016) guideline of 25 µg m<sup>-3</sup>.

The highest average PM<sub>10</sub> concentration was measured at Site 4 (22.2 µg m<sup>-3</sup> which is 89% of the annual NEPM PM<sub>10</sub> objective). This was largely accounted for by a single high sample of 70 µg m<sup>-3</sup> collected during the period 6<sup>th</sup> – 13<sup>th</sup> August. This sample period coincided with a TSP exceedance at the North-AQMS on the 10<sup>th</sup> August. Field notes indicate the drill rig was moved from well COM 314 adjacent to Solar-AQMS #4 to COM 313 adjacent to North-AQMS on 10/8/2017. It is possible this high value was related to road dust caused by truck movements. The possible sources of these high values were further investigated using chemical composition analysis and are discussed in Section 4.3.

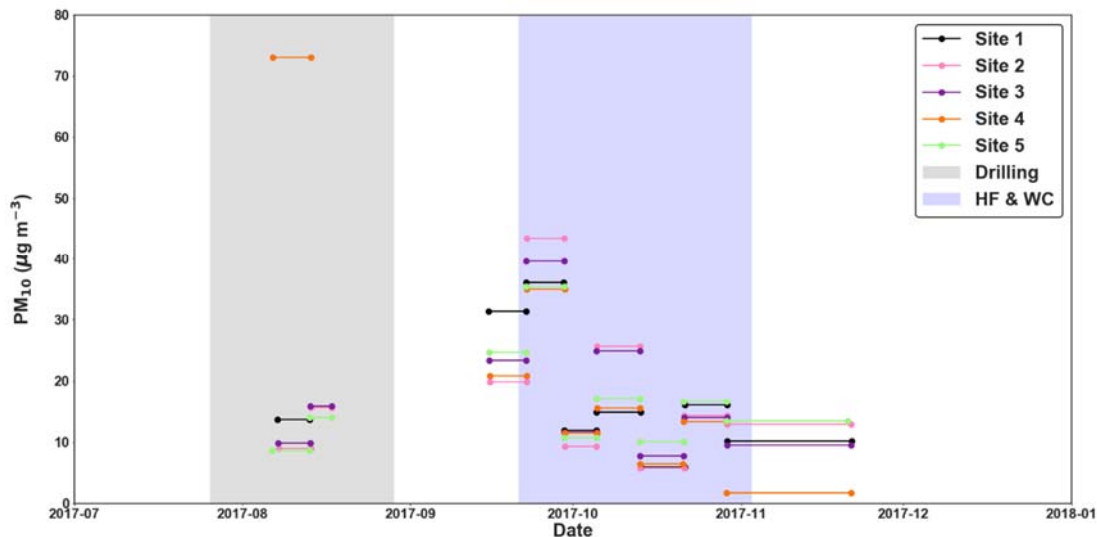


**Figure 25 Multi-day integrated averages for PM<sub>10</sub> at the five Solar-AQMS. Bars represent average PM<sub>10</sub> concentrations at each site. The length of the bar represents the sample duration. Shaded areas represent periods of well development activity on the HF study site, including drilling (grey) and HF + WC (purple).**

**Table 18 Average concentrations of all PM<sub>10</sub> filter samples collected via the Microvol low volume samplers at the five Solar-AQMS. The annual Ambient Air NEPM (2016) guideline of 25 µg m<sup>-3</sup>**

PM <sub>10</sub> - Microvol	Number of samples	Average Sample duration (days)	Total Number of days sampled	Overall average (µg m <sup>-3</sup> )
Site 1	8	9.1	72.8	17.5
Site 2	9	8.5	76.5	17.3
Site 3	9	8.5	76.5	17.4
Site 4	8	9.2	73.6	22.2
Site 5	9	8.6	77.4	16.7

NEPM Annual PM<sub>10</sub> AQ objective is 25 µg m<sup>-3</sup>

### 4.2.3 PM<sub>2.5</sub> concentrations at the North and South-AQMS and Solar-AQMS sites

Summary statistics for PM<sub>2.5</sub> concentration, including monthly 24-hour average and maximum concentrations and data capture rates for the North-AQMS and the South-AQMS are listed in Table 19. Time series of 24-hour average PM<sub>2.5</sub> concentrations measured by FIDAS from the North and South-AQMS and the NEPM 24-hour air quality objective for PM<sub>2.5</sub> (25 µg.m<sup>-3</sup>) are shown in Figure 26. There were no exceedances of the NEPM 24-hour air quality objective for PM<sub>2.5</sub> and air quality in terms of PM<sub>2.5</sub> was classified as ‘good’ to ‘very good’ for 98% of these observations from the North and South-AQMS (Table 20).

In addition to the measurements of PM<sub>2.5</sub> at the North-AQMS and South-AQMS using Palas FIDAS instruments, PM<sub>2.5</sub> was also measured at the five Solar-AQMS sites by MetOne E-samplers. Time series of 24-hour average PM<sub>2.5</sub> concentrations from the five Solar-AQMS sites, and the NEPM 24-hour air quality objective for PM<sub>2.5</sub> are shown in Figure 26. No exceedances of the NEPM 24-hour air quality objective for PM<sub>2.5</sub> were observed at the five Solar-AQMS sites. Air quality in relation to PM<sub>2.5</sub> was classified as ‘good’ to ‘very good’ for 97% - 100% of the observations at the five Solar-AQMS sites. PM<sub>2.5</sub> levels observed at the North-AQMS and South-AQMS were fairly typical of the Surat Basin region with similar PM<sub>2.5</sub> AQI values also reported from FIDAS data from Hopeland and Miles Airport during the same period (Table 20). Note that PM was not measured at the Burncluth site.



**Table 19 Ambient concentrations of PM<sub>2.5</sub> including average and monthly maximum and average 24-hour concentrations (µg.m<sup>-3</sup>), monthly data capture (%), overall average PM<sub>2.5</sub>, percentage of data collected downwind of activities including HF, and average and maximum PM<sub>2.5</sub> downwind of HF +WC activities for North and South-AQMS for 2017.**

PM <sub>2.5</sub> - 2017	Jul	Aug	Sep	Oct	Nov	Dec	Aug – Dec 2017	HF + WC period 21 <sup>st</sup> Sept – 2 <sup>nd</sup> Nov
<b>North-AQMS – FIDAS</b>								
Max 24-hour	3	14	22	14	11	7	22	22
Average 24-hour	i.d.	3	8	6	4	4	5	7
% Data Avail	39 <sup>c</sup>	100	100	100	93	100	88 <sup>c</sup>	100
<b>South-AQMS - FIDAS</b>								
Max 24-hour	3	13	23	13	10	6	23	23
Average 24-hour	i.d.	3	9	6	4	4	5	7
% Data Avail	33 <sup>c</sup>	99	71 <sup>a</sup>	100	97	100	83 <sup>a,c</sup>	100

n.d. indicates no data are available; i.d. indicates insufficient data were available to calculate value (< 60% data available). Reasons for data availability < 90 %: a = power outage; b = instrument failure; c = instrument commissioned/de-commissioned part way through month; d = air-conditioning failure; e = calibration out of tolerance; f = communication / logger failure; g = sample manifold inlet fault.

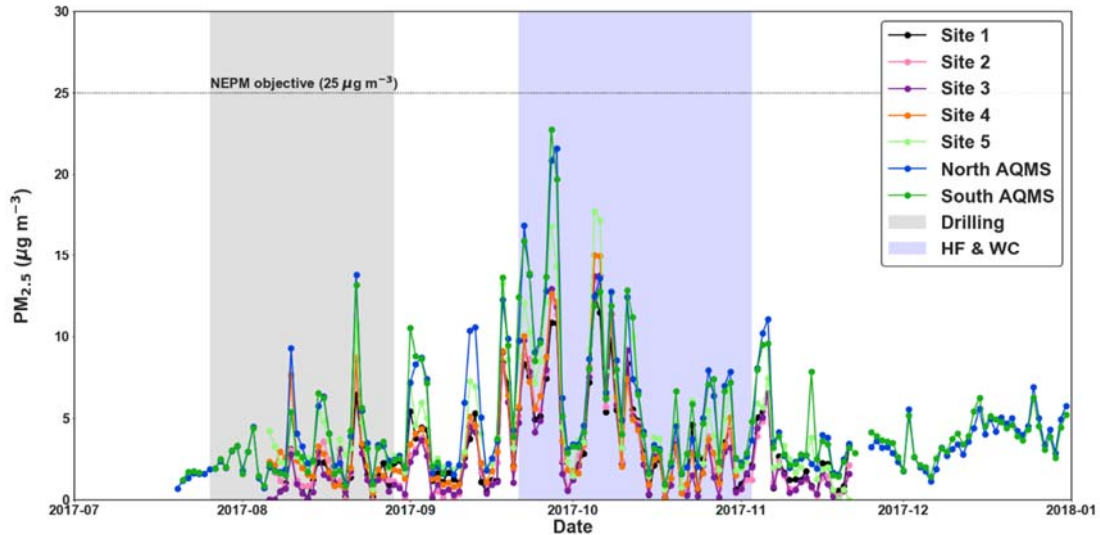


Figure 26 24-hour average  $PM_{2.5}$  measured at the North and South-AQMS by Palas FIDAS and at the five Solar-AQMS sites measured by MetOne E-Sampler. Site 5 was co-located with the South-AQMS. Shaded areas represent periods of well development activity on the HF study site, including drilling (grey) and HF + WC (purple).

Table 20 Proportion of total 24-hour observations of  $PM_{2.5}$  in each air quality index category from the North and South-AQMS' and five Solar-AQMS at the HF study site, and from Hopeland and Miles Airport sites operated as part of the Surat Basin Ambient Air Monitoring Network. PM was not measured at Burncluth.

Proportion of total observations in each AQ index category						
AQ Index categories	Very Good	Good	Fair	Poor	Very Poor	
PM <sub>2.5</sub> 24-hour Average	North-AQMS (all)	85%	13%	2%	0%	0%
	North-AQMS (HF + WC)	68%	25%	7%	0%	0%
	South-AQMS	86%	13%	1%	0%	0%
	South-AQMS (HF + WC)	70%	25%	5%	0%	0%
	Site 1	92%	8%	0%	0%	0%
	Site 2	91%	9%	0%	0%	0%
	Site 3	92%	8%	0%	0%	0%
	Site 4	90%	10%	0%	0%	0%
	Site 5	85%	12%	3%	0%	0%
	Hopeland	86%	12%	1%	0%	0%
	Miles Airport	88%	11%	1%	1%	0%

### HF and non-HF related sources of PM<sub>2.5</sub>

Higher time resolution (5-minute) PM<sub>2.5</sub> and wind direction data were used to assess the likelihood that increases in PM<sub>2.5</sub> concentration were a result of well development activity.

Figure 27 shows the distributions of 5-minute average PM<sub>2.5</sub> data measured at the North and South-AQMS when downwind of drilling (A) and when downwind of HF + WC (C), alongside data from other WDRs during the same periods (B and D) and during periods where no drilling/HF/WC activities were occurring (E). The characteristics of the distributions for the PM<sub>2.5</sub> data from the North and South-AQMS were as follows:

#### North-AQMS:

- The median and inter quartile (IQR, 25<sup>th</sup> – 75<sup>th</sup>) percentiles ranges of PM<sub>2.5</sub> concentrations were similar for all activity periods and non-activity periods, and all WDRs (medians = 2 to 5 µg m<sup>-3</sup>, IQRs = 2 to 10 µg m<sup>-3</sup>);
- **Drilling** - the top 5 % of values when measuring downwind of drilling (A) were higher than the top 5% of values when measuring air masses from other WDRs during the same period (B) and higher than non-activity periods (E);
- **HF + WC** - The lowest range of concentrations was observed downwind of HF + WC (C).

#### South-AQMS:

- The median and inter quartile (IQR, 25<sup>th</sup> – 75<sup>th</sup>) ranges of PM<sub>2.5</sub> concentrations were also similar for all activity periods and WDRs (medians = 2 to 8 µg m<sup>-3</sup>, IQRs = 1 to 12 µg m<sup>-3</sup>);
- **Drilling** - the top 5 % of values when measuring downwind of drilling (A) were close to or lower than the top 5% of values when measuring air masses from other WDRs during the same period (B) and during non-activity periods (E);
- **HF + WC** - the top 5 % of values when measuring downwind of HF +WC (C) were close to or lower than the top 5% of values when measuring air masses from other WDRs (D) during the same periods and during non-activity periods (E).

Overall, drilling at the North-AQMS coincided with higher PM<sub>2.5</sub> concentrations, while HF + WC activity was not associated with the highest peaks in PM<sub>2.5</sub> at either site. This is consistent with the results for PM<sub>10</sub> and indicates that activities on site, but not necessarily on the well pads, may be the source of peak events. The sources of PM<sub>2.5</sub> at the HF study site were further investigated using chemical composition analysis in Section 4.3.

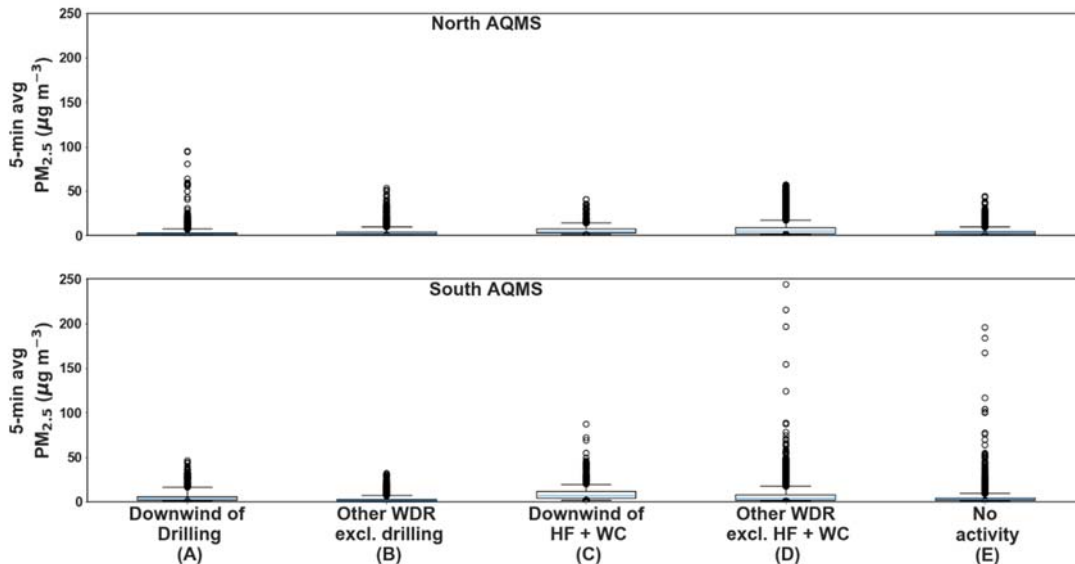


**Figure 27** Box and whisker plots of the 5-minute average  $PM_{2.5}$  data from the North and South-AQMS measured when downwind of drilling and HF + WC. For comparison  $PM_{10}$  data from other WDRs during drilling and HF +WC, as well as during non-activity periods are presented. Note the box represents the range between the 25<sup>th</sup> and 75<sup>th</sup> percentiles, the blue line is the median (50<sup>th</sup> percentile), the whiskers represent the 5<sup>th</sup> and 95<sup>th</sup> percentiles and the points above/below the whiskers represent the top/bottom 5% of values.

#### 4.2.4 Total suspended particles (TSP)

In addition to  $PM_{10}$  and  $PM_{2.5}$ , total suspended particulates (TSP) were also measured by the Palas FIDAS instruments at the North and South-AQMS in this study. In this case TSP refers to particles with a diameter  $< 18 \mu m$ . The Queensland EPP for Air prescribes an annual air quality objective value of  $90 \mu g m^{-3}$  for TSP. An Australian 24-hour ambient air objective does not exist for total TSP. Instead the 24-hour air quality objective used here is based on the New Zealand Ministry for the Environment's nuisance trigger level of  $60 \mu g m^{-3}$  for high sensitivity areas (MFE 2016) as recommended by Queensland's Department of Environment and Science (DES). Due to TSP measured by the FIDAS (up to  $18 \mu m$ ) and the Australian Standard method (up to  $100 \mu m$ ) (AS/NZS 3580.9.3:2015) being non-equivalent the data from this study can only be considered indicative and cannot be considered equivalent to Australian Standard Method (AS/NZS 3580.9.3:2015).

Summary statistics for TSP concentration including monthly 24-hour average and maximum concentrations and data capture rates for the North-AQMS and the South-AQMS are listed in Table 21. A time series showing 24-hour average TSP concentrations at both the North-AQMS and South-AQMS monitoring stations are shown in Figure 28 along with the New Zealand Ministry for the Environment's nuisance trigger level for high sensitivity areas (MFE 2016) of  $60 \mu g m^{-3}$ . In terms of TSP air quality was classified as 'good' to 'very good' in 93% of the observations at the HF

study site (Table 22). There were six exceedances of the nuisance trigger level for TSP at the South-AQMS on September 18<sup>th</sup>, 21<sup>st</sup>, 26<sup>th</sup>, 27<sup>th</sup> and October 20<sup>th</sup> and 27<sup>th</sup>, 2017. There was one exceedance of the nuisance trigger level for TSP on August 10<sup>th</sup> and one on October 27<sup>th</sup>, 2017 at the North-AQMS. The exceedance of the nuisance trigger level for TSP at the South-AQMS on September 27<sup>th</sup> coincided with an exceedance of the NEPM 24-hour air quality objective for PM<sub>10</sub> at the South-AQMS (Section 4.2.1).

As described in section 2.3, during the intensive monitoring phase of this study the CSIRO team members maintained daily written logs of the HF operations and other activities relevant to air quality that were occurring in the field during sampling. The activity occurring on site during PM exceedances are summarised in the subsequent section 4.2.5. Possible sources of the TSP exceedances at the North and South-AQMS sites were further investigated using chemical composition analysis and the results are discussed in Section 4.3.

TSP levels observed at the North and South-AQMS were fairly typical of the Surat Basin region with similar TSP air quality index values calculated from FIDAS measurements at Hopeland and Miles Airport during the same period (Table 27). TSP was not measured at the Burncluth air monitoring site.

**Table 21 Ambient concentrations of TSP including average and monthly maximum and average 24-hour concentrations ( $\mu\text{g}\cdot\text{m}^{-3}$ ) for the North and South-AQMS (Jul – Dec 2017). Data capture (%), overall average and maximum TSP, and TSP concentrations during HF + WC are also included.**

TSP - 2017	Jul	Aug	Sep	Oct	Nov	Dec	Aug – Dec 2017	HF + WC period 21 <sup>st</sup> Sept – 2 <sup>nd</sup> Nov
<b>North-AQMS – FIDAS</b>								
Max 24-hour	12	72	43	60	24	18	60	60
Average 24-hour	i.d.	16	24	13	11	12	14	18
% Data Avail	39 <sup>c</sup>	100	100	100	93	100	88 <sup>c</sup>	100
<b>South-AQMS - FIDAS</b>								
Max 24-hour	11	23	130	106	45	47	130	130
Average 24-hour	i.d.	11	39	21	16	18	19	28
% Data Avail	33 <sup>c</sup>	99	71 <sup>a</sup>	100	97	100	83 <sup>a,c</sup>	100

n.d. indicates no data are available; i.d. indicates insufficient data were available to calculate value (< 60% data available). Reasons for data availability < 90 %: a = power outage; b = instrument failure; c = instrument commissioned/de-commissioned part way through month; d = air-conditioning failure; e = calibration out of tolerance; f = communication / logger failure; g = sample manifold inlet fault.

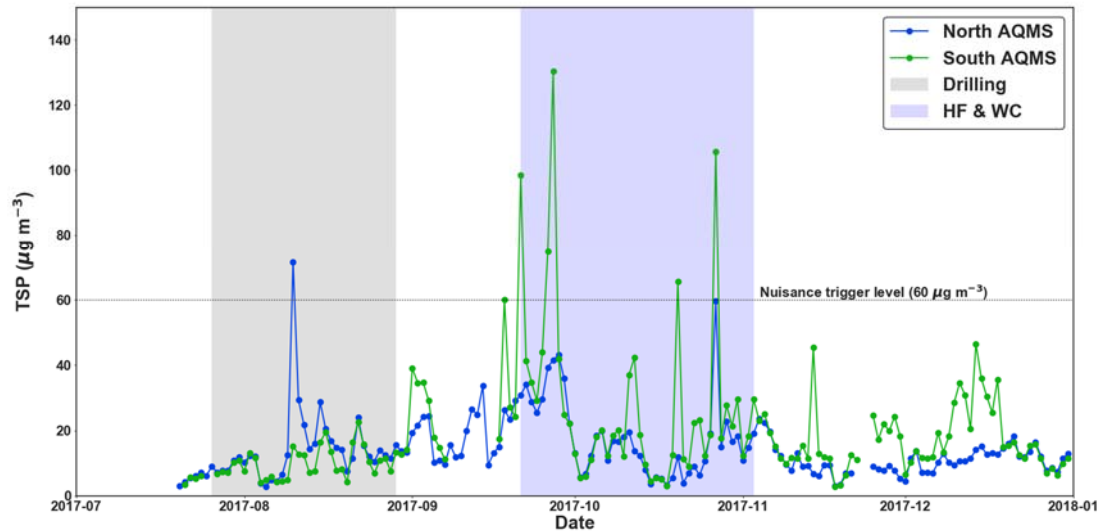


Figure 28 24-hour averages for total suspended particles at both North and South-AQMS. Shaded areas represent periods of well development activity on the HF study site, including drilling (grey) and HF + WC (purple).

Table 22 Proportion of total 24-hour observations of TSP in each air quality index category from the North and South-AQMS' at the HF study site, and from Hopeland and Miles Airport sites operated as part of the Surat Basin Ambient Air Monitoring Network. PM including TSP was not measured at Burnluith.

Proportion of total observations in each AQ index category						
AQ Index categories	Very Good	Good	Fair	Poor	Very Poor	
TSP 24-hour average	North-AQMS (all)	81%	17%	1%	1%	0%
	North-AQMS (HF + WC)	70%	23%	5%	2%	0%
	South-AQMS (all)	70%	23%	4%	2%	2%
	South-AQMS (HF + WC)	50%	30%	9%	5%	7%
	Hopeland	86%	14%	0%	0%	0%
	Miles Airport	73%	19%	6%	2%	0%

### HF and non-HF related sources of TSP

Higher time resolution (5-minute) TSP and wind direction data were used to assess the likelihood that increases in TSP concentration were a result of well development activity.

Figure 29 shows the distributions of 5-minute average TSP data measured at the North and South-AQMS when downwind of drilling (A) and when downwind of HF + WC (C) alongside data from

other WDRs during the same periods (B and D) and during periods where no drilling/HF/WC activities were occurring (E). The characteristics of the distributions for the TSP data from the North and South-AQMS were as follows-

**North-AQMS:**

- The median and inter quartile ranges of TSP were similar for all activity periods and non-activity periods, and all WDRs (medians = 10 to 14  $\mu\text{g m}^{-3}$ , IQRs = 6 to 27  $\mu\text{g m}^{-3}$ );
- **Drilling** - the top 5 % of values when measuring downwind of drilling were higher than the top 5% of values when measuring air masses from other WDRs during the same period and higher than non-activity periods;
- **HF + WC** - The lowest range of concentrations was observed downwind of HF + WC.

**South-AQMS:**

- The median and inter quartile ranges of TSP were also similar for all activity periods and WDRs (medians = 2 to 8  $\mu\text{g m}^{-3}$ , IQRs = 7 to 18  $\mu\text{g m}^{-3}$ );
- **Drilling** - The top 5 % of values when measuring downwind of drilling were close to or lower than the top 5% of values when measuring air masses from other WDRs during the same periods and during non-activity periods;
- **HF + WC** - The top 5 % of values when measuring downwind of HF + WC were close to or lower than the top 5% of values when measuring air masses from other WDRs during the same periods and during non-activity periods.

Overall drilling at the North-AQMS was associated with higher TSP concentrations while HF +WC activity was not associated with higher peaks in TSP at either site. This is consistent with the results for  $\text{PM}_{10}$  and  $\text{PM}_{2.5}$  and indicates that activities on site, but not necessarily on the well pads, may be the source of TSP during peak events. This is consistent with vehicle traffic on unsealed roads being a source of TSP at the study site. The sources of TSP at the HF study site were further investigated using chemical composition analysis in Section 4.3.

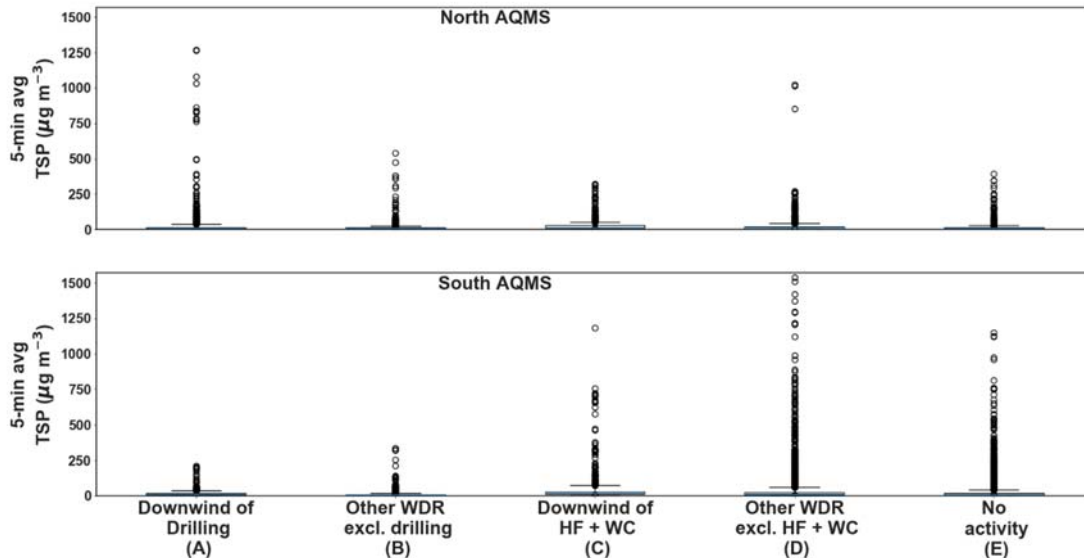


Figure 29 Box and whisker plots of the 5-minute average PM<sub>2.5</sub> data from the North and South-AQMS measured when downwind of drilling and HF + WC. For comparison PM<sub>10</sub> data from other WDRs during drilling and HF +WC, as well as during non-activity periods are presented. Note the box represents the range between the 25<sup>th</sup> and 75<sup>th</sup> percentiles, the blue line is the median (50<sup>th</sup> percentile), the whiskers represent the 5<sup>th</sup> and 95<sup>th</sup> percentiles and the points above/below the whiskers represent the top/bottom 5% of values.

#### 4.2.5 Summary of PM Exceedances

The concentrations of PM<sub>10</sub>, PM<sub>2.5</sub> and TSP measured at the North and South-AQMS and the five Solar-AQMS during the HF study were compared with relevant ambient air quality objectives and the following exceedances of air quality objectives were observed:

- **North-AQMS** - 2 exceedances of the TSP 24-hour nuisance trigger level. No exceedances of PM<sub>10</sub> or PM<sub>2.5</sub> NEPM air quality objectives;
- **South-AQMS** - 6 exceedances of the TSP 24-hour nuisance trigger level at the North-AQMS and one exceedance of the PM<sub>10</sub> NEPM air quality objective. No exceedances of PM<sub>2.5</sub> air quality objectives.

These nine exceedances occurred on seven separate days: August 10<sup>th</sup>, September 18<sup>th</sup>, 21<sup>st</sup>, 26<sup>th</sup>, and 27<sup>th</sup>, and October 20<sup>th</sup>, and 27<sup>th</sup>. As described in section 2.3 during the intensive monitoring phase of this study, CSIRO team members maintained daily written logs of the HF operations and other activities relevant to air quality that were observed in the field during sampling. The written field logs indicate that drilling, HF or WC was taking place on 6 of the 7 days when PM exceedances occurred (August 10<sup>th</sup>, September 21<sup>st</sup>, 26<sup>th</sup>, and 27<sup>th</sup>, and October 20<sup>th</sup>, and 27<sup>th</sup>). On the remaining day, 18<sup>th</sup> September, site set-up activities were occurring.

As noted in the preceding sections (4.2.1 – 4.2.4) high concentrations of PM occurred when drilling and HF + WC activities were taking place on site. However, the boxplots of high time resolution data (5-minute) presented in sections 4.2.1, 4.2.3 – 4.2.4 also showed the following:

- At the North-AQMS, 5-minute average peak values in TSP, PM<sub>10</sub> and PM<sub>2.5</sub> were highest in data collected downwind of drilling, but this was not the case at the South-AQMS;
- For both the North and South-AQMS, 5-minute average peak values in TSP, PM<sub>10</sub> and PM<sub>2.5</sub> were highest in data collected downwind of HF + WC and were close to or lower than when sampling air masses from other WDRs during the same period and lower than during non-activity periods.

Lower PM concentrations downwind of HF + WC than for other WDRs during the same period indicates that activities on site, but not on the well pads, may be a source of PM during peak events. This is consistent with vehicle traffic on unsealed roads being a source of PM at the study site. To further investigate the sources of PM at the HF study site, in particular possible sources contributing to exceedances in PM concentrations, the chemical composition of the PM collected on filters at the HF study site were analysed and the results are reported in the proceeding section (4.3).

### 4.3 Chemical Composition Analysis of Particulate Matter

As discussed in section 4.2, at the HF study site potential sources of PM include

- dust
- smoke
- sea salt
- vehicle exhaust
- industrial emissions
- agricultural chemical sprays
- storage, handling and mixing of proppant (sand) and dry chemicals (e.g. potassium chloride, gelling agents, gel breakers and biocides).
- secondary production in the atmosphere via reactions between gaseous air pollutants.

The chemical composition of PM will differ depending on the sources of PM present. In this section, chemical composition data are used to identify possible sources of PM at the HF study site and factors that may have contributed to exceedances of PM air quality objectives.

## PM Chemical Composition Analysis Methods

Three of the sampling techniques employed in this study involved the collection of PM onto Teflon filters:

- 2 x 12-hour samples of PM<sub>10</sub> collected per day using Comde-Derenda low volume samplers at North-AQMS;
- ~ 1 week samples of PM<sub>10</sub> collected by Ecotech Microvols at Solar-AQMS #1 – #5;
- ~1 week samples of PM<sub>2.5</sub> collected by MetOne e-Samplers at Solar-AQMS #1 – #5.

In addition to gravimetric mass determination (reported in Section 4.2) the filters underwent several analytical procedures to determine the chemical composition of the particle mass. Firstly, the filters underwent non-destructive ion beam analysis (IBA) conducted by ANSTO at the Lucas Heights laboratory by the ANSTO STAR 2MV accelerator using simultaneous nuclear IBA techniques:

- Proton induced X-ray emission (PIXE) –analysis of elements (e.g. aluminium zirconium)
- Proton induced gamma-ray emission (PIGE) – analysis of light elements (e.g. sodium)

The elements that were determined by IBA were:

Sodium (Na)	Potassium (K)	Nickel (Ni)	Strontium (Sr)
Aluminium (Al)	Calcium (Ca)	Copper (Cu)	Yttrium (Y)
Silicon (Si)	Titanium (Ti)	Zinc (Zn)	Zirconium (Zr)
Phosphorous (P)	Chromium (Cr)	Gallium (Ga)	
Sulfur (S)	Manganese (Mn)	Arsenic (As)	
Chlorine (Cl)	Iron (Fe)	Rubidium (Rb)	

A full description of these methods and how they are used can be found on the ANSTO web page (<http://www.ansto.gov.au/ResearchHub/OurResearch/IER/Capabilities/IBA/index.htm>).

Secondly, ANSTO measured equivalent black carbon (EBC) using a light-absorption technique called the laser integrated plate method (LIPM), the use of which has been well-established for Australian conditions (Taha et al. 2007, Hibberd et al 2015, 2013).

Lastly, the filter samples were analysed using ion chromatography at the CSIRO Aspendale laboratories for major water-soluble ions and anhydrous sugars including levoglucosan and mannosan (woodsmoke tracers).

The ionic species whose concentrations were determined by ion chromatography were:

Chloride (Cl <sup>-</sup> )	Oxalate (C <sub>2</sub> O <sub>4</sub> <sup>-</sup> )	Sodium (Na <sup>+</sup> )	Levoglucosan (C <sub>6</sub> H <sub>10</sub> O <sub>5</sub> )
Nitrate (NO <sub>3</sub> <sup>-</sup> )	Formate (HCOO <sup>-</sup> )	Ammonium (NH <sub>4</sub> <sup>+</sup> )	Mannosan (C <sub>6</sub> H <sub>10</sub> O <sub>5</sub> )
Sulfate (SO <sub>4</sub> <sup>2-</sup> )	Acetate (CH <sub>3</sub> COO <sup>-</sup> )	Magnesium (Mg <sup>2+</sup> )	
Phosphate (PO <sub>4</sub> <sup>3-</sup> )	Methanesulfonate (MSA <sup>-</sup> )	Calcium (Ca <sup>2+</sup> )	
		Potassium (K <sup>+</sup> )	

#### 4.3.1 Queensland EPP air pollutants present in PM<sub>10</sub>

The Queensland Environmental Protection Policy (EPP) for Air (2008) prescribes air quality objectives for a number of specific compounds/elements that may be present in PM<sub>10</sub>, four of which were measured in the analysis of PM<sub>10</sub> composition undertaken for this study. They were arsenic, manganese, nickel, and sulfate. Table 23 shows the frequency each species was detected above the detection limit of the method, the range of observed 12-hour average concentrations (N = 94) of each species and their relevant EPP air quality objectives. The observed concentrations of arsenic, manganese, nickel, and sulfate were always below the EPP air quality objectives.

**Table 23 Detection frequency and average concentrations of arsenic, manganese, nickel and sulfate from the North-AQMS, and the QLD EPP air quality objectives for these elements/compounds**

Component of PM <sub>10</sub>	Detection Frequency	Overall Average	Qld EPP Air Quality Objective
Arsenic	5%	≤ MDL (2 ng m <sup>-3</sup> )	6 ng m <sup>-3</sup> (annual)
Manganese	64%	0.008 µg m <sup>-3</sup>	0.16 µg m <sup>-3</sup> (annual)
Nickel	1%	≤ MDL (1 ng m <sup>-3</sup> )	20 ng m <sup>-3</sup> (annual)
Component of PM <sub>10</sub>	Detection Frequency	24-hour Maximum	Qld EPP Air Quality Objective
Sulfate	100%	5 µg m <sup>-3</sup>	27 µg m <sup>-3</sup> (24-hour)

#### 4.3.2 PM<sub>10</sub> Source Apportionment

Source Apportionment analysis was applied to the PM<sub>10</sub> chemical composition data to identify the factors that contributed to the total PM<sub>10</sub> mass concentrations observed at the HF study site. This method has been used in previous studies by CSIRO to characterize the factors contributing to PM<sub>2.5</sub> in an urban – industrial region of NSW (Hibberd et al. 2013, 2016). In this section, the source apportionment analysis is used to identify possible sources of PM at the HF study site, the average contribution of these sources to PM<sub>10</sub> and the factors that coincided with exceedances of PM air quality objectives.

The concentration of 26 chemical species measured on the 93 PM<sub>10</sub> samples collected at the North-AQMS (9/8 – 15/8/2017, 18/9 – 25/10/2017) were entered into a positive matrix factorisation (PMF) receptor model (Norris & Duvall, 2014). This receptor model relies on internal correlations between species in the data set to identify both the factors contributing to the samples and the amount that each factor contributed to the total PM<sub>10</sub> mass collected on the filter.

The methods used to determine the concentrations of the 26 chemical species, the quality assurance and control methods employed to ensure high quality data and the methods used to select the species to incorporate into the PMF model are described in detail in Appendix 10. Appendix 10 also includes a description of the PMF model and how it was used.

#### **4.3.2.1 PMF factors and source tracers**

Using the PMF model, eight factors were identified to be contributing to the PM<sub>10</sub> chemical composition during the study. Each of the eight factors was characterised by a chemical ‘fingerprint’ which is a pattern of chemical species and their concentrations. Figure 30 shows the fingerprints for each factor and includes information on the average concentrations of each species contributing to the fingerprint (vertical blue columns) and the fraction of the total mass of the species accounted for by the Factor (red squares).

Table 24 lists the Factors identified by the PMF, the chemical species that contribute to the factors, the average contribution of each factor to total PM<sub>10</sub> mass and the possible sources of each factor. Each of these factors is discussed in more detail below. In summary, PM<sub>10</sub> mass was dominated by the Soil and Secondary Ammonium Sulfate Factors, which on average accounted for 37% and 16% of the PM<sub>10</sub> mass respectively. Fresh Sea Salt and Secondary Nitrate-Aged Sea Salt together contributed on average a further 22% of the PM<sub>10</sub> mass. The combined smoke factors (Woodsmoke and Aged Biomass Smoke) contributed on average 18% of the PM<sub>10</sub> mass. The remaining 7% was made up of aerosols of biological origin including fungal spores and biota found in soils.

These sources are typical of PM<sub>10</sub> sources measured in other rural locations e.g. at a rural location in the north of Spain four factors identified to contribute to PM<sub>10</sub> were crustal (equivalent to Soil), secondary sulphate (equivalent to Secondary Ammonium Sulfate), secondary nitrate (equivalent to Secondary Nitrate-Aged Sea Salt) and sea salt (Aldabe et al., 2011). The work presented here appears to be the first report of source apportionment for PM<sub>10</sub> in an Australian rural location. Other source apportionment studies in rural or background areas in Australia have been carried out on PM<sub>2.5</sub> including at Cape Grim in NorthWest Tasmania (Crawford et al., 2017) and Yarrangobilly in the Snowy Mountains, SE Australia (Tadros et al., 2018), where similar factors were identified.

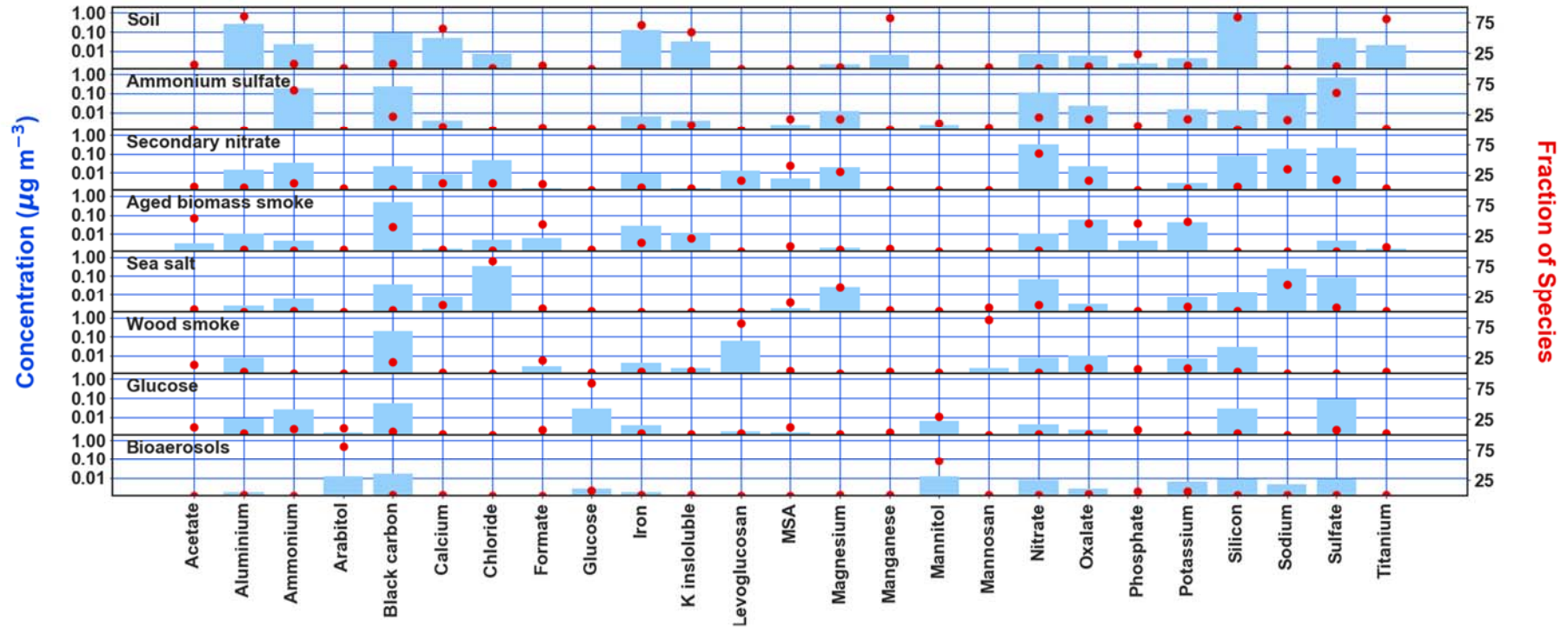


Figure 30 Chemical fingerprints for each Factor. Left axis and blue bars represents the concentration of each species contributing to the fingerprint. Right axis and red square represent the fraction of the total mass of the species accounted for by the factor

**Table 24 Summary of factors identified by the PMF, the chemical species that contribute to the factors, the percentage of total mass that the factor comprises and the potential sources that contribute to the factor.**

Factor	Main species contributing to the factor (largest contributors in bold)	Average contribution of the factor to PM <sub>10</sub> mass over the whole study period (uncertainty range)	Potential sources (primary/secondary)
Factor 1 Soil	<b>Silicon (Si):Aluminium (Al):Titanium (Ti)</b> , Iron, Calcium, insoluble Potassium (K), Black Carbon (BC)	37% (25-42%)	Primary particles - Soil dust.
Factor 2 Secondary Ammonium Sulfate	<b>Ammonium (NH<sub>4</sub><sup>+</sup>) :non-sea salt sulfate (nssSO<sub>4</sub><sup>2-</sup>)</b> , BC	16% (9-18%)	Secondary Ammonium sulfate aerosol Products of reactions between local & regional sources of SO <sub>2</sub> (e.g. fossil fuel burning) and ammonia (agriculture, industry, vehicles, non-road diesel equipment, soils)
Factor 3 Secondary Nitrate-Aged Sea Salt	<b>Sodium (Na<sup>+</sup>): Magnesium (Mg<sup>2+</sup>), nitrate (NO<sub>3</sub><sup>-</sup>)</b> , BC, almost no Chloride (Cl <sup>-</sup> )	13% (7-19%)	Mixed primary and secondary aerosol Sea salt reacted with industrial, commercial, road & non-road transport emission from local & regional sources, esp. NO <sub>2</sub>
Factor 4 Aged Biomass Smoke	<b>BC, potassium (K<sup>+</sup>), Oxalate, Formate, Acetate</b>	11% (8-21%)	Mixed primary and secondary aerosol Mixture of primary emissions from biomass burning and/or biofuels (BC, K <sup>+</sup> ) with secondary aerosol from oxidation of VOCs emitted in smoke.
Factor 5 Fresh Sea Salt	<b>Na<sup>+</sup>, Mg<sup>2+</sup>, Cl<sup>-</sup></b>	9% (8-14%)	Primary aerosol Fresh sea salt aerosol from wave-breaking
Factor 6 Wood Smoke	<b>Levoglucosan</b> , BC, K <sup>+</sup> , <b>Mannosan</b>	7% (5-10%)	Primary aerosol Domestic woodheaters, bushfires, hazard reduction burns
Factor 7 Glucose	<b>Glucose</b> , Mannitol	5% (3-9%)	Primary aerosol Fungi, lichen and soil biota
Factor 8 Primary Biological Aerosols	<b>Arabitol, Mannitol</b>	2% (2-9%)	Primary aerosol Natural fungal spores found in soil.

#### 4.3.2.2 Source indicator species

The PMF analysis was based on the 12-hour PM<sub>10</sub> samples collected by the low volume sampler at the North-AQMS. The key species identified in each factor in the PMF analysis listed in Table 24 can be used as tracers for the factors that contributed to PM<sub>10</sub> mass measured on the multi-day

samples collected with the Microvols at the Solar-AQMS. The key species used for this analysis are listed in Table 25.

**Table 25 Key species used to identify sources contributing to the multi-day samples collected with the Microvol samplers at the Solar-AQMS sites**

Factor	Indicator species
Factor 1 Soil	Si and Al
Factor 2 Secondary Ammonium Sulfate	nssSO <sub>4</sub> <sup>2-</sup>
Factor 3 Secondary Nitrate-Aged Sea Salt	NO <sub>3</sub> <sup>-</sup>
Factor 4 Aged Biomass Smoke	K <sup>+</sup> (and BC)
Factor 5 Fresh Sea Salt	Cl <sup>-</sup>
Factor 6 Wood Smoke	Levoglucosan (and BC)
Factor 7 Glucose	Glucose
Factor 8 Primary Biological Aerosols	Arabitol

The average concentrations of the indicator species and other key species from each factor from the multiday samples of PM<sub>10</sub> collected by Microvols and PM<sub>2.5</sub> collected by E-Samplers at the Solar-AQMS sites are shown in Figure 31. Silicon, the Soil Factor tracer (Factor 1), was the dominant contributor to PM<sub>10</sub> mass collected on the Microvol filters across all five Solar-AQMS during the sampling period (Aug – Nov). Black carbon (BC), associated with the two smoke Factors (Factor 4 Aged Biomass Smoke and Factor 6 Wood Smoke), was on average the second largest contributor to PM<sub>10</sub> mass at the Solar-AQMS sites, with other significant contributions from non-sea salt sulfate (nss SO<sub>4</sub><sup>2-</sup>) associated with Secondary Ammonium Sulfate Factor (Factor 2) and Na<sup>+</sup> associated with Secondary Nitrate-Aged Sea Salt Factor (Factor 3).

The dominant species in PM<sub>2.5</sub> at the Solar-AQMS sites was BC associated with the two smoke Factors (Factor 4 Aged Biomass Smoke and Factor 6 Wood Smoke), followed by key species associated with Secondary Ammonium Sulfate Factor (Factor 2) and Secondary Nitrate-Aged Sea Salt Factor (Factor 3). Since soil particles exist primarily in the coarse size (> PM<sub>2.5</sub>), the lower concentrations of Silicon in the PM<sub>2.5</sub> samples collected at the Solar-AQMS sites is expected (Figure 31).

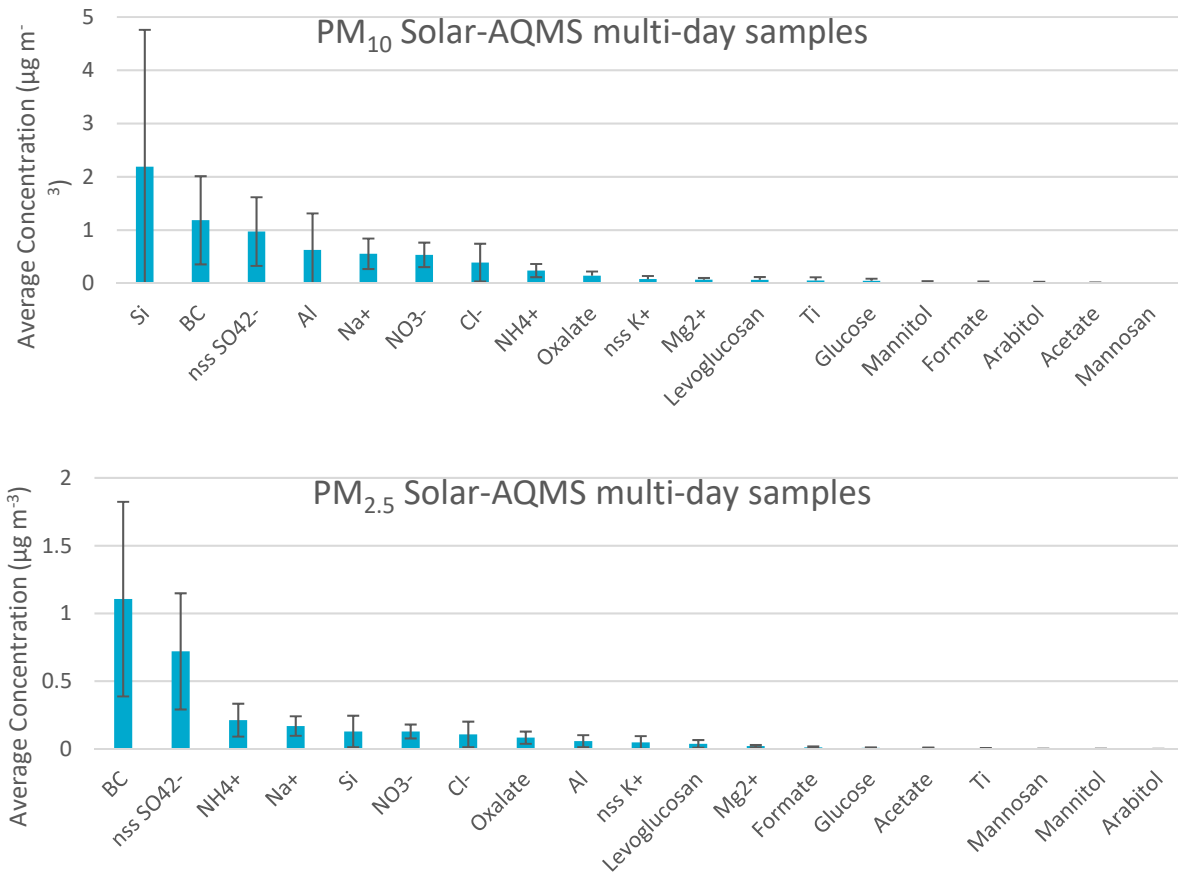


**Figure 31** The average concentration of the indicator species and other key species from each factor from the 12-hour samples of PM<sub>10</sub> collected by the Comde-Derenda low volume sampler (top) and the multi-day samples of PM<sub>10</sub> collected by Microvolts (middle) and PM<sub>2.5</sub> collected by E-Samplers (bottom) at the Solar-AQMS sites (#1 - #5). Error bars represent ± one standard deviation.

Overall, the data presented in the preceding sections (4.3.2.1, and 4.3.2.2) identified the factors which on average made the largest contribution to PM<sub>10</sub> and PM<sub>2.5</sub> over the study period. However, the contribution of each of the factors to PM varied with time as shown in the time series of the contribution of each PMF Factor to 24-hour average PM<sub>10</sub> at the North-AQMS (µg m<sup>-3</sup>) presented in Figure 32. For example, Fresh Sea Salt contributed on average 9% to PM<sub>10</sub> at the North-AQMS (Table 25), however there were multiple 24-hour periods where Fresh Sea Salt was the dominant contributor to PM<sub>10</sub> (Figure 32). Variability in the contribution of each factor was likely due to changes in emissions (e.g. the occurrence of smoke from fires, traffic related dust emissions) and meteorology (e.g. rainfall which suppressed air borne PM, and prevailing winds which influence regional transport of pollutants to the site). The following sections discuss the characteristics of each factor in turn, including their possible role in PM exceedances, the likely sources of each factor including well development activity, and the influence of meteorology on their contribution to PM at the HF study site.

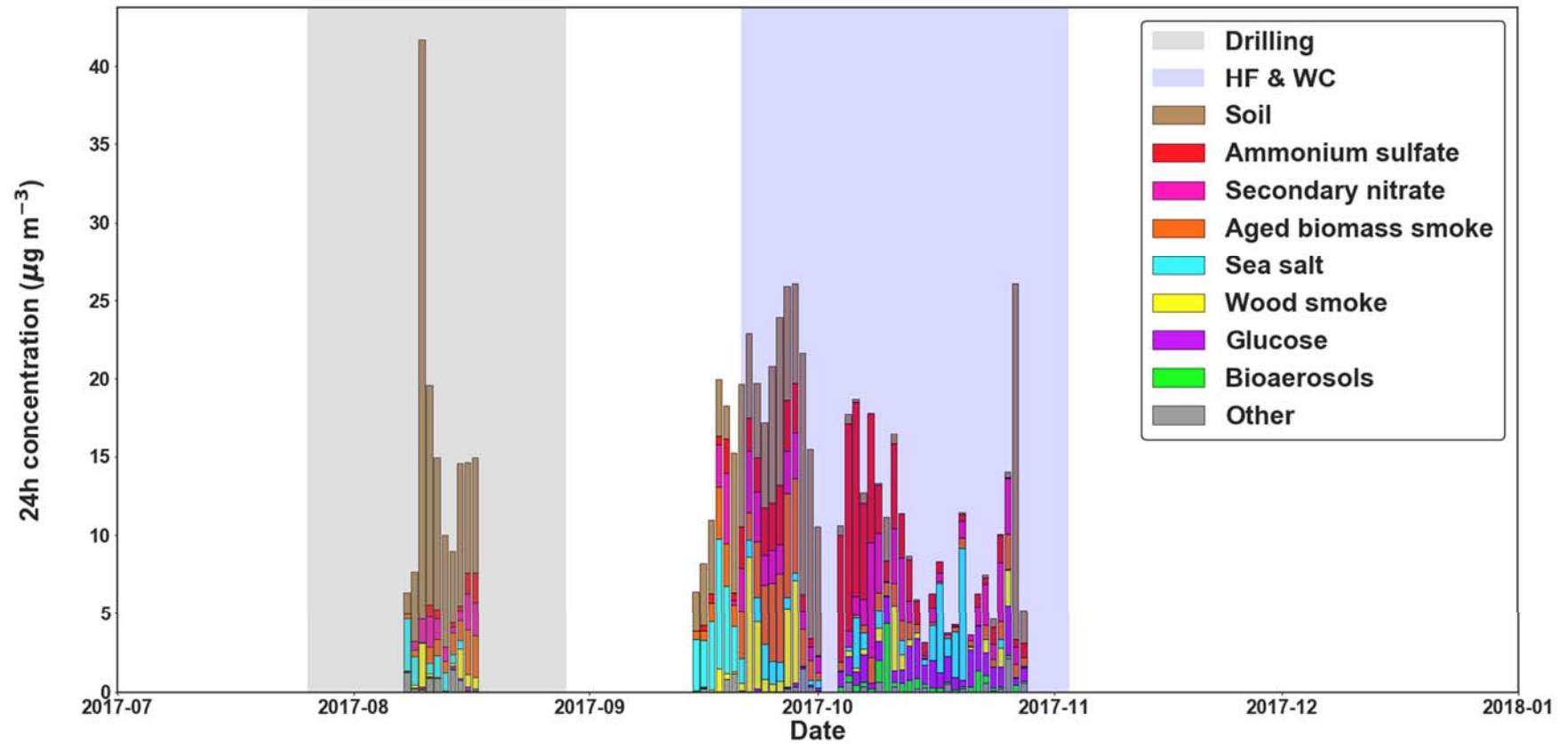


Figure 32 Time series of the contribution of each PMF Factor to PM<sub>10</sub> at the North-AQMS ( $\mu\text{g m}^{-3}$ ). Shaded areas represent drilling (grey) and HF + WC (purple) periods. "Other" refers to the PM<sub>10</sub> mass not accounted for by one of the identified PMF factors.

#### 4.3.2.3 Factor 1 Soil

The PMF analysis determined that the Soil Factor on average made up 37% of the total PM<sub>10</sub> mass at the North-AQMS and contributed over 25% to the 24-hour average PM<sub>10</sub> mass on 25 of the 52 days of sampling. The Soil Factor includes the key elements associated with crustal dust i.e. aluminium (Al), silicon (Si) and titanium (Ti). The highest proportions of these crustal elements are found in this factor.

Soil was identified as the dominant contributor to this factor because the ratios of aluminium to silica (Al/Si) and aluminium to titanium (Al/Ti), of 13.6 and 0.3 respectively, were typical of those measured in crustal composition (Lide 1997) and Australian dust (Radhi et al., 2010). It is unlikely that the silica measured in this study was derived from proppant handling as was found by Esswein et al. (2013) where significant emissions of crystalline silica dust were determined to be a result of proppant handling during HF in the US, since the correlation coefficient of 0.99 of silica with both aluminium and titanium is consistent with these elements coming from the same source (i.e. soil). If the proppant was a source of silica, the ratios of silica to both aluminium and titanium would be expected to differ from those of crustal and soil sources and the correlations would not necessarily be close to unity.

Overall the Soil Factor was identified as the major contributor to PM<sub>10</sub> mass collected in most samples at the North-AQMS from the start of sampling in early August up until the start of October (Figure 32). Dry conditions prevailed on site during this period until the start of frequent rainfall events between October and the end of sampling in December (Figure 9 Section 3) which coincided with an abrupt fall in the contribution of soil to PM<sub>10</sub> due to the suppression of airborne dust by rainfall.

Figure 33 (left panel) shows the polar frequency plot of the weighted mean statistic (i.e. concentrations are weighted by the frequency of occurrence of wind direction) for the Soil Factor contribution. This plot shows that the highest contributions of the Soil Factor at the North-AQMS were associated with winds from the 70 ° and 250 ° sectors. This is also shown in the polar frequency plot with maximum concentration being the plotted statistic (Figure 33 right panel). In this plot wind speed is represented by the radius in the plot and shows that the highest contribution of the Soil Factor in the 70 ° and 250 ° sectors occurred at low wind speeds (1-2 m s<sup>-1</sup>).

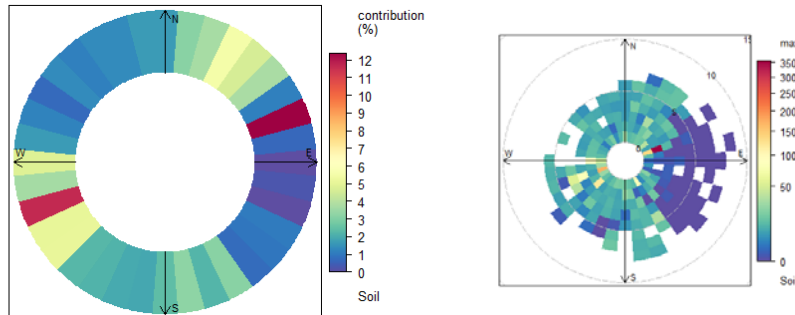


**Figure 33 Soil Factor- polar frequency plot of the weighted mean statistic (left) and polar frequency of the maximum statistic (right).**

Soil dust is generated by disturbing loose soil and other crustal matter. This disturbance can include wind blowing over the Earth's surface and the movement of vehicles and equipment traffic. Due to their large size, soil dust particles are typically not transported large distances in the air except under very high wind speeds. The highest contribution of soil dust influencing the sampling site occurred at low wind speeds, and it was likely generated locally from the movement of vehicle and equipment traffic on unsealed roads and well pads near the North-AQMS.

Soil dust was the major contributor to exceedances of TSP and PM<sub>10</sub> concentrations measured at the North and South-AQMS and a substantial peak in PM<sub>10</sub> concentrations measured at Solar-AQMS #4. These events will be discussed by site in turn below.

### **The contribution of soil to TSP exceedances at the North-AQMS**

As described in the previous section (4.2) two exceedances of the 24-hour TSP nuisance trigger level occurred at the North-AQMS on the 10<sup>th</sup> August and the 27<sup>th</sup> October 2017. The key features listed below indicate that these events were due dust emitted by vehicles traffic and equipment on unsealed roads and well pads in the vicinity of the North-AQMS:

- Soil dust is generally coarse particles (diameters > PM<sub>2.5</sub>) and in both TSP exceedance events PM was dominated by coarse particles with 87% of the TSP mass and 78% of the PM<sub>10</sub> mass due to particles with diameter > 2.5 µm (> PM<sub>2.5</sub>);
- In both events the Soil Factor was identified as the dominant contributor to PM<sub>10</sub> mass collected, contributing 90% of PM<sub>10</sub> on the 10<sup>th</sup> August and 88% of PM<sub>10</sub> on the 27<sup>th</sup> October (Figure 32);
- The event on the 10<sup>th</sup> August coincided with the movement of the drill rig from COM314 (site 4) to COM313 (North-AQMS) (Table 3, Section 2.3). Well COM 314 was approximately one kilometre to the east of the North-AQMS with associated vehicle movements on roads between the sites being consistent with the directional dependence of maximum concentrations with winds from the 70° sector (see Figure 33);

- The event on the 27<sup>th</sup> October also coincided with HF the transition to WC activity at COM314 (Table 3, Section 2.3) approximately one kilometre to the east of the North-AQMS. Peak TSP and PM<sub>10</sub> concentrations during this 24 -hour period occurred when winds were from the SW consistent with the directional dependence of maximum concentrations with winds from the 250° sector and was likely a result of dust from vehicle traffic on roads to the SW of the North-AQMS (Figure 34).

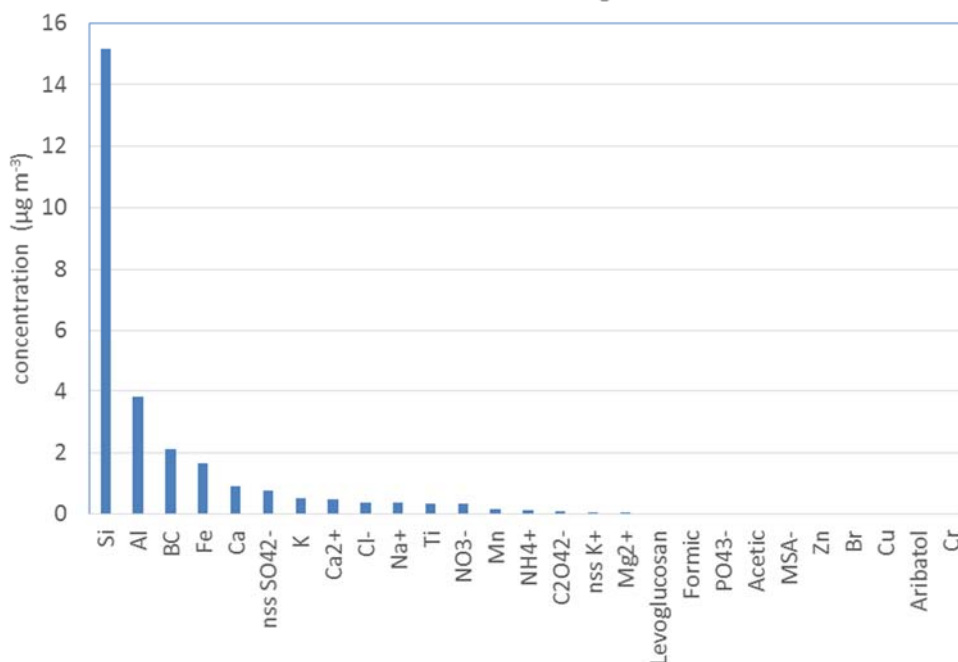


Figure 34 Map of HF study site with North and South-AQMS (red dots), roads, wells (COM###) and laydown area near South-AQMS shown. Source: Origin Energy.

#### The contribution of soil to high PM<sub>10</sub> at Solar-AQMS #4

As reported in Section 4.2.2, the highest PM<sub>10</sub> mass concentration from the multi-day Microvol samples of 70 µg m<sup>-3</sup> occurred for the period 6<sup>th</sup> – 13<sup>th</sup> August at Solar-AQMS #4 located adjacent to well COM314. This sample period coincided with the TSP exceedance at the North-AQMS on the 10<sup>th</sup> August discussed above.

As mentioned previously we can use the key species contributing to each factor from the PMF analysis listed in Table 24 to understand the sources potentially contributing to the chemical composition measured on the multi-day samples collected with the Microvols at the Solar-AQMS sites. Silica, the Soil Factor tracer, was the dominant contributor to PM<sub>10</sub> mass collected on the Microvol filter (Figure 35) at Solar-AQMS #4 during the period 6-13<sup>th</sup> August suggesting that dust emissions during drilling at COM 314 and drill rig movements were the dominant contributors to the high PM<sub>10</sub> mass of 70 µg m<sup>-3</sup> measured during this period.



**Figure 35 Composition of multi-day sample collected at Solar-AQMS #4 with Microvol 6-13 Sept 2017. The species are plotted in order of decreasing concentration. In this sample the soil indicator species Si displayed the highest concentrations indicating a substantial soil dust contribution to this sample.**

### The contribution of soil to TSP and PM<sub>10</sub> exceedances at the South-AQMS

As summarised in Section 4.2.5 there were six exceedances of the TSP nuisance trigger level at the South-AQMS occurring on the 18<sup>th</sup>, 21<sup>st</sup>, 26<sup>th</sup>, 27<sup>th</sup> September and the 20<sup>th</sup> and 27<sup>th</sup> October 2017 with a coincident exceedance of the PM<sub>10</sub> NEPM air quality objective that occurred on the 27<sup>th</sup> September.

Again, the concentration of silica, in the multi-day PM<sub>10</sub> samples collected with the Microvols at the South-AQMS (Solar-AQMS #5) was used to indicate the contribution of soil to TSP and PM<sub>10</sub> exceedances at the South-AQMS. The key features listed below indicate that these events were most likely due to dust emitted by vehicle traffic and equipment on unsealed roads and well pads near the South-AQMS:

- Soil dust is generally coarse particles (diameter > PM<sub>2.5</sub>) and in six TSP and PM<sub>10</sub> exceedance events PM was dominated by coarse particles with 77 - 93% of the TSP mass and 60 – 83 % of the PM<sub>10</sub> mass due to particles with diameter > 2.5 µm;
- In all exceedance events the Soil Factor tracer silica was the dominant contributor to PM<sub>10</sub> mass collected on the Microvol filters. For example, Figure 36 shows the composition of PM<sub>10</sub> from the Microvol sample for the period 22 – 29 September from the South-AQMS, which included three exceedances of TSP and one of PM<sub>10</sub> on the 21<sup>st</sup>, 26<sup>th</sup>, and 27<sup>th</sup> September.

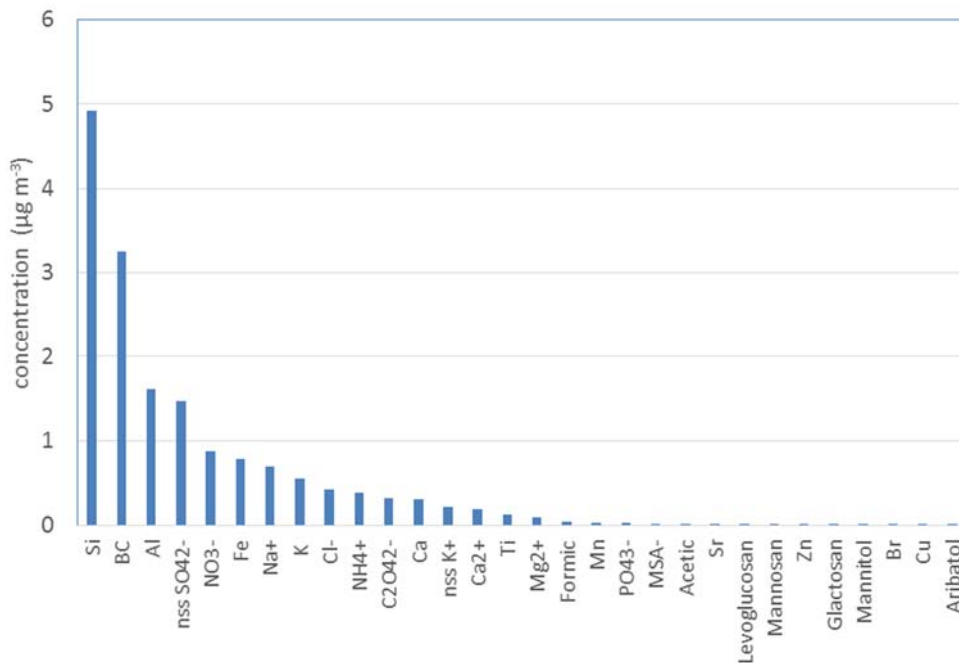


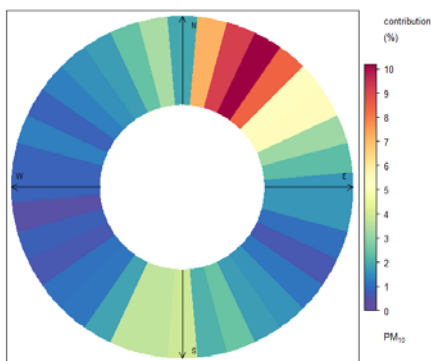
**Figure 36 Composition of multi-day sample collected at South-AQMS with Microvol 22-29 Sept 2017. The species are plotted in order of decreasing concentration. In this sample the soil indicator species Si displayed the highest concentrations, with significant BC concentrations as well indicating substantial contributions of soil dust and biomass smoke (fresh / aged) to this sample.**

As previously discussed, a truck laydown area was located < 100 m to the NE of the South-AQMS (Figure 34). The laydown area was a cleared area that contained a large above ground water tank used to store groundwater for HF sourced from a nearby bore. This area also served as a storage area for diesel refuelling tanks, trailers holding HF chemicals and proppant, trucks and equipment and the area experienced frequent truck traffic.

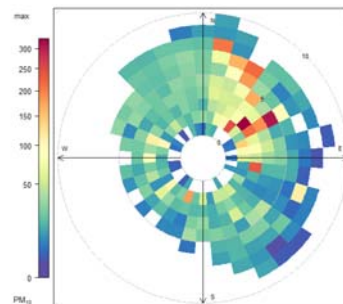
Figure 37 (left panels) show the polar frequency plots of the weighted mean statistic for PM<sub>10</sub> and TSP measured by the Palas FIDAS at the South-AQMS. These plots show that the highest concentrations of PM<sub>10</sub> and TSP at the South-AQMS were associated with winds from the 50 °- 70° sectors. The polar frequency plots, with maximum concentration being the plotted statistic (Figure 37right panels), indicate that the highest concentrations of PM<sub>10</sub> and TSP at the South-AQMS were

associated with winds in the 70 ° and 250 ° sectors at low wind speeds ( $2-4 \text{ m s}^{-1}$ ). Soil dust emissions from the frequent vehicle traffic at the laydown area to the NE of the South-AQMS provide a possible explanation for the high TSP and  $\text{PM}_{10}$  concentrations observed from the NE wind sector at this site.

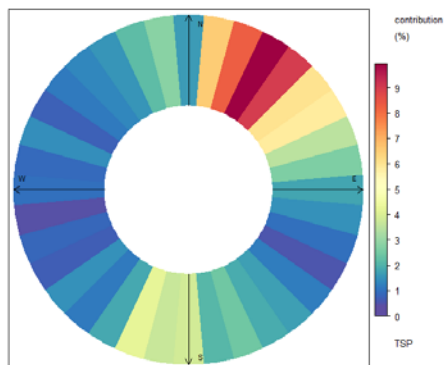
**$\text{PM}_{10}$**



**$\text{PM}_{10}$**



**TSP**



**TSP**

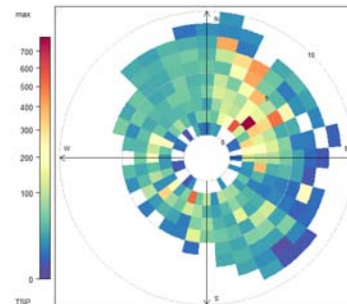


**Figure 37  $\text{PM}_{10}$  (top) and TSP (bottom) mass measured at the South-AQMS by Palas FIDAS - polar frequency plot of the weighted mean statistic (left) and polar frequency of the maximum statistic (right).**

In summary, soil was identified as a major contributor to  $\text{PM}_{10}$  mass on average over the study period. Local emissions of soil dust from vehicle traffic and equipment on unsealed roads and well pads were associated with exceedances in  $\text{PM}_{10}$  and TSP mass concentrations. The contribution of soil to  $\text{PM}_{10}$  was lower following the onset of rainfall events in October which likely suppressed airborne dust.

#### 4.3.2.4 Factor 2 Secondary Ammonium Sulfate

Factor 2 made up on average 16% of the PM<sub>10</sub> mass and contributed over 25% to the 24-hour average PM<sub>10</sub> mass on 12 of the 52 days of sampling. Key species in this factor were the soluble ions ammonium and sulfate with the highest proportions of these soluble ions found in this factor. Ammonium sulfate is a secondary aerosol component i.e. is produced by the chemical reactions of gases within the atmosphere. Secondary aerosols, including secondary ammonium sulfate, are generally fine and are predominantly measured in the PM<sub>2.5</sub> size fraction.

Sulfate is produced by the photo-oxidation of SO<sub>2</sub> that is generally emitted during the combustion of fossil fuels e.g. in coal fired power stations. Sources of ammonia include agriculture (mostly from animal excrement and fertiliser application), industrial processes, vehicular emissions and volatilization from soils and oceans (Behera et al. 2013). The National Pollution Inventory (NPI) lists basic non-ferrous metal manufacturing and electricity generation as the two largest contributors to SO<sub>2</sub> and sheep, beef and grain farming as the largest contributor to ammonia emissions in Queensland.

The nearest well to the North-AQMS was COM 313, located 100 m to the east (Figure 34), and underwent HF on the 6-7 October which coincided with the two highest concentrations of the Ammonium Sulfate Factor in 24- hour average PM<sub>10</sub> mass. Some of the chemicals used in HF to break down the gel fluids used to hydraulically fracture the coal seam contained ammonium peroxydisulfate and diammonium peroxydisulfate. Quantities of several hundred kilograms per well were used. These chemicals were used in dry powder form so that there was a potential for emissions to air during the transport, mixing and handling at the HF study site. However, primary emissions of particles as chemical dusts are dominated by coarse particles (> PM<sub>2.5</sub>) and during HF at COM 313 on the 6-7 October fine particles (PM<sub>2.5</sub>) were the dominant size fraction, contributing 77% and 73% respectively of the PM<sub>10</sub> mass. This indicates the observed ammonium sulfate was due to fine secondary ammonium sulfate aerosols and therefore not due to primary emissions of chemical dusts from HF.

Potentially significant contributions to PM from secondary formation of ammonium nitrate aerosols by photo-oxidation of ammonia in evaporated HF wastewater under high NO<sub>x</sub> conditions (> 200 ppb) have been reported for U.S. gas fields (Bean et al. 2018). Ammonia was detected in 100% of flowback/produced water samples from wells COM313 and COM359R (range 0.02 – 44 mg/L) during the study period as part of the water monitoring for this project (Apte et al., 2019). However, significant contributions of secondary ammonium nitrate to PM were not identified in the PMF analysis in this study. This can be explained by the practice of storage and handling of flowback/produced water occurring in enclosed tanks and pipelines which limited evaporative losses of ammonia to air. In addition, the very low NO<sub>x</sub> concentrations observed at the study site (1- hour average ~ 1 ppb, max ~ 30 ppb) also limit the potential for ammonia photo-oxidation at the HF site.

The polar frequency plot of the weighted mean statistic (Figure 38 left) shows the concentration of the Ammonium Sulfate Factor was greatest in winds from the 5° to 50° sector. The polar frequency plot for the maximum statistic (Figure 38 right) shows these maximum concentrations were often associated with wind speeds between 3 - 5 m s<sup>-1</sup>.

The coincidence of high Ammonium Sulfate Factor concentrations with wind directions from the NE provides further evidence that HF at wells on the study site did not significantly contribute to the observed ammonium sulfate component of PM<sub>10</sub> as all wells were located to the south and east of the North-AQMS (between 80° - 230°) (Figure 32).

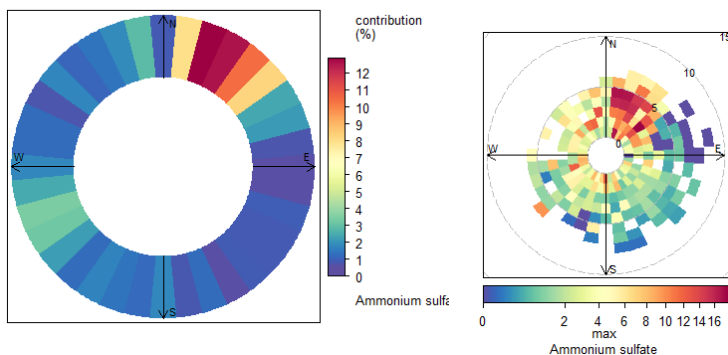


**Figure 38 Ammonium Sulfate Factor- polar frequency plot of the weighted mean statistic (left) and polar frequency of the maximum statistic (right).**

The largest contributions (50 – 80%) of the Ammonium Sulfate Factor to 24-hour average PM<sub>10</sub> mass were observed at the start of October (Figure 32). This period also coincided with a shift from predominantly SW winds in July - August to NE winds in September – November. Four coal fired power stations (Callide B and C, Gladstone and Stanwell) and three non-ferrous metal manufacturing sites located near Gladstone lie to the NE of the site. This provides a possible explanation for the coincidence of high Ammonium Sulfate Factor concentrations with the NE sector at moderate wind speeds. Regional transport of the products of reactions between industrial SO<sub>2</sub> emissions and the large agricultural sources of ammonia in the region provided a source of secondary ammonium sulfate PM.

#### 4.3.2.5 Factor 3 Secondary Nitrate-Aged Sea Salt

On average, Factor 3 contributed 12% of the PM<sub>10</sub> mass and contributed over 25% to the 24-hour average PM<sub>10</sub> mass on eight of the 52 days of sampling (Figure 32). Key species in this factor were the soluble ions nitrate and sodium. The highest proportions of these soluble ions were found in this factor. It also included magnesium and methane sulfonate, both markers of sea-salt.

The likely source of Factor 3 was identified as secondary nitrate-aged sea salt because the ratio of magnesium to sodium was similar to the ratio of these ions in sea water while the ratio of chloride to sodium is lower than the ratio found in seawater (Millero et al. 2008). These ratios result when

chloride is displaced from the sea-salt by reaction with nitric acid in the atmosphere to form sodium nitrate ( $\text{NaNO}_3$ ) (Seinfeld & Pandis., 2006).

The sources of nitric acid are industrial and transport emissions. Nitric acid is produced from the oxidation of nitrogen oxides from fossil fuel combustion. The NPI lists electricity generation as the largest contributor to emissions of nitrogen oxides in Queensland.

The polar frequency plot of the weighted mean statistic (Figure 39 left) shows the contribution of the Secondary Nitrate-Aged Sea Salt Factor was greatest in winds from the 5° to 50° sector. The polar frequency plot for the maximum statistic (Figure 39 right) shows these maximum concentrations were associated with wind speeds between 0-7  $\text{m s}^{-1}$ .

As mentioned in the previous section, multiple electricity generators lie to the NE of the site. The study site was also approximately 350 km directly inland of the coast to the east. This can explain the coincidence of high nitrate aged sea salt concentrations with the NE sector where the products of reactions between the industrial emissions of nitric oxide and the oceanic sources of sea salt provided a source of nitrate aged sea salt PM in the HF study region.

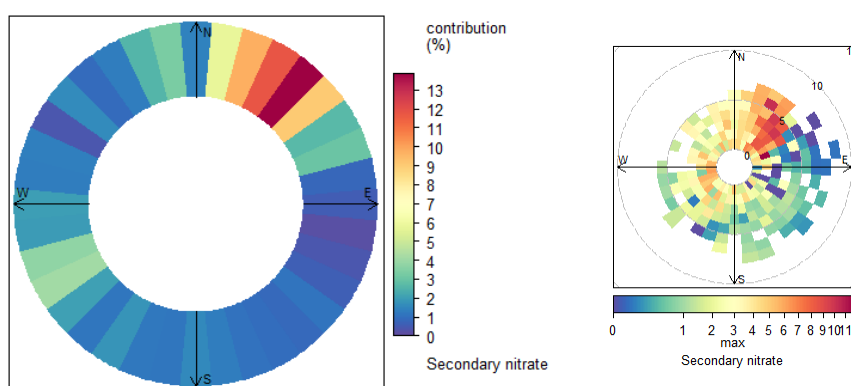


**Figure 39 Secondary Nitrate-Aged Sea Salt Factor- polar frequency plot of the weighted mean statistic (left) and polar frequency of the maximum statistic (right).**

#### 4.3.2.6 Factor 4 Aged Biomass Smoke

On average Factor 4 made up 11% of the  $\text{PM}_{10}$  mass at the North-AQMS and contributed over 25% to the 24-hour average  $\text{PM}_{10}$  mass on one day of the 52 days of sampling (Figure 32). The key species in this factor included black carbon and soluble potassium. Black carbon is formed from the combustion of biomass, biofuel or fossil fuels. Soluble potassium can be produced during the combustion of cellulose found in plant matter. The factor also contained large fractions of the soluble ions oxalate, formate and acetate. As an air mass ages these soluble ions are produced by the photo oxidation of VOCs. At the same time the woodsmoke tracer levoglucosan is removed as the air mass ages (Bhattacharai et al.,2019). The presence of these species and the absence of the woodsmoke tracer levoglucosan suggests this factor is most likely aged biomass smoke.

The highest 24-hour average concentrations of the Aged Biomass Smoke Factor were observed on the 27<sup>th</sup> – 28<sup>th</sup> September (Figure 32). The Wood Smoke (Factor 6) also made large contributions to PM<sub>10</sub> on these days. Geoscience Australia’s Sentinel website and NASA Worldview website (see Appendix.15) confirm fires in the region during this period with large fires burning in state forests approximately 200 km to the NW of the site and approximately 400 km to the NE of the site near Rockhampton resulting in regional smoke over the study site that was a mixture of fresh and aged emissions (Figure 41).



**Figure 40** NASA Worldview map of fire hotspots (Appendix 15) on the 27th September 2017 when the highest 24-hour average concentrations of the Aged Biomass Smoke Factor (Factor 4) were recorded. Note the mixing of Wood Smoke (Factor 6) from forest fires ~ 200 km to the NW and Aged Biomass Smoke (Factor 4) from fires further afield (~ 400 km) to the NNE over the study site.

However, it is also possible that non-wood biomass combustion may have contributed to this factor e.g. prescribed and non-prescribed burning of grasses, agricultural crops and other plants as well as energy production from biofuels such as sugar cane. Combustion of these materials typically produce only small amounts of levoglucosan and elevated levels of the other key species (oxalate, formate, acetate, potassium) as shown for sugar cane in a study during cane burning in south eastern Brazil (Allen et al., 2004).

The polar frequency plot of the weighted mean statistic (Figure 41 left) shows the contribution of the Aged Biomass Smoke Factor was greatest in winds from the 5° to 50° sector. The polar

frequency plot for the maximum statistic (Figure 41 right) shows the highest concentrations were associated with wind speeds between 6 -7 m s<sup>-1</sup> and moderate concentrations were also observed at low speeds in the NW sector. The coincidence of high concentrations of Aged Biomass Smoke Factor with the NNE sectors, positively associated with higher wind speeds, suggests regional transport of aged smoke was the dominant source of non- wood smoke in the HF study region.

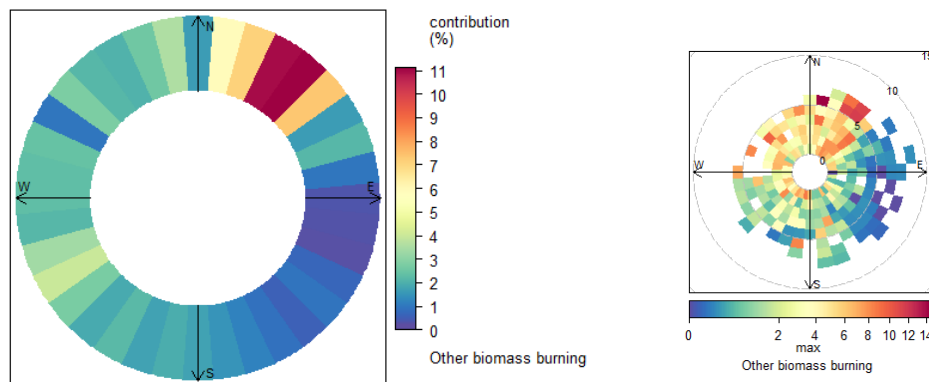


**Figure 41 Aged Biomass Smoke Factor- polar frequency plot of the weighted mean statistic (left) and polar frequency of maximum statistic (right).**

On average, the Aged Biomass Smoke Factor (Factor 4) made a minor contribution (11%) to PM<sub>10</sub> mass at the study site. On occasion aged smoke from regional fires was transported to the site in the prevailing NE winds also making a contribution to PM<sub>10</sub> concentrations.

#### 4.3.2.7 Factor 5 Fresh Sea Salt

On average Factor 5 contributed 9% of the PM<sub>10</sub> mass and contributed over 25% to the 24-hour average PM<sub>10</sub> mass on 12 of the 52 days of sampling (Figure 32). The Fresh Sea Salt Factor is dominated by the seawater soluble ions sodium, chloride, magnesium and sulfate and their ratios closely match those for standard sea water (Millero et al., 2008) show in Table 26.

It is not unusual to observe fresh sea salt aerosol at locations more than 700 km inland e.g. sea salt aerosol were reported at a site in Alabama more than 320 km from the Gulf of Mexico (Bondy et al., 2017) and at a rural site in Michigan more than 700 km from the nearest body of sea water (May et al., 2018).

Brine ponds associated with CSG water treatment facilities (WTF) are another potential source of salt aerosol in the study region. The ratio of magnesium to sodium (Mg/Na) was determined for produced waters from wells and for water samples from a WTF in the study region as part of the water quality component of this project (Apte et al 2018). The ratio Mg/Na for seawater, CSG waters and the Fresh Sea Salt Factor identified in this work are shown in Table 26. The ratio of Mg/Na was the same as the ration for seawater and greater than the ratios measured in the CSG waters, strongly indicating that Factor 5 was fresh sea salt and not salt from CSG waters.

**Table 26 Ratios of chloride and magnesium to sodium in seawater (Millero et al., 2008), produced waters and influent and brine from the water treatment facility and the Fresh Sea Salt Factor identified by PMF in the PM<sub>10</sub> samples.**

Mean ratios (by mass) summary	Mg/Na
Seawater	<b>0.12</b>
Produced waters	0.0057
WTF (influent & brine combined)	0.0028
Fresh Sea Salt Factor	0.12

The polar frequency plot of the weighted mean statistic (Figure 42 left) shows the contribution of the Fresh Sea Salt Factor was greatest in winds from the 5° to 50° sector. The polar frequency plot for the maximum statistic (Figure 42 right) shows the highest concentrations were associated with wind speeds between 1-7 m s<sup>-1</sup>. The coincidence of the maximum concentrations of this factor with the NNE sectors and positive association with higher wind speeds, indicates regional transport from the coast was the most likely source of fresh sea salt in the HF study region.

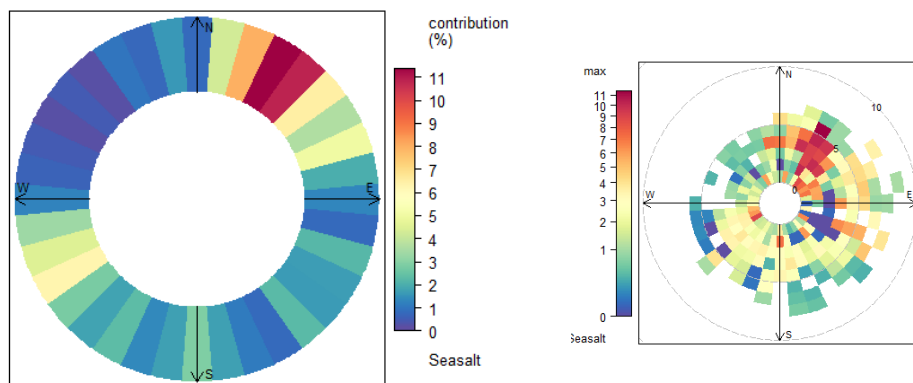


**Figure 42 Sea salt Factor- polar frequency plot of the weighted mean statistic (left) and polar frequency of maximum statistic (right).**

#### 4.3.2.8 Factor 6 Wood Smoke

Factor 6 makes up 7% of PM<sub>10</sub> and it contributed over 25% to the 24-hour average PM<sub>10</sub> mass on three of the 52 days of sampling (Figure 32). Key species in this factor included the woodsmoke tracer species levoglucosan and mannosan. Black carbon also contributed to this factor.

Potential sources of wood smoke at the HF study site were prescribed burns, bushfires and domestic wood heating. The time series in Figure 32 shows the highest Wood Smoke Factor contributions occurred on the 22-23 September and 28- 29 September. Geoscience Australia’s Sentinel website and NASA Worldview website (see Appendix.15) confirm fires in the region

during both of these periods with large fires burning in state forests approximately 200 km to the NW of the site during all of these periods which were likely to have contributed to regional smoke events. A smaller fire was observed on the 22<sup>nd</sup> September in a forested area approximately 20 km to the NE of the study site which coincided with the highest 24-hour PM<sub>10</sub> woodsmoke concentration. Written logs confirmed smoke was observed by CSIRO personnel on site that day.

The polar frequency plot of the weighted mean statistic (Figure 43 left) shows the contribution of the Wood Smoke Factor was greatest in winds from the 30-50 ° sector. The polar frequency plot for the maximum statistic (Figure 43 right) shows these maximum concentrations were associated with wind speeds between 1-4 m s<sup>-1</sup>. Overall, smoke generally made a minor contribution to PM<sub>10</sub> mass at the study site. On occasion, smoke from regional and local fires was transported to the site in the prevailing NE winds and most likely contributed to PM<sub>10</sub> concentrations.

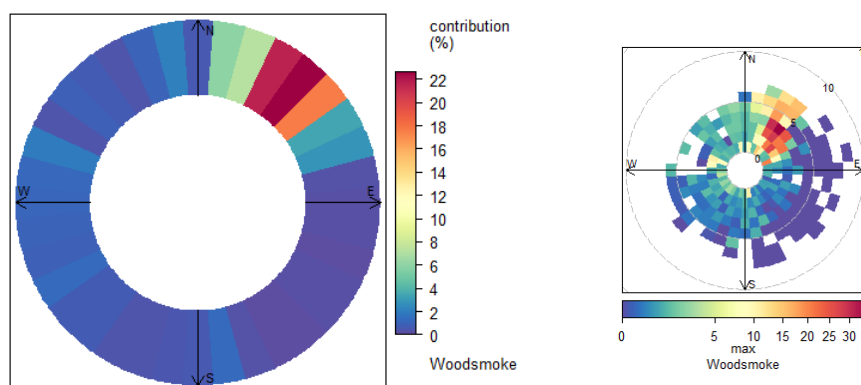


**Figure 43 Wood Smoke Factor- polar frequency plot of the weighted mean statistic (left) and polar frequency of maximum statistic (right).**

#### 4.3.2.9 Factor 7 Glucose

Factor 7 on average contributed 5% of PM<sub>10</sub> and contributed over 25% to the 24-hour average PM<sub>10</sub> mass on nine of the 52 days of sampling (Figure 32). Key species in this factor included glucose and mannitol, both of which are found in fungi, lichens and soil biota.

The time series in Figure 32 shows an abrupt increase in the contribution of this factor to PM<sub>10</sub> mass at the start of October coinciding with the onset of rainfall events which may have triggered an increase in biological activity in the soil and vegetation at the HF study site.

The polar frequency plot of the weighted mean statistic (Figure 44 left) shows the contribution of the Glucose Factor was distributed across different wind directions with the highest contributions in the 15° to 30° sector and the 235° to 270° sector. The polar frequency plot for the maximum statistic (Figure 44 right) shows these maximum concentrations were associated with low wind speeds (< 3 m s<sup>-1</sup>). The lack of any strong coincidence in concentrations with a particular sector and the association with lower wind speeds indicate dispersed local sources surrounding the

sampling site were the most likely contributors to this factor. Emissions from biological activity in the soil and vegetation surrounding the North-AQMS are consistent with this observation and are a likely source of this factor.

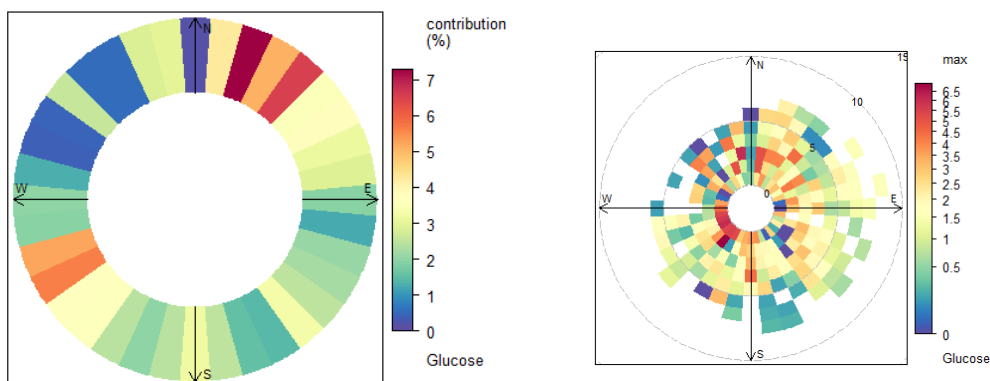


**Figure 44** Glucose Factor- polar frequency plot of the weighted mean statistic (left) and polar frequency of maximum statistic (right).

#### 4.3.2.10 Factor 8 Primary Biological Aerosol

On average Factor 8 made only minor contributions (2%) to PM<sub>10</sub> mass, however on two of the 52 days of sampling this factor contributed over 25% to the 24-hour average PM<sub>10</sub> mass (Figure 32). Key species in this factor were arabinol and mannitol which are found in fungal spores and bioaerosols.

Like the Glucose Factor, there was an abrupt increase in the contribution of this factor to PM<sub>10</sub> mass at the start of October that coincided with the onset of rainfall events which likely triggered an increase in biological activity at the HF study site.

The polar frequency plot of the weighted mean statistic (Figure 45 left) shows the contribution of the Primary Biological Aerosol Factor occurred in winds from the 220° to 250° sector. The polar frequency plot for the maximum statistic (Figure 45 right) shows these maximum concentrations were associated with very low wind speeds (< 2 m s<sup>-1</sup>) indicating local biological activity in the soil and vegetation to the SW of the North-AQMS was the source of this factor.

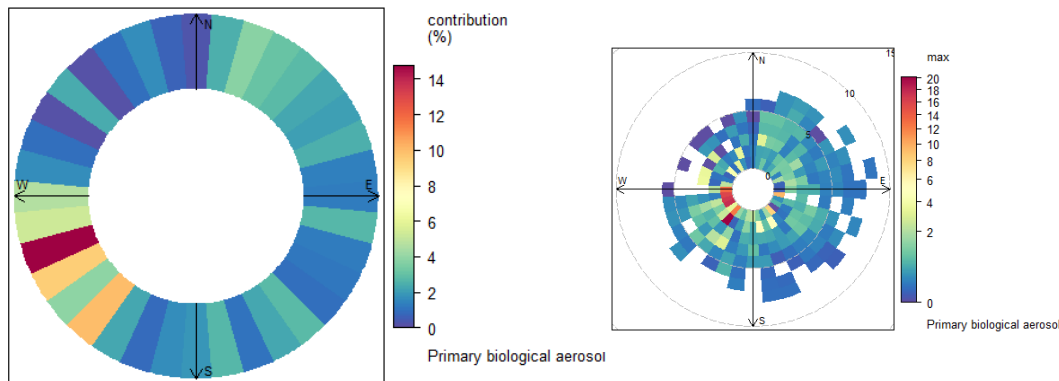


**Figure 45 Primary Biological Aerosol Factor- polar frequency plot of the weighted mean statistic (left) and polar frequency of maximum statistic (right).**

### 4.3.3 Summary of the sources of PM at the HF study site

Source Apportionment analysis was applied to the PM<sub>10</sub> chemical composition data to identify the factors that contributed to the total PM<sub>10</sub> mass concentrations At the North-AQMS. Eight factors, ranked in order of their contribution to average PM<sub>10</sub>, were identified.

- Factor 1 Soil
- Factor 2 Secondary Ammonium Sulfate
- Factor 3 Secondary Nitrate-Aged Sea Salt
- Factor 4 Aged Biomass Smoke
- Factor 5 Fresh Sea Salt
- Factor 6 Wood Smoke
- Factor 7 Glucose
- Factor 8 Primary Biological Aerosol

Contributions from Factors 2 – 6 were the result of regional transport (tens to hundreds of kilometres) of PM to the study site from both natural and industrial sources in the region. PM from these factors were predominantly in the fine size fraction (PM<sub>2.5</sub>). Contributions from Factors 7 and 8 were from natural biological sources at the study site. Combined these sources comprise the background PM in the atmosphere of the study region and well development activities on site did not significantly contribute to these factors.

Only local emissions of soil dust from vehicle traffic and equipment on unsealed roads and well pads were attributable to CSG well development activities. On seven days during this study dust emissions from vehicles and equipment on site resulted in exceedances in 24-hour PM<sub>10</sub> and TSP air quality objectives. The frequency and extent of these events was dependent on meteorology, particularly rainfall, which suppressed airborne dust.



## 5 NEPM Air Toxics, other VOCs and hydrogen sulphide

This section presents data on the air toxics: benzene, toluene, xylenes, formaldehyde and polycyclic aromatic hydrocarbons (PAHs); along with data on other organic compounds and hydrogen sulphide. Benzene, toluene, xylenes and formaldehyde belong to a class of chemicals known as volatile organic compounds (VOCs) which are organic compounds that predominantly exist in the gas phase at ambient temperatures and are generally observed at low concentrations (parts per billion to parts per trillion). Polycyclic aromatic hydrocarbons are a class of chemicals that are considered semi-volatile and typically exist in both the particle and gas phase in the atmosphere and often attach to other particulate matter (e.g. soot).

Air toxics are emitted during combustion including vehicle exhaust and wood smoke, evaporation from fuels, solvents and industrial chemicals and processes, as well as consumer products. Some VOCs including formaldehyde, can also be formed in the atmosphere as a secondary product of reactions between other gaseous air pollutants. At the HF study site potential sources of air toxics include exhaust and evaporative emissions from fuel powered vehicles and equipment on site, evaporation of air pollutants from HF fluids, flowback /produced waters during transport handling and storage at the surface, and secondary production.

### Relevant Air Quality Objectives

In this section the concentrations of air toxics, other VOCs and hydrogen sulphide are compared to relevant federal and state air quality objectives, specifically, the NEPM Air Toxics (2011) and Queensland EPP for Air (2008).

Air toxics are sometimes referred to as hazardous air pollutants (HAPs) to differentiate them from the common criteria air pollutants: NO<sub>2</sub>, CO, SO<sub>2</sub>, O<sub>3</sub>, PM and lead included in the Ambient Air NEPM (2016). Substances listed in the NEPM for Air Toxics (2011) are:

- benzene, toluene, and xylenes collectively known as BTX. Sometimes ethylbenzene is also included in this group which is then referred to as BTEX;
- Formaldehyde;
- benzo(a)pyrene (BaP) as a marker for polycyclic aromatic hydrocarbons (PAHs).

The primary aim of the air toxics NEPM is the collection of data on the ambient levels of these five air toxics at locations where elevated levels are expected to occur and there is a likelihood that significant population exposure could occur. The air toxics NEPM (2011) specifies Monitoring Investigation Levels (MILs) for each air toxic. MILs are levels of air pollution below which long-term exposure, or exposure for a given averaging time, does not pose a significant health risk. Short-

term exceedances of MILs do not mean that adverse health effects automatically occur. Instead, it is a trigger for some form of further investigation by the relevant jurisdiction of the cause of the exceedance.

The Queensland Government's Environment Protection Policy (EPP) for Air (2008) includes objectives for other air pollutants, not included in the NEPM standards (2011, 2016), four of which were measured in the present study and are reported in Section 5.3. These pollutants include hydrogen sulphide, 1,2-dichloroethane, styrene and tetrachloroethylene.

An additional set of recognised air quality objectives/criteria- the Texas AMCVs and the Texas Commission on Environmental Quality Effects Screening Levels (Texas ESLs) are referred to here to provide context to the measurements of 12 other VOC species detected in air at the HF study site and reported in Section 5.4.

### **Methods for Measurement of Air Toxics**

During the measurement program five different sampling and analysis methods were employed for the measurement of air toxics. Details of each of the sampling and analysis procedures have been provided in previous reports for this project (Dunne et al 2017, 2018a, 2018 b) and further details of the analysis and performance is provided in the Appendices to this report. Briefly, the five methods employed for measurement of the NEPM air toxics are described below.

Four methods for VOCs including BTX and formaldehyde:

- **Active sampling and derivatization of formaldehyde onto DNPH cartridges** followed by off-line analysis using Ultra High Performance Liquid Chromatography. Samples were collected on DNPH-coated solid silica adsorbent cartridges (Supleco LpDNPH S10). Two 12-hour samples per day of formaldehyde were collected at the North-AQMS one ~24-hour sample per day was collected at each of the five the Solar-AQMS sites;
- **Active sampling of VOCs onto adsorbent tubes (AT-VOC)** followed by thermal desorption and off-line gas chromatography with flame ionisation and mass spectrometric detection (GC-FID-MS) analysis. Two 12-hour samples per day were collected at the North-AQMS and at each of the five Solar-AQMS sites. Data for benzene, toluene, xylenes (BTX), and styrene are reported here;
- **Proton transfer reaction mass spectrometry (PTR-MS)** provided continuous (10 min resolution) measurements of a range of VOCs including formaldehyde and BTX. A commercially built PTR-MS instrument (Ionicon Analytik GmbH, Innsbruck, Austria) was operated by CSIRO continuously in an enclosure at the North-AQMS site from July – November 2017. Note that the PTR-MS measures ethylbenzene at the same mass channel as the xylenes and the concentrations of xylene reported from the PTR-MS data contain minor contributions of ethylbenzene;

- **Passive Radiello Sampling.** Radiello cartridges were deployed at the North and South-AQMS and at the Solar-AQMS #1 site between Jun – Dec 2017. The sampling and analysis was conducted by a third-party contractor, SGS-Leeder, on behalf of GISERA. The cartridges were deployed on purpose-built poles ~2 m high and each cartridge was exposed to air for approximately two weeks. Three different Radiello cartridges and analysis methods were used to capture air pollutants including BTEX, formaldehyde and hydrogen sulfide. In addition to BTX and formaldehyde four other compounds included in Queensland Government's EPP for Air (2008) were measured by passive Radiello VOC sampling at the HF study site from 14 June – 30 November 2017. These were hydrogen sulphide, the VOCs 1,2-dichloroethane, styrene and tetrachloroethylene. Styrene was also measured in the 12-hour AT-VOC samples at the study site from 7/8 – 19/8 and 15/9 – 29/10. Details of the Radiello methodology and data from another HF site in the Surat Basin were provided in a previous report for this project (Dunne et al., 2018b).

This study also employed one method for measuring semi-volatile PAH compounds:

- **Active sampling of PAHs onto quartz filters and PUF sorbent cartridges** using a high-volume sampler followed by chemical desorption in hexane and acetone, then subsequent analysis with gas chromatography coupled to a DFS Magnetic Sector high-resolution mass spectrometer (GC-HRMS). Approximately 48 hour PAH samples were collected by CSIRO staff and analysed at the Queensland Alliance for Environmental Health Sciences at the University of Queensland laboratories in Brisbane.

### Comparison on VOC Measurement Methods

Co-located measurements by PTR-MS, DNPH and VOC adsorbent tube (AT-VOC) methods have been employed in the past by CSIRO O&A laboratories and published as reports (Cope et al., 2014, CSIRO 2008, Galbally et al 2008) and in the international scientific literature (Dunne et al., 2018c) showing reasonable agreement between measurement methods with correlations of  $R^2 > 0.9$  and slopes of 1.2 – 1.5 for the BTEX species and formaldehyde.

In the current study the different measurement methods for the air toxics generated comparable results for toluene, xylenes and formaldehyde, however, this was not the case for benzene. While the range of concentrations of formaldehyde, toluene and xylenes reported by all methods were similar, the concentrations of benzene measured at the Solar-AQMS sites were an order of magnitude higher than the other measurement methods. Median and mean benzene concentrations of 0.02 – 0.03 ppb were reported by the passive Radiello method, the active sampling method at the North-AQMS and the measurements by PTR-MS. Concentrations of benzene reported by the active sampling method employed at the Solar-AQMS sites were an order of magnitude higher with mean and median values of 0.15 – 0.20 ppb.

Post-study testing showed that the precision of the benzene measurements collected by active sampling at the Solar-AQMS sites were unacceptable. Relative standard deviation values less than 25% are considered acceptable (US EPA 1999). The relative standard deviation (%) of a set of replicate measurements of benzene at the five Solar-AQMS sites was 131 %. Given the poor precision of the Solar-AQMS sampling for benzene and the reasonable agreement between the other three independent measurement methods (North-AQMS AT-VOC, the PTR-MS and the passive Radiello), benzene data from the Solar-AQMS samples was excluded from reporting in this study. It is important to note that the overall average concentrations of benzene reported by the active sampling at the Solar-AQMS sites were still well below the NEPM air toxics annual objective for benzene.

The following Sections (5.1 – 5.5) provide a summary of the data for each of these toxic air pollutants. Air quality in relation to the concentrations of each air pollutant observed at the study site and Australian federal and state air quality objectives are discussed further. Additional comparisons are provided with data from other air quality studies undertaken in areas not directly impacted by HF operations.

Using high time resolution data (10-minute average), the concentrations of formaldehyde and BTX measured at the North-AQMS when downwind of drilling, HF + WC activities are presented. For comparison, data for periods when the AQMS was upwind of drilling, HF + WC, and during periods where none of these activities were occurring are also presented. The differences between the concentrations downwind of drilling, HF + WC and concentrations of air pollutants from other wind directions and/or when non-activity periods occurred provides information on potential enhancements in air toxics levels above background that occurred during these well development activities.

## 5.1 Formaldehyde

Formaldehyde belongs to a class of oxygenated organic compounds known as aldehydes. Potential sources of formaldehyde detected in air at the HF site include:

- secondary production from photochemical oxidation of other VOCs and methane in the atmosphere often in the presence of sunlight (photochemical reactions);
- emissions from prescribed burning, bushfires or wood heater emissions;
- exhaust emissions from vehicles and diesel-powered equipment;
- emissions from HF or other CSG development activity on site e.g. HF fluids, flowback fluids and CSG;
- other industrial, commercial or domestic emissions in the region.

Formaldehyde was measured using three methods in this study:

- Continuous measurements by PTR-MS at the North-AQMS only;
- 2 x 12-hour samples per day at the North-AQMS and ~ 24-hour samples at the five Solar-AQMS collected using active sampling onto DNPH cartridges;
- ~ 14-day samples collected by Radiello passive sampling at the North and South-AQMS and at Site 1.

In this section, data on the concentration of formaldehyde observed at the study site is presented. Concentrations are compared with air quality guidelines and with data from other sites in the Surat Basin. Changes in formaldehyde levels above background that occurred during HF operations are investigated and potential contributions from HF and non-HF related sources of formaldehyde are discussed.

#### **Summary Statistics and Comparison with Air Quality Objectives**

Summary statistics of formaldehyde concentrations including monthly average and maximum concentrations and data capture rates for the North-AQMS and Solar-AQMS #1 –# 5 are listed in Table 27. Note Solar-AQMS #5 was co-located with the South-AQMS. A time series of the 24-hour average formaldehyde concentrations measured across the six monitoring sites by PTR-MS and DNPH methods is shown in Figure 46 along with the NEPM 24-hour formaldehyde monitoring investigation level (MIL) of 0.04 ppm (40 ppb). The maximum 24-hour average concentrations of formaldehyde across the six sampling sites were 3.7 – 4.9 ppb which are 8 to 10 times lower than the Air Toxics NEPM (2011) MIL of 40 ppb (0.04 ppm).

**Table 27 Monthly maximum and average 24-hour concentrations of formaldehyde (ppm) for North-AQMS (PTR-MS & DNPH methods) and for Solar-AQMS #1-#5 (DNPH method) for the HF study period (Jul – Dec 2017). Data capture (%), overall average formaldehyde, and concentrations during HF +WC are also presented. The NEPM 24-hour MIL for formaldehyde is 0.040 ppm.**

Formaldehyde - 2017	Jul	Aug	Sep	Oct	Nov	Dec	Overall	HF + WC period
<b>North-AQMS- PTR-MS</b>							<b>Jul - Nov</b>	<b>21<sup>st</sup> Sept – 2<sup>nd</sup> Nov</b>
Max 24-hour	1.96	2.87	4.92	2.42	3.01	n.d.	4.92	4.92
Average 24-hour	i.d.	1.65	2.77	1.37	1.64	n.d.	1.87	1.94
% Data Avail	10 <sup>c</sup>	100	100	100	70 <sup>c</sup>	0 <sup>c</sup>	76 <sup>c</sup>	100
<b>North-AQMS- DNPH</b>							<b>Aug - Oct</b>	<b>21<sup>st</sup> Sept – 2<sup>nd</sup> Nov</b>
Max 24-hour	n.d.	2.21	2.51	2.00	n.d.	n.d.	2.51	2.51
Average 24-hour	n.d.	i.d.	i.d.	0.98	n.d.	n.d.	1.22	1.08
% Data Avail	0 <sup>h</sup>	26 <sup>h,b</sup>	27 <sup>h,b</sup>	61 <sup>h,b,i</sup>	0 <sup>h</sup>	0 <sup>h</sup>	38 <sup>h,b,i</sup>	49 <sup>h,b,i</sup>
<b>Solar-AQMS #1- #5 DNPH</b>							<b>Aug - Oct</b>	<b>21<sup>st</sup> Sept – 2<sup>nd</sup> Nov</b>
Max 24-hour	n.d.	2.61	3.72	2.62	n.d.	n.d.	3.72	3.72
Average 24 - hour	n.d.	i.d.	i.d.	1.03	n.d.	n.d.	1.40	1.45
% Data Avail <sup>k</sup>	0 <sup>h</sup>	23 – 32 <sup>h,b</sup>	47 – 53 <sup>h,b</sup>	48 – 74 <sup>h,b,i</sup>	0 <sup>h</sup>	0 <sup>h</sup>	41 – 51 <sup>h,b,i</sup>	26 – 36 <sup>h,b,i</sup>

n.d. indicates no data are available; i.d. indicates insufficient data were available to calculate value (< 60% data available). Reasons for data availability < 90 %: a = power outage; b = instrument failure; c = instrument not commissioned or commissioned /decommissioned part way through month; h = sampling only conducted when CSIRO personnel on site 8/8/2017 – 17/8/2017 and 15/9/2017 – 28/10/2017; i= samples not collected due to bad weather or sample media shortage; k= data availability differed between Solar-AQMS #1 –#5, range of values presented.

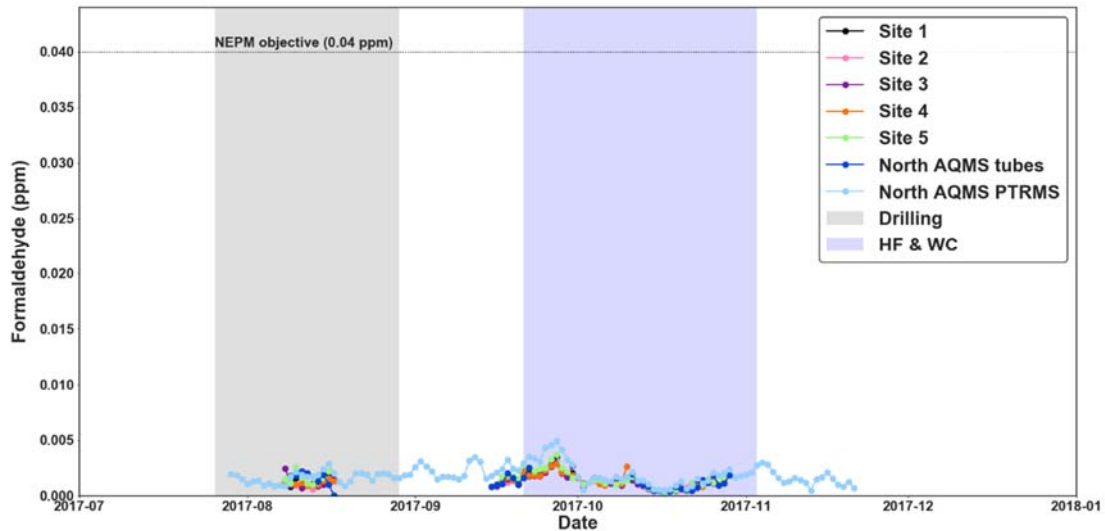


**Figure 46 24-hour averages of formaldehyde measured at the North-AQMS and Solar-AQMS sites by active sampling on the DNPH tubes and the NEPM 24-hour objective. Shaded areas represent periods of well development activity on the HF study site, including drilling (grey) and HF + WC (purple).**

### Comparison with other sites in the Surat Basin

The approximately 14 day integrated average concentrations of formaldehyde reported from the Radiello method in this study were similar to those reported from 134 Radiello samples collected at two other HF sites in the Miles-Condamine region of the Surat Basin in 2016-17 shown in Table 28 and reported previously in Dunne et al. (2018). The concentrations were comparable to Radiello data from four other sampling sites operated over the same period as part of the Surat Basin Ambient Air Quality (SBAAQ) Study (Lawson et al., 2018). Overall the range of concentrations and detection frequencies of each compound measured using Radiello samplers at the HF sites were similar to those observed across the two regional sites (Burncluith and Tara) which were > 10 km from CSG infrastructure, and at two other gas field sites (Miles Airport and Hopeland) which were not known to be directly impacted by HF activities.

**Table 28** The detection frequency (% samples > Detection limit, DL) and the range of ~ 14-day integrated average concentrations of formaldehyde measured by Radiello at the HF study site, another HF site in the Miles-Condamine region in 2016/17 (Dunne et al., 2018), and from two regional sites (Burncluith & Tara region) and two gas field sites (Wilgas & Hopeland) operated as part of the Surat Basin Ambient Air Monitoring Network (Lawson et al. 2018).

Location		Range (ppb)	Detection Frequency (% samples > DL)
HF site (This Study)	Jun – Dec 2017	≤ 0.04 – 1.30	94%
HF site 2016/17 (Miles-Condamine)	Oct 2016 – Sept 2017	0.33 – 2.12	100%
Regional Sites (Tara region & Burncluith)	Jun – Dec 2017	≤ 0.04 – 1.30	83%
Gas-Field Sites (Wilgas & Hopeland)	Jun – Dec 2017	0.39 – 1.30	100%

#### **HF and non-HF related sources of formaldehyde at the HF study site**

In addition to being a significant source of PM, biomass burning is also a major source of gases, including VOCs, to the atmosphere. Formaldehyde is both directly emitted during biomass burning and is also produced as a smoke plume ages in the atmosphere via secondary reactions between primary pollutants (e.g. VOCs and NO<sub>x</sub>). The PTR-MS, used to measure formaldehyde at the North-AQMS, also measured acetonitrile which is almost exclusively emitted from biomass burning. With an atmospheric lifetime of many months, acetonitrile is commonly used as a tracer for biomass burning in PTR-MS measurements of the atmosphere (Dunne et al 2012, de Gouw et al, 2003). A time series of 24-hour average formaldehyde and acetonitrile concentrations presented in Figure 47 shows a clear relationship between formaldehyde and acetonitrile concentrations, indicating contributions from regional smoke were a highly likely source of formaldehyde at the HF study site. Notably, the highest 24-hour average values of formaldehyde occurred during 25 – 28 September which coincided with the highest 24-hour maximum acetonitrile concentrations.

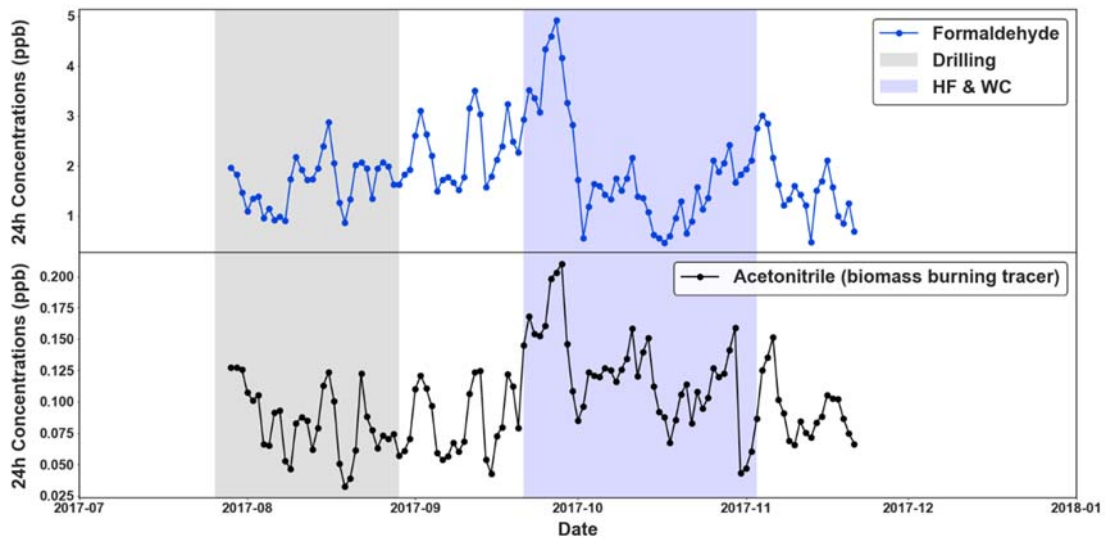


**Figure 47 Time series of the 24-hour averages of formaldehyde and the biomass burning tracer acetonitrile measured by PTR-MS at the North-AQMS.**

The time series in Figure 47 also shows a gradual increasing trend in formaldehyde concentrations from August through September coinciding with the transition to spring, followed by a visible decline in formaldehyde concentrations at the start of October that corresponded with a shift in local meteorology and the arrival of rainfall events. This behaviour can be explained by the increasing warmth and sunlight of spring favouring secondary photochemical production of formaldehyde, followed by the onset of rainfall resulting in loss of formaldehyde by wet deposition to the surface. In addition, overcast conditions associated with wet weather would likely have suppressed secondary photochemical production of formaldehyde in the atmosphere. Thus, biomass burning and secondary reactions in the atmosphere in the region of the HF study site are deemed to be the likely sources of formaldehyde.

Potential enhancements in formaldehyde concentrations above background due to local well development activity were assessed using higher time resolution (10-minute) PTR-MS formaldehyde data and wind direction at the North-AQMS. Figure 48 shows the distributions of 10-minute average formaldehyde data at the North-AQMS when downwind of drilling (A) and when downwind of HF + WC (C) along with data from other WDRs during the same periods (B and D) and during periods where no drilling, HF or WC activities occurred (E). The distribution characteristics of the formaldehyde data from the North-AQMS were as follows:

- The median and inter quartile ranges (IQR, 25<sup>th</sup> – 75<sup>th</sup> percentiles) of formaldehyde concentrations for all activity periods and non-activity periods, and all WDRs were similar (medians = 1.5 to 1.9 ppb, IQRs = 0.75 to 2.8 ppb), however the 75<sup>th</sup> and 95<sup>th</sup> percentile

when measuring downwind of HF + WC (C) were higher than for the other periods and WDRs;

- **Drilling** - the top 5 % of values when measuring downwind of drilling (A) were higher than the top 5% of values when measuring air masses from other WDRs during the same period (B) but were within the range of concentrations measured during non-activity periods (E);
- **HF + WC** - the top 5 % of values when measuring downwind of HF + WC (C) were within the same range as the top 5% of values when measuring air masses from other WDRs during the same period (D) and during non-activity periods (E);
- The highest 10-minute average formaldehyde concentrations were observed during the periods when there was no activity occurring.

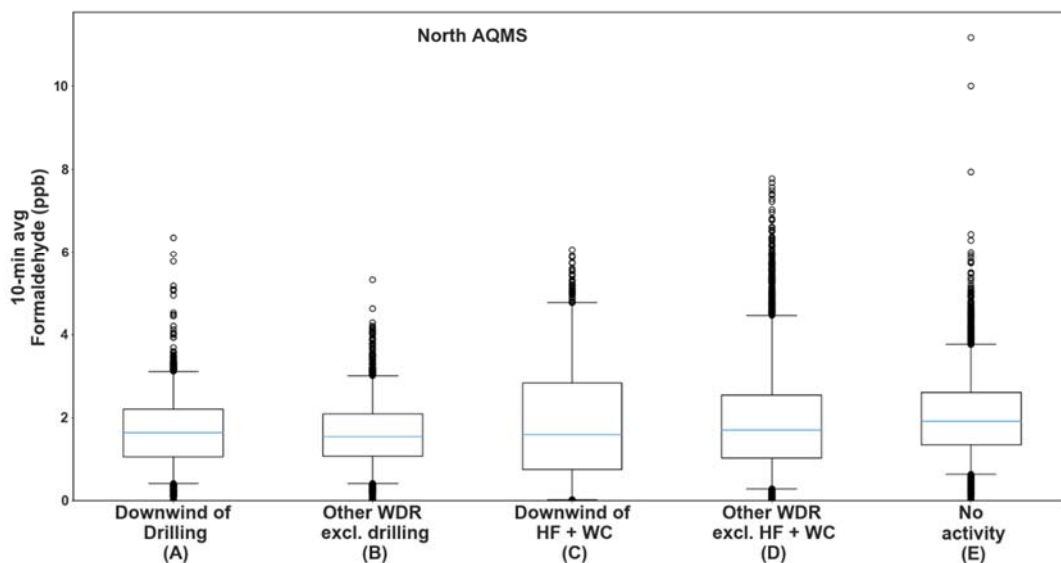


**Figure 48** Box and whisker plots of the 10 min average formaldehyde data from the North-AQMS measured by PTR-MS when downwind of drilling and HF + WC. For comparison formaldehyde data from other WDRs during drilling and HF +WC, as well as during non-activity periods are presented. Note the box represents the range between the 25<sup>th</sup> and 75<sup>th</sup> percentiles, the blue line is the median (50<sup>th</sup> percentile), the whiskers represent the 5<sup>th</sup> and 95<sup>th</sup> percentiles and the points above/below the whiskers represent the top/bottom 5% of values.

In a previous report for this project, at another HF site in the Surat Basin region (Dunne et al 2018), approximately 14-day integrated averages of formaldehyde collected on Radiello samples were higher downwind from well pads during HF activity. In the previous study, elevated levels did not appear to be related to emissions from vehicles and equipment on site and did not coincide with peaks related to smoke. The elevated long term averages (~ 14 days) associated with HF +WC in the previous study and the higher 75<sup>th</sup> and 95<sup>th</sup> percentiles of formaldehyde when measuring

downwind of HF + WC (C) observed in this study suggest HF + WC activities may increase formaldehyde concentrations above background.

The potential sources of formaldehyde emissions to air associated with well development activity currently remain poorly understood. An Australian Government assessment of chemicals used in CSG extraction in Australia which identified 113 chemicals used in drilling and HF during the period 2010 – 2012 did not list formaldehyde as a component of drilling or HF fluids (NICNAS 2017a). Hydraulic Fracturing Well Completion reports were submitted to the Queensland Government for each well at the study site by the well operator as part of their requirements under the *Petroleum Regulation Act 2004*. No use of formaldehyde was reported as a chemical additive in the HF fluids injected into the wells (APLNG, 2016). Likewise, the well operator did not report the use of chemical additives in drilling fluids that contained formaldehyde (APLNG, 2017). However the presence of formaldehyde in HF fluids as a result of interactions between chemical additives or as a trace contaminant in the chemical additives used has been reported but is currently not well understood (Kahrilas et al., 2014; Stringfellow et al., 2014).

Formaldehyde is highly soluble and has low volatility. If present in HF fluids it is likely to largely remain in the liquid phase and be carried to the surface in flowback and produced waters rather than substantially partition to the gas phase and be carried in CSG (Yost et al. 2016). In analysis of samples of flowback and produced water from 64 HF and non-HF wells in Queensland, formaldehyde was never detected above the quantitation limit of 0.2 mg/L (NICNAS, 2017). In 11 samples of water from wells in the Surat Basin, trace levels of formaldehyde (0.06 mg/L) were measured in only one sample (Lawson et al., 2017).

### **Summary**

In summary, the concentrations of formaldehyde measured by three independent methods across the study site, were always well below relevant air quality criteria. Biomass burning and secondary photochemical production were identified as the likely sources of formaldehyde in the background atmosphere in the region of the HF study site. Small enhancements in formaldehyde concentration above background were observed in measurements downwind of drilling and HF + WC activities. Aside from vehicle emissions, the potential sources of formaldehyde associated with well development activities are not well understood. Analysis of the limited data of the composition of HF fluids, drilling fluids, CSG and flowback/produced waters suggests direct emissions of formaldehyde to the air from these potential sources were unlikely to have contributed significantly to airborne concentrations.

## 5.2 Benzene, Toluene, Xylenes

Benzene, toluene and xylenes, collectively known as the BTX compounds, share similar sources. Possible sources of BTX that were detected in air at the HF site (Dunne et al., 2017) include:

- Vehicle exhaust and evaporative fuel/oil emissions;
- Evaporation / leakages from on-site tanks/pipelines holding flowback / produced water;
- Fugitive emissions of CSG;
- Emissions from prescribed burning, bushfires or wood heaters;
- Other industrial/ commercial / domestic emissions.

The addition of BTX compounds to HF fluids has been strictly regulated in Queensland (SoQ 2010) and fracturing fluids must meet the Australian Drinking Water Guideline for benzene and the Australian and New Zealand Environment Conservation Council guideline for marine and freshwater quality for toluene and xylenes. The well operator did not report any chemical additives being used in drilling fluids that contained benzene (APLNG , 2017). Consequently drilling, and HF fluids, are not considered a source of BTX here.

BTX compounds are naturally present in coal and may be mobilised from the coal seam into CSG and formation water during HF and brought to the surface as a component of either flowback/produced water or CSG. Little publicly available information exists on the levels of VOCs in CSG and formation water from Australian coal seams and more data is needed to properly characterize these sources (Stearman et al., 2014). In previous studies BTX was either not detected or detected at trace levels in CSG (< 1 ppm) and flowback / produced waters (< 0.2 mg/L). However, concentrations in water samples were higher in HF wells than in non-HF wells. (Apte et al., 2016, NICNAS 2017, Day et al., 2016, Lawson et al., 2017).

Trace levels of one or more BTX species were detected in 67% of flowback and produced water samples collected from wells (COM 313, COM337 and COM 359R) at the site of the present study as part of the water quality component of this GISERA project (Apte et al., 2018). The physicochemical properties of the BTX compounds indicate these species will partition between the formation water and the gas phase (Yost et al., 2016, Ryerson et al., 2011) and may make minor contributions to ambient BTX as a component of CSG emissions or via evaporation from flowback water stored on site.

In sections (5.2.1 – 5.2.3) summary statistics of the concentrations of benzene, toluene and xylenes observed at the study site are presented and compared with air quality guidelines and with data from other sites in the Surat Basin. In sections 5.2.4 changes in BTX levels above background that occurred during HF operations are investigated and potential contributions from HF and non-HF related sources of BTX are discussed.

## 5.2.1 Benzene

### Summary Statistics and Comparison with Air Quality Objectives

Summary statistics of benzene concentrations including monthly average and maximum concentrations and data capture rates for the North-AQMS are listed in Table 28. An annual MIL of 0.003 ppm (3 ppb) is specified for benzene in the Air Toxics NEPM (2011). The overall average for the 116 days of PTR-MS data was 0.03 ppb which is approximately 100 hundred times lower than the annual NEPM MILs. Likewise, the range of benzene concentrations integrated over approximately 14 days measured in the Radiello samples at the North and South-AQMS and Site #1 for the period Jun – Nov 2017 were 0.02 - 0.07 ppb (Table 28), well below the NEPM MILs.

A time series of the ~ 24-hour average benzene concentrations measured by the PTR-MS and the VOC adsorbent tubes (AT-VOC) at the North-AQMS is shown in Figure 49. The maximum 24-hour benzene concentration of 0.09 ppb observed during this study was well below the short-term (24-hour) Texas AMCV guideline value for benzene of 180 ppb.

**Table 29 Monthly maximum and average 24-hour concentrations of benzene (ppb) for North-AQMS by PTR-MS and AT-VOC methods for the HF study period (Jul – Dec 2017). Data capture (%), overall average benzene, and concentrations during HF +WC are also presented. The annual NEPM MIL for benzene is 180 ppb. Note: Benzene data from Solar-AQMS #1 –# 5 excluded due to poor precision (Appendix 11).**

Benzene - 2017	Jul	Aug	Sep	Oct	Nov	Dec	Overall	HF + WC period
<b>North-AQMS- PTR-MS</b>							<b>Jul - Nov</b>	<b>21<sup>st</sup> Sept – 2<sup>nd</sup> Nov</b>
Max 24-hour	0.03	0.08	0.09	0.06	0.05	0	0.09	0.09
Average 24-hour	0.02	0.03	0.03	0.03	0.02	0	0.03	0.03
% Data Avail	10 <sup>c</sup>	100	100	100	70 <sup>c</sup>	0 <sup>c</sup>	76 <sup>c</sup>	100
<b>North-AQMS - AT-VOC</b>							<b>Aug - Oct</b>	<b>21<sup>st</sup> Sept – 2<sup>nd</sup> Nov</b>
Max 24-hour	n.d.	0.04	0.04	0.06	0.09	0	0.09	0.06
Average 24 -hour	n.d.	i.d.	i.d.	i.d.	i.d.	0	i.d.	i.d.
% Data Avail	0 <sup>h</sup>	26 <sup>h,b</sup>	27 <sup>h,b</sup>	52 <sup>h,b,i</sup>	13 <sup>h</sup>	0 <sup>h</sup>	39	47

n.d. indicates no data are available; i.d. indicates insufficient data were available to calculate value (< 60% data available). Reasons for data availability < 90 %: a = power outage; b = instrument failure; c = instrument not commissioned or commissioned /decommissioned part way through month; h = sampling only conducted when CSIRO personnel on site 8/8/2017 – 17/8/2017 and 15/9/2017 – 28/10/2017; i= samples not collected due to bad weather or sample media shortage;

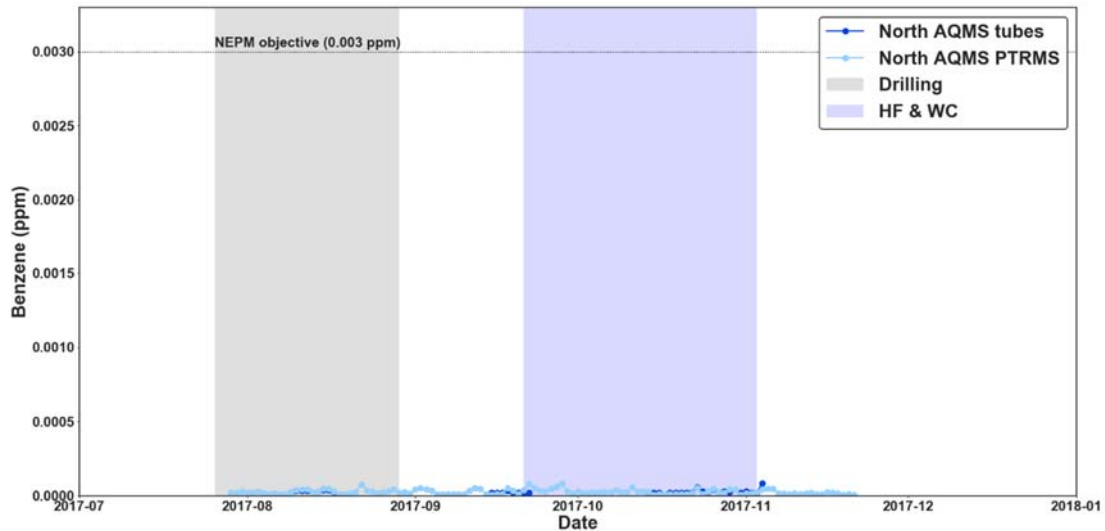


**Figure 49 24-hour averages of benzene measured at the North-AQMS by PTR-MS and NEPM Air Toxics annual objective for benzene. Shaded areas represent periods of well development activity on the HF study site, including drilling (grey) and HF + WC (purple). Note that North AQMS tubes represents the samples collected using the AT-VOC method at the North-AQMS.**

### Comparison with other sites in the Surat Basin

The ~14-day integrated average concentrations of benzene reported from the Radiello method in this study were similar to those reported from 134 Radiello samples collected at two other HF sites in the Miles-Condamine region of the Surat Basin in 2016-17 shown in Table 30 and reported previously in Dunne et al. (2018), and similar to Radiello data from four other sampling sites operated over the same period as the present study as part of the Surat Basin Ambient Air Quality (SBAAQ) Study (Lawson et al., 2018). Overall, the range of concentrations and detection frequencies of each compound collected using Radiello samplers at the HF sites were similar to those observed across the two regional sites (Burncluith and Tara) which were > 10 km from CSG infrastructure, and at two other gas field sites (Miles Airport and Hopeland) which were not known to be directly impacted by HF activities.

**Table 30 Comparison of the detection frequency (% samples > DL) and concentration ranges of benzene measured by Radiello at the HF study site, with data from another HF site in the Miles-Condamine region collected in 2016/17 (Dunne et al., 2018), and with data from two regional sites (Burncluith & Tara region) and two gas field sites (Wilgas & Hopeland) operated as part of the Surat Basin Ambient Air Monitoring Network (Lawson et al., 2018).**

Location	Range (ppb)	Detection Frequency (% samples > DL)
HF site (This Study)	0.02 – 0.07	18%
HF site (Miles-Condamine, 2016/17)	0.01 – 0.09	21%
Regional Sites (Tara region & Burncluith)	0.02 – 0.05	25%
Gas-Field Sites (Wilgas & Hopeland)	0.01 – 0.09	29%

## 5.2.2 Toluene

### Summary Statistics and Comparison with Air Quality Objectives

Summary statistics of toluene concentrations, including monthly average and maximum concentrations and data capture rates for the North-AQMS are listed in Table 31. A time series of the approximately 24-hour average toluene concentrations measured by the AT-VOC at the North-AQMS and Solar-AQMS #1- #5 and 24-hour average PTR-MS data from the North-AQMS are shown in Figure 50. The maximum 24-hour toluene concentration of 0.06 ppb observed during this study was well below the 24-hour Air Toxics NEPM MIL value for toluene of 1 ppm. An annual NEPM MIL of 0.1 ppm (100 ppb) is also specified for toluene in the Air Toxics NEPM (2011). The overall average for the 116 days of PTR-MS data was 0.02 ppb, and the average from the AT-VOC at the North-AQMS and Solar-AQMS #1-#5 were 0.01 ppb (Table 31) which is well below the annual NEPM MIL value. Likewise, the range of ~ 14-day integrated toluene concentrations measured in the Radiello samples at the North and South-AQMS and Solar-AQMS #1 for the period Jun – Nov 2017 were 0.01 -0.03 ppb (Table 32), well below the NEPM MIL.

**Table 31 Monthly maximum and average 24-hour concentrations of toluene (ppm) for North-AQMS by the PTR-MS and active sampling on adsorbent tube methods (AT-VOC) and for Solar-AQMS #1-#5 for the HF study period (Jul – Dec 2017). Data capture (%), overall average toluene, and concentrations during HF +WC are also presented. The NEPM 24-hour MIL for toluene is 0.1 ppm.**

Toluene - 2017	Jul	Aug	Sep	Oct	Nov	Dec	Overall	HF + WC period
<b>North-AQMS- PTR-MS</b>							<b>Jul - Nov</b>	<b>21<sup>st</sup> Sept – 2<sup>nd</sup> Nov</b>
Max 24-hour	0.015	0.034	0.045	0.053	0.053	n.d.	0.053	0.053
Average 24-hour	0.013	0.015	0.020	0.025	0.020	n.d.	0.020	0.025
% Data Avail	10 <sup>c</sup>	100	100	100	70 <sup>c</sup>	0 <sup>c</sup>	76 <sup>c</sup>	100
<b>North-AQMS- AT-VOC</b>							<b>Aug - Oct</b>	<b>21<sup>st</sup> Sept – 2<sup>nd</sup> Nov</b>
Max 24-hour	n.d.	0.028	0.020	0.032	0.018		0.032	0.032
Average 24-hour	n.d.	i.d.	i.d.	i.d.	i.d.		0.012	0.009
% Data Avail	0 <sup>h</sup>	26 <sup>h,b</sup>	27 <sup>h,b</sup>	52 <sup>h,b,i</sup>	13 <sup>h</sup>	0 <sup>h</sup>	39 <sup>h,b,i</sup>	47 <sup>h,b,i</sup>
<b>Solar-AQMS Sites #1-5 AT-VOC</b>							<b>Aug - Oct</b>	<b>21<sup>st</sup> Sept – 2<sup>nd</sup> Nov</b>
Max 24-hour	n.d.	0.060	0.033	0.050	n.d.		0.060	0.050
Average 24-hour	n.d.	i.d.	i.d.	i.d.	i.d.		0.011	0.012
% Data Avail	0 <sup>h</sup>	19 - 35 <sup>h,b</sup>	48 - 52 <sup>h,b</sup>	39 - 55 <sup>h,b,i</sup>	0 <sup>h</sup>	0 <sup>h</sup>	41 - 47 <sup>h,b,i</sup>	51 - 63 <sup>h,b,i</sup>

n.d. indicates no data are available; i.d. indicates insufficient data were available to calculate value (< 60% data available). Reasons for data availability < 90 %: a = power outage; b = instrument failure; c = instrument not commissioned or commissioned /decommissioned part way through month; h = sampling only conducted when CSIRO personnel on site 8/8/2017 – 17/8/2017 and 15/9/2017 – 28/10/2017; i= samples not collected due to bad weather or sample media shortage; k= data availability differed between Solar-AQMS #1 –# 5, range of values presented.

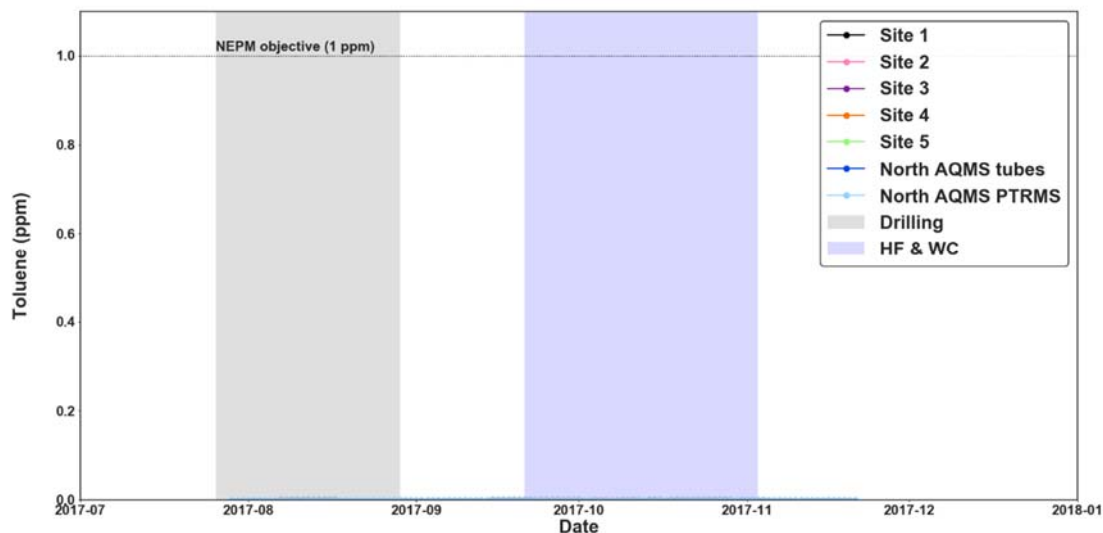


**Figure 50 24-hour averages of toluene measured at the North-AQMS by PTR-MS and by absorbent tubes (AT-VOC) at the Solar-AQMS sites with the NEPM Air Toxics annual objective for toluene. Shaded areas represent periods of well development activity on the HF study site, including drilling (grey) and HF + WC (purple).**

### Comparison with other sites in the Surat Basin

The range of ~ 14-day integrated average concentrations of toluene reported from the Radiello method in this study were lower than those reported from 134 Radiello samples collected at two other HF sites in the Miles-Condamine region of the Surat Basin in 2016-17 shown in Table 32 and reported previously in Dunne et al. (2018). , and similar to Radiello data from four other sampling sites operated over the same period as the present study as part of the Surat Basin Ambient Air Quality (SBAAQ) Study (Lawson et al., 2018). Overall, the range of concentrations and detection frequencies of each compound collected using Radiello samplers at the HF sites were similar to those observed across the two regional sites (Burncluith and Tara) which were > 10 km from CSG infrastructure, and at two other gas field sites (Wilgas and Hopeland) which were not known to be directly impacted by HF activities.

**Table 32 Comparison of the detection frequency (% samples > DL) and concentration ranges of toluene measured by Radiello at the HF study site, with data from another HF site in the Miles-Condamine region collected in 2016/17 (Dunne et al 2018), and with data from two regional sites (Burncluith & Tara region) and two gas field sites (Wilgas & Hopeland) operated as part of the Surat Basin Ambient Air Monitoring Network (Lawson et al 2018).**

Location	Range (ppb)	Detection Frequency (% samples > DL)
HF site (This Study)	0.01 – 0.03	18%
HF site (Miles-Condamine)	0.01 – 0.18	29%
Regional Sites (Tara region & Burncluith)	0.01 – 0.04	21%
Gas-Field Sites (Wilgas & Hopeland)	0.01 – 0.04	43%

### 5.2.3 Xylenes

#### Summary Statistics and Comparison with Air Quality Objectives

Summary statistics of xylene concentrations including monthly average and maximum concentrations and data capture rates for the North-AQMS are listed in Table 33. A time series of the approximately 24-hour average xylene concentrations measured by the AT-VOC method at all six sampling sites and the PTR-MS at the North-AQMS is shown in Figure 51. It is important to note that the PTR-MS measurement of xylenes include minor contributions from ethylbenzene, another aromatic compound with the same mass as xylene, which may lead to a small overestimation in the PTR-MS reported concentrations for xylenes.

An annual MIL of 0.20 ppm (200 ppb) is specified for xylenes in the Air Toxics NEPM (2011). The overall average for the 116 days of PTR-MS data was 0.017 ppb. The average xylene concentrations from the AT-VOC sampling at the North-AQMS and the Solar-AQMS sites was 0.014 ppb and 0.008 ppb respectively. Likewise, the range of ~ 14-day xylene concentrations measured in the Radiello samples at the North and South-AQMS as well as Site 1 for the period Jun – Nov 2017 were 0.01 – 0.06 ppb (Table 33).

The maximum 24-hour xylene concentration of 0.077 ppb observed during this study was well below the 24-hour Air Toxics NEPM MIL value for xylene of 0.25 ppm.

**Table 33 Monthly maximum and average 24-hour concentrations of xylenes (ppm) for North-AQMS and for Solar-AQMS 1-5 for the HF study period (Jul – Dec 2017). Data capture (%), overall average xylenes, and concentrations during HF +WC are also presented. The NEPM 24-hour MIL for formaldehyde is 0.04 ppm.**

Xylenes - 2017	Jul	Aug	Sep	Oct	Nov	Dec	Overall	HF + WC period
<b>North-AQMS- PTR-MS</b>							<b>Jul - Nov</b>	<b>21<sup>st</sup> Sept – 2<sup>nd</sup> Nov</b>
Max 24-hour	0.016	0.032	0.041	0.039	0.039	n.d.	0.041	0.041
Average 24-hour	0.012	0.012	0.017	0.021	0.018	n.d.	0.017	0.020
% Data Avail	10 <sup>c</sup>	100	100	100	70 <sup>c</sup>	0 <sup>c</sup>	76 <sup>c</sup>	100
<b>North-AQMS- AT-VOC</b>							<b>Aug - Oct</b>	<b>21<sup>st</sup> Sept – 2<sup>nd</sup> Nov</b>
Max 24-hour	n.d.	0.021	0.009	0.010	0.018	n.d.	0.032	0.032
Average 24-hour	n.d.	i.d.	i.d.	i.d.	i.d.	n.d.	0.012	0.009
% Data Avail	0 <sup>h</sup>	26 <sup>h,b</sup>	27 <sup>h,b</sup>	52 <sup>h,b,i</sup>	13 <sup>h</sup>	0 <sup>h</sup>	39 <sup>h,b,i</sup>	47 <sup>h,b,i</sup>
<b>Solar-AQMS #1-#5 AT-VOC</b>							<b>Aug - Oct</b>	<b>21<sup>st</sup> Sept – 2<sup>nd</sup> Nov</b>
Max 24-hour	n.d.	0.028	0.017	0.020	n.d.	n.d.	0.028	0.020
Average 24-hour	n.d.	i.d.	i.d.	i.d.	n.d.	n.d.	0.006	0.006
% Data Avail	0 <sup>h</sup>	19 - 35 <sup>h,b</sup>	48 - 52 <sup>h,b</sup>	39 - 55 <sup>h,b,i</sup>	0 <sup>h</sup>	0 <sup>h</sup>	41 - 47 <sup>h,b,i</sup>	51 - 63 <sup>h,b,i</sup>

n.d. indicates no data are available; i.d. indicates insufficient data were available to calculate value (< 60% data available). Reasons for data availability < 90 %: a = power outage; b = instrument failure; c = instrument not commissioned or commissioned /decommissioned part way through month; h = sampling only conducted when CSIRO personnel on site 8/8/2017 – 17/8/2017 and 15/9/2017 – 28/10/2017; i= samples not collected due to bad weather or sample media shortage; k= data availability differed between Solar-AQMS #1 –# 5, range of values presented.

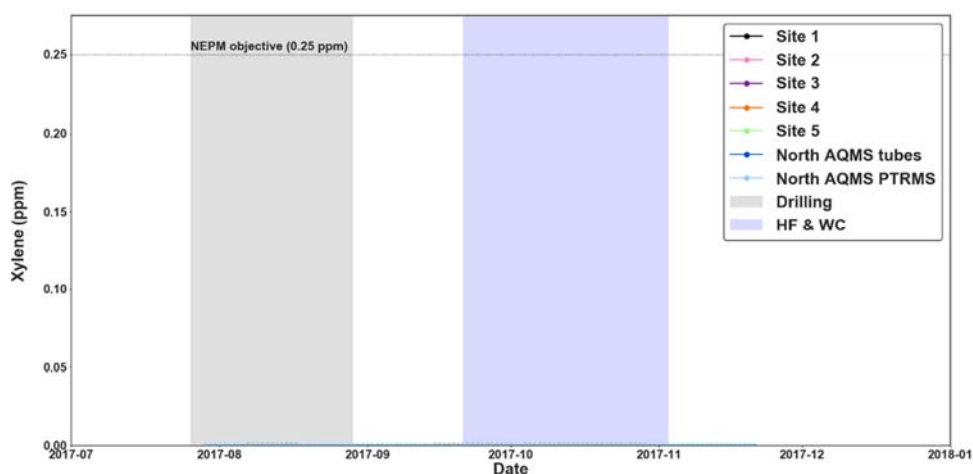


**Figure 51 24-hour averages of xylenes measured at the North-AQMS by PTR-MS and by absorbent tubes at the Solar-AQMS sites with the NEPM Air Toxics annual objective for xylene. Shaded areas represent periods of well development activity on the HF study site, including drilling (grey) and HF + WC (purple).**

### Comparison with other sites in the Surat Basin

The range of ~ 14-day integrated average concentrations of xylene reported from the Radiello method in this study were similar to those reported from 134 Radiello samples collected at two other HF sites in the Miles-Condamine region of the Surat Basin in 2016-17 shown in Table 34 and reported previously in Dunne et al. (2018), and similar to Radiello data from four other sampling sites operated over the same period as the present study as part of the Surat Basin Ambient Air Quality (SBAAQ) Study (Lawson et al., 2018). Overall, the range of concentrations and detection frequencies of each compound collected using Radiello samplers at the HF sites were similar to those observed across the two regional sites (Burncluth and Tara) which were > 10 km from CSG infrastructure, and at two other gas field sites (Miles Airport and Hopeland) which were not known to be directly impacted by HF activities.

**Table 34 Comparison of the detection frequency (% samples > DL) and concentration ranges of xylenes measured by Radiello at the HF study site, with data from another HF site in the Miles-Condamine region collected in 2016/17 (Dunne et al., 2018), and with data from two regional sites (Burncluth & Tara region) and two gas field sites (Wilgas & Hopeland) operated as part of the Surat Basin Ambient Air Monitoring Network (Lawson et al., 2018).**

Location	Range (ppb)	Detection Frequency (% samples > DL)
HF site (This Study)	0.01 – 0.06	12%
HF site (Miles-Condamine)	0.01 – 0.08	9%
Regional Sites (Tara region & Burncluth)	0.01 – 0.06	13%
Gas-Field Sites (Wilgas & Hopeland)	0.01 – 0.03	19%

#### 5.2.4 HF and non-HF related sources of BTX

As has previously been discussed in relation to particulate matter (PM) (Section 4.3) and formaldehyde (Section 5.1), biomass burning was a significant source of air pollutants in the region during the HF study period. In addition to PM and formaldehyde, biomass burning is also a source of BTX to the atmosphere. The time series of 24-hour average BTX and acetonitrile concentrations (a tracer for biomass burning as discussed in Section 5.1) are presented in Figure 52. Similarity in the BTX and acetonitrile time series indicates that contributions from regional smoke were a significant source of BTX at the HF study site.

Also notable in the time series in Figure 52 is that the concentration of benzene was almost always greater than the concentrations of toluene and xylenes and the mean benzene to toluene ratio from the 24-hour average data was 1.6 and ranged from 0.4 – 3.7. The ratio of benzene to toluene differs with source type. Benzene/toluene ratios of 0.2 – 0.6 are typical in urban areas where emissions are dominated by petrol fuelled vehicle emissions, whereas diesel exhaust generally coincides with benzene/ toluene ratios  $>1$  (Cope et al., 2014, Day et al., 2016). Benzene / toluene ratios of approximately 0.9 and approximately 3 have been observed in air impacted by emissions from rural fires and wood smoke respectively (Cope et al., 2014, Akagi et al., 2011). In addition, once emitted into the atmosphere the benzene/toluene ratio generally increases as the air mass ages since the atmospheric lifetime of benzene (months) is greater than that for toluene and xylenes (days). Therefore, the mean benzene/toluene ratio of 1.6 observed in this study indicates background concentrations of BTX at the HF study site were dominated by smoke with lower values of toluene and xylene associated with aged air masses.

However, on occasion benzene/toluene ratios were  $\leq 1$ . From the start of sampling in early August up until the start of October benzene/toluene ratios at the North-AQMS were on average 1.9. followed by a visible decline in benzene concentrations at the start of October (1/10 – 10/10) that corresponded with a shift in local meteorology and the arrival of rainfall events likely resulting in loss of benzene in the background atmosphere by wet deposition to the surface, and suppression of emissions from regional fires. During this period, benzene concentrations were lower, and the benzene/toluene ratios were  $\leq 1$  indicating fresh vehicle emissions were the dominant source of benzene at the site likely related to equipment and vehicles used in HF + WC activity which occurred from 6/10 - 10/10 at the nearest well to the North-AQMS. There were several subsequent intermittent periods similar to this one where, in the absence of smoke, vehicle emissions appeared to be the dominant source of BTX on site.

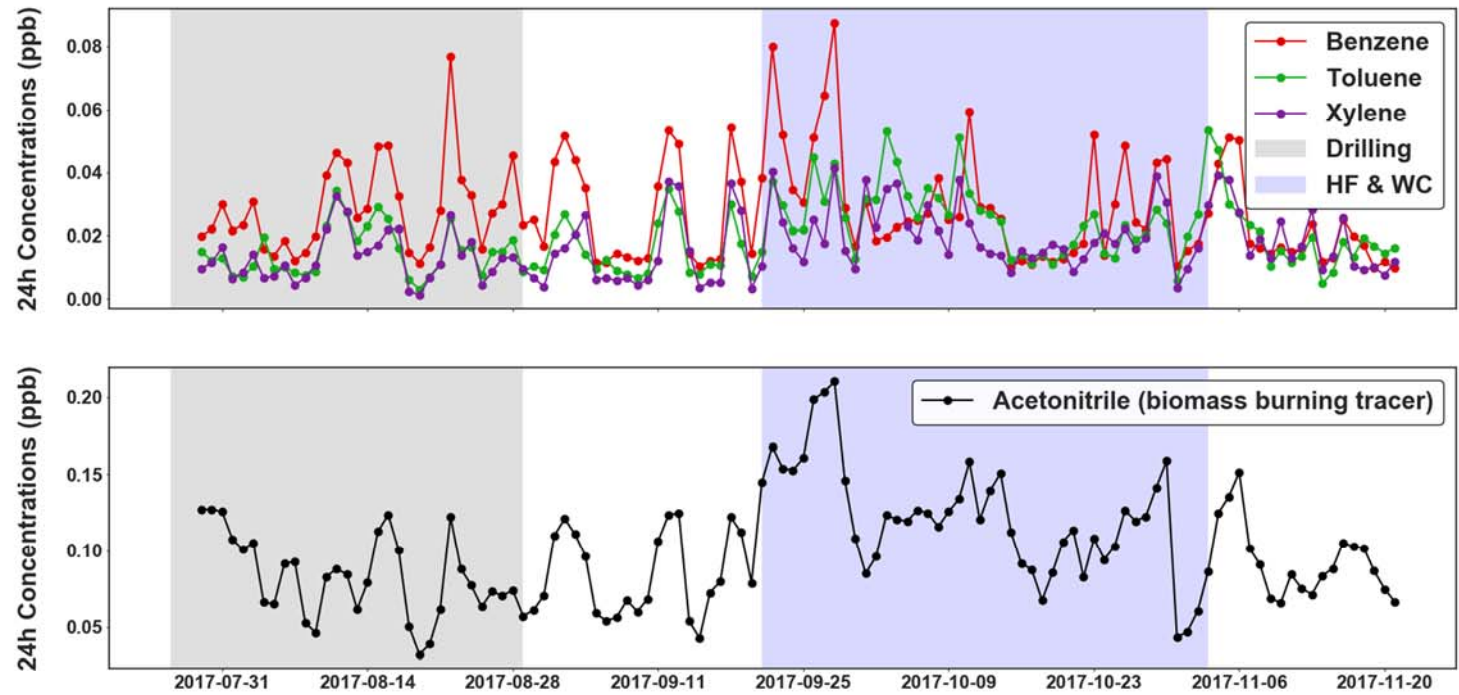


Figure 52 Time series of 24-hour concentrations of BTX species benzene, toluene and xylene (top panel) and acetonitrile (bottom panel) measured by PTR-MS measured at the North-AQMS. Shaded areas represent periods of well development activity on the HF study site, including drilling (grey) and HF + WC (purple).

Potential enhancements in BTX concentrations above background due to well development activity were further assessed using higher time resolution (10-minute) BTX and wind direction data. Figure 53 shows the distributions of 10-minute average benzene data measured with the PTR-MS at the North-AQMS when downwind of drilling (A) and when downwind of HF + WC (C), alongside data from other WDRs during the same periods (B and D) and during periods where no drilling, HF or WC activities were occurring (E). The characteristics of the distributions for the benzene data from the North-AQMS were as follows:

- For each of the BTX species, the median and inter quartile ranges were similar between activity periods and non-activity periods, and all WDRs;
- **Drilling** - The top 5 % of values when measuring downwind of drilling were higher than the top 5% of values when measuring air masses from other WDRs during the same period;
- **HF + WC** - With the exception of one peak event during HF + WC activity, the top 5 % of values when measuring downwind of HF + WC were generally within the range of the top 5% of values when measuring air masses from other WDRs during the same period and in comparison to non-activity periods.

The maximum 10-minute average benzene value measured downwind of HF + WC of 0.53 ppb (Figure 53) was recorded at midday on 10/10/2017 and coincided with 10-minute average maxima for toluene of 1.09 ppb, and xylenes 2.29 ppb. Well completions activity was occurring at the nearest well (COM 313) to the North-AQMS during this period.

Potential sources of BTX at the well pad during this period include emissions from equipment and vehicles on site and volatilisation/evaporation of BTX from flowback water stored in tanks at the well pad. Two samples of water flushed from well COM313 during completions on the 10/10/2017 were analysed as part of the water quality component of this GISERA project (Apte et al., 2018). Benzene, toluene and xylenes in these samples were all below the detection limits ( $1 - 2 \mu\text{g L}^{-1}$ ) of the analytical method employed and it is unlikely BTX emissions from flowback water stored on site significantly contributed to the observed peaks in benzene, toluene and xylene during WC activities. Rather, the benzene/toluene ratio of 0.5 during this peak event suggests the influence of emissions from vehicles or equipment on site. This is consistent with a previous report for this project at another HF site in the Surat Basin region (Dunne et al., 2018), in which small peaks in BTX concentrations, measured by Radiello sampling, were associated with HF activity and appeared to be related to emissions from vehicles and equipment on site.

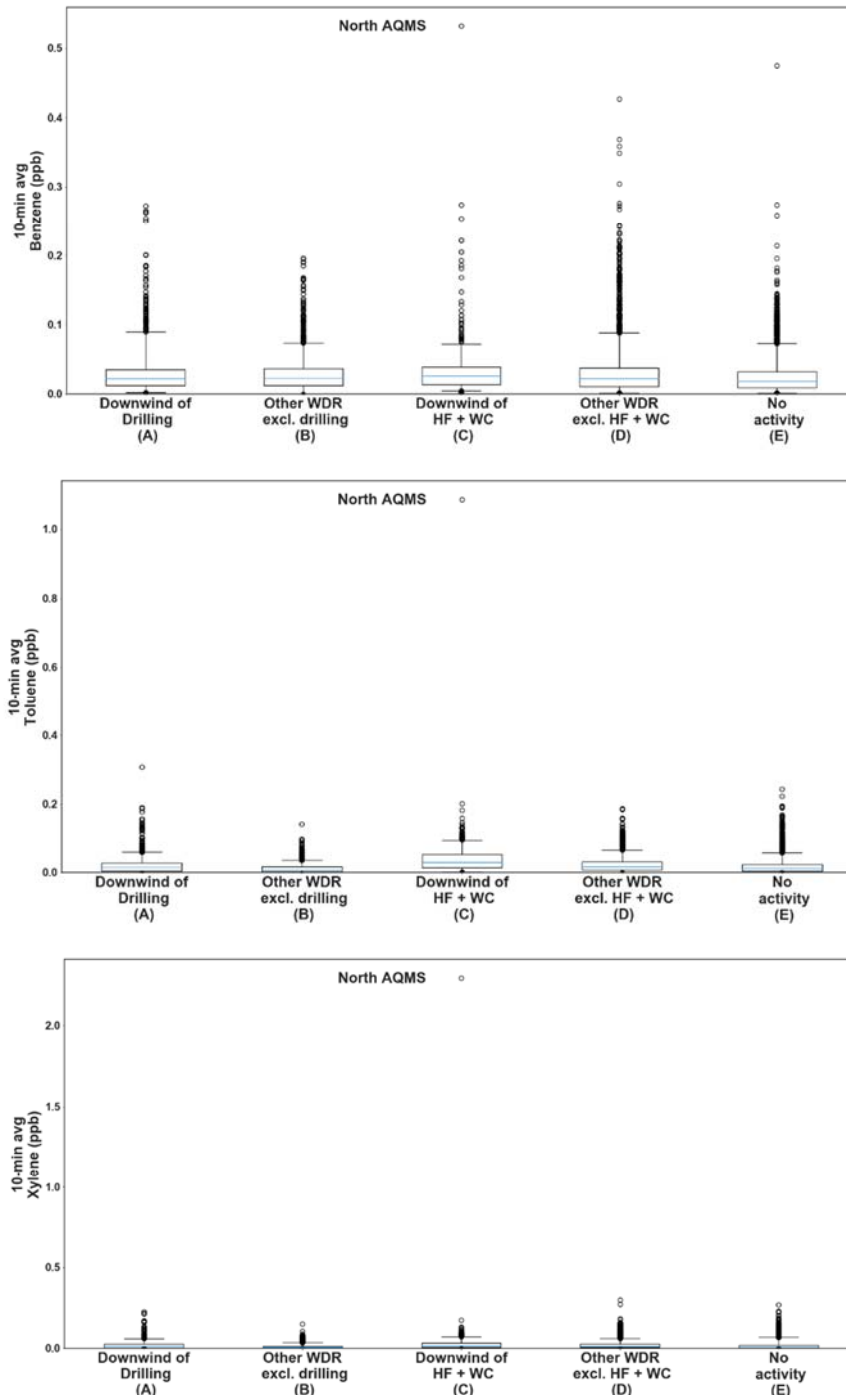


Figure 53 Box and whisker plots of the 10 min average benzene, toluene, xylene data from the North-AQMS measured by PTR-MS when downwind of drilling (A) and HF + WC (C). For comparison BTX data from other WDRs during drilling (B) and HF +WC (D), as well as during non-activity periods (E) are presented. Note the box represents the range between the 25<sup>th</sup> and 75<sup>th</sup> percentiles, the blue line is the median (50<sup>th</sup> percentile), the whiskers represent the 5<sup>th</sup> and 95<sup>th</sup> percentiles and the points above/below the whiskers represent the top/bottom 5% of values.

### 5.2.5 BTX Summary

In summary, the concentrations of BTX measured by three independent methods (PTR-MS, AT-VOC and Radiello) across the study site were always well below NEPM monitoring investigation levels. Biomass burning was identified as the most likely source of BTX in the background atmosphere at the study site. Small enhancements in BTX concentrations above background were observed in measurements downwind of drilling and HF + WC. Analysis of the benzene/toluene ratio suggests emission from vehicles and equipment on site were responsible for these enhancements. This is consistent with limited data of the composition of HF fluids, drilling fluids, CSG and flowback/produced waters which suggests direct emissions of benzene to the air from these HF-specific sources were unlikely to have contributed significantly to airborne concentrations.

## 5.3 Polycyclic Aromatic Hydrocarbons

Polycyclic aromatic hydrocarbons (PAHs) occur naturally in coal tars, crude oil and shale oil and are also formed during incomplete combustion of organic materials. Being semi-volatile, some PAHs in ambient air exist in a gaseous state or condense onto aerosols, for example, by attaching to smoke or dust particles. More than 100 PAH molecular species exist, some of which may cause adverse health effects. Benzo-a-pyrene (BaP) in particular has been included in the NEPM Air Toxics because of its behaviour as a human carcinogen.

PAH compounds typically share similar sources. PAHs detected in air at the HF site may be due to the following (Dunne et al., 2017):

- Emissions from vehicles and diesel-powered equipment;
- Emissions from prescribed burning, bushfires or wood heaters;
- Evaporation / leakages from on-site tanks or pipelines holding flowback / produced water;
- Fugitive emissions of CSG;
- Energy production, industry;

An Australian Government assessment of chemicals used in CSG extraction in Australia which identified 113 chemicals used in drilling and HF during the period 2010 – 2012 did not list PAHs as a component of drilling or HF fluids (NICNAS 2017a). Hence, HF fluids are not considered as a source of PAHs here.

In previous studies PAHs were not detected in CSG ( $< 0.02 \text{ mg m}^{-3}$ ) and were either not detected or only detected at trace levels in flowback/produced waters ( $< 0.2 \text{ mg L}^{-1}$ ) in samples from HF and non-HF wells (NICNAS, 2017; Lawson et al., 2017). The concentrations of PAHs in 36 flowback/produced water samples collected from three wells at the HF study site (N = 36), were

below the detection limit ( $< 0.05 \mu\text{g L}^{-1}$ ) with the exception of one sample containing trace amounts of naphthalene ( $1.1 \mu\text{g L}^{-1}$ ) (Apte et al., 2019).

### Summary Statistics and Comparison with Air Quality Objectives

The Air Toxics NEPM prescribes a MIL for the mass concentration of benzo-a-pyrene (BaP) as a marker of typical concentrations for the remaining PAH species. In this study, 24 samples each of a 48-hour duration were collected between 11 August to 22 November 2017 following the Australian standard method for sampling and analysis of PAHs in ambient air (AS/NZS 2014). Sample periods of 48 hours were used to ensure sufficient mass was deposited on the sample cartridges to allow for detection and quantification. Nine of the 16 US EPA priority PAHs were quantified, including BaP, which enables comparison to the Air Toxics NEPM guideline. Sample statistics for BaP are reported in Table 38 with 22 of the 24 samples having BaP concentrations greater than the method detection limit of  $0.0003 \text{ ng m}^{-3}$ .

**Table 35 Summary statistics for Benzo[a]Pyrene concentrations**

	Method	Averaging period	MDL ( $\text{ng m}^{-3}$ )	25 <sup>th</sup> %ile ( $\text{ng m}^{-3}$ )	Median ( $\text{ng m}^{-3}$ )	Mean ( $\text{ng m}^{-3}$ )	75 <sup>th</sup> %ile ( $\text{ng m}^{-3}$ )	Max ( $\text{ng m}^{-3}$ )	N
BaP	Active sampling of PAHs onto quartz filters and PUF sorbent	48-hour	0.0003	0.0008	0.0024	0.0045	0.0067	0.0219	24

*Sample concentrations were blank-corrected. The sample MDL was calculated as 3 times the standard deviation in the field blank.*

Figure 54 shows the time series of 48-hour BaP concentrations compared to the annual Air Toxics NEPM guideline. The average concentration of BaP during the study (August to November) was  $0.0045 \text{ ng m}^{-3}$ . If the average BaP concentration measured from August to November is representative of the concentration across one full year, then the inferred annual concentration of BaP is well below the annual air Toxics NEPM guideline of  $0.30 \text{ ng m}^{-3}$ . While Australia has no short-term health objectives for BaP, comparison to a Texas AMCV short-term guideline of  $30 \text{ ng m}^{-3}$  (which is 100 times higher than the annual NEPM guideline) also indicates that the 48-hour average concentrations are very low, with a maximum measured 48-hour concentration of  $0.0219 \text{ ng m}^{-3}$ .

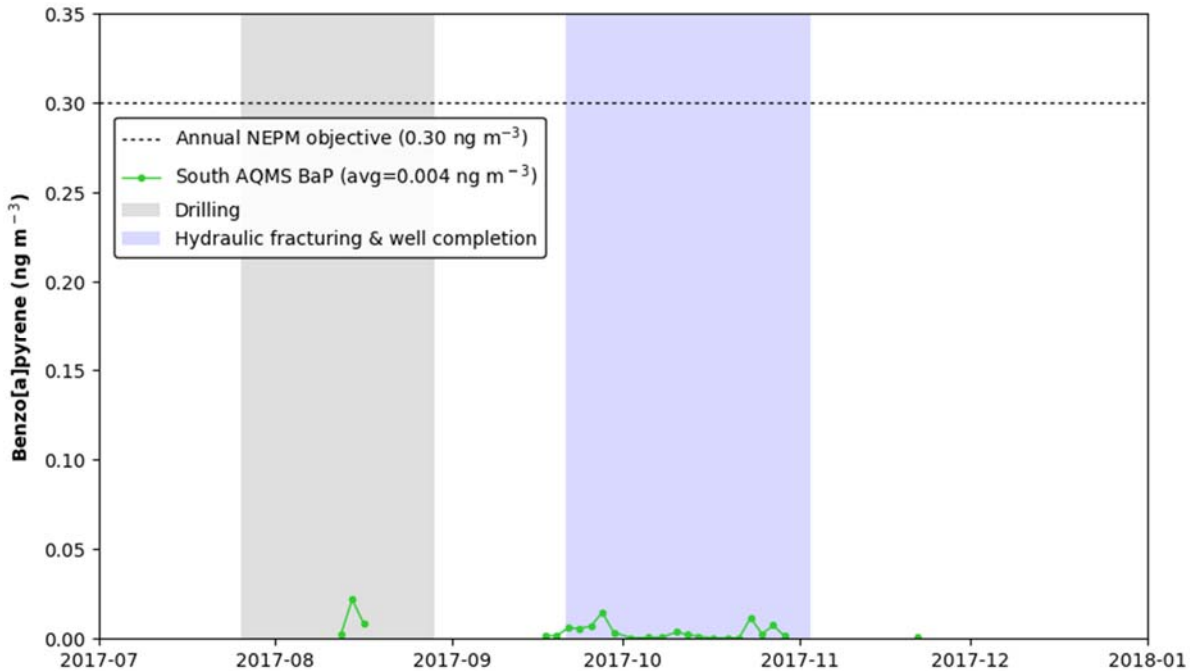


**Figure 54** Time series of 48-hour average benzo[a]pyrene concentrations in  $\text{ng m}^{-3}$  during the study compared to the annual NEPM objective of  $0.3 \text{ ng m}^{-3}$ . Shaded areas represent periods of well development activity on the HF study site, including drilling (grey) and HF + WC (purple).

### Comparison with other sites in Australia

The concentrations of PAHs measured in this study, particularly BaP, are amongst the lowest observed in Australia and New Zealand. The range in BaP concentrations observed at the South-AQMS site is lower than or similar to concentrations measured at other sites in Queensland (Table 39) such as Mutdapilly, a Queensland Department of Environment and Science background air quality site located in inland rural Queensland. The Mutdapilly site has been part of the South East Queensland monitoring network since 1995 and was used in 2007 by Kennedy et al. (2010) to measure PAHs in summer and winter. The reported levels of  $<0.0055 \text{ ng/m}^3$  in summer and  $0.0071 \text{ ng/m}^3$  in winter are similar to concentrations observed in this study.

Benzo[a]pyrene is a 5- ring PAH species used as a marker for total PAH concentrations. Nine additional 4-ring to 6-ring PAH species were also measured during this study. The concentrations of these species were also lower than concentrations observed at urban monitoring sites and were comparable to concentrations measured at the inland background site at Mutdapilly in Queensland (Table 39).

**Table 36 Concentrations of ten PAH species measured at other Queensland sites. BaP, the marker used to assess levels of PAHs against the annual NEPM, is highlighted in bold.**

	Concentration of PAHs (ng m <sup>-3</sup> )									
	Flu	Pyr	BaA	Chr	BbF+BkF	BeP	BaP	I123cdP	DahA	BghiP
This study min <sup>a</sup>	<0.0566	<0.0430	<0.0010	<0.0019	<0.0008	<0.0003	<b>&lt;0.0003</b>	<0.0004	<0.0002	<0.0007
This study max <sup>a</sup>	0.4657	0.3838	0.0434	0.0888	0.1439	0.0782	<b>0.0219</b>	0.0533	0.0119	0.0464
This study average	0.1692	0.1411	0.0058	0.0174	0.0254	0.0125	<b>0.0045</b>	0.0120	0.0020	0.0119
Rural Qld summer <sup>b</sup>	0.08	0.064	0.008	0.021	0.010	0.0047	<b>&lt;0.0055</b>	<0.0055	<0.0055	<0.0055
Rural Qld winter <sup>b</sup>	0.34	0.20	0.013	0.056	0.026	0.016	<b>0.0071</b>	0.012	<0.0059	0.056
Regional Qld min <sup>c</sup>	0.069						<b>&lt;0.0052</b>			
Regional Qld max <sup>c</sup>	1.5						<b>0.14</b>			
Industrial Qld average <sup>d</sup>							<b>0.005</b>			
Industrial Qld max <sup>d</sup>							<b>0.012</b>			
Urban Qld average <sup>e</sup>							<b>0.028</b>			
Urban Qld max <sup>e</sup>							<b>0.051</b>			

<sup>a</sup>48-hour gas and aerosol active measurements at the study site in the Darling Downs, rural inland Queensland, 2017

<sup>a</sup>40 to 50-day passive measurements at Mutdapilly, a rural inland background site, Queensland, 2007 (Kennedy et al 2010a)

<sup>b</sup>Monthly gas and aerosol active measurements at sites around Gladstone, a coastal region, Queensland, 2008/09 (Kennedy et al 2010b)

<sup>c</sup>Monthly PM<sub>10</sub> active measurements at Fisherman's Landing, an industrial area north of Gladstone, Queensland, 2016 (NEPC 2017)

<sup>d</sup>Monthly PM<sub>10</sub> active measurements at Woolloongabba, a traffic-impacted urban site, Brisbane, Queensland, 2016 (NEPC 2017)

Flu Fluoranthene (206-44-0), Pyr=Pyrene (129-00-0), BaA=Benzo[a]anthracene (56-55-3), Chr=Chrysene (218-01-9), Bbf+BkF= Benzo[b+k]fluoranthene (205-99-2+207-08-9), Bep= Benzo[e]pyrene, BaP=Benzo[a]pyrene (50-32-8), i123cdP= Indeno[1,2,3-cd]pyrene (193-39-5), DahA= Dibenz[ah]anthracene (53-70-3), BghiP= Benzo[ghi]perylene (191-24-2)

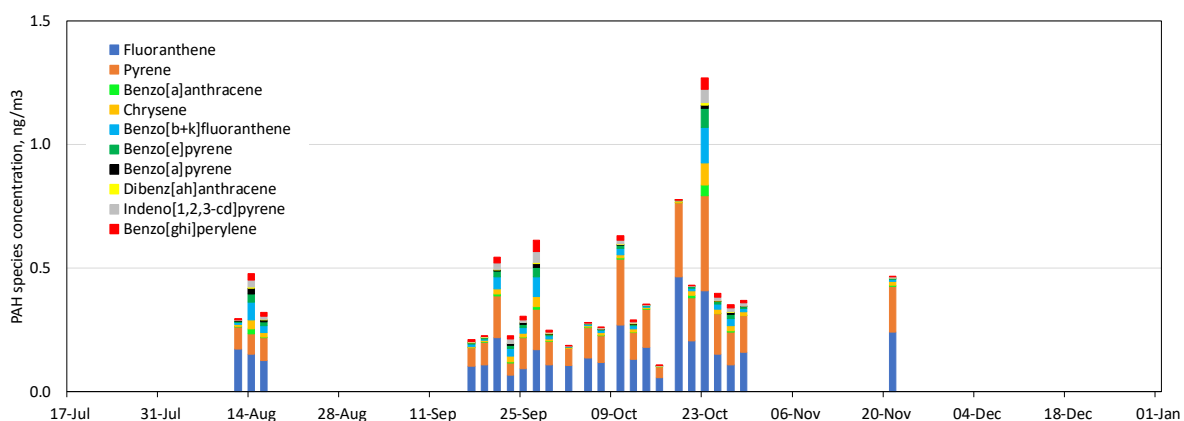


**Figure 55 Time series of 48-hour PAH concentrations measured at the South-AQMS site.**

A time series of all PAH species shows that the two most volatile species, Fluoranthene (Flu) and Pyrene (Pyr), are most abundant, comprising on average 77% of total PAH concentration. Measurements at other locations in Queensland show these two species typically exist as gases and the eight heavier, less volatile species, including BaP, Benzo[a]anthracene (BaA), Chrysene (Cr), Benzo[b+k]fluoranthene, (Bbf+BkF), Benzo[e]pyrene (Bep), Indeno[1,2,3-cd]pyrene (i123cdP), Dibenz[ah]anthracene (DahA), Benzo[ghi]perylene (BghiP) typically occur in the particle phase

(Wang et al., 2017). At the study site there were strong correlations between the gas phase PAHs, Flu and Pyr ( $R^2 = 0.85$ ) indicating they had similar sources. There were also strong correlations between aerosol phase PAHs ( $R^2=0.39-0.99$ ), with strongest agreement between the less volatile 5-ring and 6-ring species. Weaker correlations between gas and aerosol phase PAH concentrations may have been due to different transport and removal processes for gas and particle PAHs, resulting in different atmospheric lifetimes.

### **HF and non-HF related sources of PAHs**

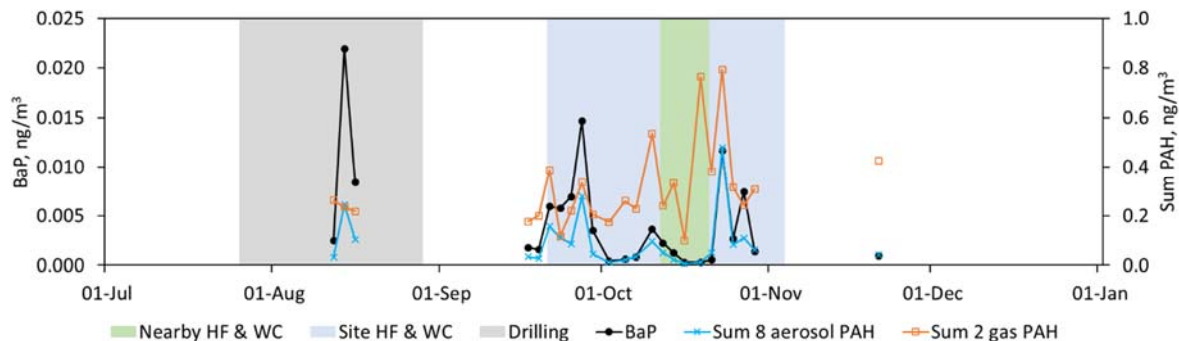
Potential enhancement of PAHs during HF + WC activities were examined by looking at PAH concentrations when wells nearest to the South-AQMS underwent HF +WC. No drilling of nearby wells occurred during the six days of sampling from August 11 to 17 so enhancement during drilling could not be assessed.

Figure 56 shows the concentrations of BaP, the sum of eight aerosol phase PAH (i.e. BaA, BaP, Cr, BbF+BkF, Bep, i123cdP, DahA and BghiP) and the sum of the two gas phase PAH concentrations (Flu and Pyr) during periods of activity at nearby wells COM 444 and COM 359R (shaded in green):

- Well COM 444 was located approximately 320 m to the NW ( $340^\circ$ ) of the PAH sampler at the South-AQMS. The period of HF + WC of COM 444 coincided with three consecutive samples collected from 11/10 to 18/10 corresponding to the first three points in the green shaded section in Figure 56. The PAH sampler was downwind of this well pad for 37% of the HF + WC period;
- Well COM 359R was located approximately 420 m to the S ( $170^\circ$ ) of the PAH sampler at the South-AQMS. HF + WC of COM 359R occurred over three samples from 15/10 - 20/10 corresponding to the last three data points in the green shaded section in Figure 56. The PAH sampler was downwind of COM359R for 28% of the HF + WC period. Aerosol phase PAHs were not elevated for the three samples.

Statistical analysis of PAH concentrations showed there was no significant enhancement in PAH concentrations ( $p < 0.05$ ) during nearby HF + WC activity ( $n = 4$ ) compared to other times ( $n = 20$ ). Gas phase PAHs were elevated in one sample from 18/10 - 20/10, coinciding with HF + WC activities at COM 359R, however during this time winds were not from the direction of the well pad undergoing HF + WC.

Three samples were collected while wells across the HF field were drilled. The highest BaP concentration of  $0.022 \text{ ng m}^{-3}$  for the study occurred for the sample period from 13th August 11 am to 15th August 11 am. However, the closest wells to the South-AQMS (COM 44 and COM 359R) were not undergoing drilling at the time this sample was collected. Instead, wells COM313 and COM 337 located N and NW of the South-AQMS were being drilled.



**Figure 56** Time series of BaP, the sum of 8 aerosol phase PAH (BaA, BaP, Cr, Bbf+BkF, Bep, i123cdP, DahA and BghiP) and 2 gas phase PAH (Flu and Pyr). Shaded areas represent periods of well development activity on the HF study site, including drilling (grey) and HF + WC (purple). The green shaded area represents activity at COM 359R and COM 444.

PAH profiles have been used to indicate the contributions of different sources of PAHs since the profile depends on the processes producing the PAHs (Tobiszewski and Namieśnik 2012). For example, low molecular weight PAHs form during low temperature combustion (e.g. biomass burning) and high molecular weight PAHs form during high temperature combustion (e.g. in combustion engines). A number of studies have developed and used specific values of PAH diagnostic ratios for different sources. Khalili et al. (1995) and Guo et al. (2003) suggested a BaP/(BaP+Cr) ratio of 0.5 indicated diesel combustion; Rogge et al. (1993a, b), Mandalakis et al. (2002), Fang et al. (2004) and Ravindra et al. (2006a, b) suggested a Flu/(Flu+Pyr) ratio of > 0.5 indicated diesel combustion while a Flu/(Flu+Pyr) ratio of < 0.5 indicated gasoline combustion; Kavouras et al. (2001) identified a i123cdP / (i123cdP + BghiP) ratio between 0.35 and 0.70 indicated diesel combustion. Many authors advise that caution is required when using binary diagnostic ratios to identify PAH sources due to complexities associated with photodegradation and chemical reactions in the atmosphere (Ravindra et al., 2008). However, combining the results obtained with PAH diagnostic ratios with other marker compounds provides support for the interpretation of PAH profiles.

The ratios discussed above that were measured in this study are shown in Table 37. The ratios of Fu/(Fu+Py) and I123cdP/(I123cdP+BghiP) indicate the contribution of diesel combustion to the PAHs measured at the South-AQMS. The maximum BaP/(BaP+Chr) also suggested a diesel combustion contribution to PAHs.

**Table 37 Diagnostic ratios of different PAH sources from the literature and measured in this study.**

	Flu/(Flu+Pyr)	BaP/(BaP+Chr)	I123cdP/ (I123cdP+BghiP)
wood			0.7 <sup>i</sup>
diesel	>0.5 <sup>abcdef</sup>	0.5 <sup>g h</sup>	0.35-0.7 <sup>i</sup>
petrol	<0.5 <sup>abcdef</sup>		
average	1.3	0.05	0.5
median	1.2	0.2	0.5
min	0.7	0.0	0.4
max	1.9	0.4	0.5

<sup>a</sup>Rogge et al. (1993a), <sup>b</sup>Rogge et al.(1993b), <sup>c</sup>Mandalakis et al.(2002), <sup>d</sup>Fang et al. (2004), <sup>e</sup>Ravindra et al. (2006a) <sup>f</sup>Ravindra et al. (2006 b), <sup>g</sup>Khalili et al. (1995), <sup>h</sup>Guo et al. (2003), <sup>i</sup>Kavouras et al. (2001)

These diesel combustion emissions may have originated from the laydown area and unsealed road located approximately 20 metres NE of the South AQMS. This area contained a large above-ground bore water tank, diesel refuelling tanks and trailers holding HF chemicals and proppant. There was frequent truck traffic to the area for refilling fuel, water or chemicals. The truck activity could be seen through short-term peaks in coarse PM and NO<sub>x</sub> (NO<sub>2</sub> and NO) concentrations. As discussed in the particle section, the highest concentrations of PM<sub>10</sub> and TSP at the South-AQMS were associated with winds from the NE sector, particularly during low wind speeds. The chemistry of particles at the South-AQMS site show much of the PM<sub>10</sub> and TSP was associated with soil dust. However short events in NO<sub>x</sub> coinciding with TSP show the site was also impacted by exhaust emissions from vehicles, a known source of PAHs.

Non-HF sources of PAHs that could contribute to regional background levels include biomass burning emissions from prescribed burns, wild-fires, agriculture burns, domestic heating/cooking, fugitive emissions from CSG infrastructure and emissions associated with burning of fuels for energy production, other industries, machinery or transport. The source apportionment of North-AQMS PM<sub>10</sub> comprised an average of 11% aged biomass smoke and 7% smoke from wood burning fires. There is a weak but significant correlation between PM<sub>10</sub> from these two smoke sources at the North-AQMS and BaP measured at the South-AQMS (R<sup>2</sup>=0.27), suggesting that regional smoke may have also contributed to PAH levels measured at the South-AQMS.

In summary, diagnostic ratios of PAH species and relationships with other marker species suggested that diesel combustion and biomass burning smoke contribute to PAH concentrations measured at the South-AQMS.

## 5.4 Other Queensland EPP air pollutants

Four additional gaseous air pollutants which are included in the Queensland Government's Environment Protection Policy (EPP) for Air (2008) were measured by passive Radiello VOC sampling at the HF study site from 14 June – 30 November 2017. These included hydrogen sulphide, the VOCs- 1,2-dichloroethane, styrene, and tetrachloroethylene. Styrene was also measured in the AT-VOC samples at the study site (7/8 – 19/8 and 15/9 – 29/10) and continuously from July – Nov by the PTR-MS at the North-AQMS.

Each passive Radiello sampler was deployed for approximately 14 days and the results from each sample represent an average concentration over the exposure period. Given the long averaging time the most appropriate comparison to make with the reported concentrations is to longer term air quality objectives (e.g. annual) as opposed to short-term objectives (e.g. 24-hour). Since the Queensland EPP only specifies 24-hour goals for 1,2-dichloroethane and hydrogen sulphide the levels of these pollutants reported from the 14-day Radiello samples cannot be assessed against these short-term objectives. Instead, the Radiello results for 1,2-dichloroethane were compared to annual Texas AMCV values and concentrations of hydrogen sulphide were compared against the Western Australian Department of Health 90-day guideline of 14 ppbv (WA DOH 2009).

### **Styrene**

An annual objective of 0.110 ppm (110 ppb), and 1-week objective of 60 ppb is specified for styrene in the Queensland EPP (2008). The overall average for the 116 days of PTR-MS data was 0.007 ppb. The average from the active sampling at the North-AQMS and the Solar-AQMS sites was 0.001 ppb. Styrene was never reported above the detection limit of 0.02 ppb in the Radiello samples on any occasion at the HF site (Table 38).

A time series of the ~ 24-hour average xylene concentrations measured by the VOC adsorbent tubes and the PTR-MS at the North-AQMS and by AT-VOC at the Solar-AQMS sites is shown in Figure 57. The maximum 24-hour styrene concentration of 0.034 ppb observed in this study was well below the Texas AMCV guideline value for styrene of 5.2 ppm (5200 ppb).

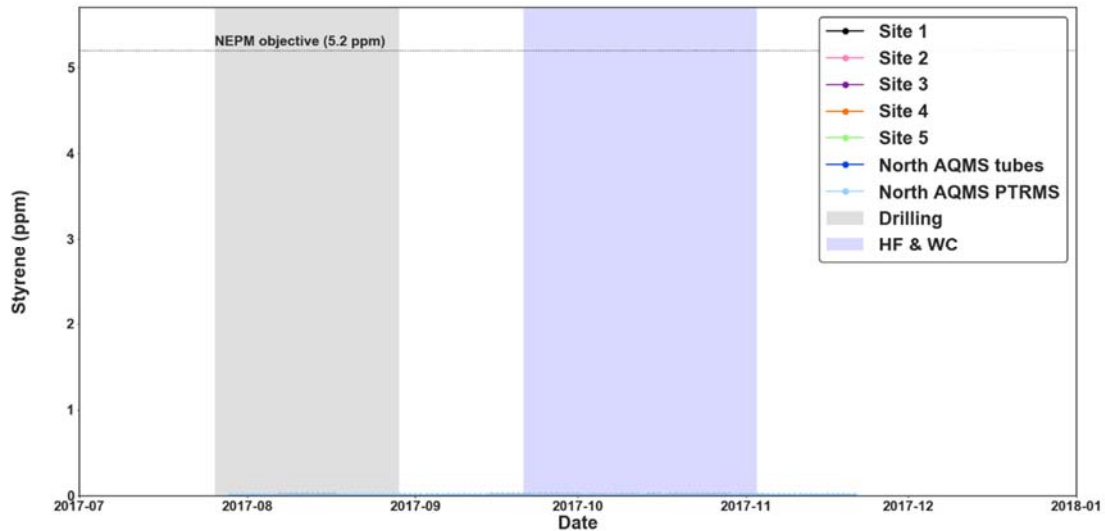


Figure 57 24-hour averages of styrene measured at the North-AQMS by PTR-MS and by absorbent tubes at the Solar-AQMS sites with the NEPM Air Toxics annual objective for styrene. Shaded areas represent periods of well development activity on the HF study site, including drilling (grey) and HF + WC (purple).

**Hydrogen sulphide, 1,2-dichloroethane, and tetrachloroethylene**

Hydrogen sulphide, and the VOCs- 1,2-dichloroethane and tetrachloroethylene were never detected at levels greater than their respective detection limits in either of the Radiello samples on any occasion during this study. The detection limits refer to the lower concentration limit of the Radiello measurement method, below which the concentration of a pollutant could not be reliably measured. Detection limits for each pollutant are listed in Table 38 along with their relevant air quality objectives. The maximum detection limits for these compounds were tens to thousands of times lower than their relevant air quality guideline values. This suggests that these compounds were either not present in the air at the HF study site or present in concentrations too low to be reliably measured with the Radiello sampling method employed in this study and were all well below relevant long-term ambient air objectives.

Table 38 Mean and max concentrations, detection frequency, detection limit method employed, averaging time and air quality objective for 1,2 dichloromethane, styrene, Tetrachloroethylene and Hydrogen Sulphide.

Compound	Method	Detection limit	Detection Frequency	Median (Max)	Ambient air objective		
		(ppbv)	(%)	(ppbv)	(ppbv)	Averaging period	Source
1,2-Dichloroethane	Radiello (~14-day avg)	0.02	0%	≤ 0.02	170 0.72	24-hour annual	Qld EPP Texas AMCV

Styrene	Radiello (~14-day avg)	0.02	0%	≤ 0.02	110	annual	Texas AMCV
	PTR-MS (24-hour avg)	0.002	97%	0.007 (0.034)	60 5200	1 week 24-hour	Qld EPP Texas AMCV
	AT-VOC (~24-hour avg)	0.001	13%	0.001 (0.029)			
Tetrachloroethylene	Radiello (~14-day avg)	0.02	0%	≤ 0.02	36 2	annual annual	Qld EPP Texas ESL
Hydrogen sulphide	Radiello (~14-day avg)	0.56	0%	≤ 0.56	110 14	24-hour 90 days	Qld EPP WA DOH

## 5.5 Other VOCs

In addition to formaldehyde, BTX and the four Queensland EPP air pollutants an additional 48 other VOCs were measured by the Radiello method at the HF study site from June to November 2017. Thirty-nine of these compounds were measurable by the passive Radiello method but never reported above their detection limits at the HF study site.

- Bromochloromethane
- Butanol
- 2-butoxyethanol
- Butyl acetate
- Chlorobenzene
- Cyclohexane
- Cyclohexanone
- Dichlorobenzene
- Dichloroethane
- Dichloropropane
- 2-Ethylhexanol
- Ethyl tertiary butyl ether
- n-heptane
- Isobutanol
- Isooctane
- Isopropylbenzene
- 1-methoxy-2-propanol
- 1-methoxy-2-propyl acetate
- Methyl methacrylate
- Methylcyclohexane
- Methylcyclopentane
- Methyl ethyl ketone
- Methyl isobutyl ketone
- 2-methyl pentane
- 3-methylpentane
- Methyl tertiary butyl ether
- Naphthalene
- n-Nonane
- n-Octane
- n-propylbenzene
- styrene
- Tetrachloroethylene
- 1,1,1-trichloroethane
- Trichloroethylene
- Trichloromethane
- 1,2,4-trimethylbenzene

- o-xylene
- pentanal
- benzaldehyde

The detection limits for the passive Radiello measurements of these species were tens to hundreds of times lower than the relevant long-term Texas AMCV air quality objectives suggesting that these compounds were either not present in the air at the HF study site or present in concentrations too low to be reliably measured with the Radiello sampling method employed in this study.

Table 39 lists the 13 compounds that were reported above the detection limits of the Radiello method on one or more occasions during this study, alongside their reported concentration range, detection frequency ( % samples > DL) and relevant air quality objectives. Australian federal or state ambient air objectives were not available for most of the VOCs reported in Table 39. In the absence of Australian objectives, Texas AMCV objectives that covered the range of VOCs measured in this study were used for comparison. The maximum concentrations for all 13 compounds detected at the HF study site during this study were tens to thousands of times below the long-term (annual) Texas AMCV objectives referenced here.

Overall, the range of concentrations and detection frequencies of each compound measured using Radiello samplers at the HF site were generally similar to those observed during the same period across the two regional sites (Burncluth and Tara) which were > 10 km from CSG infrastructure, at two other gas field sites (Miles Airport and Hopeland) which were not known to be directly impacted by HF activities, as well as at another HF site in the Miles-Condamine area measured in 2016-17 and reported previously (Dunne et al., 2018).

**Table 39** The concentration range and detection frequency (DF) for each VOC detected in Radiello samples at the HF study site and their relevant annual/ long term ambient air quality objective values. Also presented are data from another HF study site in the Miles-Condamine region collected in 2016/17 (Dunne et al 2018), and data from the regional sites (Tara and Burncluith) and gas field sites (Miles Airport and Hopeland) collected over the same period as the present study.

Compound	HF site (this study)		HF Sites 2016/17		Regional sites		Gas-field sites		Annual/ long-term ambient air quality objective	
	Roma-Yuleba region		Miles-Condamine region		Tara region & Burncluith		Wilgas, Hopeland,		ppb	Source
	Range (ppb)	DF (%)	Range (ppb)	DF (%)	Range (ppb)	DF (%)	Range (ppb)	DF (%)		
<i>N (Radiello samples)</i>	33		134		24		21			
<b>n-Hexane</b>	0.01 – 0.05	6%	0.01 – 0.09	13%	0.02 – 0.08	8%	0.01 – 0.09	24%	190	Texas AMCV
<b>n-Decane</b>	0.01 – 0.03	9%	0.01 – 0.08	21%	< 0.03	0%	0.01 – 0.04	10%	175	Texas AMCV
<b>n-Undecane</b>	0.03 – 0.14	33%	0.02 – 0.08	15%	0.02 – 0.10	38%	0.02 – 0.13	48%	55	Texas AMCV
<b>Benzene</b>	0.02 – 0.07	18%	0.01 – 0.09	21%	0.02 – 0.05	25%	0.01 – 0.09	29%	3	NEPM/EPP
									1	Texas AMCV
<b>Toluene</b>	0.01 – 0.03	18%	0.01 – 0.18	29%	0.01 – 0.04	21%	0.01 – 0.04	43%	100	NEPM/EPP
									1100	Texas AMCV
<b>m &amp; p-xylenes</b>	0.01 – 0.06	12%	0.01 – 0.08	9%	0.01 – 0.06	13%	0.01 – 0.03	19%	200	NEPM/EPP
									140	Texas AMCV
<b>o-Xylene</b>	< 0.02	0 %	0.01 – 0.03	4%	0.01 – 0.03	4%	0.01 – 0.04	5%	200	NEPM/EPP
									140	Texas AMCV

Compound	HF site (this study)		HF Sites 2016/17		Regional sites		Gas-field sites		Annual/ long-term ambient air quality objective	
	Roma-Yuleba region		Miles-Condamine region		Tara region & Burncluith		Wilgas, Hopeland,		ppb	Source
	Range (ppb)	DF (%)	Range (ppb)	DF (%)	Range (ppb)	DF (%)	Range (ppb)	DF (%)		
<b>Ethylbenzene</b>	0.01 – 0.05	12%	0.01 – 0.06	3%	0.01 – 0.04	8%	0.01 – 0.03	14%	440	Texas AMCV
<b>Styrene</b>	< 0.02	0%	< 0.02	0%	0.01 – 0.10	4%	< 0.04	0%	110	Texas AMCV
									60*	Qld EPP(* 1 week)
									5200*	Texas AMCV (*24-hour)
<b>Carbon tetrachloride</b>	0.05 – 0.11	88%	0.03 – 0.15	100%	0.05 – 0.11	100%	0.03 – 0.11	100%	2	Texas AMCV
<i>N(Aldehyde samples)</i>	33		116		25		21			
<b>Formaldehyde</b>	0.04 – 1.30	94%	0.33 – 2.12	100%	0.04 – 1.30	83%	0.39 – 1.30	100%	40* 9	NEPM/EPP (*24-hour) Texas AMCV
<b>Acetaldehyde</b>	0.03 – 0.56	94%	0.08 – 0.94	100%	0.07 – 0.81	83%	0.13 – 0.72	100%	25	Texas AMCV
<b>Propanal</b>	0.04 – 0.13	30%	0.03 – 1.14	58%	0.05 – 0.17	42%	0.04 – 0.18	48%	55	Texas AMCV
<b>Butanal</b>	0.09 – 0.27	9%	0.08 – 0.37	34%	0.13 – 0.24	13%	0.08 – 0.30	14%	34	Texas AMCV
<b>Hexanal</b>	0.04 – 0.12	21%	0.05 – 0.14	22%	0.05 – 0.12	17%	0.03 – 0.13	5%	200	Texas AMCV

## 6 Mercury and Radon

### 6.1 Mercury

While atmospheric mercury mostly exists in gaseous elemental form, trace amounts can also be present as organic or inorganic molecules. Mercury naturally occurs in most environmental reservoirs (rock, soil, air, water, biota). Emissions of mercury from these reservoirs includes volatilization from the ocean, release from soils during wild fires, release from the earth's crust during volcanic activity and release from decaying organic matter.

Release of mercury to the atmosphere from anthropogenic sources includes evaporation from unburnt fossil fuels and combustion of fossil fuels for transport, energy production, domestic heating or cooking. Mercury can be released during mining of the earth's crust for metals, during smelting/refining of metals and during production of materials such as cements and vinyl chloride. Mercury can also be released during incineration or evaporation from manufactured items containing mercury including paints, lamps, batteries, biocides, temperature and pressure sensors etc. The 2016/2017 National Pollutant Inventory for Australia reports the largest sources of mercury emission to air are dust from roads, emissions from non-ferrous metal manufacture (alumina, nickel etc.), electricity generation (burning of coal and coal seam gas), biomass burning (prescribed burns, agricultural burns, wildfires) and metal ore mining (mainly gold).

Relevant to the study reported here, possible on-site sources of mercury include natural emissions from soil, water or vegetation and emissions from CSG-related activities such as use of fossil-fuel powered vehicles and equipment for drilling, pad preparation, HF and well completion. Mercury may also be naturally present in CSG and in ground water from the coal seam and may be released at the surface during HF and well completion or as fugitive emissions from CSG infrastructure.

An Australian Government assessment of chemicals used in CSG extraction in Australia which identified 113 chemicals used in drilling and HF during the period 2010 – 2012 did not list mercury as a component of drilling or HF fluids (NICNAS 2017a) and HF fluids are not considered as a source of mercury here. Mercury was either not detected or detected in trace amounts in CSG ( $< 0.1 \mu\text{g m}^{-3}$ ) and produced water ( $< 0.5 \mu\text{g L}^{-1}$ ) from well head samples in Queensland gas fields (Apte et al., 2019, NICNAS 2017, Lawson et al., 2017).

Sampling of mercury was undertaken at the South-AQMS. Semi-continuous measurements were made using a Model 2537A Vapor Phase Mercury Analyser, which collected mercury onto a pair of gold traps that were alternately analysed and cleaned every 5 minutes. The sampling and analysis method follows the Global Mercury Observation System (GMOS) Standard Operational Procedure for the determination of GEM [http://www.gmos.eu/public/GMOS%20SOP%20TGM\\_GEM.pdf](http://www.gmos.eu/public/GMOS%20SOP%20TGM_GEM.pdf) and Appendix 13 of this report.

### Summary Statistics and Comparison with Air Quality Objectives

Table 40 shows the summary statistics for mercury. The mean 1-hour concentration measured throughout the sample period from 15<sup>th</sup> August 2017 to 6<sup>th</sup> December 2017 was 0.57 ng m<sup>-3</sup> with a maximum concentration of 0.94 ng m<sup>-3</sup>.

**Table 40 Summary statistics for mercury concentrations, in ng/m3 sampled from 15<sup>th</sup> August 2017 to 6<sup>th</sup> December 2017**

	Method	Averaging period	MDL (ng m <sup>-3</sup> )	25 <sup>th</sup> %ile (ng m <sup>-3</sup> )	Median (ng m <sup>-3</sup> )	Mean (ng m <sup>-3</sup> )	75 <sup>th</sup> %ile (ng m <sup>-3</sup> )	Max (ng m <sup>-3</sup> )	N
Hg	Active sampling onto gold traps	1h	<0.1	0.48	0.57	0.57	0.65	0.94	2609

Sample concentrations were blank-corrected. The sample MDL was calculated as 3 times the standard deviation in the field blank.

Figure 58 shows a time series of mercury concentrations compared to the annual Queensland EPP air quality objective for mercury vapour 1.1 µg m<sup>-3</sup>. To compare the measurements to the objective, the concentrations were divided by 1000 to convert from units of ng m<sup>-3</sup> to µg m<sup>-3</sup>. The measurements are so low compared to the standard that any variations cannot be seen in the time series.

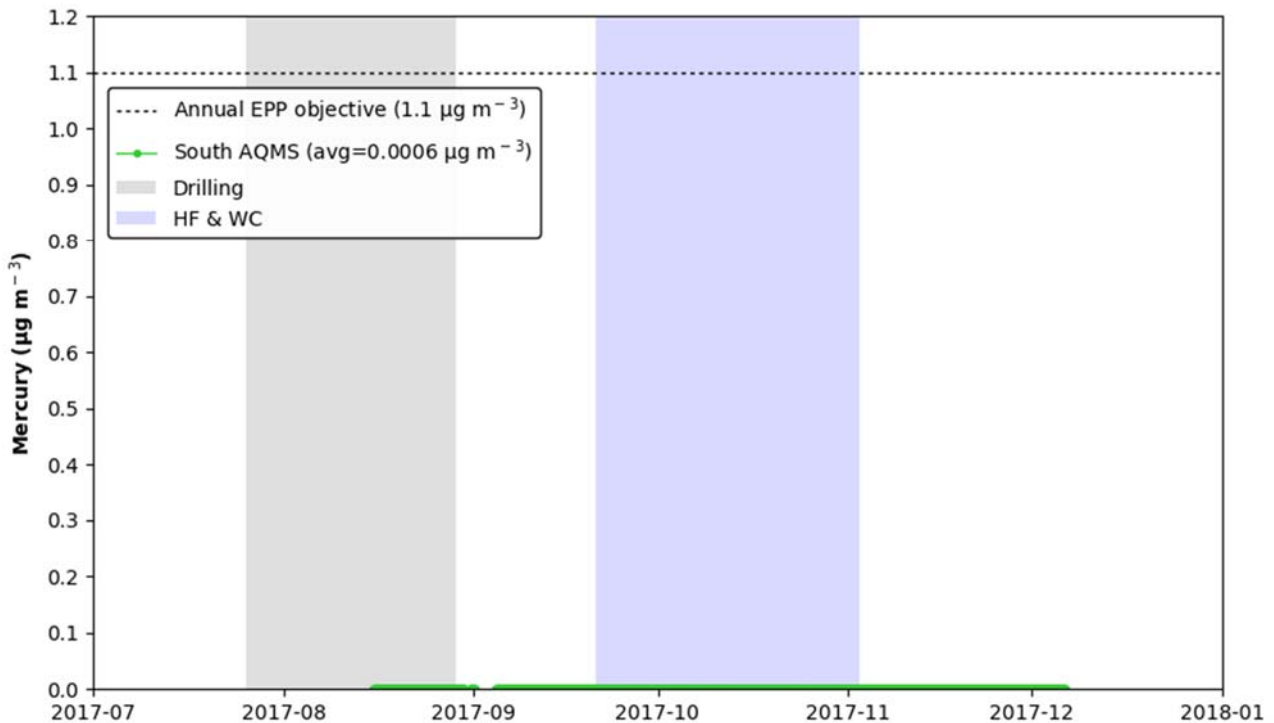


**Figure 58 Time series of mercury concentrations. Shaded areas represent periods of well development activity on the HF study site, including drilling (grey) and HF + WC (purple).**

## Comparison with other sites in Australia

The concentrations measured at the South-AQMS in this study were lower or similar to other sites in Australia (Table 41). Mercury levels at background sites in the Southern Hemisphere are typically 0.8 – 1.0 ng m<sup>-3</sup>, but lower concentrations of 0.6 ng m<sup>-3</sup> were observed at an inland alpine site and are similar to those observed in this study.

**Table 41 Concentrations of mercury measured in other locations in Australia.**

Location	Hg, ng/m <sup>3</sup> , average and standard deviation
This study	0.57 ± 0.12 (10-minute data)
Background mercury in the Southern hemisphere tropics near Darwin, 2015 <sup>a</sup>	0.93 ± 0.12 (5-minute data)
Background mercury in the Southern hemisphere Southern Ocean, Tasmania, 2013 <sup>b</sup>	0.848 ± 0.112 (5 to 15-minute data)
Inland site, Hunter Valley NSW 2019 <sup>c</sup>	0.8-1.0 (5-minute data)
Alpine grassland site, Snowy Mountains, NSW, 3-week period, summer <sup>d</sup>	0.59 ± 0.10 (10-minute data)

<sup>a</sup>Howard et al. 2017, <sup>b</sup>Slemr et al 2017, <sup>c</sup>Nelson et al., (2017), <sup>d</sup>Howard et al., 2018

## HF and non-HF related sources of Mercury

Potential enhancements in mercury concentrations above background due to well development activity were further assessed using higher time resolution (5-minute) mercury and wind direction data. Figure 59 shows the distributions of 5-minute average mercury data measured at the South-AQMS when downwind of drilling (A) and when downwind of HF + WC (C), alongside data from other WDRs during the same periods (B and D) and during periods where no drilling, HF or WC activities were occurring (E). The characteristics of the distributions for the mercury data from the South-AQMS were as follows:

- the median mercury concentrations for all activity periods and non-activity periods, and all WDRs were similar (medians ~ 0.5 µg m<sup>-3</sup>, IQRs = 0.4 – 0.6 .5 µg m<sup>-3</sup>);
- **Drilling** - The top 5 % of values when measuring downwind of drilling were slightly lower than the top 5% of values when measuring air masses from other WDRs during the same period and during non-activity periods;
- **HF + WC** - The top 5 % of values when measuring downwind of HF + WC were within the range of the top 5% of values when measuring air masses from other WDRs during the same period and similar to the top 5% of values measured during non-activity periods.

## Summary

In summary, the concentrations of mercury measured at the South-AQMS were always well below Queensland EPP air quality objectives and were comparable to levels measured at other rural and remote sites in Australia. Increases in mercury above background concentrations were not associated with measurements taken downwind of well development activity. This is consistent with limited data of the composition of HF fluids, drilling fluids, CSG and flowback/produced

waters which suggest direct emissions of mercury to the air from these HF-specific sources was unlikely to have contributed significantly to airborne concentrations.

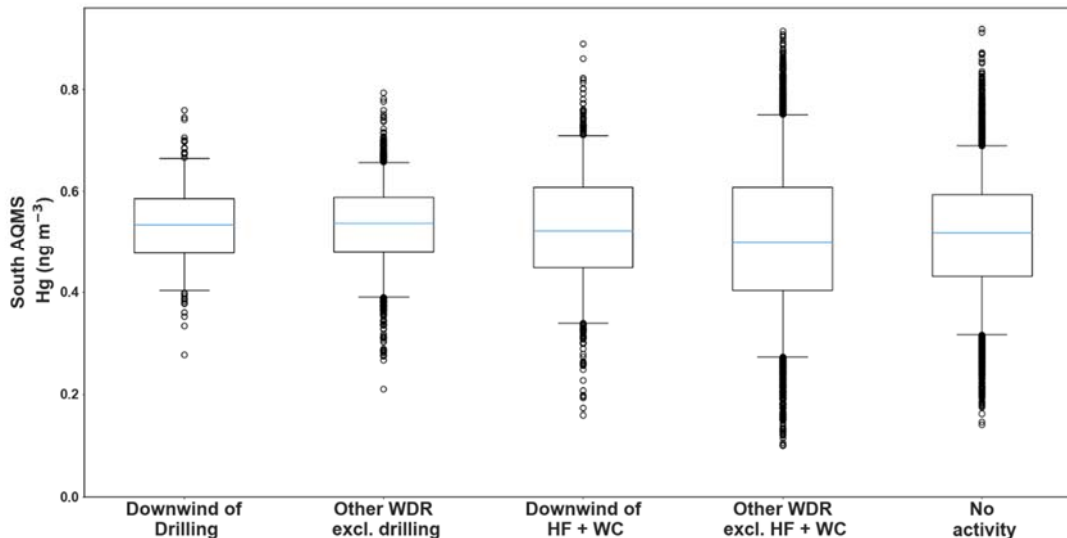


**Figure 59** Box and whisker plots of the 5-minute average mercury data from the South-AQMS measured when downwind of drilling and HF + WC. For comparison mercury data from other WDRs during drilling and HF +WC, as well as during non-activity periods are presented. Note the box represents the range between the 25<sup>th</sup> and 75<sup>th</sup> percentiles, the blue line is the median (50<sup>th</sup> percentile), the whiskers represent the 5<sup>th</sup> and 95<sup>th</sup> percentiles and the points above/below the whiskers represent the top/bottom 5% of values.

## 6.2 Radon

Radon is a radioactive noble gas is a product of the decay of Uranium 238. Radon is present in almost all rocks and sediments and consequently, natural emissions from soils are the largest source of radon to the atmosphere.

Continuous measurements of radon in ambient air were undertaken by the Australian Nuclear Science and Technology Organisation (ANSTO) at the South-AQMS using their 1500 L dual flow loop two-filter radon detector from 8th August to 25th November 2017 with data capture of 92% for that period. As a reference, radon monitoring was also conducted using a smaller 100 L radon detector over the same period at the Tara site which was 117 km to the SE of the HF study site and > 10 km from large CSG industry sources.

### Summary Statistics and Comparison with Air Quality Objectives

Summary radon concentration statistics including monthly average and maximum concentrations from the South-AQMS and the Tara reference site are listed in Table 42. The time series of 10-minute average radon concentrations from the South-AQMS and the reference site are shown in

Figure 60. Radon concentrations observed at the HF study site can be assessed against the action levels for radon-222 concentrations in air for households and workplaces described in ARPANSA’s Recommendations for Limiting Exposure to Ionizing Radiation (ARPANSA 2002) (Guidance note [NOHSC:3022(1995)]). The exposure limits listed are 200 Becquerel per cubic metre (Bq m<sup>-3</sup>) for households and 1000 Bq m<sup>-3</sup> for workplaces. The guideline states that if long-term average radon concentrations in a home or workplace are found to exceed these values, remedial action is recommended. The average radon concentration at the HF study site and reference site were 4.4 and 9.2 Bq m<sup>-3</sup> respectively, well below the ARPANSA recommended action levels for workplaces and households.

**Table 42 Summary radon concentration statistics, including monthly average and maximum concentrations from the South-AQMS and the Tara region reference measurements. The ARPANSA Recommendations for Limiting Exposure to Ionizing Radiation (ARPANSA 2002) (Guidance note [NOHSC:3022(1995)]) are: 200 Becquerel per cubic metre Bq m<sup>-3</sup> for households and 1000 Bq m<sup>-3</sup> for workplaces.**

Radon - 2017	All	Aug	Sep	Oct	Nov	Dec
<b>South-AQMS</b>						
Max 24 hour	9.96	9.96	8.04	6.82	7.20	-
Average 24 hour	4.44	6.01	5.36	3.64	2.95	-
% Data Avail	92%					
<b>Tara region</b>						
Max 24 hour	34.2	29.7	34.2	13.9	24.6	-
Average 24 hour	9.2	18.1	12.9	3.3	3.4	-
% Data Avail	98%					

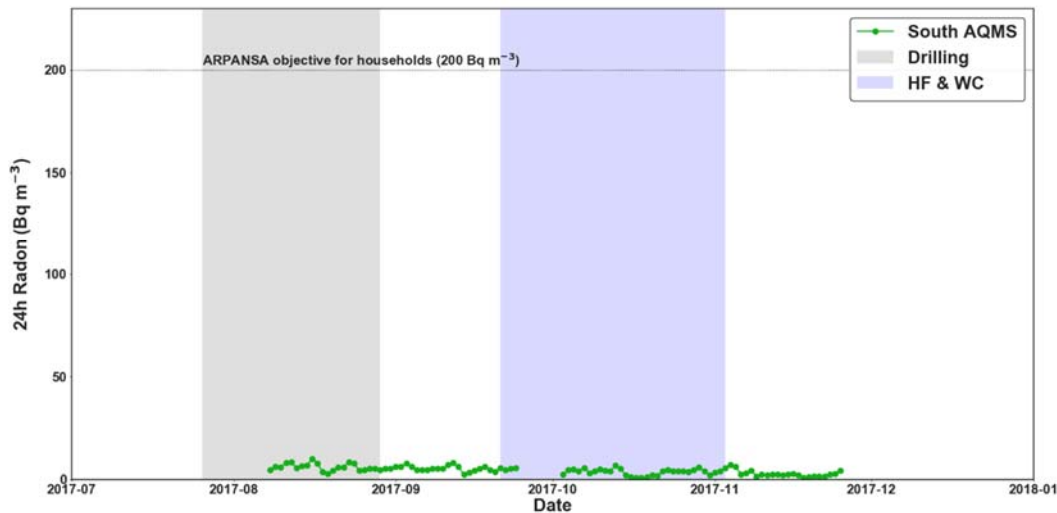


**Figure 60** Time series of 24-hour average radon concentrations from the South-AQMS. Shaded areas represent periods of well development activity on the HF study site, including drilling (grey) and HF + WC (purple). The ARPANSA Recommendations for Limiting Exposure to Ionizing Radiation (ARPANSA 2002) (Guidance note [NOHSC:3022(1995)]) are: 200 Becquerel per cubic metre  $\text{Bq m}^{-3}$  for households and  $1000 \text{ Bq m}^{-3}$  for workplaces.

### HF and non-HF related sources of Radon

Potential enhancements in radon concentrations above background due to well development activity were assessed using higher time resolution (10-minute) radon and wind direction data. Figure 61 shows the distributions of 10-minute average radon data measured at the South-AQMS when downwind of drilling (A) and when downwind of HF + WC (C), alongside data from other WDRs during the same periods (B and D) and during periods where no drilling, HF, or WC activities were occurring (E). Because wind speed can have a significant influence on radon concentration, the radon concentrations for calm conditions (wind speed  $< 1 \text{ m s}^{-1}$ ) are also included in the plot. The characteristics of the distributions for the radon data from the South-AQMS were as follows:

- **Drilling** - the distribution of radon concentrations downwind of drilling were visibly higher than for other WDRs during the same period and during non-activity periods;
- **HF + WC** - The median and IQR of radon concentrations when measuring downwind of HF + WC were slightly higher than the median and IQRs for data when measuring air masses from other WDRs during the same period and during non-activity periods;
- **Calm conditions** - The median and IQR of radon concentrations measured during calm conditions (wind speed  $< 1 \text{ m s}^{-1}$ ) were close to or higher than the median and IQRs for data during drilling and HF + WC.

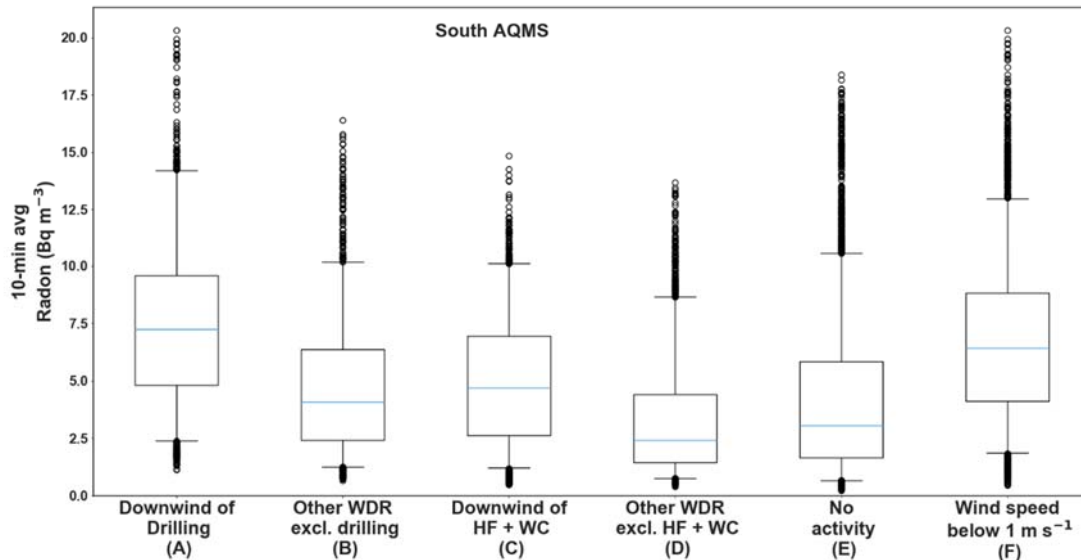


**Figure 61** Box and whisker plots of the 10 min average radon data from the South-AQMS measured when downwind of drilling and HF + WC. For comparison radon data from other WDRs during drilling and HF +WC, as well as during non-activity periods are presented. Note the box represents the range between the 25<sup>th</sup> and 75<sup>th</sup> percentiles, the blue line is the median (50<sup>th</sup> percentile), the whiskers represent the 5<sup>th</sup> and 95<sup>th</sup> percentiles and the points above/below the whiskers represent the top/bottom 5% of values.

As discussed previously, natural emissions from soils were most likely a significant source of radon to the background atmosphere in the study region. During cooler, calmer conditions (i.e. winter nights), radon emissions can pool in low lying areas, whereas stronger winds and warmer temperatures (i.e. spring/summer days) result in greater mixing and dilution of radon emissions thus lowering ambient concentrations. The relationship between wind speeds and radon concentrations at the South -AQMS is shown in the time-series in Figure 62. At the lowest wind speeds radon concentrations measured at the South-AQMS are highest.

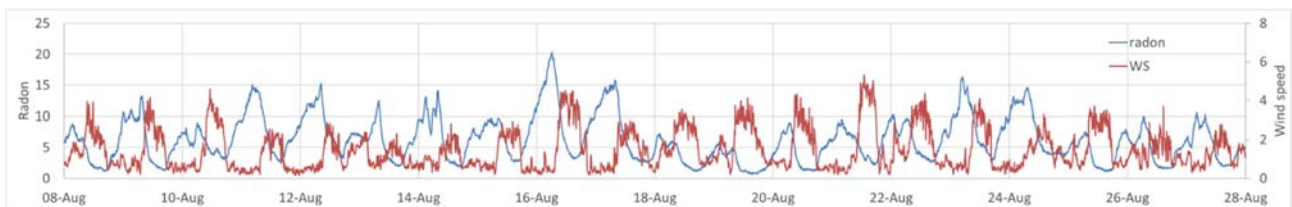


**Figure 62** Time series of radon concentration and wind speed (WS) measured at the South-AQMS

As initially described in section 4, the definitions for “downwind of drilling”, “downwind of HF + WC” and “No-activity” included data when calm conditions prevailed (wind speed < 1 m s<sup>-1</sup>), whereas “other wind directions (WDR) excluding downwind of drilling” or “other WDRs excluding downwind of HF + WC” did not include periods when calm conditions prevailed. The inclusion of

calm conditions provides an explanation for the slightly higher concentrations in the periods defined as “downwind of drilling”, “downwind of HF+WC” and “No-activity” in comparison to the periods defined as “other WDRs excluding downwind of drilling / HF+WC” which excluded calm conditions. This effect was more pronounced during drilling as this activity occurred in the winter months where calm, cool conditions resulted in higher ambient radon concentrations.

In addition to natural emissions from soils, radon could potentially be emitted at the well pad as a component of CSG or via emissions from flow back fluids. Radon concentrations of 40 – 190 Bq m<sup>-3</sup> were reported from analysis of a limited number of CSG samples from wellheads in the Surat Basin (Lawson et al., 2017). Radon is not a component of chemical additives used in HF but may be emitted as a decay product of <sup>238</sup>U present in groundwater used in HF fluid mixtures. The samples of the bore water used for HF operations at the site of the present study were sampled on five occasions between August 2017 and February 2018 and the concentration of <sup>238</sup>U was always < 1 mBq kg<sup>-1</sup>. Also, <sup>238</sup>U was detected in only 50% of flow back and produced water samples (N = 27) from three wells at the HF study site and radon in these samples was present in trace quantities (< 20 mBq kg<sup>-1</sup>). Consequently, HF fluids and flow back water are not considered a significant source of radon here.

### **Summary**

In summary, the concentrations of radon measured at the South-AQMS were always well below ARPANSA Recommendations for Limiting Exposure to Ionizing Radiation and were lower than levels at a background reference site in the Surat Basin (>10 km from CSG infrastructure) and comparable to levels measured at other gas field sites in the Surat Basin. Higher radon concentrations were associated with low wind speeds and cooler conditions which likely limited the dilution and mixing of natural emissions of radon from soils in the region of the study site. Limited data of the composition of HF fluids, drilling fluids, CSG and flowback/produced waters suggests direct emissions of radon to the air from these HF-specific sources was not likely to have contributed significantly to airborne concentrations.

## 7 Methane

Coal seam gas is predominantly composed of methane (98%) and CSG emissions to the atmosphere can occur as a result of deliberate venting/flaring from CSG infrastructure (e.g. wells, pipelines, processing facilities) and during activities including well development and well operation activities. It can also be emitted inadvertently via leaks from CSG infrastructure. In addition to CSG sources, methane is also emitted from other natural and man-made sources including:

- decomposition of organic matter, such as in lakes, rivers, wetlands and soils;
- smoke from bushfires and planned burns;
- natural and man-made connections between the coal seam and the surface including methane seeps and legacy coal bores;
- livestock and other animals.

Time series of hourly methane concentrations from the North and South-AQMS from July to December 2017 are shown in Figure 63. The overall averages of the 1-hour methane data were 1.8 - 1.9 ppm with occasional 1-hour average peaks up to 2.8 ppm.

There is no ambient air quality objective for methane, as it is not considered harmful to humans at ambient concentrations. Instead methane was measured in this study as a tracer for other components of CSG including BTX, PAHs, as well as hydrogen sulphide, mercury and radon which as discussed in previous sections may be present in trace quantities in CSG. Assuming trace levels ( $\leq 1$  ppm) of air toxics in CSG, concentrations of CSG methane in ambient air as high as 10 ppm will only result in minor (parts per trillion) additions to the ambient concentrations of air toxics (Lawson et al., 2018; Day et al., 2016). Given the low ambient methane levels observed in this study ( $< 3$  ppm) the potential contribution of CSG to ambient levels of air toxics was unlikely to be significant.

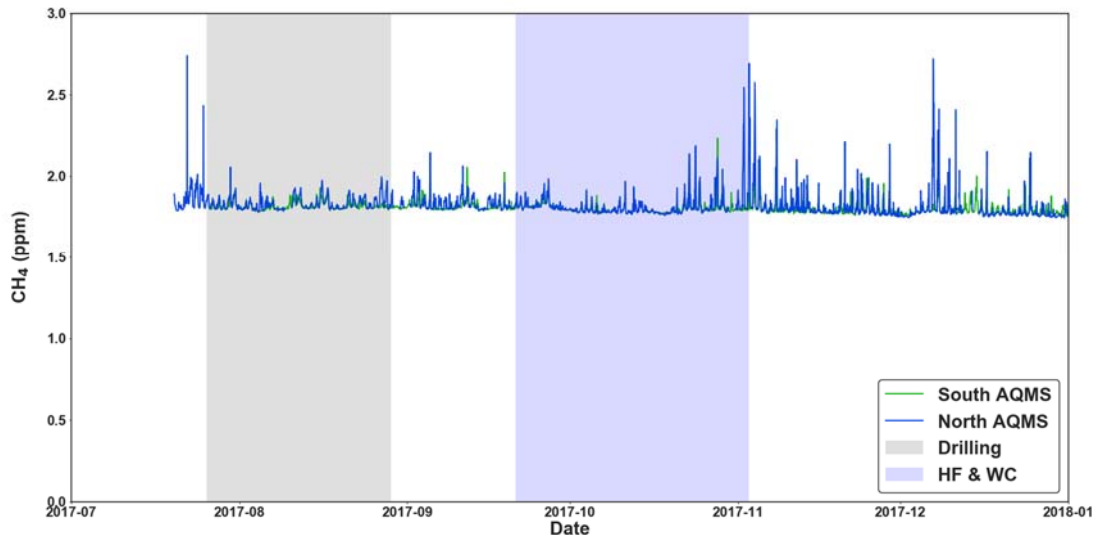


**Figure 63** Time series of methane measured at the North and South-AQMS. Shaded areas represent periods of well development activity on the HF study site, including drilling (grey) and HF + WC (purple).

### Comparison with other sites in the Surat Basin

The overall averages of the 1-hour data were 1.8 - 1.9 ppm at the HF study site in good agreement with annual average methane concentrations of ~ 1.8 ppm – 1.9 ppm reported in previous studies for 3 other gas field sites and two regional sites in the Surat Basin (Lawson et al., 2018; Luhar et al., 2018). Methane peaks up to 2.8 ppm (1-hour average) were observed in this study which are significantly lower than 1-hour average peaks over 10 ppm and up to 25 ppm observed at other gas field sites in the Surat Basin (Lawson et al., 2018).

### HF and non-HF sources of methane

Sources of methane to the background atmosphere at the HF study site included cattle, biomass burning as well as the decomposition of organic matter especially following the shift to warmer weather and the onset of rainfall in October.

The time series in Figure 63 shows generally higher concentrations at the end of HF + WC into the non-activity period after. During drilling and perforation operations methane concentrations measured at both the North and South- AQMS were low. This was expected since during drilling the wells are essentially closed to the atmosphere and no water was removed to minimise emissions. Consequently, only background methane would be expected, consistent with the low concentrations observed during drilling.

During HF methane emissions are only expected to occur during backflow operations. During well completions the well is ‘flowed’ and significantly larger quantities of methane are released compared to during drilling and HF activities (Day et al., 2017). After connection to the gathering

lines emissions will be observed from the operating wells and high point vents located along the water gathering lines. Such releases may have been responsible for the observed methane peaks towards the end of the HF + WC completion period and the early production period as more wells were brought on line.

Potential enhancements in methane concentrations above background due to well development activity were assessed using higher time resolution (5-minute) methane and wind direction data. Figure 64 shows the distributions of 5-minute average methane data measured at the North and South-AQMS when downwind of drilling (A) and when downwind of HF + WC (C), alongside data from other WDRs during the same periods (B and D) and during periods where no drilling, HF or WC activities were occurring (E). The characteristics of the distributions for the methane data were as follows:

#### **North-AQMS**

- The median and IQRs were similar between activity periods and non-activity periods, and all WDRs;
- **Drilling** – Methane was not measured at the North-AQMS during drilling due to instrument failure;
- **HF + WC** - the top 5 % of methane values when measuring downwind of HF + WC were similar to higher the top 5% of values when measuring air masses from other WDRs during the same period and lower than the top 5% of values measured during non-activity periods.

#### **South-AQMS:**

- The distributions of methane concentrations were similar between activity periods and non-activity periods, and all WDRs.

Overall, enhancements in methane concentrations were not associated with measurements downwind of drilling, HF + WC. This is consistent with our understanding of only minor CSG emissions over the drilling and HF process, followed by an increase in emissions associated with WC and the production phase of well development.

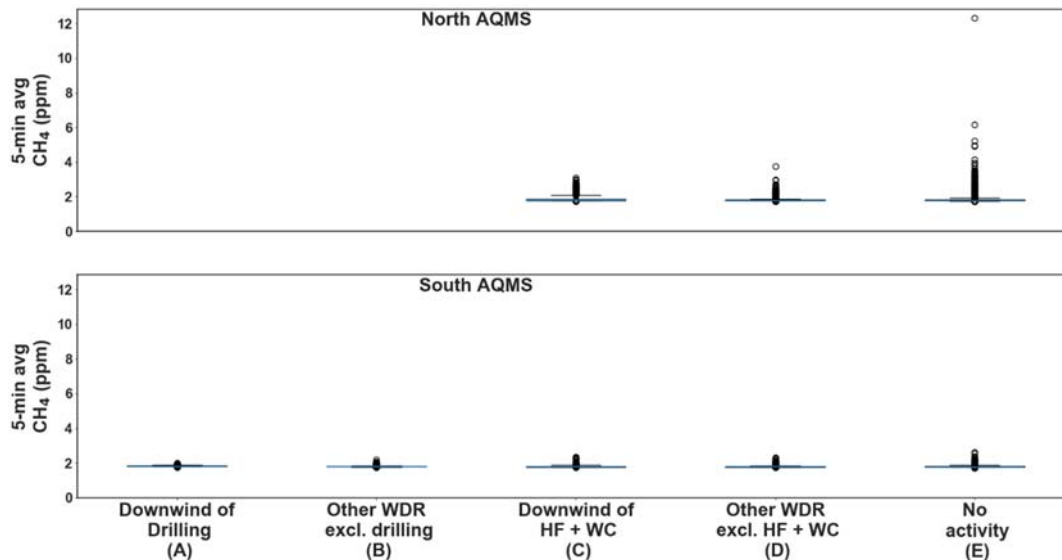


Figure 64 Box and whisker plots of the 5-minute average methane data from the North and South-AQMS measured when downwind of drilling and HF + WC. For comparison methane data from other WDRs during drilling and HF + WC, as well as during non-activity periods are presented. Note the box represents the range between the 25<sup>th</sup> and 75<sup>th</sup> percentiles, the blue line is the median (50<sup>th</sup> percentile), the whiskers represent the 5<sup>th</sup> and 95<sup>th</sup> percentiles and the points above/below the whiskers represent the top/bottom 5% of values.

## Summary

In summary, average concentrations of methane measured at the HF study site were generally close to background levels and similar to average concentrations observed at other sites in the Surat Basin. Maximum concentrations in this study of approximately 3 ppm were substantially lower than peaks of up to 25 ppm observed at other Surat Basin sites. Based on limited data of the composition of CSG and the low concentrations of methane observed in this study it was concluded that CSG emissions did not contribute significantly to airborne concentrations of air toxics.

## 8 Discussion and Summary

The potential impact on air, surface water, groundwater and soil of HF operations in CSG production are of concern to communities living in gas development regions (Cham and Stone 2013). The GISERA Air, Water and Soil Impacts of Hydraulic Fracturing: Phase 2 (W.12) project aimed to address some of these concerns by carrying out a comprehensive investigation of air, water and soil quality during HF at a site in the Surat Basin in Queensland. The project is the continuation of the Phase 1 project (W.11) during which comprehensive peer-reviewed study designs were developed for air quality (Dunne et al., 2017) and water and soil quality (Apte et al., 2017) studies.

Presented here is the final report for the air quality component of the study. A comprehensive air monitoring program was undertaken from July – December 2017 in a CSG field containing 10 CSG wells which underwent HF in September – November 2017. This was the first comprehensive study to assess the impact of HF on air quality in an Australian gas field to date.

Measurement systems were deployed across six sites in the CSG field and collected data on a suite of air pollutants prescribed in the NEPM and Queensland EPP air quality objectives and a range of additional atmospheric components.

The study objectives and the data presented in this report that addressed each objective are outlined below. Note that in this final report we have reordered the objectives to facilitate the flow of the summary below.

**Objective 1 (previously Objective 3)- *Perform comparisons of the data with Australian federal and state air quality objectives, as well as data from other air quality studies undertaken in areas not directly impacted by HF operations both within the Surat Basin and in other locations in Australia.*** This objective was addressed by

- Comparing data collected using Australian Standard measurement techniques and validated methods with NEPM, Qld EPP and other relevant ambient air quality objectives. The data presented showed that for:
  - **Gaseous NEPM Ambient Air Pollutants (NO<sub>2</sub>, CO, O<sub>3</sub> and SO<sub>2</sub>)** measured at the North and South-AQMS - Air quality at the study site in relation to these four pollutants was classified as ‘good’ to ‘very good’ in 99% to 100% of the measurements during the period August – December 2017. The concentrations of NO<sub>2</sub>, CO and SO<sub>2</sub> never approached or exceeded relevant air quality objectives with concentrations always less than two-thirds of the NEPM /EPP objectives. Air quality in relation to O<sub>3</sub> was occasionally classified as ‘fair’ (> two-thirds of the NEPM



objective) however more than 98% of the time it was classified as 'good' to 'very good';

- **Particulate NEPM Ambient Air Pollutants (PM<sub>10</sub> and PM<sub>2.5</sub>) and TSP** measured at the North and South-AQMS - Air quality at the study site in relation to particulate pollutants was classified as 'good' to 'very good' in 96% to 99% of the measurements during the period August – December 2017. While air quality in relation to PM<sub>2.5</sub> was occasionally classified as 'fair', for more than 96% of the time it was classified as 'good' to 'very good'. There were infrequent occasions ( $\leq 4\%$ ) during the study period when concentrations of PM<sub>10</sub> and TSP exceeded the relevant air quality objectives and air quality was classified as 'poor' to 'very poor' however generally air quality in relation to PM<sub>10</sub> and TSP was 'good' to 'very good' with 96% to 99% of the measurements being less than two-thirds of the relevant air quality objectives;
- **NEPM Air Toxics (formaldehyde, benzene, toluene, xylene and benzo(a)pyrene as a marker for PAHs)**. The concentrations of these pollutants were always well below NEPM air toxics monitoring investigation levels;
- **Other Queensland EPP air pollutants** - The species measured included arsenic, manganese, nickel and sulfate as components of PM<sub>10</sub> and were always well below Qld EPP air quality objectives. The concentrations of the gaseous pollutant's mercury, hydrogen sulphide, 1,2-dichloroethane, styrene and tetrachloroethylene also listed in the Qld EPP were always well below relevant long-term air quality objectives (Qld EPP, Texas AMCV and WA DoE objectives);
- **48 other VOCs** were measured at the HF study site and concentrations were always well below relevant NEPM, Qld EPP and Texas AMCV long-term objectives;
- **Radon concentrations at the HF study site were always well below** ARPANSA's Recommendations for households and workplaces for Limiting Exposure to Ionizing Radiation (ARPANSA 2002) (Guidance note [NOHSC:3022(1995)]).
- Data for NO<sub>2</sub>, CO, O<sub>3</sub>, PM<sub>10</sub>, PM<sub>2.5</sub>, TSP, formaldehyde, BTX, other VOCs and methane from the HF study site were compared with other measurements in the Surat Basin Ambient Air Quality study network. These comparison sites were two regional sites (Burncluth and Tara) which were > 10 km from CSG infrastructure and two other gas field sites (Miles Airport and Hopeland). HF activities were not known to have occurred near these Surat Basin Air monitoring sites during the period of the present study, hence data from these sites provides a useful comparison of regional air quality from locations not directly impacted by HF activities. The data presented showed that:



- **NEPM Ambient Air Pollutants (NO<sub>2</sub>, CO, O<sub>3</sub>, PM<sub>10</sub>, PM<sub>2.5</sub>) and TSP** concentrations observed at the HF study site were similar to those measured at other sites in the Surat Basin Ambient Air Quality study network (Hopeland, Miles Airport and Burncluith) during the same period as the HF study;
- **NEPM Air Toxics, hydrogen sulphide and other VOCs** concentration ranges and detection frequencies of each compound collected using Radiello samplers at the HF site were generally similar to those observed during the same period across other regional and gas field sites in the Surat Basin (Burncluith, Tara, Miles Airport and Hopeland) as well as at another HF site in the Miles-Condamine area measured in 2016-17 and reported previously (Dunne et al., 2018);
- **Radon** concentrations were found to be consistently higher at the reference site located >10km away from CSG infrastructure than at the HF Study site and these differences were likely a result of differences in local climatology and geography at each site. The radon concentrations observed at the HF study site were also similar to the values measured at five other sites in a previous study in the Surat Basin (Tait et al., 2013);
- **Methane** concentrations at the HF study site were on average approximately 1.8 ppm and in good agreement with background concentrations reported in previous studies for three other gas field sites and two regional sites in the Surat Basin (1.8 – 1.9 ppm) (Lawson et al., 2018, Luhar et al., 2018). The maximum concentrations of methane observed in this study (3 ppm) were significantly lower than peaks of up to 25 ppm observed at other gas field sites in the Surat Basin (Lawson et al., 2018).
- In lieu of data from other Surat Basin sites, comparison of data for sulfur dioxide, PAHs, and mercury were undertaken with data from other suburban, rural and remote sites in Australia. Data from these sites provides a useful comparison of concentrations typical of other areas in Australia. The data presented showed that:
  - **Sulfur dioxide** concentrations measured in this study were similar to those observed over the same period at a Queensland Department of Environment and Science air quality monitoring site at Flinders View, a suburban air quality monitoring site located in the Ipswich area of southeast Queensland;
  - **PAH** concentrations observed in this study are amongst the lowest observed in Australia and were similar to those reported from a rural background site (Mutdapilly) in Queensland;
  - **Mercury** concentrations observed in this study were similar to or lower than concentrations observed in other rural sites in NSW and NT and in air masses from the Southern Ocean.



In summary, with the exception of a few infrequent PM values atmospheric concentrations of a range of pollutants were well below relevant air quality objectives for the entire duration of the study period. The range of concentrations observed at the HF study site, including occasional exceedances of PM<sub>10</sub> and TSP, were not distinctly different to those observed at other sites in the Surat Basin and in Australia that were not directly impacted by HF activity.

**Objective 2 (Previously Objective 1)- Quantify enhancements in air pollutant levels above background that occur during HF operations.** This objective has been addressed in this report by:

- Comparison of high time resolution measurements collected downwind of drilling, HF + WC with data from other wind directions during the same period, and comparison with non-activity periods at the HF site. In this case, background is defined as concentrations measured from other wind directions during the same period and during non-activity periods. The data presented showed that for:
  - **Gaseous NEPM Ambient Air Pollutants (NO<sub>2</sub>, CO, O<sub>3</sub> and SO<sub>2</sub>).** Small, short term enhancements in NO<sub>2</sub> and CO above background concentrations were associated with air masses sampled downwind of drilling and/or HF +WC activities. Well development activity was not associated with enhancements in O<sub>3</sub> or SO<sub>2</sub> above background and the concentrations observed on site were the result of regional emissions and transport of these pollutants to the study site;
  - **Particulate NEPM Ambient Air Pollutants (PM<sub>10</sub>, PM<sub>2.5</sub>) and TSP.** Concentrations of airborne particles were higher when drilling, and HF + WC activity was occurring on site however, peak concentrations were not associated with air masses sampled downwind of drilling and/or HF +WC activities indicating that activities on site but not necessarily on the well pads contributed to the source of peak events;
  - **NEPM Air Toxics**, benzene, toluene, xylenes and formaldehyde concentrations above background were observed in measurements downwind of drilling, HF + WC activities;
  - **Mercury and radon** concentrations measured downwind of well development activity were similar to the range of concentrations measured during non-activity periods (background);
  - **Methane** - Well development activity was not associated with enhancements in methane above background which are typically associated with the production phase of the well rather than development.

In summary, short term enhancements in the concentrations of NO<sub>2</sub>, CO, PM<sub>10</sub>, PM<sub>2.5</sub>, TSP, BTX and formaldehyde above background were associated with well development activities in this study. These impacts generally occurred at levels below air quality objectives, except for some

infrequent dust events. Well development activity was not associated with measurable enhancements in O<sub>3</sub>, SO<sub>2</sub>, mercury, radon and methane.

**Objective 3 (Previously Objective 2)- Provide information on the contribution of HF and non-HF related sources of air pollutants to local air quality at the selected study site.** This objective has been addressed in this report by:

- Comparison of the composition of gaseous and particulate air pollutants observed in the atmosphere with known source profiles such as the composition of HF fluids, CSG, and flowback fluids, vehicle exhaust, smoke etc, and comparisons with tracer species. The data presented showed that for:
  - **NEPM Ambient Air Pollutants NO<sub>2</sub> and CO** - Small, short term peaks in NO<sub>2</sub> and CO were associated with drilling, HF + WC activities, these compounds were not components of drilling fluids, HF fluids, flowback fluids or CSG and peaks in their concentrations were likely due to exhaust emissions from diesel powered equipment and vehicles on site which are known sources of these pollutants;
  - **NEPM Air Toxics – formaldehyde.** Relationships with smoke tracer species showed biomass burning and was a dominant source of formaldehyde in the background atmosphere at the study site along with secondary photochemical production. Small enhancements in formaldehyde concentration above background were observed in measurements downwind of drilling, HF + WC. Aside from known vehicle emission sources, the potential sources of formaldehyde associated with well development activities are not well understood, and analysis of the limited data of the composition of HF fluids, drilling fluids, CSG and flowback/produced waters suggests direct emissions of formaldehyde to the air from these potential sources were unlikely to have contributed significantly to airborne concentrations;
  - **NEPM Air Toxics- benzene, toluene, xylene.** Relationships with smoke tracer species showed biomass burning was a dominant source of BTX in the background atmosphere at the study site. Small enhancements in BTX concentrations above background were observed in measurements downwind of drilling, HF + WC and analysis of the benzene/toluene ratio during these peaks suggests emission from vehicles and equipment on site were responsible for these enhancements rather than HF-specific sources. Limited data of the composition of HF fluids, drilling fluids, CSG and flowback/produced waters which either did not contain BTX or contained BTX in trace amounts, suggest direct emissions of BTX to the air from these HF-specific sources was unlikely to have contributed significantly to airborne concentrations;



- **NEPM Air Toxics- PAHs** Diagnostic ratios of PAH species and relationships with other marker species suggested that diesel combustion and biomass burning smoke contributed to PAH concentrations measured at the South-AQMS;
- **Mercury and radon** concentrations measured downwind of well development activity were similar to the range of concentrations measured during non-activity periods (background). Higher radon concentrations were associated with low wind speeds and cooler conditions which limited the dilution and mixing of natural emissions of radon from soils in the region of the study site. Limited data of the composition of HF fluids, drilling fluids, CSG and flowback/produced waters which either did not contain mercury and radon or contained these species in trace amounts, suggesting direct emissions of mercury and radon to the air from these HF-specific sources was unlikely to have contributed significantly to airborne concentrations.
- Application of a statistical model known as the positive matrix factorisation (PMF) receptor model to the PM<sub>10</sub> chemical composition data was used to identify the most likely sources of particulate matter (PM) at the study site. The PMF analysis identified eight dominant Factors that likely contributed to PM. They were as follows, ranked in order of their contribution.
  - Factor 1 Soil
  - Factor 2 Secondary Ammonium Sulfate
  - Factor 3 Secondary Nitrate-Aged Sea Salt
  - Factor 4 Aged Biomass Smoke
  - Factor 5 Fresh Sea Salt
  - Factor 6 Wood Smoke
  - Factor 7 Glucose
  - Factor 8 Primary Biological Aerosol

Contributions from Factors 2 – 6 were the result of regional transport (tens to hundreds of km) of PM to the study site from both natural (smoke, sea salt) and industrial sources (secondary ammonium sulfate and nitrate aged sea salt) in the region. Particulate matter from these factors were predominantly in the fine size fraction (PM<sub>2.5</sub>). Contributions from Factors 7 and 8 were from natural biological sources at the study site. When combined, the sources contributing to Factors 2 to 8 comprise the background PM in the atmosphere of the study region and well development activities on site did not significantly contribute to these factors. Only local emissions of soil dust from vehicle traffic and equipment on unsealed roads and well pads could be attributed to CSG well development activities using this analysis technique. On seven days during this study, dust emissions from vehicles and equipment on site resulted in exceedances in 24-hour PM<sub>10</sub> and TSP air quality objectives.

In conclusion, with the exception of very infrequent dust events associated with the movement of vehicles and equipment on unsealed roads on site, atmospheric concentrations of a range of pollutants were well below relevant air quality objectives for the entire duration of the study period. Emissions from diesel powered vehicles and equipment on site also likely contributed to small enhancements in NO<sub>2</sub>, CO, PM<sub>2.5</sub>, formaldehyde, BTX and PAHs during well development which were still well within relevant ambient air quality objectives. Impacts on air quality associated with well development were short term (hours to days) and are likely to be transient within gas development regions as drilling, HF and well development operations move from well site to well site.

Analysis of limited data of the composition of HF fluids, drilling fluids, CSG and flowback/produced waters showed these HF-specific sources did not contain high levels of contaminants which may potentially impact air quality, or they were only present in trace amounts, suggesting that direct emissions of pollutants to the air from these HF-specific sources was unlikely to have contributed significantly to airborne concentrations. It is important to note, accidental or uncontrolled releases (spills, leaks) of HF fluids and CSG were not observed during this study and the impact on air quality of these events could not be assessed.

This is the first comprehensive study of the impact of HF on air quality in an Australian onshore gas field and this study provides important information about the concentrations and sources of air pollutants associated with well development activities. The data generated in this study will be made publicly available on the CSIRO data access portal in late 2019. This report and the data provided will assist the assessment of human health risks from exposures via ambient air (NICNAS 2017c) including the GISERA health study - Keywood et al., (2018) and other studies of the environmental and health impacts of CSG development in Australia. The data also provides a useful resource for policy makers, landholders and other stakeholders to inform decision making around future well development in the region and for industry to improve practice.

## References

- Akagi SK, Yokelson RJ, Wiedinmyer C, Alvarado MJ, Reid JS, Karl T, Crouse JD and Wennberg PO (2011) Emission factors for open and domestic biomass burning for use in atmospheric models. *Atmos. Chem. Phys.* 11(9): 4039-4072. doi: 10.5194/acp-11-4039-2011
- Aldabe J, Elustondo D, Santamaria C, Lasheras E, Pandolfi M, Alastuey A, Querol X and Santamaria JM (2011) Chemical characterisation and source apportionment of PM<sub>2.5</sub> and PM<sub>10</sub> at rural, urban and traffic sites in Navarra (North of Spain). *Atmospheric Research* 102(1-2): 191-205. doi: 10.1016/j.atmosres.2011.07.003
- Allen AG, Cardoso AA and da Rocha GO (2004) Influence of sugar cane burning on aerosol soluble ion composition in Southeastern Brazil. *Atmospheric Environment* 38(30): 5025-5038. doi: 10.1016/j.atmosenv.2004.06.019
- APLNG (2016) Hydraulic Fracture Simulation Fact Sheet  
<https://www.originenergy.com.au/content/dam/origin/about/our-approach/docs/OurApproach-2016-Hydraulic-Fracture-Stimulation.pdf>.
- APLNG (2017) Material Safety Data Sheets. Available: <https://www.aplng.com.au/about-us/compliance/material-safety-data-sheets.html>.
- Apte S C, Kookana R S, Batley G E and Williams M (2017) Literature review: Geogenic contaminants associated with coal seam gas operations, Project report prepared by the Land and Water Flagship, Commonwealth Scientific and Industrial Research Organisation (CSIRO) as part of the National Assessment of Chemicals Associated with Coal Seam Gas Extraction in Australia, Commonwealth of Australia, Canberra.
- Apte S C, Williams M, King J J, Angel B M, Kookana R S and Craig A (2018) Water and Soil sample analysis: data report. Project W12 Milestone 5 Report to the Gas Industry Social and Environmental Research Alliance (GISERA). CSIRO, Canberra.
- Apte S C, Williams M, King J J, Angel B M, Kookana R S and Craig A (2019) Water and Soil Quality Final Report. Project W12 Milestone 7 Report to the Gas Industry Social and Environmental Research Alliance (GISERA). CSIRO, Canberra
- Apte S, Kookana R and Williams M (2017) Potential impacts of hydraulic fracturing on air, soil and water quality in the vicinity of coal seam gas well sites in the Surat Basin, Queensland: water and soil monitoring plan. A task report to the Gas Industry Social and Environmental Research Alliance (GISERA). July 2017. CSIRO, Canberra. p 30.
- ARPANSA (2002) Australian Radiation Recommendations for limiting exposure to ionizing radiation (Guidance note [NOHSC:3022(1995)]). Australian Radiation Protection and Nuclear Safety Authority, Yallambie Victoria. Available: <http://www.arpansa.gov.au/pubs/rps/rps1.pdf>.
- AS/NZS (2007). AS/NZS 3580.1.1:2007 . Methods for sampling and analysis of ambient air. Part 1.1: Guide to siting air monitoring equipment.
- AS/NZS (2014). AS/NZS 3580.16:2014 Methods for sampling and analysis of ambient air. Method 16: Determination of polycyclic aromatic hydrocarbons (PAH)
- Bauer H, Claeys M, Vermeylen R, Schueller E, Weinke G, Berger A and Puxbaum H (2008) Arabitol and mannitol as tracers for the quantification of airborne fungal spores. *Atmospheric Environment* 42(3): 588-593. doi: 10.1016/j.atmosenv.2007.10.013
- Behera SN, Sharma M, Aneja VP and Balasubramanian R ( 2013) Ammonia in the atmosphere: a review on emission sources, atmospheric chemistry and deposition on terrestrial bodies. *Environmental Science and Pollution Research* 20: 8092–8131.

- Bhattarai H, Saikawa E, Wan X, Zhu HX, Ram K, Gao SP, Kang SC, Zhang QG, Zhang YL, Wu GM, Wang XP, Kawamura K, Fu PQ and Cong ZY (2019) Levoglucosan as a tracer of biomass burning: Recent progress and perspectives. *Atmospheric Research* 220: 20-33. doi: 10.1016/j.atmosres.2019.01.004
- Bondy AL, Wang B, Laskin A, Craig RL, Nhliziyo MV, Bertman SB, Pratt KA, Shepson PB and Ault AP (2017) Inland Sea Spray Aerosol Transport and Incomplete Chloride Depletion: Varying Degrees of Reactive Processing Observed during SOAS. *Environmental Science & Technology* 51(17): 9533-9542. doi: 10.1021/acs.est.7b02085
- Cham S T and Stone P (2013) How can understanding community concerns about hydraulic fracturing help to address them? *Effective and Sustainable Hydraulic Fracturing*, Ed Jeffery R, Intech Open, DOI: 10.5772/45724.
- Cope M, Keyword MD, Emmerson K, Galbally IE, Boast K, Chambers S, Cheng M, Crumeyrolle S, Dunne E, Fedele R, Gillett R, Griffiths A, Harnwell J, Katzfey J, Hess D, Lawson S, Miljevic B, Molloy S, Powell J, Reisen F, Ristovski Z, Selleck P, Ward J, Zhang C and Zeng J (2014) Sydney Particle Study- Stage II. Report to the Office of Environment and Heritage NSW, 152p  
<http://www.environment.nsw.gov.au/resources/aqms/SydParticleStudy10-13.pdf>.
- Crawford J, Cohen DD, Stelcer E and Atanacio AJ (2017) Long term fine aerosols at the Cape Grim global baseline station: 1998 to 2016. *Atmospheric Environment* 166: 34-46. doi: 10.1016/j.atmosenv.2017.07.012
- CSIRO (2008) Sources of ozone pre-cursors and atmospheric chemistry in a typical Australian city, A report to Air Quality Section, Environment Standards Branch, Department of the Environment, Water, Heritage and the Arts, Commonwealth of Australia, Canberra.
- CSIRO (2015) What is Hydraulic Fracturing? Available: <https://www.csiro.au/en/Research/Energy/Hydraulic-fracturing/a-What-is-hydraulic-fracturing>; Accessed 20/4/2017.
- Day S, Marvig P, White S and Halliburton B (2017) Methane emissions from CSG well completion activities. CSIRO, Australia.
- Day S, Tibbett A, Sestak S, Knight C, Marvig P, McGarry S, Weir S, White S, Armand S, van Holst J, Fry R, Dell'Amico M, Halliburton B and Azzi M (2016) Methane and Volatile Organic Compound Emissions in New South Wales. CSIRO, Australia. Accessed: 8/6/2017, Available: <http://www.epa.nsw.gov.au/resources/air/methane-volatile-organic-compound-emissions-nsw-3063.pdf>.
- de Gouw JA, Warneke C, Parrish DD, Holloway JS, Trainer M and Fehsenfeld FC (2003) Emission sources and ocean uptake of acetonitrile (CH<sub>3</sub>CN) in the atmosphere. *Journal of Geophysical Research-Atmospheres* 108(D11). doi: 4329 10.1029/2002jd002897
- Despres VR, Huffman JA, Burrows SM, Hoose C, Safatov AS, Buryak G, Frohlich-Nowoisky J, Elbert W, Andreae MO, Poschl U and Jaenicke R (2012) Primary biological aerosol particles in the atmosphere: a review, . *Tellus B: Chemical and Physical Meteorology* 64,(15598, DOI: 10.3402/tellusb.v64i0.15598).
- Dunne E, Galbally IE, Cheng M, Selleck P, Molloy SB and Lawson SJ (2018) Comparison of VOC measurements made by PTR-MS, adsorbent tubes-GC-FID-MS and DNPH derivatization-HPLC during the Sydney Particle Study, 2012: a contribution to the assessment of uncertainty in routine atmospheric VOC measurements. *Atmospheric Measurement Techniques* 11(1): 141-159. doi: 10.5194/amt-11-141-2018
- Dunne E, Galbally IE, Lawson S and Patti A (2012) Interference in the PTR-MS measurement of acetonitrile at m/z 42 in polluted urban air-A study using switchable reagent ion PTR-MS. *International Journal of Mass Spectrometry* 319: 40-47. doi: 10.1016/j.ijms.2012.05.004
- Dunne E, Keyword M and Selleck P (2017) Design of a study to assess the potential impacts of hydraulic fracturing on air quality in the vicinity of well sites in the Surat Basin, Queensland (Draft 3 – Revised study design for Combabula site) Milestone of 4.1 of Air, Water and Soil Impacts of Hydraulic Fracturing

- Dunne E, Powell J and Henson S (2018) Measurements of VOCs by passive Radiello sampling at a hydraulic fracturing site in the Surat Basin, Queensland. Milestone of 6 of Project W.11- Air, Water and Soil Impacts of Hydraulic Fracturing. Available: <https://gisera.csiro.au/wp-content/uploads/2018/07/Water-11-Milestone-6-report.pdf>.
- EPP (2008). Environment Protection (Air) Policy (2008) <https://www.legislation.qld.gov.au/LEGISLTN/CURRENT/E/EnvProtAirPo08.pdf> accessed on 25 April 2017
- Esswein EJ, Breitenstein M, Snawder J, Kiefer M and Sieber WK (2013) Occupational Exposures to Respirable Crystalline Silica During Hydraulic Fracturing. *Journal of Occupational and Environmental Hygiene* 10(7): 347-356. doi: 10.1080/15459624.2013.788352
- Fang GC, Wu YS, Chen MH, Ho TT, Huang SH and Rau JY (2004) Polycyclic aromatic hydrocarbons study in Taichung, Taiwan, during 2002-2003. *Atmospheric Environment* 38(21): 3385-3391. doi: 10.1016/j.atmosenv.2004.03.036
- Field RA, Soltis J and Murphy S (2014) Air quality concerns of unconventional oil and natural gas production. *Environmental Science-Processes & Impacts* 16(5): 954-969. doi: 10.1039/c4em00081a
- Galbally I E, Lawson S J, Hibberd M F, Bentley S T, Cheng M, Weeks I A, Gillet R W, Selleck P W and Dunne E (2008) A study of VOCs during winter 2006 at Wagerup, Western Australia. A report to Alcoa World Alumina Australia. CSIRO Marine and Atmospheric Research, Aspendale, Australia.
- GISERA (2018) Potential health impacts from CSG (website), Gas Industry Social and Environmental Health Alliance (GISERA), Available: <https://gisera.csiro.au/project/potential-health-impacts-from-csg/>.
- Goncalves C, Alves C, Evtugina M, Mirante F, Pio C, Caseiro A, Schmidl C, Bauer H and Carvalho F (2010) Characterisation of PM10 emissions from woodstove combustion of common woods grown in Portugal. *Atmospheric Environment* 44(35): 4474-4480.
- Griffiths AD, Zahorowski W, Element A and Werczynski S (2010) A map of radon flux at the Australian land surface. *Atmospheric Chemistry and Physics* 10(18): 8969-8982. doi: 10.5194/acp-10-8969-2010
- Guo H, Lee SC, Ho KF, Wang XM and Zou SC (2003) Particle-associated polycyclic aromatic hydrocarbons in urban air of Hong Kong. *Atmospheric Environment* 37(38): 5307-5317. doi: 10.1016/j.atmosenv.2003.09.011
- Hibberd M, Keywood M, Cohen D, Stelcer E, Scorgie Y and Thompson S (2015) Lower Hunter Particle Characterisation Study. 4th Progress Report (Summer).
- Hibberd MF, Selleck P, Keywood MD, Cohen DD, Stelcer E and Atanacio A (2013) Upper Hunter Particle Characterisation Study. CSIRO, Australia. <http://www.environment.nsw.gov.au/resources/aqms/UHFPCSFinal.pdf>.
- Howard D and Edwards GC (2018) Mercury fluxes over an Australian alpine grassland and observation of nocturnal atmospheric mercury depletion events. *Atmospheric Chemistry and Physics* 18(1): 129-142. doi: 10.5194/acp-18-129-2018
- Howard D, Nelson PF, Edwards GC, Morrison AL, Fisher JA, Ward J, Harnwell J, van der Schoot M, Atkinson B, Chambers SD, Griffiths AD, Werczynski S and Williams AG (2017) Atmospheric mercury in the Southern Hemisphere tropics: seasonal and diurnal variations and influence of inter-hemispheric transport. *Atmospheric Chemistry and Physics* 17(18): 11623-11636. doi: 10.5194/acp-17-11623-2017
- Kahrilas GA, Blotvogel J, Stewart PS and Borch T (2015) Biocides in Hydraulic Fracturing Fluids: A Critical Review of Their Usage, Mobility, Degradation, and Toxicity. *Environmental Science & Technology* 49(1): 16-32. doi: 10.1021/es503724k
- Kavouras IG, Koutrakis P, Tsapakis M, Lagoudaki E, Stephanou EG, Von Baer D and Oyola P (2001) Source apportionment of urban particulate aliphatic and polynuclear aromatic hydrocarbons (PAHs) using multivariate methods. *Environmental Science & Technology* 35(11): 2288-2294. doi: 10.1021/es001540z

- Kennedy K, Bentley C, Heffernan A, Paxman C, Stevenson G and Mueller J (2010) Gladstone Air Study 2009 – 2010: Monitoring for polycyclic aromatic hydrocarbons (PAHs), and polychlorinated dibenzo-p-dioxins (PCDDs) & furans (PCDFs) and polychlorinated biphenyls (PCBs). The National Research Centre for Environmental Toxicology (Entox), The University of Queensland. 45 pp.
- Kennedy K, Macova M, Bartkow ME, Hawker DW, Zhao B, Denison MS and Mueller JF (2010) Effect based monitoring of seasonal ambient air exposures in Australia sampled by PUF passive air samplers. *Atmospheric Pollution Research* 1(1): 50-58. doi: 10.5094/apr.2010.008
- Keywood M and Dunne E (2017) State of the knowledge about the potential sources of air pollutants associated with CSG extraction using hydraulic fracturing. Task 2 Report for Air, Water and Soil Impacts of Hydraulic Fracturing (W.11) July 2017 38 p.
- Keywood M, Grant S, Walton A, Aylward L, Rifkin W, Witt K, Kumar A, and M, W.: Human Health Effects of Coal Seam Gas Activities –A Study Design Framework. Final report to the Gas Industry Social and Environmental Research Alliance (GISERA). January 2018. CSIRO, Canberra. <https://gisera.csiro.au/wp-content/uploads/2018/06/Health-1-Final-Report.pdf>, 2018.
- Keywood M D, Hibberd M F and Emmerson K M (2017) Australia state of the environment 2016: atmosphere, independent report to the Australian Government Minister for the Environment and Energy, Australian Government Department of the Environment and Energy, Canberra, doi:10.4226/94/58b65c70bc372.
- Khalili NR, Scheff PA and Holsen TM (1995) PAH SOURCE FINGERPRINTS FOR COKE OVENS, DIESEL AND GASOLINE-ENGINES, HIGHWAY TUNNELS, AND WOOD COMBUSTION EMISSIONS. *Atmospheric Environment* 29(4): 533-542. doi: 10.1016/1352-2310(94)00275-p
- Lawson S, Powell J, Noonan J, Dunne E and Etheridge D (2018) Ambient air quality in the Surat Basin, Queensland Overall assessment of air quality in region from 2014 -2018 <https://gisera.csiro.au/wp-content/uploads/2018/09/G3-final-AQ-assessment-report.pdf>.
- Lawson S.J., Hibberd M.F. and Keywood M.D. (2017) Ambient Air Quality in the Surat Basin- Overview of Study Design, Report for the Gas Industry Social and Environmental Research Alliance (GISERA), Project No G.3, Available: [https://gisera.org.au/wp-content/uploads/2016/02/GISERA-AQ-study-design\\_final.pdf](https://gisera.org.au/wp-content/uploads/2016/02/GISERA-AQ-study-design_final.pdf). Accessed: 4/4/2017.
- Lide D R (Ed) (1997) CRC Handbook of Chemistry and Physics, 78th edition, CRC Press, Boca Raton, FL, USA.
- Malm WC, Sisler JF, Huffman D, Eldred RA and Cahill TA (1994) Spatial and seasonal trends in particle concentration and optical extinction in the United-States. *Journal of Geophysical Research-Atmospheres* 99(D1): 1347–1370.
- Mandalakis M, Tsapakis M, Tsoga A and Stephanou EG (2002) Gas-particle concentrations and distribution of aliphatic hydrocarbons, PAHs, PCBs and PCDD/Fs in the atmosphere of Athens (Greece). *Atmospheric Environment* 36(25): 4023-4035. doi: 10.1016/s1352-2310(02)00362-x
- May NW, Gunsch MJ, Olson NE, Bondy AL, Kirpes RM, Bertman SB, China S, Laskin A, Hopke PK, Ault AP and Pratt KA (2018) Unexpected Contributions of Sea Spray and Lake Spray Aerosol to Inland Particulate Matter. *Environmental Science & Technology Letters* 5(7): 405-412. doi: 10.1021/acs.estlett.8b00254
- MFE (2016) Good Practice Guide for Assessing and Managing Dust, Wellington: Ministry for the Environment Publication number: ME 1277
- Millero FJ, Feistel R, Wright D G and McDougall TJ (2008) The composition of Standard Seawater and the definition of the Reference-Composition Salinity Scale. *Deep-Sea Research* 55: 50–72.
- Nelson P, Morrison A, Howard D and Edwards G (2017) Ambient atmospheric mercury in the vicinity of two large coal fired power stations and open cut coal mines, ICMGP 2017, 13th International Conference on Mercury as a Global Pollutant, Providence Rhode Island, July 16-21 2017.

- NEPC (2017) National Environment Protection Council Annual Report 2016–17 Commonwealth of Australia, 2018 ISBN: 978-1-921069-10-9, 207 pp. <http://www.nepc.gov.au/system/files/resources/afef0a22-b780-41ed-ab10-416162bb201e/files/nepc-annual-report-2016-17.pdf>.
- NEPM (2011) National Environment Protection (Air Toxics) Measure <https://www.legislation.gov.au/Details/F2011C00855> accessed on 25 April 2107.
- NEPM (2015). National Environment Protection (Ambient Air Quality) Measure <https://www.legislation.gov.au/Details/F2016C00215> accessed on 25 April 2017
- NICNAS (2017a) Human health hazards of chemicals associated with coal seam gas extraction in Australia, Project report prepared by the National Industrial Chemicals Notification and Assessment Scheme (NICNAS) as part of the National Assessment of Chemicals Associated with Coal Seam Gas Extraction in Australia, Commonwealth of Australia, Canberra.
- NICNAS (2017b) Human health risks associated with surface handling of chemicals used in coal seam gas extraction in Australia, Project report prepared by the National Industrial Chemicals Notification and Assessment Scheme (NICNAS) as part of the National Assessment of Chemicals Associated with Coal Seam Gas Extraction in Australia, Commonwealth of Australia, Canberra.
- NICNAS (2017c) Identification of chemicals associated with coal seam gas extraction in Australia, Project report prepared by the National Industrial Chemicals Notification and Assessment Scheme (NICNAS) as part of the National Assessment of Chemicals Associated with Coal Seam Gas Extraction in Australia, Commonwealth of Australia, Canberra.
- Norris G and Duvall R (2014) EPA Positive Matrix Factorization (PMF) 5.0 Fundamentals and User Guide [https://www.epa.gov/sites/production/files/2015-02/documents/pmf\\_5.0\\_user\\_guide.pdf](https://www.epa.gov/sites/production/files/2015-02/documents/pmf_5.0_user_guide.pdf)
- Radhi M, Box MA, Box GP, Mitchell RM, Cohen DD, Stelcer E and Keywood MD (2010) Size-resolved mass and chemical properties of dust aerosols from Australia's Lake Eyre Basin. *Atmospheric Environment* 44(29): 3519-3528. doi: 10.1016/j.atmosenv.2010.06.016
- Ravindra K, Bencs L, Wauters E, de Hoog J, Deutsch F, Roekens E, Bleux N, Berghmans P and Van Grieken R (2006) Seasonal and site-specific variation in vapour and aerosol phase PAHs over Flanders (Belgium) and their relation with anthropogenic activities. *Atmospheric Environment* 40(4): 771-785. doi: 10.1016/j.atmosenv.2005.10.011
- Ravindra K, Wauters E and Van Grieken R (2008) Variation in particulate PAHs levels and their relation with the transboundary movement of the air masses. *Science of The Total Environment* 396(2-3): 100-110. doi: 10.1016/j.scitotenv.2008.02.018
- Ravindra K, Wauters E, Tyagi SK, Mor S and Van Grieken R (2006) Assessment of air quality after the implementation of compressed natural gas (CNG) as fuel in public transport in Delhi, India. *Environmental Monitoring and Assessment* 115(1-3): 405-417. doi: 10.1007/s10661-006-7051-5
- Rogge WF, Hildemann LM, Mazurek MA, Cass GR and Simoneit BRT (1993) SOURCES OF FINE ORGANIC AEROSOL .2. NONCATALYST AND CATALYST-EQUIPPED AUTOMOBILES AND HEAVY-DUTY DIESEL TRUCKS. *Environmental Science & Technology* 27(4): 636-651. doi: 10.1021/es00041a007
- Rogge WF, Hildemann LM, Mazurek MA, Cass GR and Simoneit BRT (1993) SOURCES OF FINE ORGANIC AEROSOL .5. NATURAL-GAS HOME APPLIANCES. *Environmental Science & Technology* 27(13): 2736-2744. doi: 10.1021/es00049a012
- Ryerson TB, Aikin KC, Angevine WM, Atlas EL, Blake DR, Brock CA, Fehsenfeld FC, Gao RS, de Gouw JA, Fahey DW, Holloway JS, Lack DA, Lueb RA, Meinardi S, Middlebrook AM, Murphy DM, Neuman JA, Nowak JB, Parrish DD, Peischl J, Perring AE, Pollack IB, Ravishankara AR, Roberts JM, Schwarz JP, Spackman JR, Stark H, Warneke C and Watts LA (2011) Atmospheric emissions from the Deepwater Horizon spill constrain air-water

- partitioning, hydrocarbon fate, and leak rate. *Geophysical Research Letters* 38. doi: L07803  
doi:10.1029/2011gl046726
- Schinteie R, Pinetown K and Douglas G SS (2015) Literature review of dissolved hydrocarbons in groundwater with emphasis on the Australian Surat and Bowen basins. CSIRO, Australia. Available: <https://gisera.org.au/wp-content/uploads/2016/04/GISERA-Hydrocarbons-Lit-Review-2015.pdf>. Accessed: 20/4/2017.
- Schinteie R, Pinetown K, Douglas G and S S (2015) Literature review of dissolved hydrocarbons in groundwater with emphasis on the Australian Surat and Bowen basins. CSIRO, Australia. Available: <https://gisera.org.au/wp-content/uploads/2016/04/GISERA-Hydrocarbons-Lit-Review-2015.pdf>. Accessed: 20/4/2017.
- Seinfeld JH (1986) Atmospheric chemistry and physics of air pollution. Atmospheric chemistry and physics of air pollution.: 738 pp.
- Slemr F, Angot H, Dommergue A, Magand O, Barret M, Weigelt A, Ebinghaus R, Brunke E-G, Pfaffhuber K, Edwards G, Howard D, Powell J, Keywood M and Wang F (2015) Comparison of mercury concentrations measured at several sites in the Southern Hemisphere *Atmos. Chem. Phys. Discuss.* <http://www.atmos-chem-phys-discuss.net/14/30611/2014/> L1 - <http://www.atmos-chem-phys-discuss.net/14/30611/2014/acpd-14-30611-2014.pdf> DO - 10.5194/acpd-14-30611-2014 ER
- SoQ (2010) Natural Resources and Other Legislation Amendment Bill (No. 2) 2010. State of Queensland, <http://www5.austlii.edu.au/au/legis/qld/bill/nraolab22010521/>.
- State of the knowledge about the potential sources of air pollutants associated with CSG extraction using hydraulic fracturing Milestone 2.1 of W.11. doi: <https://doi.org/10.4225/08/5a0f23f8f10fb>
- Stearman WM, Taulis M and et al. (2014) Assessment of Geogenic Contaminants in Water Co-Produced with Coal Seam Gas Extraction in Queensland, Australia: Implications for Human Health Risk. *Geosciences* 4(3): 219.
- Tadros CV, Crawford J, Treble PC, Baker A, Cohen DD, Atanacio AJ, Hankin S and Roach R (2018) Chemical characterisation and source identification of atmospheric aerosols in the Snowy Mountains, south-eastern Australia. *Science of The Total Environment* 630: 432-443. doi: 10.1016/j.scitotenv.2018.02.231
- Taha G, Box GP, Cohen DA and Stelcer E (2007) Black carbon measurement using laser integrating plate method. *Aerosol Science and Technology* 41(3): 266-276. doi:10.1080/02786820601156224
- Tait DR, Santos IR, Maher DT, Cyronak TJ and Davis RJ (2013) Enrichment of Radon and Carbon Dioxide in the Open Atmosphere of an Australian Coal Seam Gas Field. *Environmental Science & Technology* 47(7): 3099-3104. doi: 10.1021/es304538g
- TCEQ ( 2016 ) Air monitoring comparison values, Texas Commission on Environmental Quality, Accessed: 18/5/2018, Available: <https://www.tceq.texas.gov/toxicology/amcv/abou>.
- TCEQ (2016) Effects screening levels, Texas Commission on Environmental Quality, Accessed: 18/5/2018, Available: [https://www.tceq.texas.gov/toxicology/esl/list\\_main.html/#esl\\_1](https://www.tceq.texas.gov/toxicology/esl/list_main.html/#esl_1).
- Tobiszewski M and Namieśnik J (2012) PAH diagnostic ratios for the identification of pollution emission sources. *Environmental Pollution* 162: 110-119. doi: <https://doi.org/10.1016/j.envpol.2011.10.025>
- Yost EE, Stanek J, DeWoskin RS and Burgoon LD (2016) Estimating the Potential Toxicity of Chemicals Associated with Hydraulic Fracturing Operations Using Quantitative Structure-Activity Relationship Modeling. *Environmental Science & Technology* 50(14): 7732-7742. doi: 10.1021/acs.est.5b05327
- Aldabe J, Elustondo D, Santamaria C, Lasheras E, Pandolfi M, Alastuey A, Querol X and Santamaria JM (2011) Chemical characterisation and source apportionment of PM<sub>2.5</sub> and PM<sub>10</sub> at rural, urban and traffic sites in Navarra (North of Spain). *Atmospheric Research* 102(1-2): 191-205. doi: 10.1016/j.atmosres.2011.07.003

## 9 Appendix: Comparison of particulate matter (PM) measurement methods

There were four methods used in this study to measure air quality in relation to PM:

1. Sampling of PM<sub>10</sub> by Low Volume Sampler-Gravimetric Method: Two x 12-hour samples of PM<sub>10</sub> were collected per day on Teflon Filters using Comde-Derenda low volume samplers at the North-AQMS: This method complies with AS/NZ 3580.9.9.2006. The average of the twice daily samples was directly comparable with the 24-hour NEPM/EPP air quality objective for PM<sub>10</sub>.
2. PM<sub>10</sub> by Low Volume Sampler-Gravimetric Method: Multi-day (~ 9 days) samples of PM<sub>10</sub> were collected on Teflon Filters using Ecotech Microvol low volume samplers at the five Solar-AQMS sites. This method also complies with Australian Standard Method AS/NZ 3580.9.9.2006. Due to the multi-day duration of sampling the Microvol PM<sub>10</sub> data was not directly comparable with the 24-hour NEPM/EPP air quality objective. For the purposes of this study, the overall average of PM<sub>10</sub> measured using Microvols at the five Solar-AQMS sites was compared to the NEPM/EPP annual air quality objective of 25 ug m<sup>-3</sup> to provide context to these longer-term measurements.
3. Continuous measurements of PM<sub>2.5</sub> by MetOne E-Sampler: E-samplers were operated at the five Solar-AQMS sites and provided continuous measurement of PM<sub>2.5</sub> by near forward light scattering technique plus gravimetric PM<sub>2.5</sub> mass by multi-day sampling on 47 mm Teflon filters. The continuous measurements by light scattering were corrected based on the gravimetric mass scattering (K) factor determined from the filter sample. The continuous PM<sub>2.5</sub> from light scattering is not an Australian Standard Method for determination of PM<sub>2.5</sub> but the filter measurements used for calibration did comply with Australian Standard Method AS/NZ 3580.9.10:2017.
4. Continuous measurements of PM<sub>10</sub> and PM<sub>2.5</sub> were performed simultaneously by Palas FIDAS 200s aerosol spectrometer located at both the North and South-AQMS: This method is not an Australian Standard Method for determination of PM<sub>10</sub> or PM<sub>2.5</sub>. Notably, FIDAS

instruments were also used for PM measurements at Miles Airport and Hopeland sites operated as part of the Surat Basin Ambient Air Quality Study (Lawson et al., 2018).

Good agreement with slopes of 0.98 – 1.09, intercepts of -2 to 1  $\mu\text{g m}^{-3}$ , and  $R^2$  values of 0.84 – 0.97 (Figure 65) were observed between FIDAS instruments and co-located Australian Standard PM<sub>10</sub> Low Volume Sampler-Gravimetric Methods (Derenda and Microvol) and co-located continuous measurements of PM<sub>2.5</sub> by E-Sampler. An ideal comparison would give a slope of 1, and intercept of 0 and  $R^2$  of 1. For the purposes of this study the non-standard and Australian Standard PM measurement methods provided comparable results and were of sufficient quality for direct comparison with the NEPM/EPP PM<sub>10</sub> and PM<sub>2.5</sub> air quality objectives.

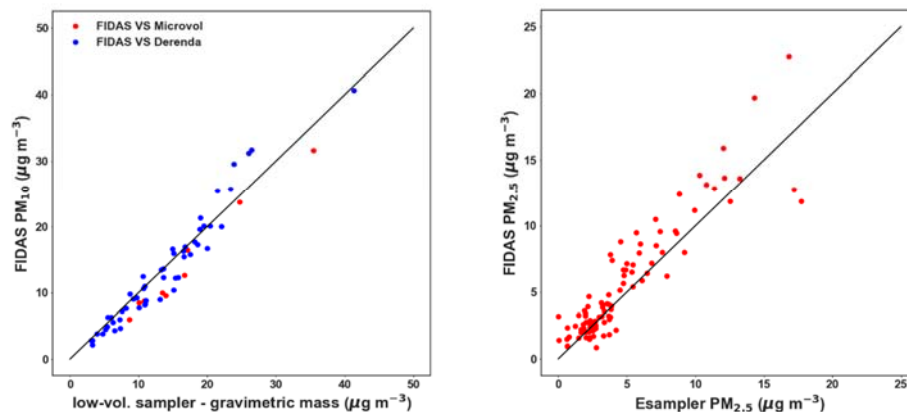


**Figure 65 Comparison of PM<sub>10</sub> and PM<sub>2.5</sub> measurement methods employed during the HF study. Lines represent 1:1 agreement. (Left panel) (blue) 24-hour average PM<sub>10</sub> by low-volume Derenda sampler with gravimetric mass determination versus 24-hour average of continuous PM<sub>10</sub> measurement by FIDAS light scattering method ( $R^2 = 0.94$ ). (red) Multi-day integrated average PM<sub>10</sub> by low-volume Microvol sampler with gravimetric mass determination versus FIDAS PM<sub>10</sub> integrated average over the same sample duration as Microvol ( $R^2 = 0.97$ ). (Right Panel) 24-hour average of continuous PM<sub>10</sub> measurements by E-Sampler light scattering technique with gravimetric mass correction versus 24-hour average of continuous PM<sub>10</sub> measurement by FIDAS light scattering method ( $R^2 = 0.84$ ).**

## 10 Appendix - Analysis of PM<sub>10</sub> chemical composition data

As described in Section 4.3 12-hour PM<sub>10</sub> samples were collected on Teflon filters at the North-AQMS using Comde-Derenda low volume samplers following the method described in the AS/NZ 3580.9.9.2006. The Teflon filters underwent analysis for gravimetric mass and elemental (by Ion Beam Analysis), soluble ion and anhydrous sugar composition analysis (by ion chromatography). Many of these data were then analysed using Positive Matrix Factorisation receptor model to determine factors contributing to the source of particles collected on the samples.

The methods used to collect the samples and perform the chemical composition analysis are described in detail in Dunne et al. (2017). In this section we report on data quality analysis, describe the PMF method and the results of the PMF,

### 10.1 Data Quality

#### 10.1.1 Blank filters

Blank filters were analysed throughout the study. The average of the blank concentration is subtracted from each measurement. The blanks are also used to calculate the method detection limit (MDL). We followed the Standards Australia procedures which are those of the International Standard ISO 6879:1995 Air quality – Performance characteristics and related concepts for air quality measuring methods. Section 5.2.7 of the Standard states that a zero sample has a 5% probability of causing a measured concentration above the detection limit, so that:

$$Sc(0) * t_{0.95} \quad (1)$$

where:

Sc(0) is the standard deviation of the blanks, and

t<sub>0.95</sub> is value of the 1-tailed t distribution for P<0.05 (i.e. the 95 % confidence limit).

#### 10.1.2 Ion balance

The ion balance (IB) gives an indication of the water soluble aerosol chemistry data quality in that the total cation equivalents (positive charged ions) should equal the total anion equivalents (negative charged ions).

Note that a poor IB does not always indicate bad data quality. For example pH is not measured in this project and samples with high pH levels might have a poor IB due to high levels of bicarbonate; these samples usually also have high levels of calcium. Similarly, samples with low pH may have excess anions. Samples that have been flagged as invalid have been reanalysed. The IB plot is shown in Figure 66 and shows excellent data quality.

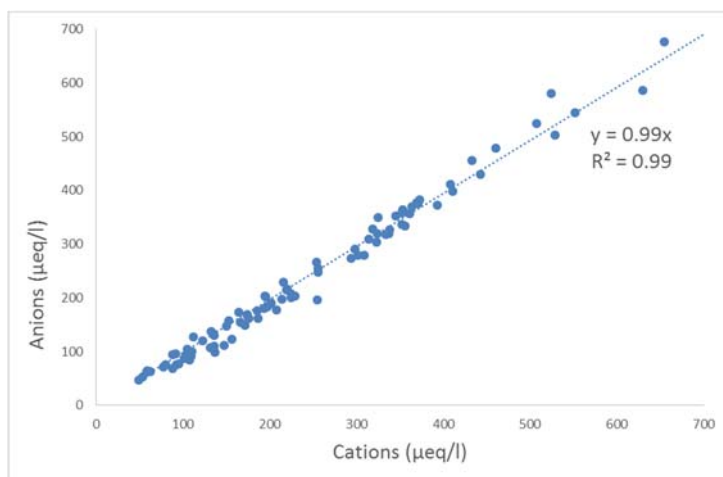
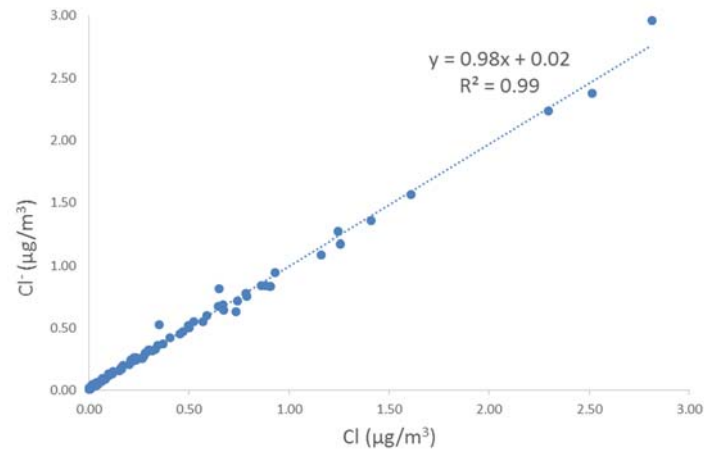


Figure 66 Ion balance for the ion chromatography measurements with the anions and cations

### 10.1.3 Comparison of species from IC and IBA analysis

Ion chromatography (IC) and ion beam analysis (IBA) techniques analyse some common species, allowing for an independent check of the quality of the analytical methods. It is important to note that IC measures the concentrations of soluble species concentrations in ionic form whereas IBA measures total concentration of the species. In general we would expect IC concentrations to be lower than the IBA concentrations. In addition, both techniques have an uncertainty of approximately  $\pm 5\%$ . In the case of chlorine however, most atmospheric chlorine is generally water soluble, hence the two techniques should compare well if both data sets are of good quality. Figure 67 shows that the concentration of Cl measured by IBA and Cl<sup>-</sup> measured by IC agree well, providing us with confidence in amalgamating the IBA and IC data sets for PMF analysis.



**Figure 67 Comparison of chloride ion (Cl<sup>-</sup>) concentrations determined by ion chromatography and elemental chlorine (Cl) concentrations determined by ion beam analysis**

#### 10.1.4 Species correlations and tracer time series

Correlations between chemical species can be qualitative indicators of the sources of these species.

The identification of soil dust relies on the presence of aluminium, silicon, titanium, iron and calcium; in particular aluminium, silicon, titanium have few other sources and are the most useful identifiers. Figure 68 shows a scatter plot of titanium against aluminium with a linear relationship of 13.58 and Figure 69 shows a scatter plot of silicon against aluminium with a linear relationship of 0.27 both of which are very similar to the typical value for crustal dust (Lide 1997). The correlation coefficient of 0.99 indicates that both aluminium and titanium are from the same source.

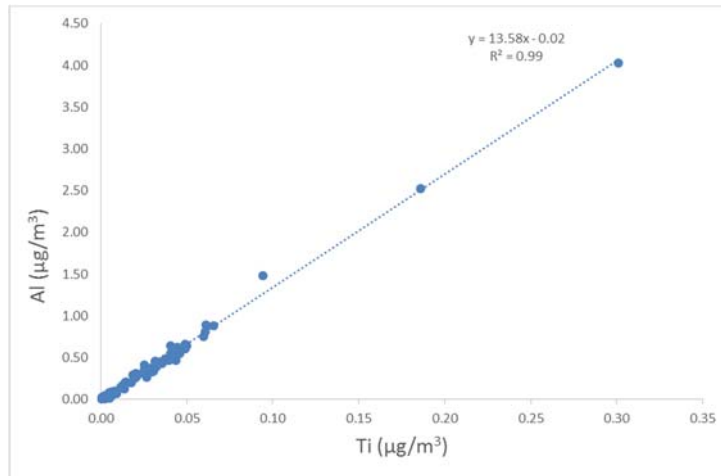


**Figure 68 Scatter plot of titanium versus aluminium**

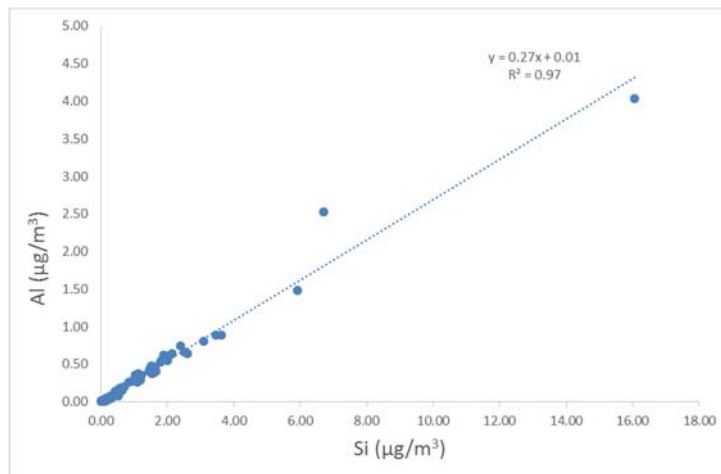
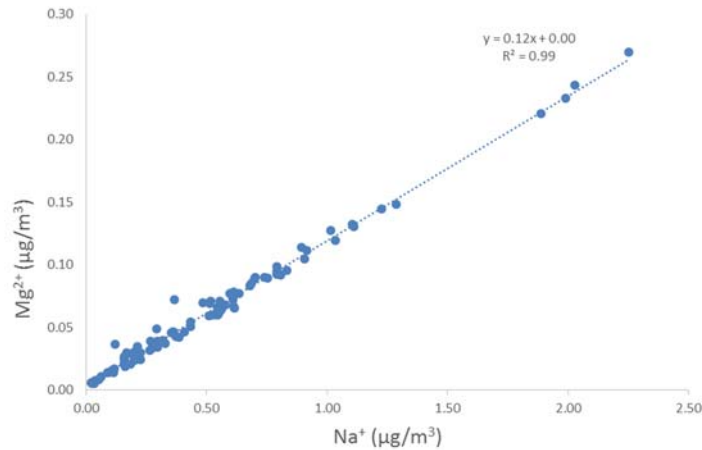


**Figure 69 Scatter plot of silicon versus aluminium**

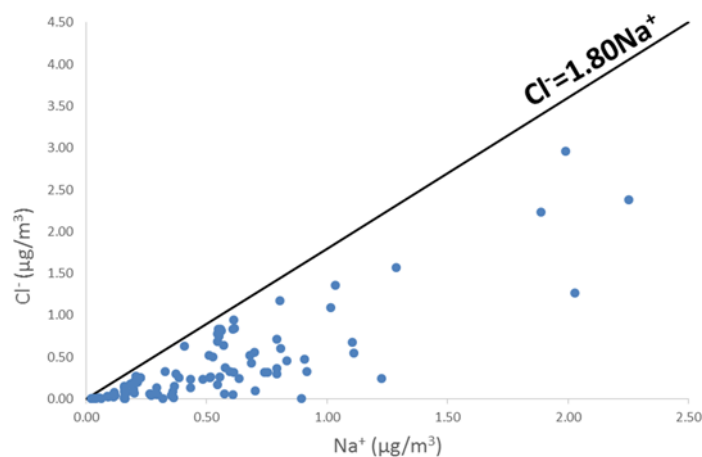
Figure 70 shows that the linear relationship between magnesium and sodium is the same as the  $Mg^{2+}/Na^+$  ratio in standard sea water of 0.12 (Millero et al. 2008). In addition, the correlation coefficient of 0.99 suggests that both sodium and magnesium are from the same source. This provides strong evidence that most of the sodium and magnesium in the samples are derived from sea salt.

Unlike the magnesium and sodium component of sea salt which remains present in the particles, chloride can be displaced during reaction sulfuric and nitric acids (Seinfeld and Pandis 2006). Figure 71 shows the scatter plot of chloride and sodium with all points lying below the line for fresh sea salt ( $Cl^-/Na^+ = 1.80$ ). This plot shows that observed chloride concentration is always lower

than the ratio of pure sea salt. This displacement of chloride is referred to as ‘aging’ of the sea salt and is discussed in more detail below.

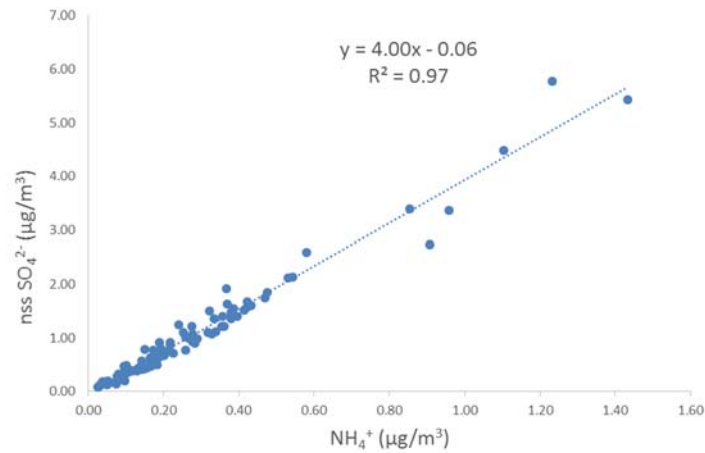


**Figure 70** Scatter plot showing the strong linear relationship between magnesium and sodium concentrations



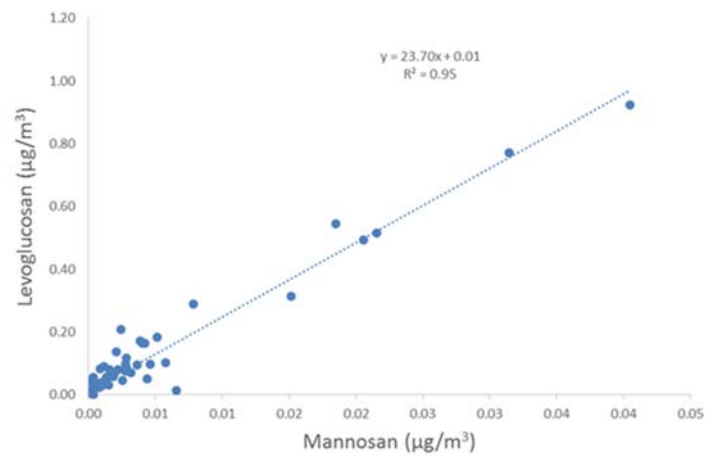
**Figure 71** Scatter plot showing that for a given sodium concentration, the observed chloride concentrations are always lower than for fresh sea salt ( $Cl^-/Na^+ = 1.80$ ).

Figure 72 shows the linear relationship between non sea salt (nss) sulfate and ammonium, with a ratio of 4.00 and high correlation coefficient ( $r^2$ ) of 0.97, suggesting that most of the ammonium and nss sulfate have similar sources. The  $SO_4/NH_4$  ratio for neutralised ammonium sulfate is 2.7 and for ammonium bisulfate it is 5.0. This indicates that the ammonium and nss sulfate measured at this site is likely to be a mix of ammonium sulfate and ammonium bisulfate which form as secondary inorganic aerosols in the atmosphere.



**Figure 72 Scatter plot showing the strong linear relationship between nss sulfate and ammonium concentrations**

Levoglucosan and mannosan are unique tracers for the combustion of cellulose found in trees and plants (Iinuma et al. 2007). Figure 73 shows a good correlation between these species with the ratio of 23.7 representative of wood smoke from the combustion of hardwood (Goncalves et al. 2010). Figure 74 shows the times series plot of levoglucosan with the peaks indicating the times that woodsmoke impacted on the AQMS nth site.



**Figure 73 Scatter plot of mannosan versus levoglucosan in the PM<sub>10</sub> measured during the study**

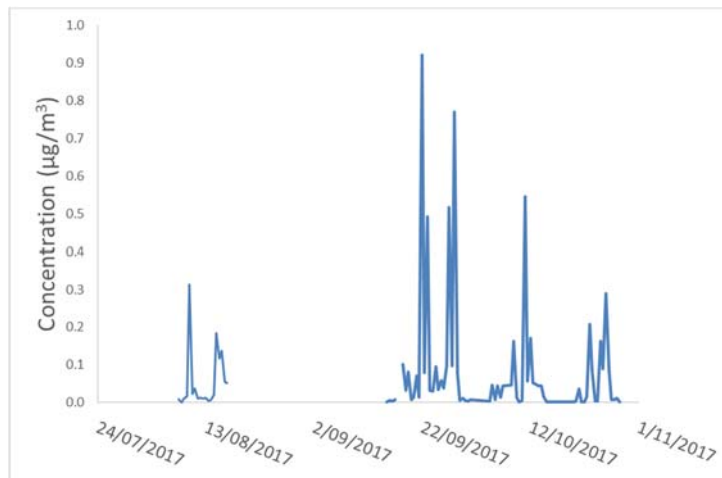


**Figure 74 Time series plot of levoglucosan in the PM<sub>10</sub> measured during the study**

Figure 75 shows the time series plot of arabitol and mannitol which are tracers for fungal spores and have been used to assess the abundance of primary bio-aerosols (PBA) in the atmosphere (Bauer et al. 2008; Despres et al. 2012).

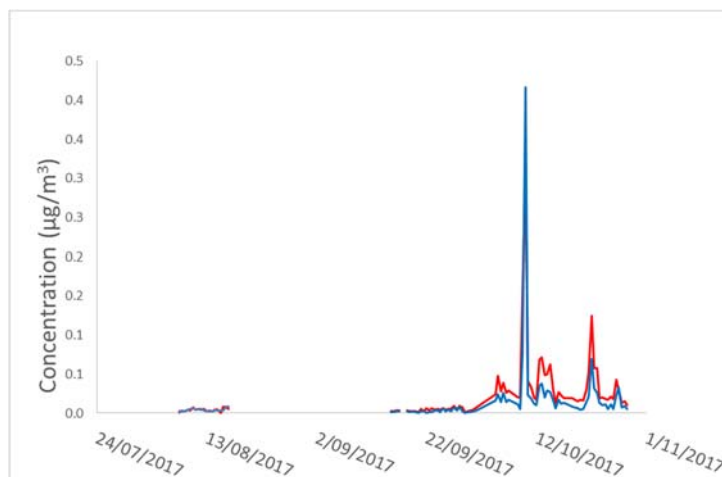


**Figure 75 Time series plot of arabitol and mannitol in the PM<sub>10</sub> measured during the study**

### 10.1.5 Reconstructed chemical mass

We can sum the concentrations of the chemical species measured on the filters by IBA and IC to calculate the reconstructed chemical mass and compare the reconstructed chemical mass to the total gravimetric mass determined by weighing the filters before and after sampling. Differences provide us with an indication of the completeness of the chemical analysis i.e. have we quantified all of the chemical components that make up the PM<sub>10</sub> mass?

The soil mass concentration can be estimated from the following equation (Malm et al. 1994).

$$\text{Soil} = 2.20 \times \text{Al} + 2.49 \times \text{Si} + 1.63 \times \text{Ca} + 1.94 \times \text{Ti} + 2.42 \times \text{Fe}$$

noting that the soil species measured only include their elements and not their associated oxides.

Figure 76 shows the linear relationship between the measured and reconstructed mass with a R<sup>2</sup> of 0.93. The chemical species measured make up 70% of the measured mass with the difference likely to be moisture and some organic compounds that were not measured.

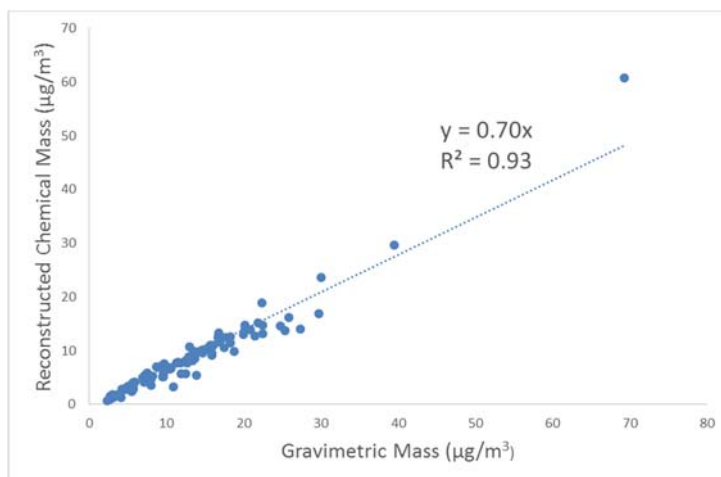


**Figure 76 Scatter plot of gravimetric mass versus reconstructed chemical mass in the PM<sub>10</sub> measured during the study**

## 10.2 Data analysis by PMF (positive matrix factorisation)

Positive matrix factorisation (PMF) is a type of receptor modelling for analysing data collected at receptors. It is a mathematical method that relies on internal correlations between species in the data set to identify both the factors contributing to the samples and the amount that each factor contributes to the composition measured on the filter.

Once the factors are obtained, further analysis is undertaken to identify the source(s) in each factor. This uses the species information in the factor and other knowledge of atmospheric chemistry as well as wind sector and seasonal analysis to identify the most likely source(s) of emissions for each factor. In many cases, there is a single dominant source in a factor and this is often used to name the factor. However, if sources are co-located or otherwise correlated, they can appear together in a single factor or across several factors. It is important to note that the sources identified by PMF are not necessarily the same as the sources listed in an emissions inventory.

An advantage of PMF is that it is often able to identify factors representing species or groups of species that are not directly emitted as particles (primary particles) but are formed by chemical reactions in the atmosphere and gas-to-particle conversions (secondary particles), such as secondary ammonium sulfate which is not directly emitted from a source, and will not be listed in a source emissions inventory.

In the PMF analysis for this study, the chemical composition data of all the samples was analysed using the EPA PMF 5.0 software (Norris and Duvall 2014).

### 10.2.1 Selection of species

The analytical methods used for the analysis of samples in this project have produced a data set consisting of 45 species. In a number of cases different methods have measured the same or similar species (e.g. sulfate by IC and S by PIXE). In these cases, we have selected one of the species for inclusion in the PMF analysis.

**Table 43 Species excluded from the PMF analysis**

Species excluded	Reason
Na by PIXE	used Na <sup>+</sup> by IC
S by PIXE	used SO <sub>4</sub> <sup>2-</sup> by IC
Cl by PIXE	used Cl <sup>-</sup> by IC, much better detection limit
K by PIXE	used K <sup>+</sup> by IC and insoluble K
Ca <sup>2+</sup> by IC	used Ca by PIXE
P, Cr, Ni, Cu, Zn, Ga, As, Rb, Sr, Y, Zr by PIXE F <sup>-</sup> , Br <sup>-</sup> , galactosan, by IC	Low S/N or poorly fitted by PMF model (correlation between observed and modelled $r^2 < 0.4$ )

S/N: signal-to-noise (ratio)

For a number of species, a significant proportion of the measured concentrations were below the method detection limit (MDL). The EPA PMF 5.0 User Guide (Norris and Duvall 2014) recommends the exclusion of species if more than 95% of samples have concentrations less than the MDL. In addition, species with more than 75% of samples less than the MDL were examined closely and their inclusion was dependent on how well the modelled time series fit the observational data.

We also used the criteria of the signal-to-noise (S/N) ratios as calculated by EPA PMF to assign an uncertainty weighting to the species. Variables were initially defined to be strong, weak or bad depending on their S/N ratio. Species with S/N ratios less than 0.5 were excluded. Species with S/N

ratios between 0.5 and 1 were considered weak variables and by flagging them as such their estimated uncertainties were increased by a factor of three to reduce their weight in the solution. We also set the mass variable to weak by assigning it as a totalising variable.

Finally, we evaluated the ability of PMF to model each species and have excluded species whose observed concentrations were not fitted well by the PMF analysis ( $r^2 < 0.4$ ) since these species act as 'noise' in the PMF analysis and can worsen the factor fit for other species. It is worth noting that PMF identifies the principal factors that determine most of the variance in the data set. In so doing, PMF does not describe unusual episodes such as, for example, once-a-year fireworks. The species not included in the PMF analysis are listed in Table 43. Table 44 lists the strength of the various species used in the PMF analysis. There was a total of 93 samples, with 26 species used for the analysis.

**Table 44 Species included in PMF analysis of PM<sub>2.5</sub> data listing PMF category, and the median concentration and signal-to-noise ratio calculated by EPA PMF at each site.**

Species	Category	S/N	Median	Species	Category	S/N	Median
Na <sup>+</sup>	Strong	10.00	0.51	Na	Bad	0.46	0.00
NH <sub>4</sub> <sup>+</sup>	Strong	10.00	0.20	Al	Strong	5.07	0.17
K <sup>+</sup>	Strong	8.52	0.08	Si	Strong	5.92	0.58
Mg <sup>2+</sup>	Strong	10.00	0.06	P	Bad	0.01	0.00
Ca <sup>2+</sup>	Bad	9.78	0.05	S	Bad	7.47	0.33
Cl <sup>-</sup>	Strong	8.92	0.25	Cl	Bad	5.76	0.23
NO <sub>2</sub> <sup>-</sup>	Bad	4.45	0.00	K	Bad	6.59	0.12
Br <sup>-</sup>	Bad	6.88	0.00	Ca	Strong	5.27	0.05
NO <sub>3</sub> <sup>-</sup>	Strong	10.00	0.51	Ti	Strong	3.36	0.01
SO <sub>4</sub> <sup>2-</sup>	Strong	10.00	0.88	Cr	Bad	0.01	0.00
C <sub>2</sub> O <sub>4</sub> <sup>2-</sup>	Strong	9.75	0.10	Mn	Strong	2.04	0.00
PO <sub>4</sub> <sup>3-</sup>	Strong	9.75	0.01	Fe	Strong	6.83	0.12
F <sup>-</sup>	Bad	4.71	0.00	Ni	Bad	0.00	0.00
Acetic	Strong	5.64	0.00	Cu	Bad	0.11	0.00
Formic	Strong	8.35	0.01	Zn	Bad	0.32	0.00
MSA <sup>-</sup>	Strong	9.75	0.01	Ga	Bad	0.00	0.00

<b>Levogluconan</b>	Strong	8.39	0.02	<b>As</b>	Bad	0.00	0.00
<b>Aribatol</b>	Strong	10.00	0.01	<b>Rb</b>	Bad	0.05	0.00
<b>Sorbitol</b>	Bad	0.00	0.00	<b>Sr</b>	Bad	0.00	0.01
<b>Mannosan</b>	Strong	3.87	0.00	<b>Y</b>	Bad	0.21	0.01
<b>Mannitol</b>	Strong	9.89	0.01	<b>Zr</b>	Bad	0.03	0.00
<b>Glactosan</b>	Bad	0.86	0.00	<b>BC</b>	Strong	9.78	1.06
<b>Glucose</b>	Strong	7.74	0.01	<b>K insoluble</b>	Strong	4.32	0.03
<b>mass</b>	Weak	-	12.31				

### 10.2.2 Species correlations and tracer time series

The analysis using EPA PMF 5.0 is an iterative process requiring a physical interpretation of the results in order to select the appropriate number of factors, and to identify and name them. Correlations between species in the data provide a useful indication of the key species in the PMF factors and also indicate the extent to which markers from different source types may be evident in the same factor. These correlations which were discussed above provide a good starting point for determining the number of factors to use in the initial PMF run. These correlations identified a soil, sea-salt, aged sea-salt and ammonium sulfate source and the time series plots of tracer species indicate a wood smoke and primary biogenic aerosol source. This indicated that 6 factors may be a starting point for the PMF analysis.

### 10.2.3 PMF configuration

The PMF model was executed with 100 base runs, a random seed until the final solution was found, with various numbers of factors and an extra modelling uncertainty of 5% to account for errors not considered in calculating measurement or analytical errors.

Examination of the ability to model the observed time series of the species concentrations was used in arriving at the final solution, along with the need for physically sensible interpretations of the factors. The best fit with factors that could be explained physically was obtained using 8 factors.

The G-space plots showed little rotation and Fpeak was not used. All runs converged and the Q values were stable. The uncertainty in the factor contributions is derived from the bootstrapping

and displacement methods in the EPA PMF 5.0 software (Norris and Duvall 2014) and are reported in the EPA PMF diagnostic tables shown in Figure 77.

<b>Base run summary</b>									
Number of base runs:	100								
Base random seed:	9								
Number of factors:	8								
Extra modelling uncertainty (%):	5								
<b>DISP summary</b>	<b>Err.code</b>	<b>Max dQ</b>							
	0	-0.014							
	<b>Factor 1</b>	<b>Factor 2</b>	<b>F 3</b>	<b>F 4</b>	<b>F 5</b>	<b>F 6</b>	<b>F 7</b>	<b>F 8</b>	
<b>dQmax = 4</b>	0	0	0	0	0	0	0	0	
<b>dQmax = 8</b>	0	0	0	0	0	0	0	0	
<b>dQmax = 15</b>	0	0	0	0	0	0	0	0	
<b>dQmax = 25</b>	0	0	0	0	0	0	0	0	
<b>Bootstrap summary of base run</b>									
Number of bootstrap runs:	100								
Bootstrap random seed:	9								
Min. Correlation R-Value:	0.6								
<b>BS mapping:</b>									
									Unmapped
Boot Factor 1	100	0	0	0	0	0	0	0	0
Boot Factor 2	0	76	7	9	0	5	0	1	2

Figure 77 EPA PMF diagnostic tables

### 10.2.4 PMF mass closure

Figure 78 compares the PM<sub>10</sub> concentrations measured by the gravimetric method to the reconstructed mass from the PMF analysis. It shows that the modelled PMF mass has a very good agreement with the measured mass.

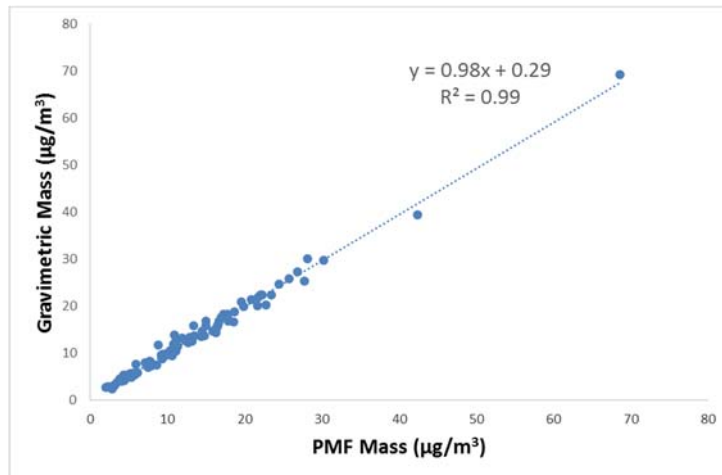


Figure 78 Scatter plot of 24-hour PM<sub>10</sub> concentrations from the gravimetric mass determination and the reconstructed mass from the PMF solution

## 11 Appendix –VOC Measurements

### 11.1 Proton Transfer Reaction – Mass Spectrometer (PTR-MS)

The PTR-MS was housed in an air-conditioned enclosure at the North-AQMS site. A flow of 1.5 L min<sup>-1</sup> of ambient air was drawn via ~ 12 m of 3/8 inch O.D. PTFE tubing inlet by a constant flow sampling pump through the PTR-MS auxiliary system and the PTR-MS sampled 300 mL min<sup>-1</sup> from the auxiliary system. A commercially built PTR-MS (Ionicon Analytik, GmbH, Innsbruck Austria) was utilised for continuous VOC measurements.

The drift tube was operated at 60° C, and an applied voltage of ~600 V and a pressure of ~2 mbar. The PTR-MS quadrupole continuously scanned 181 masses between 14 and 200 amu with a dwell time for a single mass (m/z) of 1 s, generating a full mass scan approximately every 3 min (20 data points h<sup>-1</sup> m/z<sup>-1</sup>).

The PTR-MS operated with the aid of custom-built auxiliary equipment that regulated the flow of air in the sample inlet and controlled whether the PTR-MS was sampling ambient or zero air or calibration gas. Zero readings were made by diverting ambient air through a zero furnace (350° C) with a platinum wool catalyst that destroyed VOCs in the air before entering the PTR-MS. This zero air had the same mole fractions of H<sub>2</sub>O and CO<sub>2</sub> as the ambient air being sampled, neglecting minor contributions from the oxidation of the VOCs present. Zero measurements were made for 1h commencing at each of the following times on every sampling day: 00:00 h, 17:00 h. All PTR-MS ion signals from calibration and ambient measurements were background corrected.

The minimum detectable limit for each m/z scanned by the PTR-MS was determined from the scatter in the zero measurements using the principles of ISO6879 (ISO 1995). The MDL for a single measurement was set at the 95th percentile of the deviations about the mean zero. The PTR-MS was calibrated daily for 1 hour. For each calibration measurement a set flow of 10-20 mL min<sup>-1</sup> of a ~1 ppm calibration standard was diluted in a flow 1500 mL min<sup>-1</sup> of ambient air that had been passed through the zero furnace. The PTR-MS was calibrated with three certified gas standards containing > 20 VOC species including benzene, toluene, o- xylene and formaldehyde. These certified gas standards were supplied by Apel-Reimer Environmental Inc (Miami Florida, USA). The stated accuracy for each component in the standards was ± 5%.

Detection limits for this method are typically 0.003 – 0.200 ppb with calculated measurement uncertainties of ~ 9 – 22% depending on the species under consideration (Dunne et al 2018).

As with almost all other systems used to measure trace gas concentrations, the PTR-MS records a non-zero value when measuring "zero" air that has passed through the zero furnace. For the PTRMS, this value is always positive. The zero correction applied to the ambient data was the median of the two quality assured zeros to either side of the data point. This means that a maximum of four and minimum of two zero averages are used for the zero correction of each data point. At the beginning and end of the measurement period, where only one side of the ambient data had a zero associated with it, then only the one zero was used for correction. Due to this subtraction process and the underlying measurement noise in the instrument, measurements of ambient air that has, for a particular VOC, zero concentration, will lead to the detection of a scatter of concentrations with in most cases small negative and positive deviations from zero. This "noise" is used to determine the minimum detection limit of the measurement of that VOC (see next section).

The PTR-MS instrument was operated at the HF study site in a scanning mode sequentially measuring each mass, at 1 amu intervals, between masses 21 and 150 (excluding masses 32 and 35 - 37) and then commencing again at mass 21. This range is chosen to cover the molecular masses of most VOCs that potentially could occur in the atmosphere that are detectable by PTR-MS with reasonable sensitivity but exclude masses associated with the ionization source which are not atmospherically relevant.

Data were obtained from 30 July to 21 November 2017. Initially, the dwell time for a single mass measurement was 0.5 second which was increased to 1s on 12 August to improve instrument sensitivity. Thus, for the bulk of the study period, for each of the 159 masses there is a 1 second measurement roughly every 2-3 minutes. In all, during this Study, 116 days of PTR-MS measurements were obtained, providing more than 8.8 million measurements made up of, in most cases, 55680 measurements of each individual mass (of the 159 masses measured) of which 46,400 measurements were of the ambient concentration of each mass. During the period of the Study, 10 August to 7 October 2006, the data acquisition rate (not counting zeros and calibration) was 85% for the PTR-MS.

The raw data files from the PTR-MS are processed with proprietary software developed by CSIRO that takes the ion counts and an array of other instrument information, makes corrections for zeros and calculates either indicative concentrations, or (for those species present in the calibration gases) calibrated concentrations. The algorithm used in this software is based on the physical principles underlying the design of the PTR-MS as outlined in Lindinger et al. (1998) and other documents.

The PTR-MS was calibrated with three certified gas standards containing > 20 VOC species including benzene, toluene, o- xylene and formaldehyde. These certified gas standards were supplied by Apel-Reimer Environmental Inc (Miami Florida, USA).

The PTR-MS calibration response through the study varied with a relative standard deviation of  $\pm 4.8$  to  $\pm 6.2$  %. Changes in the calibration response occurred due to periodic optimisation of the instrument by varying the instrument operating parameters. The effect of changes in the instrument response on the calculation of the ambient concentrations were accounted for by applying a moving calibration response factor across the study period. For each data point the mean of the calibration response that occurred before and after a given data point were applied to convert the instrument signal to atmospheric concentrations.

Table 45 presents the MDL and calibration response for the NEPM air toxics compounds presented in this report: formaldehyde, benzene, toluene, xylenes. These calibration factors have been applied to these mass numbers. The calibration factors for each compound were calculated by averaging several PTR-MS response values measured throughout the study, then taking an inverse of this average response. Note: in measurements of the atmosphere, the PTR-MS response at mass 107 represents the sum of xylene isomers and ethylbenzene.

**Table 45 MDL and calibration response for the NEPM air toxics compounds**

Compound	Primary protonated mass	MDL for 1-hour average (ppb)	Average PTR-MS calibration response. Units: ncps /ppb ( $\pm$ rel. std dev)
Formaldehyde	31	0.308	$1.20 \pm 6.2$ %
Benzene	79	0.005	$9.31 \pm 4.8$ %
Toluene	93	0.004	$9.42 \pm 5.0$ %
m - xylene	107	0.003	$9.63 \pm 5.3$ %

## 11.2 Active sampling of formaldehyde and BTX on adsorbent cartridges

Active sampling of formaldehyde and BTX on adsorbent cartridges was undertaken at the North-AQMS, South-AQMS (Site 5), and Sites 1 - 4. Details of the sampling methodology were described

in previous reports for this project (Dunne et al 2017, 2018). Briefly, at the North-AQMS, ambient air was actively drawn through a ~ 12 m length of 3/8 inch O.D. PTFE tubing inlet (inlet height ~ 6 m) into a CSIRO custom designed automated sampler. The automated sampler is a programmable continuous air sampler with two channels allowing for simultaneous active sampling onto VOC adsorbent tubes and DNPH cartridges. With 16 sampling ports per channel.

- Channel 1 - Two 12-hour samples of VOCs per day (00:00 – 12:00 and 12:00 – 0:00 by active sampling onto multi-adsorbent VOC tubes (Markes Carbograph 1TD/ Carbopack X) using a constant flow air sampling pump (SKC Model 222-4) at a set flow rate of 20 ml min<sup>-1</sup> with a sample volume ~14.4 litres for each VOC sample.
- Channel 2 - Two 12-hour samples of carbonyls per day (00:00 – 12:00 and 12:00 – 0:00 by active sampling onto Supleco LpDNPH S10 air monitoring cartridges using a constant flow air sampling pump at a set flow rate of 1L min<sup>-1</sup> with a sample volume ~12 litres for each carbonyl sample.

Samples of VOCs on adsorbent tubes and carbonyls on DNPH cartridges were also collected at the five Solar-AQMS sites via a ~1.5 m length of 1/4 inch Teflon tubing (inlet height ~2 m):

- ~ 24-hour samples of carbonyls were collected on DNPH coated solid silica adsorbent cartridges (Supleco LpDNPH) via a using a constant flow air sampling pump (TSI Sidepak) at a set flow rate of 1 l min<sup>-3</sup>.
- Two ~12-hour samples per day of VOCs were collected onto adsorbent tubes using two constant flow air sampling pumps (SKC) at a set flow rates of 20 ml min<sup>-3</sup>.

The DNPH cartridges and VOC adsorbent tubes were analysed at the CSIRO Ocean & Atmosphere laboratories at Aspendale Victoria. Co-located measurements by PTR-MS, DNPH and AT-VOC methods have been undertaken in the past by CSIRO O&A laboratories and published as reports (SPS Cope et al 2014, Galbally et al 2008 a, b ) and in the international scientific literature (Dunne et al 2018).

### **11.3 Analysis of DNPH tubes for formaldehyde.**

The DNPH samples were sent back to Aspendale in cooler bags with freezer blocks to keep the samples cool during transportation. The samples were then stored in the fridge and then extracted in 2.5ml of HPLC grade acetonitrile within 2 weeks of sampling. The extracts were then stored in the fridge until analysis, which was within 1-7 days of extraction.

The DNPH extracts were analysed by ultra-high performance liquid chromatography (UHPLC) consisting of a Thermo Scientific Dionex Ultimate 3000 RS system with diode array (DAD) and mass spectrometry (MS) detection. Compound separation was performed with a RSLC acclaim carbonyl column (2.2  $\mu\text{m}$ , 2.1 mm I.D., 150 mm length, Part No. 077973). The chromatographic conditions included a flow rate of 0.4 mL min<sup>-1</sup> and an injection volume of 3.0  $\mu\text{L}$ , and the DAD was operated in the 220–520 nm wavelength range with 360 nm used for mono-carbonyl quantification and the MS used for carbonyl identification. The peaks were separated by gradient elution with an initial mobile phase of 52% acetonitrile and 48% deionized water (18.2  $\Omega\text{M cm}$ , Millipore Milli-Q Advantage) for 8.3 min, followed by a linear gradient to 100% acetonitrile for 8 min, and with a column temperature of 30 °C. A certified liquid standard (Supelco Carb Method 1004 DNPH mix 2 p/n 47651-U) of the DNPH-carbonyl derivative containing 30  $\mu\text{g mL}^{-1}$  of each formaldehyde in addition to other aldehydes and ketones was diluted 1:25 in a volumetric flask. This prepared standard was then used to perform a multi-point calibration (0.15, 0.30, 0.6 and 1.2  $\mu\text{g mL}^{-1}$ ).

Detection limits for this method are typically 0.01– 0.02 ppb with a calculated measurement uncertainties of  $\sim 9\%$  depending on the sampling conditions. Further details of the DNPH method can be found in Dunne et al. (2017).

The MDL for formaldehyde was 0.013 – 0.014 ppb and formaldehyde was detected above the MDL in 99% of the samples at the HF study site.

Excluding samples affected by instrument failures, or sampling integrity issues a total number of 303 formaldehyde samples were collected on DNPH tubes and successfully analysed from across the five Solar-AQMS sites and the automated sampler at the North-AQMS during the intensive phase of the measurement period.

## 11.4 Analysis of VOC adsorbent tubes

The VOC adsorbent tube samples and blanks were analysed by an automated thermal desorber (ATD) and a gas chromatograph (GC) equipped with flame ionization detection (FID) and a mass spectrometer (MS). Compounds were identified by retention times and/or mass spectrometry (MS): Toluene and m+p- xylenes were quantified by flame ionization detection (FID); benzene and o-xylene were quantified by mass spectrometry due to co-elution. The ATD-GC-FID-MS analysis procedure was as follows: The tube was thermally desorbed at 250°C for 5 minutes by a PerkinElmer TurboMatrix™ 650 ATD. The desorbed gases were then analysed by an Agilent 7890A GC-FID and a 5975C MS. Analysis was carried out on an DB5-MS capillary column (60 m  $\times$  0.32 mm internal diameter  $\times$  1.0  $\mu\text{m}$  film thickness) using a GC temperature program from 35–250°C.

Calibration of the VOCs was carried out using a series of certified standard gas mixtures (Apel Reimer Environmental Inc, Miami, Florida, USA). The calibration involved an injection of the calibration gas onto an adsorption tube using a fixed volume temperature stabilised loop for standards with >2 ppm individual VOCs and via sampling a known volume of calibration gas onto an adsorption tube using a calibrated mass flow controller for standards with <2 ppm individual VOCs.

Tubes were cleaned by a Markes TC-20™ tube conditioner according to Markes' specifications prior to shipping to the field site. The cleaned tubes were capped with a Swagelok fitting with PTFE ferrules and then stored in sealed containers.

Field blanks were used to determine the blank levels and the limit of detection (LOD) of the compounds in this study. The blank level was taken as the mean of the field blank measurements of a compound. The LOD was calculated as the mean standard deviation multiple by the student's t value for 99 percent confidence of the sampling number of field blanks and ranges from 0.002 – 0.02. 70 laboratory blanks were analysed. These laboratory blanks showed equivalent or lower concentrations than the field blanks. All concentrations (in ppbv) of VOCs were blank corrected and calculated at 25°C and at 101.3 kPa.

All tubes were loaded with a TO14a Internal Standard (Linde SPECTRA Environmental Gases, Alpha, NJ, USA) prior to analysis to assess the instrument performance. Samples with an internal standard (IS) response outside of the mean  $\pm$  3 standard deviations of the IS response of the calibrations were excluded.

27% of samples from the Solar-AQMS sites 1 - 5, and 14% of samples from the North AQMS were excluded largely due to their internal standard response being outside of the mean  $\pm$  3 standard deviations of the IS response of the calibrations. The variability in IS response was predominantly observed for samples collected from 30/9/2016 onwards which coincided with a significant increase in ambient relative humidity from a 24 h average of 20 – 60% RH to 60 – 100% RH and the onset of rainfall events at the site (Section 3 – Meteorology). It is likely interference due to the presence of liquid water from the sample matrix retained in the VOC adsorbent tubes resulted in the observed changes in the IS response during analysis.

A total number of 398 VOC samples were collected on adsorbent tubes and successfully analysed across the five Solar-AQMS sites and the automated sampler at the North-AQMS during the measurement period. This excluded samples that were compromised by instrumental and sampling failures.

## 11.5 Precision of active sampling on VOC adsorbent tubes and DNPH cartridges

### 11.5.1 VOC adsorbent tubes

Following the conclusion of the field campaign a comparison study was conducted at CSIRO's Aspendale laboratories in which the Solar-AQMS systems were set-up side by side and replicate 12-hour samples on VOC adsorbent tubes were collected on each Solar-AQMS (2 per Solar-AQMS) on the 15/3/2018. Due to a power failure in one of the Solar-AQMS, only 8 replicate samples were available for analysis. The precision, expressed as percent relative standard deviation (%RSD), of the 8 replicate samples ranged from 131% for benzene, and 11, 7 and 16% for toluene, m+p xylene and o- xylene respectively (Table 46). Agreement within  $\pm 25\%$  is desirable (TO – 17, US EPA 1999). The cause of the poor precision for benzene remains unresolved but may be due to sampling artefacts, and/or variability introduced by the ambient sample matrix, which differs to the blank and calibration matrices especially in terms of the presence of water.

### 11.5.2 DNPH cartridges

Replicate 24-hour samples on DNPH tubes were collected on each Solar-AQMS (1 per Solar-AQMS). Two sets of 5 replicates were collected, the first on the 15/3/2018 and the second on the 20/3/2018. The precision, expressed as percent relative standard deviation (%RSD), of the 2 sets of 5 replicate formaldehyde samples ranged from 8 - 22% (Table 46). Agreement within  $\pm 20\%$  is desirable (TO – 11A, US EPA 1999).

**Table 46 MDL, mean range of replicates and %RSD for replicate analyses on DNPH and VOC adsorbent tubes**

Compound	Date	MDL (ppb)	Mean (range) of 8 replicates (ppb)	%RSD
Formaldehyde	15/3/2018	0.016	3.247 (2.431 – 4.390)	22 %
	20/3/2018		0.456 (0.392 – 0.493)	8%
Benzene	15/3/2018	0.083	0.258 ( $\leq 0.083 - 1.102$ )	131 %
Toluene	15/3/2018	0.012	0.137 (0.122 – 0.170)	11 %
m+p- Xylenes	15/3/2018	0.007	0.068 (0.061 – 0.076)	7 %
o-xylene	15/3/2018	0.001	0.019 (0.016 – 0.026)	16 %

## 11.6 Passive Radiello sampling

One way to measure VOCs and hydrogen sulphide in the atmosphere is known as passive Radiello sampling (Radiello Manual, 2006). In the present study the Radiello sampling and analysis was conducted by a third party contractor, SGS-Leeder, on behalf of GISERA. SGS Leeder Chinchilla Qld conducted the sampling. The cartridges were deployed at 3 sites (North-AQMS, South-AQMS and Site 1) on purpose built poles ~2 m height, fitted with manufacturer supplied shelters to protect the Radiello samplers from adverse weather. Each cartridge was exposed to air for approximately 2 weeks, and then packed in a sealed container and sent to SGS Leeder's laboratories in Notting Hill, Victoria for analysis.

The method of Radiello passive sampling used in this study has been described in more detail in a previous report for this project (Dunne et al 2018). Briefly, during sampling, gases passively migrate through a diffusive surface on the cartridge at a known rate (the sampling rate), and are trapped on an adsorbent surface. Different sampling and analysis methods are used to capture different types of VOCs and hydrogen sulphide. In the present study three different Radiello methods were employed:

- VOCs chemically desorbed with carbon disulphide (CS<sub>2</sub>)
- Aldehydes by DNPH Derivatization
- Hydrogen sulphide by zinc acetate chemi-adsorption

For the VOCs detection limits were typically between 0.01 – 0.05 ppbv depending on the species measured, the sampling rate and the sampling period. Likewise the detection limits for aldehydes were 0.03 – 0.15 ppbv and hydrogen sulphide was 0.31 – 0.56 ppb.

An analysis of the performance of Radiello sampling was provided in a previous report for this project (Radiello report, Dunne et al 2018). Field duplicates are two samplers which are co-deployed in the same location side by side, exposed for the same amount of time, and treated and analysed identically and agreement between duplicate measurements is ideally within 40%. Overall the agreement between the paired duplicate measurements was generally good (correlation coefficient  $R^2=0.96$ ) and typically within 40% of each other (Figure 4). At low concentrations, there were more occasions when the relative difference between the paired measurements was > 40% but these were considered acceptable as the absolute difference (ppb) between duplicate measurements overall were very small with average absolute differences ranging from 0.00 – 0.10 ppb, and maximum absolute differences ranging from 0.00 – 0.41 ppb.

Method spikes are Radiello samplers that are identical to those used for sampling except that they are spiked with a known amount of a set of chemicals of interest and analysed alongside the samples. Method spikes are used to determine the analytical bias and ideally reported values are within 30% of the spiked mass that was added. Average method spike recoveries for the radiello study were:

- 92 to 103 % recovery for 7 VOC species (benzene, toluene, m & p- xylene, o-xylene, ethylbenzene, chlorobenzene, 1,4-dichlorobenzene)
- 52 to 92 % recovery for 4 aldehydes (formaldehyde, acetaldehyde, butanal, benzaldehyde)
- 102 % recovery for hydrogen sulfide

Formaldehyde recoveries ranged from 63 – 131% with one fifth of method spikes reporting recoveries of < 70% indicating a moderately frequent negative bias in the analysis of formaldehyde by this method. The sample data for formaldehyde was reported for this study however due to the negative analytical bias the atmospheric concentrations could have been underestimated on occasions. It is important to note that even if the maximum concentration of formaldehyde of 1.30 ppb reported in this study was underestimated by 30% it would still be almost 7 times lower than the relevant air quality standard of 9 ppb referenced here (see section 5.1).

Typically 2 method spikes were analysed alongside each batch of samples. The agreement between the paired duplicate method spikes provides an estimate of the analytical precision. Analytical precision is expressed as the relative percent difference (RPD) and is calculated from the ratio of the absolute difference between the duplicates to the average of the duplicates and is reported as percentage. Ideally RPD values are < 20%. For the radiello Study (Dunne et al 2018) average RPD values were:

- RPD = 4 to 6% for 7 VOC species (benzene, toluene, m & p- xylene, o-xylene, ethylbenzene, chlorobenzene, 1, 4-dichlorobenzene).
- RPD = 7 to 9% for 4 aldehydes (formaldehyde, acetaldehyde, butanal, benzaldehyde).
- RPD = 6 % for hydrogen sulfide
- Less than 3% of the paired method spike measurements had RPD values > 20%.

## 11.7 Comparison of VOC measurements made by PTR-MS, VOC adsorbent tubes, DNPH and Passive Radiello sampling

The following comparison of the reported values from the passive Radiello sampling method, the active sampling methods (AT-VOC and DNPH) and continuous measurements of PTR-MS. Summary statistics for each of the methods is provided in Table 47. The measurement methods provided comparable results with the exception of benzene. Median and mean benzene concentrations of 0.02 – 0.03 ppb were reported by the passive Radiello method, the automated sampler at the North-AQMS, and the measurements by PTR-MS. Concentrations of benzene reported by the active sampling method employed at Solar-AQMS sites were an order of magnitude higher with mean and median values of 0.15 – 0.20 ppb. Poor precision for benzene measurements on the Solar-AQMS stands was reported in section 8.3.3 with relative percent difference between 8 replicate measurements of 131 % where agreement within  $\pm 25\%$  is considered acceptable.

Possible reasons for this discrepancy due to sampling or analytical factors include:

- Contamination of the samples by the sampling apparatus used at the Solar-AQMS. However, the inlet materials and sample pumps used in this study were identical to those used in previous studies where this discrepancy was not observed.
- Interference in the GC-FID-MS analysis of benzene due to water in the samples collected at the Solar-AQMS. This may not have occurred at the same rate in the samples collected at the North-AQMS as the automated sampler used there for active sampling, was housed in a climate controlled laboratory which would have minimised the amount of condensation in the VOC adsorbent tubes.

The reason for the discrepancy remain unresolved, and further work is need to characterize the potential sources of contamination from sampling apparatus and to understand the influence of water on the quantification of benzene.

Given the poor precision of the Solar-AQMS sampling for benzene, and the reasonable agreement between the other three independent measurement methods (automated sampler, the PTR-MS, passive Radiello), benzene data from the Solar-AQMS samples was excluded from reporting in this study. It is important to note, the overall average concentrations of benzene reported by the active sampling at the Solar-AQMS sites was 0.21 ppb which is substantially less than the NEPM air toxics annual guideline value of 3 ppb. The maximum 24-hour concentration of benzene reported at the Solar-AQMS was 0.91 ppb which is also substantially less than the short term Texas AMCV guideline of 180 ppb.

**Table 47** Ambient concentrations of air toxics formaldehyde, benzene, toluene and xylenes measured with the different methods outlined in Section 5.

Compound	Method	Averaging period	Detection Limit (ppb)	25 <sup>th</sup> %ile (ppb)	Median (ppb)	Mean (ppb)	75 <sup>th</sup> %ile (ppb)	Max (ppb)	N
<b>Formaldehyde</b>	PTRMS – North-AQMS	12-hour	0.31	1.28	1.74	1.88	2.25	6.27	228
	DNPH – North-AQMS	12-hour	0.14	0.68	1.14	1.24	1.77	2.55	65
	DNPH - Sites 1 - 5	~ 24-h	0.13	0.94	1.20	1.35	1.70	3.73	238 (~ 45/site)
	Radiello – North & South-AQMS, Site 1	~ 14-days		0.51	0.66	0.68	0.90	1.30	33 (~ 11/site)
<b>Benzene</b>	PTRMS – North-AQMS	12-hour	0.005	0.014	0.023	0.028	0.034	0.125	228
	AT-VOC – North-AQMS	12-hour	0.020	≤ 0.020	≤ 0.020	0.028	0.033	0.086	63
	AT-VOC - Sites 1 – 5*	~ 12-hour	0.004 - 0.024	0.082*	0.156*	0.205*	0.270*	0.913*	335 (~ 67/site)
	Radiello - North & South-AQMS, Site 1	~ 14-days	0.011 – 0.021	≤ 0.018	≤ 0.019	0.023	≤ 0.021	0.069	33 (~ 11/site)
<b>Toluene</b>	PTRMS – North-AQMS	12-hour	0.004	0.011	0.015	0.020	0.026	0.068	228
	AT-VOC – North-AQMS	12-hour	0.004	≤ 0.004	0.010	0.012	0.018	0.046	63
	AT-VOC - Sites 1 - 5	~ 12-hour	0.003	0.004	0.008	0.012	0.014	0.127	335 (~ 67/site)
	Radiello - North & South-AQMS, Site 1	~ 14-days	0.010 – 0.019	≤ 0.017	≤ 0.018	≤ 0.018	≤ 0.019	0.026	33 (~ 11/site)
<b>Xylenes</b>	PTRMS – North-AQMS	12-hour	0.003	0.007	0.013	0.017	0.021	0.077	228
	AT-VOC – North-AQMS	12-hour	0.009 – 0.012	≤ 0.012	≤ 0.012	0.014	≤ 0.012	0.040	63
	AT-VOC - Sites 1 - 5	~ 12-hour	0.005	≤ 0.005	0.007	0.008	0.009	0.053	335 (~ 67/site)
	Radiello – North & South-AQMS, Sites 1	~ 14-days	0.010 – 0.018*	≤ 0.032	≤ 0.034	≤ 0.034	≤ 0.034	0.076	33 (~ 11/site)

\* Data excluded from further reporting here due to poor method precision

## 12 Appendix-Sampling and Analysis of polycyclic aromatic hydrocarbons

The method of active sampling of PAH and analysis using GC-MS was compatible with AS/NZS 3580.16:2014 Methods for sampling and analysis of ambient air. Method 16: Determination of polycyclic aromatic hydrocarbons (PAH) and US EPA Methods TO-4, TO-9 and TO-13.

Samples comprised of a filter for collecting aerosol phase followed by an adsorbent bed for collecting gas phase PAHs. Binderless, pure 142 mm diameter quartz filters (Tissuquartz, 2500 QAT-UP, Pall Corporation) were used for collection of aerosol phase PAHs. The filters were cleaned by baking for 2 hours at 850 °C, then wrapped in baked aluminium foil and stored at <4°C. Pre-cleaned 65 mm x 125 mm polyurethane foam (PUF) sorbent tubes (#226-131, SKC Inc, PA, USA), loaded in a glass cartridges were used for collection of gas phase PAHs. Prior to sampling the cleaned PUFs were spiked with three deuterated species (D-Ant, D-Pyr and D-DahA; in 100 µL isooctane), sealed and stored at <4°C.

PAH sampling was performed by CSIRO staff using a FLOW-SET High Volume PUF (polyurethane foam) Sampler (Lear Siegler Caringbah, Australia) located at the South-AQMS. Volumetric flow was achieved using a mass flow sensor with temperature and pressure compensation. The volumetric flow rate was verified prior to deployment and during the field campaign using an orifice flow rate calibration unit. An electronic manometer (TSI Velocicalc 9565, Shoreview, USA) was used to measure the ambient temperature and pressure and the differential pressure over a calibrated orifice plate installed on the unit. The average flow rate over the duration of the study was 227.7 lpm, which is within 1% of the operating flow rate of 225 lpm. The variation in the flow, expressed as % RSD was 4.9% (n=9).

Over the campaign, two laboratory blanks, three field blanks and 24 samples were collected. Sampling start date and time, initial flow rate and sample finish time and final flow rate were recorded. Total volume was logged by the sampler. Sample times were typically 48 hours. On three occasions, sampling was extended by up to 2 days due to site closure from heavy rainfall. Sample volumes ranged from 601 to 1290 m<sup>3</sup>. The exposed filter and PUF were sealed in aluminium foil separately and taken to a site laboratory where the filter was folded and sealed in baked aluminium foil and the PUF was returned to the storage cartridge and sealed.

Field blanks were obtained by loading the filter and PUF cartridge into the sampler at the site but the high volume sampler was not turned on. The sample was then immediately removed. It was subjected to the same sample handling, storage and transport procedures as for a sample.

Samples and field blanks were stored at  $<4^{\circ}\text{C}$  and transported in one batch (at  $<4^{\circ}\text{C}$ ) to Queensland Alliance for Environmental Health Sciences at the University of Queensland laboratories in Brisbane. Laboratory blanks were subject to the same preparation as samples but they were retained by the laboratory and stored at  $<20^{\circ}\text{C}$  until analysis of the field blanks and samples.

Prior to extraction, blank and sample PUFs were spiked with a solution (in 200  $\mu\text{L}$  isooctane) containing 7 deuterated PAHs: D-Phe, D-Flu, D-Chr, D-BbF, D-BaP, D-I123cdP and D-BghiP. The deuterated compounds were used as internal reference standards to quantify the native compounds using a modified isotopic dilution method.

Both filter and PUF components of each sample or blank were combined for extraction by an Accelerated Solvent Extractor (ASE) using a mixture of hexane and acetone (1:1; V:V). The extracts were concentrated under nitrogen and cleaned up using a chromatographic column. After clean-up, isotopically-labelled PCB-141 was added to each extract prior to instrument analysis to assess the recovery of the internal standards through-out the sample analysis.

Samples were analysed for 12 target PAHs, including BaP, the air Toxics NEPM indicator for PAH, using a Thermo TRACE GC Ultra coupled to a TSQ Quantum XLS triple quadrupole mass spectrometer equipped with a TriPlus Autosampler in selected reaction monitoring (SRM) mode. Calibration standards of target analytes were made ranging from 0.1 to 5000 ng per sample, with each containing deuterated internal standards at the specified concentration. Identification of the analytical responses was confirmed using a combination of signal to noise ratio (3:1), relative retention time to specific internal standard and response ratio for the two ion transitions monitored. Analyte concentrations were quantified based on the modified isotopic dilution method, i.e. from their relative response to a specific internal standard against the slope of a 10-point calibration curve. A minimum signal-to-noise ratio of 3:1 was used for compound identification. Target analyte concentrations in the volume of the extract analysed were quantified from their primary ion transition area divided by the deuterated internal standard primary ion transition area multiplied by the internal standard concentration divided by the response factor(s) determined across the range of calibration standards. The deuterated internal reference standard with the same/similar structure (i.e. number of rings) to the target analyte was used for quantification (see Table 48). The number of rings refers to the number of aromatic rings that each PAH species has.

**Table 48 Target compounds, internal standards and transitions monitored**

Target (native) analytes	Number of rings	Quantification ion transition	Qualification ion transition	Spiked internal standard	Quantification ion transition	Quantification ion transition
Phenanthrene (Phe)	3	178/176	178/152	<sup>2</sup> D <sub>10</sub> -Phe (500 ng)	188/160	188/158
Anthracene (Ant)	3	178/176	178/152	<sup>2</sup> D <sub>10</sub> -Phe (500 ng)	188/160	188/158
Fluoranthene (Flu)	4	202/200	202/201	<sup>2</sup> D <sub>10</sub> -Flu (200 ng)	212/210	208/206
Pyrene (Pyr)	4	202/200	202/201	<sup>2</sup> D <sub>10</sub> -Flu (200 ng)	212/210	208/206
Benzo[a]anthracene (BaA)	4	228/226	228/227	<sup>2</sup> D <sub>12</sub> -Chr (50 ng)	240/236	240/238
Chrysene (Chr)	4	228/226	228/227	<sup>2</sup> D <sub>12</sub> -Chr (50 ng)	240/236	240/238
Benzo[b+k]fluoranthene (BbF+BkF)	5	252/250	252/226	<sup>2</sup> D <sub>12</sub> -BbF (50 ng)	264/260	264/236
Benzo[e]pyrene (BeP)	5	252/250	252/226	<sup>2</sup> D <sub>12</sub> -BaP (50 ng)	264/260	264/236
Benzo[a]pyrene (BaP)	5	252/250	252/226	<sup>2</sup> D <sub>12</sub> -BaP (50 ng)	264/260	264/236
Dibenz[ah]anthracene (DahA)	5	278/276	278/277	<sup>2</sup> D <sub>12</sub> -I123cdP (50 ng)	288/284	288/286
Indeno[1,2,3-cd]pyrene (I123cdP)	6	276/274	276/275	<sup>2</sup> D <sub>12</sub> -I123cdP (50 ng)	288/284	288/286
Benzo[ghi]perylene (BghiP)	6	276/274	276/275	<sup>2</sup> D <sub>12</sub> -BghiP (50 ng)	288/284	288/286

A performance standard 13C-PCB-141 was added to the purified sample extract prior to analysis to monitor instrument variability and calculate the recoveries of the internal standard.

## 12.1 Sampling efficiency, analytical recovery and blank levels

In order to collect sufficient PAH mass, the sample volumes for the study were higher than typical 24-hour volumes of 324 m<sup>3</sup>. Sampling typically occurred for 48 hours, resulting in a mean sample volume of 692 m<sup>3</sup>, ranging from 601-1290 m<sup>3</sup>. For sample volumes in excess of 350 m<sup>3</sup>, AS/NZS 3580.16:2014 recommends that the dynamic retention efficiency of the sample be tested by adding known amounts of deuterated PAH standards to unexposed PUFs prior to deployment for sampling. PUFs were spiked with D-Anthracene (D-Ant), D-Pyrene (D-Pyr) and D-Dibenz[ah]anthracene (D-DahA), which covers a range of volatilities. Recoveries for D-Pyr (4-rings) and D-DahA (5-rings) were within acceptance limits of 75-125%, ranging from 89-107% and 88-111%, respectively, showing no break-through of species Table 49. Recoveries of field blanks were good for D-Ant, D-Pyr and D-DahA, indicating no handling issues. However D-Ant (3-rings) recoveries were about 10% for all samples except one. Field blank recoveries for D-Ant ranged from 67-87%, which indicates that D-Ant was lost from samples during sampling, not from storage and handling. The loss could be due to break-through due to excessive sample volumes 692 m<sup>3</sup> (601-1290 m<sup>3</sup>) or degradation of D-Ant, possibly from hot sampling conditions or the presence of

high levels of O<sub>3</sub>. Due to the poor dynamic retention efficiency of D-Ant, concentrations of 3-ring (more volatile) species Anthracene and Phenanthrene are not reported.

AS/NZS 3580.16:2014 also has acceptance criteria for sample extraction and analysis recovery, based on known amounts of deuterated PAHs added prior to the extraction process. Recoveries outside the criteria of 50-150% should be considered as qualitative only. As shown in Table 49 mean recoveries of seven deuterated PAHs ranged from 73-89%. The final sample, taken one month after the completion of site activity, had low recoveries of 22-34% that don't meet the acceptance criteria. The reason for the poor recovery is unknown; however note that low recoveries don't affect the quantification of the native PAHs as these are determined relative to the internal standard that had been added to the sample prior to extraction; thus the native is calibrated from the deuterated species that also had low recovery.

**Table 49 Recovery of spike deuterated PAHs added (a) before sampling; and (b) before extraction of exposed sample**

Sample start date/time	Sample end date/time	Sampling efficiency/recovery			Extraction, clean-up and analysis efficiency/recovery							
		D-Ant	D-Pyr	D-DahA	D-Phe	D-Flu	D-Chr	D-BbF	D-BaP	D-123cdP	D-BghiP	
11/08/2017 12:48	13/08/2017 11:12	35%	91%	97%	88%	75%	79%	84%	83%	88%	84%	
13/08/2017 11:32	15/08/2017 11:18	22%	95%	104%	125%	90%	98%	103%	106%	96%	90%	
15/08/2017 13:08	17/08/2017 10:48	34%	97%	96%	63%	63%	70%	74%	77%	74%	68%	
16/09/2017 10:29	18/09/2017 9:03	34%	96%	98%	70%	68%	73%	79%	78%	82%	81%	
18/09/2017 9:09	20/09/2017 8:03	31%	94%	99%	40%	56%	58%	62%	64%	74%	73%	
20/09/2017 8:28	22/09/2017 8:14	9%	93%	93%	63%	67%	74%	81%	83%	96%	91%	
22/09/2017 8:31	24/09/2017 8:45	9%	93%	97%	110%	88%	94%	108%	108%	101%	98%	
24/09/2017 8:58	26/09/2017 8:25	10%	94%	98%	129%	88%	100%	108%	108%	96%	90%	
26/09/2017 8:45	28/09/2017 8:07	7%	95%	99%	125%	85%	96%	103%	107%	96%	90%	
28/09/2017 8:38	30/09/2017 9:31	9%	89%	91%	93%	82%	89%	99%	99%	102%	97%	
30/09/2017 9:48	4/10/2017 9:37	8%	97%	95%	51%	53%	59%	64%	65%	69%	65%	
4/10/2017 10:01	6/10/2017 8:57	8%	97%	98%	135%	88%	97%	104%	104%	92%	81%	
6/10/2017 9:21	9/10/2017 8:11	4%	97%	99%	107%	80%	88%	96%	97%	88%	81%	

Sample start date/time	Sample end date/time	Sampling efficiency/recovery		Extraction, clean-up and analysis efficiency/recovery							
		D-Ant	D-Pyr	D-DahA	D-Phe	D-Flu	D-Chr	D-BbF	D-BaP	D-123cdP	D-BghiP
9/10/2017 8:24	11/10/2017 8:00	7%	97%	94%	79%	76%	79%	81%	81%	85%	81%
11/10/2017 8:15	13/10/2017 7:38	12%	90%	91%	57%	55%	60%	63%	64%	68%	66%
13/10/2017 7:53	15/10/2017 7:16	5%	100%	98%	110%	80%	93%	98%	102%	92%	89%
15/10/2017 7:31	18/10/2017 12:32	75%	100%	99%	68%	64%	72%	78%	83%	89%	82%
18/10/2017 12:53	20/10/2017 9:31	6%	89%	88%	103%	82%	93%	99%	102%	96%	86%
20/10/2017 9:51	22/10/2017 9:01	21%	97%	97%	99%	96%	107%	116%	122%	129%	120%
22/10/2017 9:22	24/10/2017 9:22	14%	96%	99%	119%	91%	96%	101%	103%	91%	83%
24/10/2017 9:55	26/10/2017 8:56	14%	96%	96%	115%	81%	90%	100%	100%	88%	82%
26/10/2017 9:10	28/10/2017 8:22	16%	93%	99%	100%	81%	89%	98%	99%	89%	82%
28/10/2017 8:53	30/10/2017 7:31	6%	95%	98%	58%	43%	47%	52%	53%	52%	48%
20/11/2017 16:29	22/11/2017 15:22	21%	107%	111%	22%	26%	29%	31%	33%	34%	33%
Min recovery (n=24)		4%	89%	88%	22%	26%	29%	31%	31%	33%	33%
Max recovery (n=24)		75%	107%	111%	135%	96%	107%	116%	116%	122%	120%
Mean recovery (n=24)		17%	95%	97%	89%	73%	80%	87%	88%	86%	81%
Median recovery (n=24)		11%	96%	98%	96%	80%	88%	97%	98%	89%	82%
Recovery doesn't meet criteria 50-150%		23/24	0/24	0/24	2/24	2/24	2/24	1/24	1/24	1/24	2/24

Table 50 shows laboratory and field blank masses compared to the range of sample masses. There was no significant difference in mass between the laboratory (n=2) and field blanks (n=3), indicating that sample and handling procedures did not impact on measured concentrations. Blank levels for 5 and 6-ring PAHs were less than 2 ng and for the more volatile 4-ring species Flu and Pyr, were less than 30 ng. These numbers are slightly higher than recommended by AS3580.16:2014 but sample masses of these two species were also higher. Sample:blank ratios ranged from <MDL to 64, with 23% of all PAHs having ratios > 10 and 33% of BaP measurements having ratios > 10. Sample concentrations reported have had the average field blank concentration subtracted.

**Table 50 Masses of laboratory blanks, field blanks, sample MDL and number of detects**

Species	Number of aromatic rings	Laboratory blank mass, min-max, ng	Field blank mass average (min-max), ng	MDL mass (3xSD field blank mass), ng	Detects>MDL n=24	Sample: blank ratio average (min-max)
Flu	4	20-26	23 (9-31)	35	23	4 (<MDL-11)
Pyr	4	13-16	17 (8-16)	26	23	5 (1-13)
BaA	4	0.8-0.9	0.9 (0.8-1.1)	0.6	22	4 (<MDL-27)
Chr	4	1.2-2.5	1.4 (1.0-2.5)	1.1	24	7 (<MDL-37)
BbF+BkF	5	1.3-2.9	1.6 (1.3-2.9)	0.5	23	9 (<MDL-53)
BeP	5	0.6-1.2	0.7 (0.6-1.2)	0.2	23	10 (<MDL-64)
BaP	5	0.2-0.3	0.3 (0.2-0.4)	0.2	22	8 (<MDL-39)
DahA	5	0.1	0.1 (0.1-0.2)	0.1	21	9 (<MDL-55)
I123cdP	6	0.5-0.6	0.5 (0.4-0.6)	0.3	22	13 (<MDL-58)
BghiP	6	0.7-0.9	0.8 (0.7-0.9)	0.4	22	8 (<MDL-33)

## 13 Appendix-Mercury sampling and analysis

Semi-continuous measurements were made using a Model 2537A Vapour Phase Mercury Analyser, which collected mercury onto a pair of gold traps (A and B) that were alternately analysed and cleaned every 5-minutes. The sampling and analysis method follows the Global Mercury Observation System (GMOS) Standard Operational Procedure for the determination of GEM [http://www.gmos.eu/public/GMOS%20SOP%20TGM\\_GEM.pdf](http://www.gmos.eu/public/GMOS%20SOP%20TGM_GEM.pdf) . However, QA/QC of the resultant output detected that data obtained from Trap A was consistently lower during operation, possibly due to a drop in the capture efficiency, as in some instances, an unknown compound may passivate the surface of the cartridge. The symptoms of this condition are that the two cartridges usually report substantially different readings while monitoring ambient air and the condition is most evident when output is plotted. The graph assumes a characteristic "sawtooth" or bi-modal pattern.

The differences noted between TRAP A and TRAP B data suggest that TRAP A was not working effectively from early on in the campaign. As a result all the Trap A data was removed from the data set. This outcome is in line with the guidance in the 2537A Tekran manual (Section 10:21) "When the readings between the A and B gold cartridges differ, the gold cartridge showing the higher values has always been found to be accurate. Data from the offending gold cartridge can be stripped from the data set."

As a consequence finer scaled data is only available for alternating 5-minute periods, with a 5-minute gap between samples.

## 14 Appendix – Fire Hotspot data

### A.4 Event investigations - Fire Hotspot data

Hotspot data has been used in previous CSIRO studies to identify fires in the Surat Basin region (Lawson et al 2018a and b) The following is an extract from these reports providing an explanation of the sources of this data:

*Hotspots referred to in Section 4 are derived from satellite-born instruments that detect light in the thermal wavelengths. The satellite data are processed with a specific algorithm that highlights areas with an unusually high temperature.*

*Two different satellite products were used to investigate the presence of fires in the study area in this report – Sentinel Hotspots and NASA Worldview.*

*Sentinel Hotspots - Sentinel is an Australian bushfire monitoring system that provides information about fire hotspots. Sources – MODIS sensor aboard NASA Terra and Aqua satellites, AVHRR (Advanced Very High Resolution Radiometer) night time imagery from NOAA satellites, VIIR on the Suomi-NPP satellite. © Commonwealth of Australia (Geoscience Australia) 2018.*

*NASA Worldview is a component of the NASA Earth Observing System Data and Information System (EOSDIS). The Worldview tool from NASA's Earth Observing System Data and Information System (EOSDIS) provides the capability to interactively browse historical fire data. FIRMS (Fire Information for Resource Management System) can be used to download the historical data. NASA Worldview provides fire products from the Moderate Resolution Imaging Spectroradiometer (MODIS) (MCD14DL) and the Visible Infrared Imaging Radiometer Suite (VIIRS) 375 m (VNP14IMGTDL\_NRT))*

*The smoke plumes are observed in NASA Worldview using corrected reflectance from Suomi NPP / VIIRS, Aqua /MODIS and /or Terra / MODIS.*

*We acknowledge the use of data and imagery from LANCE FIRMS operated by the NASA/GSFC/Earth Science Data and Information System (ESDIS) with funding provided by NASA/HQ.*



**GISERA**  
Gas Industry Social and  
Environmental Research Alliance

## Contact us

Paul Cunningham

Phone: +61 7 3833 5673

Email: [gisera@gisera.csiro.au](mailto:gisera@gisera.csiro.au)

[gisera.csiro.au](http://gisera.csiro.au)